CSIRO Earth Observation Centre

CSIRO Atmospheric Research

Evaluation of the EO-1 Hyperion Hyperspectral Instrument & its Applications at Australian Validation Sites 2001-2003

D.L.B. Jupp & Bisun Datt (Eds)

CSIRO Earth Observation Centre Report 2004/05

Evaluation of the EO-1 Hyperion Hyperspectral Instrument & its Applications at Australian Validation Sites 2001-2003.

(Collected Papers written by the Australian members of the NASA Science Validation Team)

ABSTRACT

This EOC Report has been developed and expanded primarily from work outlined in the Final report to the NASA NRA-99-0ES-01 submitted by David L. B. Jupp & Bisun Datt (CSIRO Office of Space Science and Applications, Earth Observation Centre), on behalf of the twenty-three Australian members (Principal and Co-Investigators) of the NASA EO-1 Science Validation Team (SVT) in May 2003. With a range of recent expansions and updates to the work reported to NASA, it now represents a comprehensive collection of the efforts by a number of Australian investigators at wide a range of Australian field sites between November 2000 and November 2002. The updated reports include more recent research findings and work done as part of the extended mission of EO-1 that started in early 2002. In addition to calibration, validation and applications reports from the scientists involved, it includes a description of the sites, an introduction to EO-1 and a summary of outcomes and recommendations for future space missions and instrument design based on the work done by the Australian scientists. The summary is organised both in terms of the technical issues of data pre-processing and also in terms of the current and future applications that will benefit from the availability of future operational space hyperspectral instruments. In that regard, a number of important recommendations have emerged that need to be addressed in the design and implementation of such future missions. Research and applications by the Australian members of the SVT using EO-1 data is continuing as is the EO-1 extended mission.

Cover Picture: The cover picture is a NASA illustration used with permission. It shows an impression of the EO-1 satellite in orbit using photographs and imagery.

Published by:

CSIRO Earth Observation Centre
GPO Box 3023, Canberra, ACT 2601
Australia

A PDF version of this report is available at: http://www.eoc.csiro.au

Australian Principal and Co-Investigators

Person	Email Address
Gary Bastin	Gary.Bastin@csiro.au
Vittorio Brando	Vittorio.Brando@csiro.au
Susan Campbell	Susan.Campbell@csiro.au
Vanessa Chewings	Vanessa.Chewings@csiro.au
Terry Cocks	tdc@intspec.com
Nicholas Coops	Nicholas.Coops@csiro.au
Tom Cudahy	Tom.Cudahy@csiro.au
Bisun Datt	Bisun.Datt@csiro.au
Arnold Dekker	Arnold.Dekker@csiro.au
Dean Graetz	Dean.Graetz@csiro.au
Alex Held	Alex.Held@csiro.au
Jon Huntington	Jon.Huntington@csiro.au
David Jupp	David.Jupp@csiro.au
Edward King	Edward.King@csiro.au
Tiit Kutser	Tiit.Kutser@ebc.uu.se
Jenny Lovell	Jenny.Lovell@csiro.au
Tim McVicar	Tim.McVicar@csiro.au
Ross Mitchell	Ross.Mitchell@csiro.au
Cindy Ong	Cindy.Ong@csiro.au
Fred Prata	Fred.Prata@csiro.au
Melissa Quigley	Melissa.Quigley@csiro.au
Craig Smith	Craig.Smith@auslig.gov.au
Tom Van Niel	Tom.VanNiel@csiro.au

Table of contents

Evaluation of the EO-1 Hyperion Hyperspectral Instrument & its Applications at Australian Validation Sites 2001-2003

1 INTRODUCTION

1.1 Background to Australian Participation

In 1999, Australian scientists made a successful application to the NASA Research Announcement (NRA-99-0ES-01, "EO-1 Evaluation and Validation") to carry out investigations in Australia on the performance of instruments carried on the upcoming NASA "Earth Observing – 1" (EO-1) Mission (see http://eo1.gsfc.nasa.gov). Of particular interest was the Hyperion hyperspectral sensor. The plan was to use a range of Australian field sites and the capacity and experience of the groups involved to deploy ground and airborne hyperspectral instruments and undertake detailed investigations in terms of impacts of data quality on applications. The findings were to provide a contribution to the overall evaluation and validation by the NASA Science Validation Team (SVT) of primarily US scientists who were gathered together by NASA to provide the mission with validation and scientific evaluation.

The Australian CSIRO (Commonwealth Scientific and Industrial Research Organisation) through its Earth Observation Centre (EOC) provided overall coordination of the Australian projects as "Principal Investigator" for the activity. CSIRO had previously, through the EOC (see http://www.eoc.csiro.au), conducted a range of investigations into hyperspectral applications at a number of the sites in Australia. These investigations involved organising airborne missions using the HyMap™ airborne scanner, taking supporting measurements, data management and data analysis. The hyperspectral test sites were widely distributed throughout Australia and its many environments as shown in Figure 1.3.1. In addition to CSIRO scientists, staff from the Australian Centre for Remote Sensing (ACRES), Integrated Spectronics Pty Ltd (ISPL) and HyVista Corporation provided important inputs to the NASA mission.

The EO-1 satellite was launched in November 2000 during the Northern Hemisphere winter adding an increased and critical role for Southern Hemisphere sites in the initial checkout period to carry out early investigations of data performance. During the first three months, Australian scientists worked closely with the Hyperion Instrument Team at TRW who needed to validate the instrument performance prior to handing over to NASA and the SVT. The Australian scientists brought planned field missions forward to provide support for the Instrument Team's assessment schedule of performance against specifications. Data from sites at Lake Frome, Mount Fitton and the Coleambally were specifically used for this task. Lake Frome provided initial strong confirmation of the underlying quality and stability of Hyperion in orbit, Mt Fitton demonstrated that the Signal-to-Noise Ratio (SNR) was sufficient to resolve specific minerals in the shortwave infrared (SWIR, the spectral region between 1200 and 2500 nm) and Coleambally was used in geometric studies. Other sites, such as the Moomba gas flares, were used for a variety of validation studies. Following this early activity, Australian scientists joined with the rest of the NASA SVT to undertake systematic technology evaluations and

helped achieve the situation where an operational extended mission has been activated to make EO-1 data widely used for both research and applications.

The Australian activity during the two years following the launch and in association with the SVT centred primarily on the fieldwork, processing the EO-1 and other data that was acquired at the 12 sites and reporting to NASA. Since then it has also moved on to develop advanced applications and operational uses for the EO-1 data. There have been three overlapping phases to this Australian activity:

Phase 1: Calibration, Validation & Evaluation (year 1)

Lake Frome and Mt Fitton for Hyperion calibration and checkout
Second Lake Frome visit for validation
Coleambally for Landsat/ALI/Hyperion cross comparisons
Uardry for Hyperion checkout
ACRES downlink and downlink testing

Phase 2: Applications (years 1 & 2)

Agriculture at Coleambally
Minerals at Mt Fitton and Panorama
Forestry at Tumbarumba
Water Quality at Moreton Bay
Reefs in the Great Barrier Reef (GBR) near Cape Tribulation
Rangelands at Kunoth
Lake Argyle for calibration and inland water quality

Phase 3: Extended Mission (years 2 & 3)

Extended Mission – Australian bulk order
ACRES/USGS collaboration for data supply
International projects using Hyperion data

The major findings from the calibration and Validation sites are described in Section 2 (Calibration and Validation Sites & Findings) and the outcomes from the applications studied there are provided as Section 3 (Applications Sites & Findings). In Section 4 (Mission Support & Data Management) the inputs and activities of ACRES and HyVista are described and in Section 5 (The Extended Mission) the Australian input and role in the development and pursuit of the Extended Mission is also presented. Section 6 (Conclusions & Recommendations) draws conclusions from the two years, Section 7 (Acknowledgements) acknowledges some of the many people and groups that have helped the work to its successful conclusions and Section 8 (EO-1 Related Publications & Presentations) lists many of the accessible publications, reports, conference and media presentations that have accompanied the widespread activity of the Australian contribution to the NASA EO-1 evaluation and its resulting applications.

1.2 EO-1 Mission – Summary of Instruments and Outcomes

The EO-1 satellite was launched by a Delta rocket from the Vandenburg AirForce Base in California on November 21, 2000. Following a three-month instrument and spacecraft checkout period by the instrument and operations teams, the data streams were judged to be operational and two years of evaluation started. In this phase, a team of scientists (the Science Validation Team, SVT) examined the data and actively improved all aspects of data delivery and processing. These improvements resulted in advanced processing and many successful applications.

The EO-1 satellite was launched into the same orbit as Landsat-7 and follows Landsat-7 by about 1 minute. The Delta rocket that launched EO-1 also carried a second satellite called Satelite de Aplicanciones Cientificas-C (SAC-C) developed jointly by the US and Argentina. SAC-C was also part of the resulting constellation of satellites (called the "A-Train") and followed EO-1 by about 30 minutes being about 1.7 minutes in front of the TERRA satellite as illustrated in Figure 1.2.1. Applications taking advantage of the collective information from sensors on these four satellite platforms was a major objective of the mission.

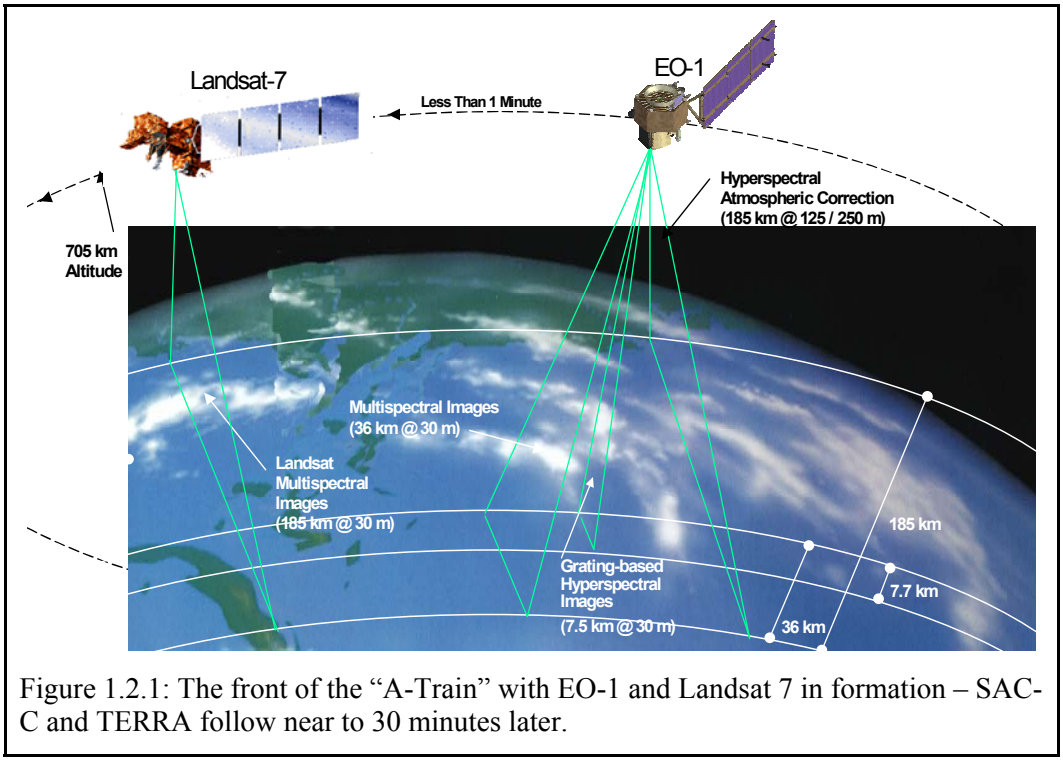

Figure 1.2.1: The front of the "A-Train" with EO-1 and Landsat 7 in formation – SAC-C and TERRA follow near to 30 minutes later.

In this section we will provide a brief and basic introduction to the mission and its experiments so that the many references that are made to its characteristics, and its many acronyms and abbreviations, are conveniently contained in one document. However, for more extensive and detailed investigation of the EO-1 mission it is best to explore the EO-1 website (http://eo1.gsfc.nasa.gov) and the papers collected in the Special Issue on EO-1 of the IEEE Transactions on Geoscience and Remote Sensing, Vol. 41, No. 6, which appeared in June 2003. Among the papers included in the Special Issue, two provide details of the background to the mission, its performance and (particularly

relevant for the work presented here) the characteristics of the Hyperion instrument. These are:

Ungar, Stephen G., Jay S. Pearlman, Jeffrey A. Mendenhall, and Dennis Reuter (2003). Overview of the Earth Observing One (EO-1) Mission. *IEEE - Transactions on Geoscience and Remote Sensing,* **41**(6), 1149-1159.

Pearlman, Jay S., Pamela S. Barry, Carol C. Segal, John Shepanski, Debra Beiso, and Stephen L. Carman (2003). Hyperion, a Space-Based Imaging Spectrometer. *IEEE - Transactions on Geoscience and Remote Sensing,* **41**(6), 1160-1173.

The "EO" in EO-1 stands for "Earth Observing" and EO-1 was launched as part of NASA's New Millenium Program. This program was designed to test new technologies and strategies for Earth Observation. EO-1 served these aims well. Firstly, it carried three experimental sensors that tested new technologies and new types of data for the space environment. One instrument was the Advanced Land Imager (ALI) that tested options for Landsat continuity. A second was the Hyperion hyperspectral sensor that provided hyperpectral data from a space platform for the first time. The third was the Linear Etalon Imaging Spectral Array (LEISA) that involved experimental hardware which achieved hyperspectral imaging in a narrower spectral range than Hyperion.

ALI has 10 bands, a 30m ground sampling distance (GSD) and a 36km swath. Its SNR is in the range 100-200 and it makes use of solar, lunar and lamp calibration to maintain its radiometric performance. Hyperion has 196 unique and useable bands, a 30m GSD, a 7.5km swath and also uses solar, lunar and lamp calibration to maintain its radiometric performance. Hyperion is aligned to be within the pan band of ALI and was radiometrically cross-calibrated with ALI prior to launch. The LAC atmospheric corrector has experimental narrow band, high spectral resolution in the near infrared (NIR, the region from 800 to 1100 nm) and part of the SWIR but since it was not used by any of the Australians it is left to the Special Issue to provide further information on this instrument and its performance. The major parameters for the three instruments are summarised in Table 1.2-1:

Table 1.2-1 Basic Parameters for the three EO-1 Earth Observing instruments

	EO-1		
Parameters	**ALI**	**HYPERION**	**AC**
Spectral Range	**0.4 - 2.4 μm**	**0.4 - 2.4 μm**	**0.9 - 1.6 μm**
Spatial Resolution	**30 m**	**30 m**	**250 m**
Swath Width	**36 Km**	**7.6 Km**	**185 Km**
Spectral Resolution	**Variable**	**10 nm**	**6 nm**
Spectral Coverage	**Discrete**	**Continuous**	**Continuous**
Pan Band Resolution	**10 m**	**N/A**	**N/A**
Total Number of Bands	**10**	**220**	**256**

The Table lists the number of Hyperion bands as 220 but users do not get access to all of these bands. Basically, Hyperion data are recorded by a single telescope but uses two 2-

D arrays of detectors. One array records the visible and near infra-red (VNIR, the region between 400 and 1000 nm) range with 70 potential bands and the other records the SWIR (900 to 2500 nm) range with 172 potential bands providing a total of 242 potential bands. However, the arrays were originally designed for a previous space hyperspectral sensor called Lewis that had been launched but failed in orbit (Pearlman *et al.*, 2003). Hyperion was brought about through the opportunity of using Lewis "spares" to meet a 12-month EO-1 deadline. In achieving this, the TRW engineers had to alter the relationship between the optics and the detectors. As a result, the SNR performance was not as high, only 220 of the potentially 242 detectors were "illuminated" and of those only 200 were useable for earth observation. Level 1 Hyperion data were therefore only delivered in the 200 bands. Of the 200 bands, four are in a spectrally overlapping region of the two detector arrays so that there are basically 196 unique bands available from Hyperion data for applications. The current standard Level 1R Hyperion data delivers 198 bands (50 VNIR and 148 SWIR) including two in the overlap region.

The three instruments are spatially aligned so that there is overlap within the standard Landsat scene geometry that EO-1 shares with Landsat-7. However, since the ALI was an experiment its full potential swath width (which would provide the same field of view (FOV) as Landsat) was not utilised and only a segment (3° of its potential of 15° FOV) on the "east" side of the Landsat scene was imaged. Hyperion was aligned to overlap with this segment and was given an off-nadir pointing of about 5° to bring it into alignment with one edge of the ALI.

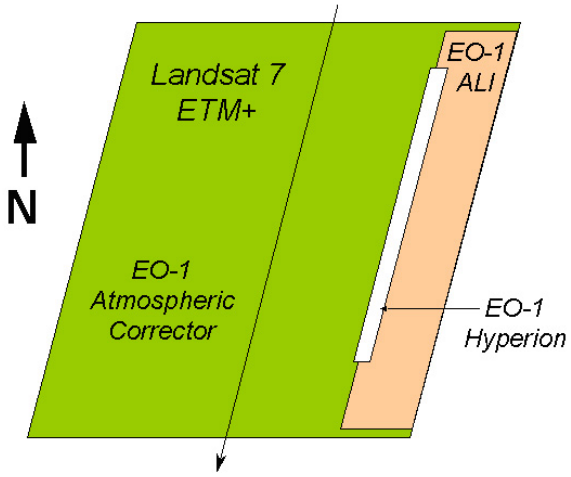

Figure 1.2.2: Alignment of the ALI, Hyperion and LEISA instruments in the EO-1 path.

The geometry for "normal" view is shown in Figure 1.2.2 although as discussed below, EO-1 has very flexible pointing capabilities and data can be taken well outside of the Landsat Path-Row framework. In all cases, however, the three instruments on EO-1 will have the relative alignment shown in Figure 1.2.2. For this reason, the ALI image was used as the reference "quick-look" for EO-1 to provide confirmation of acquisitions and of cloud free sites.

EO-1 has also been a technology prover for many other components as well as the Earth Observing instruments. Its experiments included:

- The Wide Band Advanced Recorder/Processor (WARP). This has been a key part of data downlink. It has up to 840Mbps capability, a high-density electronic board and uses advanced packaging techniques. It has been a very successful new technology;
- New RF communications technology that provided very high data rates;
- Enhanced Formation Flying (EFF) (constellation flying with Landsat-7, SAC-C and TERRA). This has been a key experiment. In the future there may also be data passing between spacecraft;
- The Lightweight Flexible Solar Array (LFSA) experiment. This tested advanced technologies for power supply to future missions;
- The Pulse Plasma Thruster (PPT). This was an experiment in advanced spacecraft manoeuvre and for future inter-planetary travel;
- Precision attitude control, which enabled EO-1 to rotate in all and every direction with very high precision. Images of stars and other experiments confirmed the extraordinary capabilities of this feature;
- A Carbon-carbon radiator that was included to test space efficient radiator designs.

All of the new technologies have performed well – much to the relief of the earth observation scientists whose hearts suffered whenever the spacecraft was shut down or scheduled for an advanced systems test.

1.3 Australian Calibration, Validation & Applications Sites

Australian seasonal conditions are characterised by widespread rains in the north in summer (December to March) with generally very hot and dry conditions in the south. There is a complementary dry season in the north in winter (June to September) and winter rains in the south. The field plan presented to NASA by the Australian scientists therefore involved twelve planned sites – six in the north and six in the south – with planned data acquisition times in the corresponding dry seasons. Figure 1.3.1 shows the geographic distribution of the sites within Australia.

The site characteristics are briefly summarised in Table 1.3-1 which indicates the (Southern Hemisphere) season when the field work was planned, the main applications for the site and the general background that made it a good selection – such as data availability. The diversity and extensive base of prior knowledge was a major factor in the success of the proposal and the success of its outcomes.

Three of the sites, Lake Frome (a salt lake or playa in northern South Australia), Uardry (an open plain site near Hay in New South Wales that is a MODIS[1] monitoring site) and Lake Argyle (a large man-made lake in the north of Western Australia) were chosen primarily for Calibration & Validation studies. They have good uniformity and specifically chosen surface characteristics.

[1] MODerate resolution Imaging Spectrometer on board the NASA TERRA satellite – 30 minutes behind EO-1.

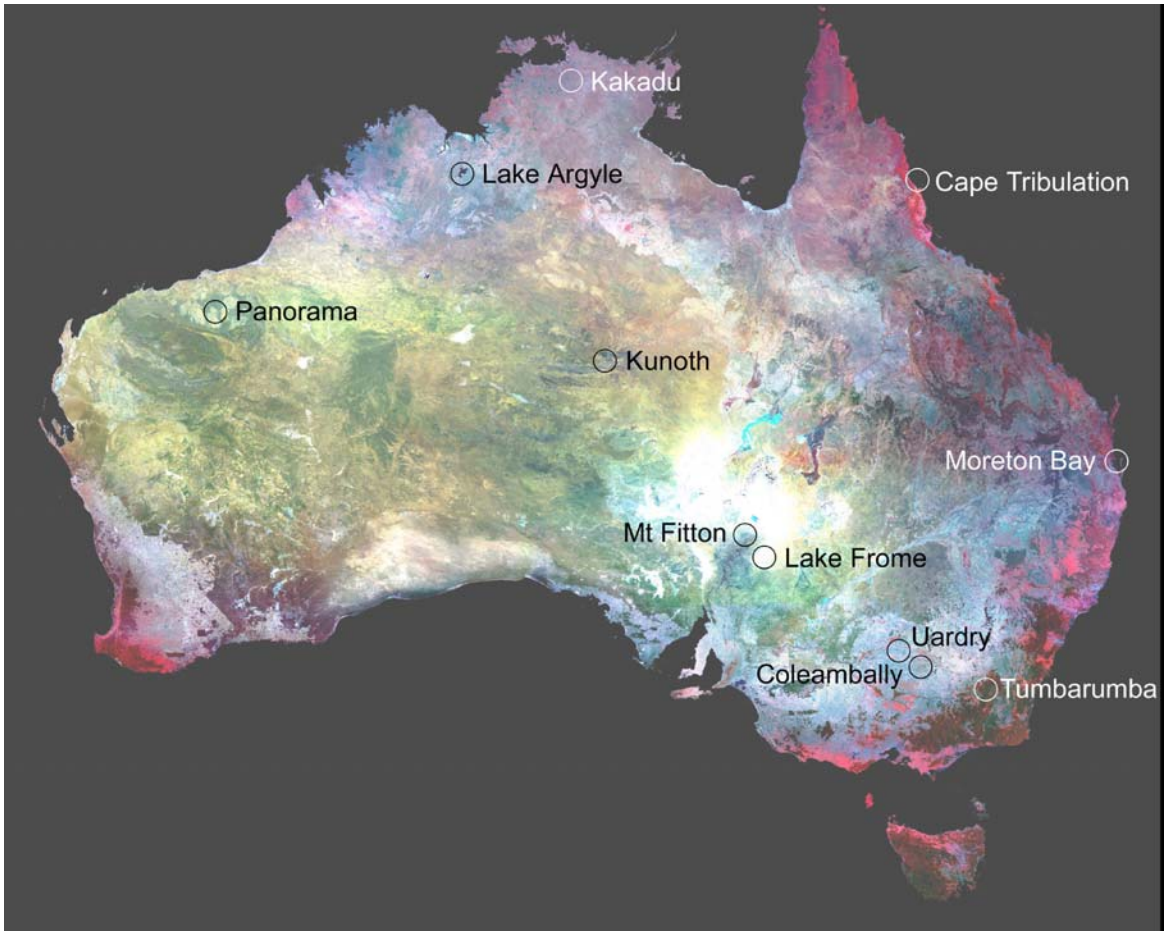

Figure 1.3.1: Locations of the Australian Calibration, validation and applications sites for the EO-1 Mission.

Two of the sites were used for both Applications and Calibration & Validation. One of these was Coleambally (an irrigated agricultural area near Uardry where a time series over two growing seasons was collected). Coleambally also played a valuable role in geometric and radiometric studies. This added role was due to the well surveyed and marked, large field structure of the region. In addition, Mount Fitton, near Lake Frome (a well-studied area of exposed mineralisation) was used for spectral studies that were used specifically to test Hyperion performance in the SWIR region.

The other seven sites were aimed at testing the performance of Hyperion data against specific areas of Applications. This led to a wide range of recommendations that will serve for any future satellite based sensor as Applications must provide the base for any choice of specifications. This side of the mission is developed later when the Extended Mission is discussed. In the event, not all of the planned acquisitions occurred and cloud cover frustrated some of the planned field missions and attempts to have field and satellite data acquired simultaneously. NASA re-scheduling was very sympathetic with these problems, especially as Geoscience Australia was providing support for added EO-1 data acquisitions world-wide through the TERSS X-Band station, and so the overall performance of each site was generally finally acceptable and only one site was unable to acquire any EO-1 data at all. This was the Kakadu site in the north of Australia. We hope to revisit that site in the future.

Table 1.3-1: Australian Sites and Summary of Site Characteristics

Site Name	Type	Notes
Lake Frome	Summer[/Winter] Radiometric Calibration & Validation	Calibration & Validation. HyMap data. A bright, uniform target in the VNIR and dry in Summer.
Lake Argyle	Winter Radiometric Calibration & Validation	Complementary dark target, CIMEL site, HyMap and OARS data.
Coleambally	Summer Agriculture Radiometric & Geometric Calibration & Validation	Irrigated rice and soybean, wheat. Ground data and support. Accurate geodetic mapping provides added opportunities.
Tumbarumba	Summer Forestry	Tall eucalyptus forest. Leaf biochemistry available. A forestry area with a flux tower and extensive field data.
Moreton Bay	Winter/Summer Water quality and coastal applications	Coastal zone, Eutrophication, Algal Blooms. Casi and Hymap data. Water quality monitoring.
Cape Tribulation (1) Cairns Reef	Winter Coral reefs	Coral reef studies enabled by the same data acquisitions as Cape Tribulation (2).
Mt Fitton	Summer[/Winter] Spectral Calibration and Validation minerals exploration	Geology Site, Mineralogy, Spectral contrasts. HyMap, OARS, MASTER, and years of data
Panorama	Winter Minerals Exploration	Minerals, HyMap data, OARS, years of ground data & recent AMS flights. Iron Ore etc
Kunoth (Alice Springs)	Summer/Winter Rangelands	Semi-Arid, Long term monitoring site. Spectral signatures collected.
Cape Tribulation (2) Tropical Agriculture	Winter, Agriculture	Sugar cane and other crops plus Rainforest & mangroves. Forestry data with tower & gondola.
Uardry	Summer Radiometric Calibration & Validation	Long term MODIS Core monitoring site. Previous data including L7 and HyMap.

An invitation for US investigators to work at Australian sites was openly made and a number of scientists took up the opportunity it provided. Table 1.3-2 lists the sites, the Australian participants and the US collaborators where this interaction occurred. The Lake Frome and Mount Fitton sites had particular use in the initial three months early checkout investigations by TRW Inc. as they worked to deliver the instrument for use by the SVT. The activities and outcomes from the sites are presented in this report in the following sections. If further information is needed, people should contact the site representative whose name is in **Bold** in Table 1.3-2. Email addresses are listed at the front of the report. The data acquisition and management is described below and the nominated person to contact is indicated in that section or they can be contacted via the site contact person.

Table 1.3-2: Site Investigators and Collaboration (Site contact in **Bold**)

Site	Australian Participants	US Collaborators
Lake Frome	Dean Graetz **Susan Campbell** Jenny Lovell Edward King David Jupp	Jay Pearlman, TRW Inc. Pamela Barry, TRW Inc. Others at TRW Inc.
Lake Argyle	Dean Graetz Susan Campbell **Jenny Lovell** Edward King Tiit Kutser	
Coleambally	**Tim McVicar** Tom Van Niel Bisun Datt David Jupp	Jay Pearlman, TRW Inc. Pamela Barry, TRW Inc. Liang Shunlin, UM Fang Hongliang, UM
Tumbarumba	**Nicholas Coops** Alex Held Bisun Datt	Mary Martin, UNE Marie-Louise Smith, UNE Scott Ollinger UNE
Moreton Bay	Arnold Dekker **Vittorio Brando** Scientists at UQ	
Cape Tribulation (1) Cairns Reef	**Tiit Kutser** David Jupp Scientists at AIMS	
Mt Fitton	**Tom Cudahy** Jon Huntington Melissa Quigley	Pamela Barry, TRW Inc.
Panorama	**Tom Cudahy** Jon Huntington Melissa Quigley	
Kunoth (Alice Springs)	**Vanessa Chewings** Geoff Pickup Gary Bastin	Melba Crawford, UTA
Cape Tribulation (2) Tropical Agriculture	**Alex Held** Armando Apan (USQ)	
Uardry	**Fred Prata** Graham Rutter	

Abbreviations for US affiliations are University of Texas at Austin, UTA; University of New England, UNE; University of Maryland, UM; US Department of Agriculture, USDA. TRW is the name for the merger of Thompson and Ramo-Wooldridge Corporations in the 1960's. For the Australian affiliations, UQ is the University of Queensland, USQ is the University of Southern Queensland and AIMS is the Australian Institute of Marine Science.

The opportunity to use the EO-1 and ancillary data from a number of the sites for research exists and the available data opportunities are listed on the CSIRO EOC web site at (http://www.eoc.csiro.au) under Hyperspectral/Australian Science Validation Team/Data Collections. At this time, ancillary data from Lake Frome, Coleambally, Tumbarumba and Kunoth are available. It is hoped to make more data collections such as these available for training and research to enable people to learn about, explore and use Hyperion data. A number of the sites also contributed image and ancillary data to the CSIRO EOC led Training Workshop for Hyperion data. The contents of the EOC Hyperion Workshop are available on two CDs for moderate cost.

1.4 Summary of findings from the Australian activity

1.4.1 Instrument performance and pre-processing

1.4.1.1 The development of Level 1R Hyperion data

The SVT took on assessing the performance of the EO-1 instruments after the instrument teams handed over the data stream to NASA. The handover occurred 3 months into the mission. The data processing path continued to be refined for each instrument as calibration and validation studies established new issues to be resolved. The Hyperion instrument data were refined over the first year of the mission and by the end had stabilised to a well-calibrated and high quality data set within the limitations defined by its technology and its specifications. At the time of the Extended Mission, when NASA acquisition operations were transferred to the USGS and the data made available to the wider public, the Hyperion data delivered by USGS were designated as Level 1R.

The work done by the instrument teams and scientists of the SVT to reach this Level was extensive and of high quality. In this aspect the EO-1 mission was highly successful and particularly so with regard to the Hyperion and ALI instruments. The Australian calibration and validation sites – as well as application sites – were instrumental in that evolution. Of particular mention are the roles played by the findings from field studies at Lake Frome, Uardry, Coleambally and Mount Fitton. In this report the main focus will be on issues and effects that remain in the Level 1R data and the recommendations of Australian scientists of how to deal with them and how they may limit applications. In future space missions that are based on similar push-broom technology, it is likely that many of the issues faced in the first two years of the EO-1 mission will need to be resolved either prior to launch or within a short check-out phase at the beginning of the mission.

Good summaries of the effort in this period and of the establishment of the instrument performance are to be found in Pearlman *et al.* (2003). However, because they will be relevant as background to the next section it is useful to note that there were many significant data-modifying processing steps between Level 0 and Level 1R. These include bad band and bad pixel handling, echo, smear and dark current correction, absolute and uniformity calibration improvements based on vicarious and on-board methods, data formatting and stabilisation and geometric modifications such as the VNIR/SWIR shift.

Perhaps the main area left out of the development of the standard Level 1R processing was geo-rectification. Most investigators were very satisfied with the geometric fidelity of all of the EO-1 instruments as well as the accuracy of pointing information. For most sites and research efforts it was also not a big problem to obtain a few good ground control points (GCPs) and bring the image(s) into alignment with maps and other data. However, for world-wide operations the data will really need ephemeris-based geo-rectification as has been demonstrated (for example) with the NASA TERRA satellite. In their conclusions following their efforts at operational processing as part of the Extended Mission, Jon Huntington and Melissa Quigley (Section 5.2 The Geoscientific Data Buy) in one of their conclusions state "*The lack of georeferencing of the Hyperion data, without having to resort to an external reference, is a disadvantage to operational users familiar with integrating data from disparate sources in a GIS, particularly where good quality maps do not exist*". This is a major operational need for a satellite based hyperspectral sensor.

The processing operations to Level 1R certainly provided good quality data but also left or added some spectral and radiometric effects that have been noticed by all scientists applying the data to their problems. It is these remaining spectral effects that we will focus on here.

1.4.1.2 Remaining scene-dependent effects

Taking the Level 1R data as base it is significant that every Australian group involved in Hyperion applications found it necessary to address and resolve a number of key remaining issues in the data. A strong point of the Australian effort was the diversity of sites and applications that were pursued – plus the interaction among these different approaches that occurred through the CSIRO EOC. Based on the collective experience of the scientists it is possible to develop a recommended pathway – or options for a recommended pathway - for data pre-processing that usually needs to be followed before they are used in applications. The steps tend to be somewhat different for different land covers and applications but have a commonality that is valuable to bring together out of the work reported by the Australian members of the SVT. Their conclusions are useful for people intending to use Hyperion as well as people designing or building future hyperspectral missions from space.

1.4.1.2.1 Outlier detection

Even after processing to Level 1R, there seem be a relatively small but still significant number of pixels in Hyperion images for which the values are highly anomalous. The cause of these "outliers" is not known. However, their presence can affect the statistics used in other data processing steps and it is best to remove them by some form of outlier detection and fixing.

The CSIRO Mineral Mapping and Technology Group (MMTG) developed a number of standard algorithms for their work and these were made available to other CSIRO scientists working with EO-1 data. As described by Cudahy (Sections 3.6 Mt Fitton and 3.7 Panorama) and Huntington and Quigley (Section 5.2 The Geoscientific Data Buy) the use of a "pixel plugger" that locates anomalous cells in the data cube and fills them has been found essential in their work. Similarly, Datt *et al.* (Section 3.2 Coleambally

and Datt *et al.*, 2003) have described the need to remove such pixels to ensure that the "de-streaking" process (described below) does not make the vertical "streaking" worse instead of better. In the Coleambally work, and in the Hyperion Workshop run by EOC a local median filter technique was used to detect and remove such pixels.

Given the harsh space environment in which the instruments must operate, it is likely this will remain an activity pursued by users in the future. Since different noise levels and different spectral areas are involved in different applications it is likely that this operation will also take into account the end-use of the data and its products.

1.4.1.2.2 Streaking/striping

A number of Australians investigated the effect known as "striping" or "streaking" in the vertical direction that was visually obvious in all Hyperion data. Every Australian activity eventually had to take action to reduce its effects – in many cases using software provided by others but with settings dependent on the application.

The Hyperion data are sensed by "push-broom" technology in which 2D detector arrays (two in the case of Hyperion) are used to record image data. The images are created by the fore-optics spectrally dispersing a slit of data (a single image line) onto the arrays such that one dimension of the array records wavebands and the other the pixels of an image line. An image of the earth's surface is formed as the imaged slit moves forward with the forward motion of the satellite.

If one detector of an array has a slightly modified or unbalanced responsivity from that of its neighbours or from its normal condition, the result is a vertical "stripe" or "streak" in the corresponding band of the image data. If the difference is persistent, the effect can be reduced or eliminated by "fine tuning" the calibrations which are normally different for each detector each array. For Hyperion this was initially done prior to launch and then refined through use of the internal lamp and solar calibration facilities. Over the period of the SVT there were significant improvements in both absolute and uniformity calibration made through these methods as well as by using targets on the earth's surface (Pearlman *et al.*, 2003). In this process, the large, uniform fields of the Coleambally site (see Datt *et al.* Section 3.2 Coleambally) were used to good effect.

However, it became clear that there was a residual of streaking in the images that was not persistent but was significant and had to be treated in a scene-dependent way. In common with similar effects found in previous satellites and in airborne data the methods used were based on matching the statistics over some or all lines of the image of the anomalous detector and either a reference set of detectors or all other detectors in the image line for the same waveband (or row of the array). This approach is then similar to methods used in the past to balance horizontal stripes in mirror scanner images by histogram equalization (Horn and Woodham, 1979), to flatten images affected by limb brightening or to balance detectors in airborne pushbroom sensors (Goetz *et al.*, 1985).

The first thing that became apparent from the work of the different groups was that the streaking effects had different characteristics in the VNIR and SWIR arrays as illustrated in Figure 1.4.1 This Figure is taken from an example used in a PowerPoint

report given by David Jupp to the SVT in 2002[2]. Since these data are generated from separate detector arrays, which utilise different detector materials, this is no great surprise.

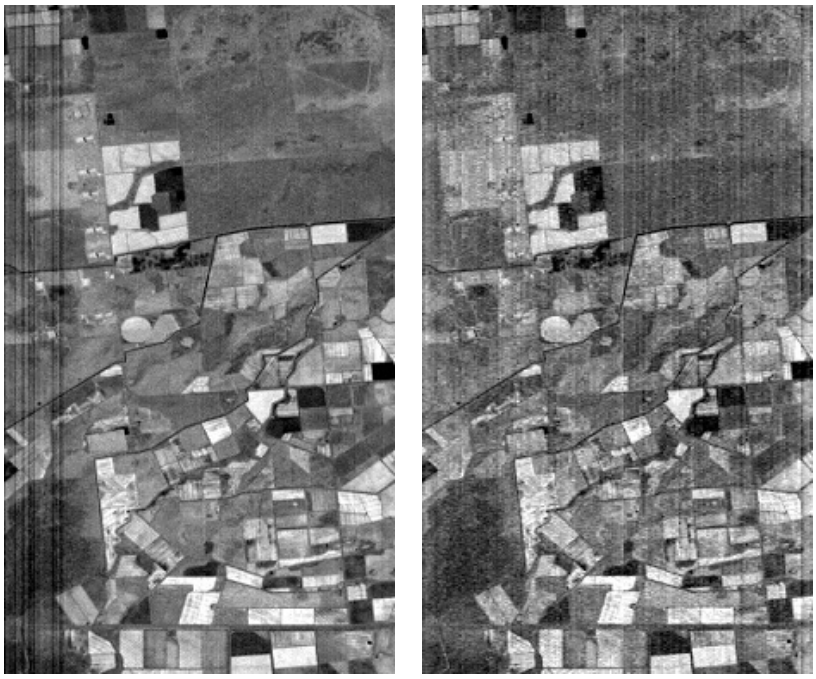

(a) (b)

Figure 1.4.1 Column Streaking in Hyperion (a) in the VNIR and (b) in the SWIR

Cudahy and Barry (Section 3.6 Mt Fitton), working primarily in the SWIR region for mineral mapping, used the method of matching the pixel mean and variance over the full column of data to the "global" mean and variance over all pixels and all lines for the band to correct for SWIR streaking. The correction factors involved an additive offset and a multiplicative gain. Their report (Section 3.6.3 Study 2 - Assessment of the stability of the SWIR module) includes a detailed study of the way in which the correction factors varied with length of the data record and how they varied over time. Both of these were significant but the method – provided that the data record had enough lines for the statistics to stabilise – still proved effective for the minerals work. The software that implemented this work is part of the MMTG toolkit mentioned previously as was used by Huntington and Quigley (Section 5.2 The Geoscientific Data Buy) as a standard pre-processing step for their work.

In the work reported from the Coleambally site (Datt, Section 3.2 Coleambally) the VNIR array data were much more important. The use of gain and offset correction in the SWIR using whole image mean and variance (called the "Global" approach) as had been used by Cudahy and Barry seemed initially to provide an effective correction but when it was applied to both arrays it was found that significant systematic effects were removed that were not related to streaking noise. This is reported in Section 3.2. To overcome this problem as well as to separate out issues of streaking from another systematic effect in the VNIR called spectral "smile" they developed an approach of

[2] Jupp, D.L.B. "Australian EO-1 Report: One year on – Applications and Experiences," SVT Meeting, Goddard Visitor's Center, MD, April 23-26, 2002.

"Local" de-streaking in which the statistics were based on a close set of neighbours of the anomalous detector rather than all pixels in the extent of the image line (Datt *et al.*, 2003). By selecting different widths of neighbourhoods in the VNIR and SWIR they were able to achieve good results for their application.

The main problem for the Global approach seems to reside in the makeup of the image and the distribution and brightness of the different land covers. This can obviously change with wavelength and so the Global method applied to a variable image or with too short a run of image lines can lead to unwanted spatial and spectral modifications in the data. On the other hand, not all vertical streaks are individual and isolated detectors but often involve blocks of detectors that seem to be anomalous but correlated. A Local method can have trouble fixing such cases. The fact that blocks of varying calibration seem common in the SWIR shows why a more "Global" approach works well with data in that array. Modulating the neighbourhood widths, applying different neighbourhoods to different band groups and carefully checking the difference images between unprocessed and processed images can, however, usually achieve good results for an application.

Among the groups working with water covered targets (Brando and Dekker, 2003 and Section 3.4 Moreton Bay and Kutser, Section 2.4 Lake Argyle) residual dark noise and low signals brought out different effects again from those found among relatively bright land covers or the SWIR array effects. Some of the effects are described and illustrated in Sections 2.4 and 3.4 and generally they found that if the de-streaking statistics were developed over areas of both water and land, the results were very poor over at least one of the major covers. They also found that additive (or offset) corrections were needed and that using multiplicative gains (variances) gave poor results. The fact that residual systematic effects due to array structure and dark current processing needed to be removed led to the use of additive Global methods by preference with the statistics being collected over areas of water that were as homogeneous as possible. It was also generally found that the corrections so obtained gave poor results if applied to land areas and land-cover "masking" proved essential to provide acceptable user-oriented products.

The streaking effect is significant in Hyperion data and needs to be addressed. Pearlman *et al.* (2003) discuss some of the technical bases for streaking and residual array effects and there are some options for reducing them in future instruments. However, such streaking is still likely to exist to some degree and be significant for applications in any similar (pushbroom) technology that is used in the future. Since it is a noise effect, having instruments with improved SNR should make it less of a problem and most likely make the job of balancing the remaining effects with software easier as well. However, having a flexible toolkit allowing Global or Local, additive, multiplicative or mixed corrections and capacity to develop statistics within a nominated region and apply corrections in other regions seems to be essential. Ultimately the needs of the application decide the best approach. The most important common need for the processing is that the effects of streaking be reduced *without sacrificing the spectral integrity of the data*.

1.4.1.2.3 Other array and digitisation effects over water

In the applications based on water covered areas as listed above in regard to de-streaking (Brando and Dekker, 2003 and Section 3.4 Moreton Bay and Kutser, Section 2.4 Lake Argyle) there were also residual array effects that were systematic and near the additive dark noise level but which are a problem for applications over the darker water covered target areas. The applications involved are important in future hyperspectral missions and so the particular issues the work has raised will be discussed in some detail.

The background to some of the effects is discussed in Pearlman *et al.* (2003). They arise because the VNIR detector array has four sub-arrays (the four quadrants defined by bands 1-35 and 36-70 and pixels 1-128 and 129-256) that are used in slightly different ways and seem to have varying noise structure. For most non-water applications, the residual effects are near the base noise level and do not affect the processing. However, over water the situation changes and one of the Figures from Section 3.4 (Moreton Bay) is repeated here to provide a visual demonstration of some of these effects. In particular, it includes the "Quadrant D" noise on the right of the image as reported by Pearlman *et al.* (2003).

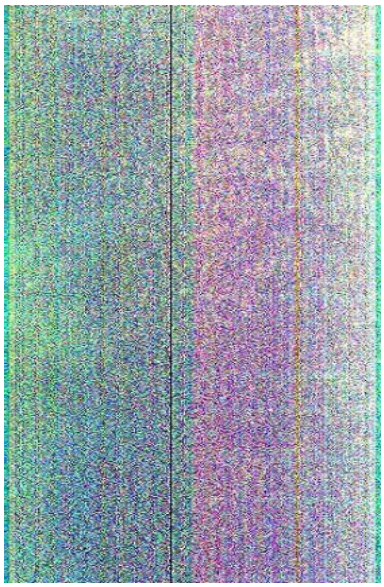

Figure 1.4.2: "Homogeneous" ocean data from Hyperion.

In addition to these effects, (Kutser, Section 2.4 Lake Argyle) has provided evidence of an effect also noticed by other Australians in which a "mirror" image of bright (or dark) areas is seen across the line of pixel 128 (Figure 2.4.7). The cause of this is not known (although it is possibly a form of "smear") but some approach to its modelling would greatly benefit applications to water covered areas. (Brando and Dekker, 2003 and Section 3.4 Moreton Bay and Kutser, Section 2.4 Lake Argyle) have managed to overcome the problem for their specific applications but their solutions (using the de-streaking tools) are still scene dependent.

The dark, water covered areas also provide examples of where image histograms show a very "spiky" behaviour. The data must be smoothed over local patches to reduce the effect. Vittorio Brando showed examples of the effect at the SVT Meeting in Buenos Aires[3]. The effect is obviously magnified by the small range of image values over the water covered areas but the processing is affected by the "spread" of the effects into clusters of values. Figure 1.4.3 shows the effect in (a) three bands at the blue end of the spectrum that are not, in fact, delivered in Level 1R data but were of great interest for people analysing water-covered areas and (b) three bands in the NIR. Vittorio Brando presented both of these graphs at the SVT meeting.

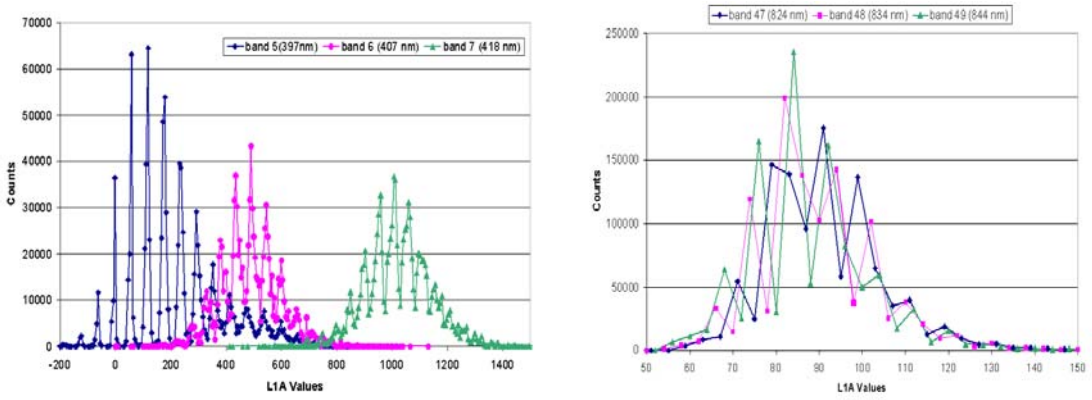

(a) (b)

Figure 1.4.3 Hyperion Level 1 data histograms over water-covered areas (a) in bands 5,6,7 and (b) in bands 47,48,49.

The cause for the effect lies primarily in the chosen dynamic range and discretisation used for the data recording and in its subsequent processing. Level 0 (satellite recorded) Digital Numbers (DN) are in the range [0,4095] (or 12 bits) and are then directly calibrated to $W\ m^{-2}\ sr^{-1}\ um^{-1}$ using detector dependent gains. The data are then re-scaled by a factor of 40 in the VNIR and 80 in the SWIR before being rounded to integer data to provide the image Digital Numbers (DN').

The resulting factors are shown in Figure 1.4.4 where the value represents the change in DN' in the image for a change of 1 DN in the recorded data. The graph shows average values for each band but these also vary across an image line due to inter-detector differences. Since high values of the gains in Figure 1.4.4 also represent low SNR performance (a statement that has been demonstrated vicariously by Brando and Dekker (2003), few of the bands with gains greater than 10 are used in the processing at most land sites but those in the blue-green region are of great interest for water-covered areas and are often retained for those applications for their potential value rather than their performance.

[3] V. E. Brando, A. G. Dekker, J. Anstee, N. Pinnel, A. Held. "Preliminary multitemporal assessment of the performance of Hyperion in coastal waters. Cal/ Val activities in Moreton, Bay, Queensland, Australia," *EO-1 SVT Meeting*, Buenos Aires, 6-8 November 2001.

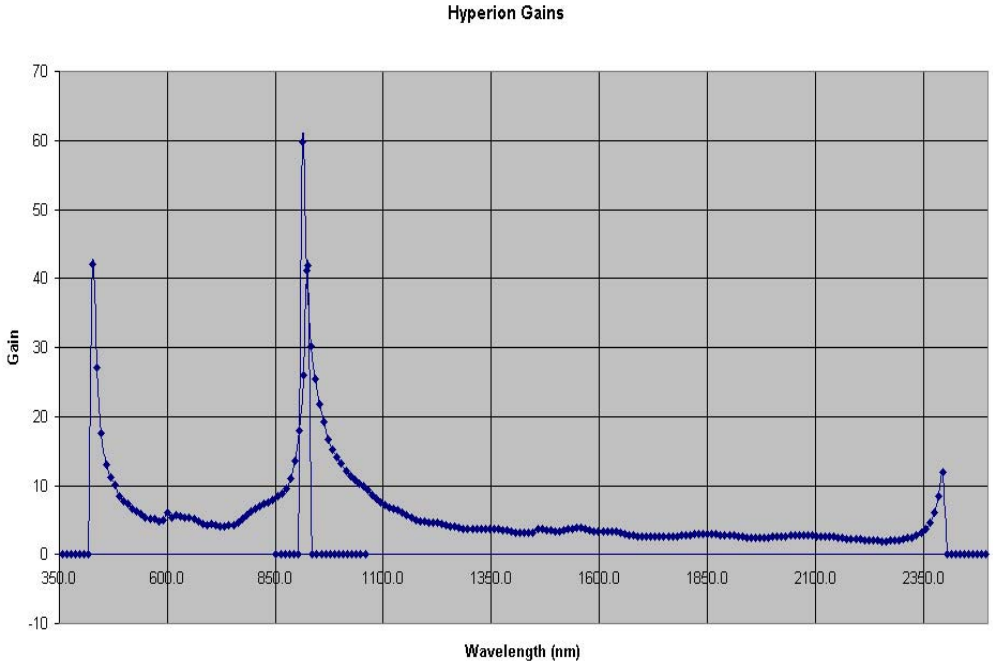

Figure 1.4.4: Hyperion gains expressing number of image DN' for one DN change in the recorded data. High values generally mean low SNR.

Calculating the predicted step between the image values shows that at the blue/green end of the spectrum over water where the image DN' range is still small, there are many "missing values" (the step is more than 50 DN' in bands 5,6,7 and 8 DN' in bands 47,48,49) but a combination of the different gain between detectors and the dark current and other corrections to the Level 1R data leads to these being "uncommon" rather than "missing" as illustrated in Figure 1.4.3. This separation occurs for two reasons. Firstly, the dynamic range of Hyperion is specified to 120% albedo without saturation (Pearlman *et al.*, 2003) so that the variation in the water is covered by only a few recorded DN values. Secondly, the low detector responsivity in the blue/green leads to the few DN values being expanded by a large amount. It follows that if water targets are seen as important for future hyperspectral sensors, there will have to be both higher SNR in the blue-green region and some trade-off developed or alternative technology investigated to serve different applications with minimal loss in precision. Alternative technology could include doping of the blue-green materials, use of nonlinear responsivity or programmable gains.

For water covered areas, there is clearly a need for future sensors to undertake very careful studies of SNR and dynamic range requirements and for the process of monitoring the dark current and modelling the array effects to be given significant and sufficient attention. Hyperspectral remote sensing of water covered areas for water quality and benthic mapping is a major area of potential applications that needs particular attention in sensor design and implementation.

1.4.1.2.4 Spectral "smile"

A systematic effect that has been noticed in Hyperion processing and applications involves problems in the spectral alignment of the VNIR array. It has been called spectral "smile" since its consequence is that the central wavelength of a band varies with spatial position across a line in a smoothly curving pattern (see Figure 1.4.5(a)). However, since the peak of the curve in Hyperion tends to be near the middle of the line it could perhaps be better called (and for more than one reason) spectral "frown".

As described by Liao *et al.* (2000), TRW used their instrument facility in the pre-launch period to measure how the spectral and spatial variation of the radiation as it is projected onto the focal plane array(s) (FPA) matches the rectilinear grid of the physical pixels of the FPA. They found very close to rectilinear behaviour in the spatial dimension and in the spectral dimension of the SWIR array. However, in the spectral dimension of the VNIR array they detected a variation of up to 2.7 nm. For reasons that may have involved the time-critical nature of the Hyperion integration and deployment on EO-1 and/or the changes in alignment needed to the original Lewis design, it was decided to characterise the effect rather than re-align the dispersed slit on the VNIR FPA.

As discussed by Cairns *et al.* (2003), given time and budget capacity it should be possible to have almost no spectral or spatial mis-alignment. However, if it cannot be avoided or if changes occur during instrument integration or during launch it may well have to be overcome by software if it is significant enough to affect applications. FPA alignment therefore needs to be carefully measured both pre- and post-launch. Goetz and Heidebrecht (1996) described a less severe effect for HYDICE data but their comments and findings have some relevance for Hyperion as well.

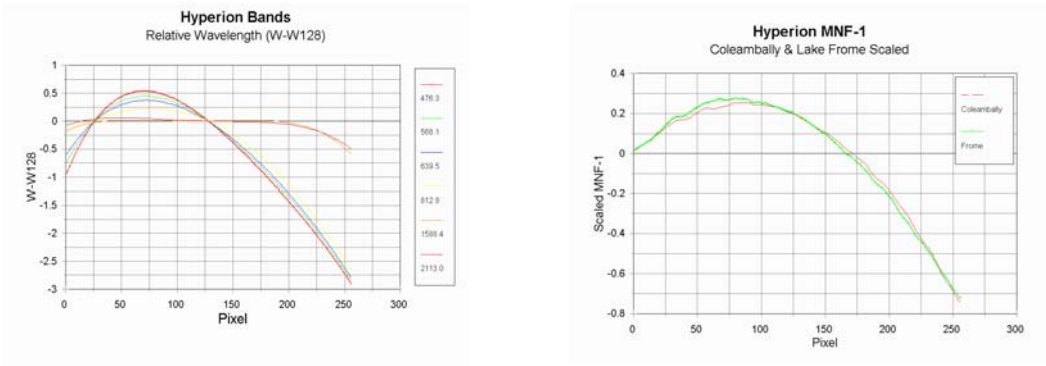

(a) (b)

Figure 1.4.5: (a) Relative spectral variation across Hyperion lines. (b) Mean MNF-1 for Coleambally and Lake Frome.

Pearlman *et al.* (2003) describe how the measurements described in Liao *et al.* (2000) were used to develop polynomial models for the "smile" over the 256 pixels for each band. The models were based on 25 points in each of the VNIR and SWIR arrays being 5 band and 5 pixel positions. Each polynomial was linear in the spectral dimension and quadratic in the wavelength dimension. The smooth curves of Figure 1.4.5(a) are the result of this modelling.

A variation of 2.7 nm does not seem to be a serious variation when the wavelength step is about 10 nm and the FWHM widths of the bands are also about 10 nm. In the VNIR, where earth surface materials generally have smooth spectra, a "smile" of this size will not cause a serious variation in the earth surface spectra. However, as discussed by Cairns *et al.* (2003), for the highly variable and sharp "spikes" that characterise many atmospheric spectra a variation of FWHM/100 or 0.1 nm can be significant. It is therefore important to take the smile into account if radiance spectra are being used that include atmospheric features or if the data are being atmospherically corrected. The "account" includes knowing the "smile" model to within a high level of accuracy.

Soon after the start of the EO-1 mission, scientists in Australia and the US had noticed a brightness variation in MNF (Green *et al.*, 1988) transformations (normally as MNF-1) of Hyperion data that had the same shape as the "smile" models. Section 3.2 (Datt *et al.*, Coleambally) provides examples in Figure 3.2.4, Figure 3.2.5 and Figure 3.2.6. The variation was found to have a consistent shape for images of widely different cover types and over time at any single site. Figure 1.4.5(b) shows graphs of the consistent relative variation of MNF-1 across the lines of two very different examples of agricultural fields and a Salt Lake.

Jupp *et al.* (2002) showed how the MNF transformation was creating the variation through loadings that simulated "derivatives" across sharp atmospheric features in the VNIR. The variation can be easily reproduced if you image the difference between Bands 40 and 42 (one each side of the Oxygen-A feature at 760 nm). Jupp *et al.* (2002) also showed how even after atmospheric correction the "smile" effect was still MNF-1 and that it could affect the spatial integrity of the Red-Edge transformation at Coleambally. They showed that among options for its removal only wavelength interpolation, in which the smile is "removed" from each vertical column by interpolating to a standard set of central wavelengths prior to atmospheric correction, could reduce it and maintain spectral integrity.

Unfortunately, interpolation was unable to remove all of the "smile" effect – just to reduce it. Also, many people are averse to modifying the radiance values prior to atmospheric correction. There was a great deal of discussion about how to "live" with the "smile" in the US and Australia and most people have worked without a specific correction in place. The good points for the situation are that:

- It is only significant in the VNIR. The SWIR has little to no "smile" effect; and
- It only affects indices, ratios or derivatives near to sharp atmospheric features or the residuals from such features after atmospheric correction.

However, the down-side is that:

- It increases the amount and intensity of residual atmospheric features in atmospherically corrected data; and
- It is a problem around the Red-Edge and liquid water regions, which are significant for vegetation analysis.

Work is still in progress involving the "smile" effect. Qu *et al.* (2003) describe modifications to the HATCH atmospheric code so that the resulting HATCH-2D can atmospherically correct each column separately. In principle this should overcome much

of the problem. However, it has not been found to provide a satisfactory solution for "smile". The likely problem is discussed by Green *et al.* (2003) and Cairns *et al.* (2003) who show how the measured "smile" based on spatial variations in the position of the Oxygen-A feature does not match the pre-launch "smile" (polynomial) model by up to 1 nm. It is also not yet clear at what stage the difference occurred although, as reported by Pearlman *et al.* (2003) it may have occurred during integration into EO-1 at GSFC prior to launch. Since most of the correction methods need an accurate (down to 0.1 nm) "smile" model as input this seems to have presented a problem that is yet to be resolved.

At this time most people have attempted to reduce the residual effects in atmospheric correction by some form of smoothing and only resort to an attempt to "correct" for "smile" if it significantly affects their results. One example of this was provided in Jupp *et al.* (2002) for the Red-Edge. In many other cases it seems to have little effect. Perhaps the main conclusion is that in the build of future sensors, sufficient time and resources need to be allocated so that sensors are launched without spectral "smile". It seems to be very difficult to overcome the effects later using software and the issue is best avoided from the start by aligning the hardware.

1.4.1.2.5 Atmospheric correction

A significant change in hyperspectral processing occurred in parallel – and quite likely stimulated by – the Hyperion mission. This change came about with the rapid maturity of a number of commercial and available software systems for atmospheric correction of hyperspectral data. Correcting the limited quantities of airborne hyperspectral data available prior to this time seemed to be something only specialists tried. However, in recent times the ENVI[4]-based modules ACORN™ (Atmospheric COrrection Now, see http://www.aigllc.com/acorn/intro.asp) and FLAASH (Fast Line-of-sight Atmospheric Analysis of Spectral Hypercubes, see Cooley *et al.*, 2002) have became commonly used. In addition to these ENVI-based modules, the direct use of MODTRAN-4 (Adler-Golden *et al.*, 1999; Matthew *et al.*, 2000) and 6S (Second Simulation of the Satellite Signal in the Solar Spectrum, see Vermote, 1997) for the task became well documented and HATCH (High-accuracy ATmospheric Correction of Hyperspectral data, see Goetz *et al.*, 2003) and its Hyperion version called HATCH-2D (see Qu *et al.*, 2003) as well as the code developed by Cairns *et al.* (2003) became provided useful challenges for the existing software with their findings.

Because of this change, all of the work described here used atmospheric correction to surface reflectance as part of the processing. Coops (Section 3.1 Tumbarumba), Chewings and Bastin (Section 3.3 Kunoth), Cudahy *et al.* (Section 3.6 Mt Fitton and Section 3.7 Panorama) and Huntington and Quigley (Section 5.2 The Geoscientific Data Buy) all used the ACORN™ software to correct to ground spectral reflectance. Brando and Dekker (Section 3.4 Moreton Bay) used a water application oriented front-end to MODTRAN-4 both for the extra tools needed for water modelling and because FLAASH and ACORN™ had problems or limitations over water covered areas. Kutser's work (Section 2.4 Lake Argyle and Section 3.5 Cape Tribulation – Coral Reef Studies) used MODTRAN-4 directly for similar reasons. Prata (Section 2.3 Uardry) used MODTRAN-3.7 to estimate top of atmosphere radiance for validation. Datt *et al.*

[4] Hyperspectral image analysis software from Research Systems Inc. Boulder, Colorado.

(Section 3.2 Coleambally) used and compared a number of packages but mainly used FLAASH or (in some specific cases) MODTRAN-4 as will be discussed below.

Despite this wide level of acceptance and application, atmospheric correction is still not free of the need for specialist attention and the many and diverse environments imaged by Hyperion have challenged the best of the codes with its interplay of noise, "smile" and the varying needs of the applications. However, the situation seems to have changed forever and for the good of all users. As discussed above in the context of the spectral "smile" that remained in Hyperion, Cairns *et al.* (2003) noted that when atmospheric effects need to be removed, the required accuracy for the band centre might need to approach 1/100 of the width of the bands. For Hyperion this would mean 0.1 nm, which was clearly not achieved. A design goal of 0.5 to 1.0 nm may still have been achieved and such levels of accuracy seem to provide good atmospheric corrections when aerosols and water vapour are low.

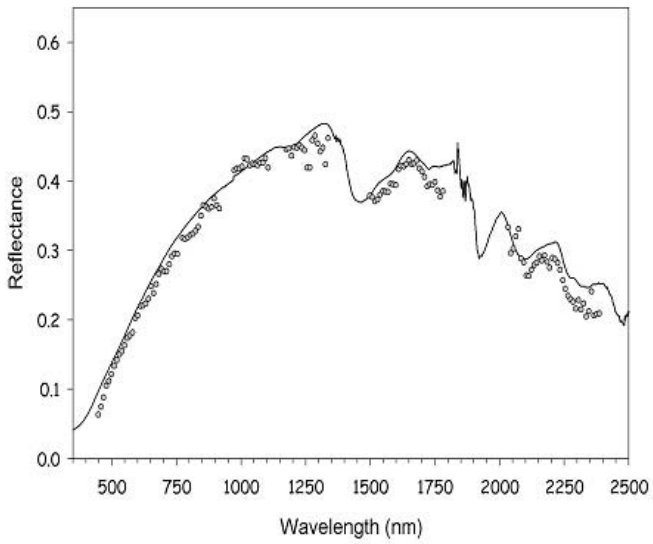

Figure 1.4.6: Atcor Comparison between field data (solid line) and FLAASH-corrected Hyperion data (circles).

The value of seeking maximum accuracy is illustrated and studied by Huntington and Quigley (Section 5.2 The Geoscientific Data Buy) who point out the difference in performance obtained if the nominal band centres used in Level 1B data (the central wavelengths at pixel 128) are replaced by the average of the central wavelengths over 256 pixel. The variation is due, as explained previously, to Hyperion's spectral "smile". The average centres are used in Level 1R released by the USGS and provide less noisy results.

Figure 1.4.6 shows the result of correcting Hyperion at Coleambally (Section 3.2 Coleambally) using the AFRL FLAASH software compared with an average soil spectrum for the same area measured with an ASD spectroradiometer that was mounted on a quad-bike for spatial coverage at Hyperion scale. The FLAASH program estimates

the overall level of aerosol needed and the amount of atmospheric water vapour for each pixel. There are a number of variations between Hyperion and the ground data but the result provides good validation for the low aerosol and low water vapour case. In Figure 1.4.6 some of the residual variations have been removed through only selecting "stable" bands after atmospheric correction. Unfortunately, this also reduces the potential extent of coverage of the spectral data for agricultural applications. The selection is especially limiting near to 2000 nm and around the liquid water bands for vegetation with centres at 980 nm and 1200 nm and a useful inflection in between.

The issue faced by Brando and Dekker (Section 3.4 Moreton Bay) and in the work reported by Kutser (Sections 2.4 Lake Argyle and 3.5 Cape Tribulation – Coral Reef Studies) was that pixel-based correction for atmospheric water vapour tended to fail badly over the water-covered areas. The FLAASH software does not allow this option to be by-passed (although ACORN™ does) and consequently MODTRAN-4 was used directly to control the column water vapour and its profile. A significant contributor to the problem was the need to use the large water vapour band near 1150 nm rather than the band near 950 nm to estimate the atmospheric water vapour. The performance of the array materials in a region including 950 nm and 980 nm was not good enough to allow its use for either atmospheric water vapour estimation (near 950 nm) or liquid water estimation (near 980 nm). The SWIR bands near 1150 nm are extremely noisy over water and also over inland lakes and irrigated fields. For fully water-covered areas, a pixel-based correction may be possible with careful use of the small water vapour bands near 730 nm and 790 nm.

The scientists working at Coleambally (Datt *et al.*, Section 3.2 Coleambally) compared a number of software systems including FLAASH, ACORN™ and MODTRAN-4 with field data and found only a few major differences among the cases used. Among the differences that did exist it was clear that the improvements to the water vapour transmission model described by Matthew *et al.* (2000) needed to be incorporated into models other than FLAASH and there is a future need for all models to handle the interactions between CO_2 and water vapour absorption near 2000 nm as successfully as Qu *et al.* (2003) have in their HATCH code. Goetz *et al.* (2003) also validated their HATCH software using this site with its carefully measured ground based data. It is not clear whether HATCH achieved its results through attention to multi-species absorption or by locally adjusting the band centres. Both may be important options in future operational systems.

Following atmospheric correction of some 15 images over two growing seasons at Coleambally it is possible to reach a number of conclusions for future developments in this activity. Combined with the findings from other Australian sites they may be summarised as follows:

- The interaction between CO_2 and water vapour absorption near 2000 nm was a major problem for atmospheric correction methods other than HATCH. All of the current vendors need to incorporate methods similar to those described by Qu *et al.* (2003) including band centre adjustment.
- The improvements to MODTRAN transmission functions implemented in FLAASH (Matthew *et al.*, 2000) should also be made available to all Modtran-4 and derivative users (including ACORN™).

- There remains significant instability in atmospheric water vapour calculations over water covered areas or even areas with significant cover of water (such as rice or irrigation areas).
- There is still a need for better separation of land cover and atmospheric water vapour and liquid water effects over land. Current use of image smoothing simply hides the problem.
- There is a need for alternative spectral methods to estimate visibility (aerosol) when the popular Kaufmann method is not reliable – especially over areas where water and crop are mixed.
- There is a need for some of the important advances developed for Modtran4.2, FLAASH 4.1, HATCH-3D and for the paper by Cairns *et al.* (2003) in the EO-1 Special Issue to be provided by all commercially available software.

1.4.1.2.6 Spectral Noise reduction

Despite all of the pre-processing described here, it is found that after atmospheric correction has been done the spectra are still generally noisy and that some quite unstable areas exist in the spectra. Many of these effects do not seem to average out over regions and there have been a variety of approaches developed to achieve products that do not show these persistent effects. Among these have been:

1.4.1.2.6.1 Reference spectrum smoothing

If some ground-based spectra are available then they can be compared with the image data. If the residuals are assumed to be "noise" the comparison can provide an additive or multiplicative correction that brings the spectra at known points into alignment.

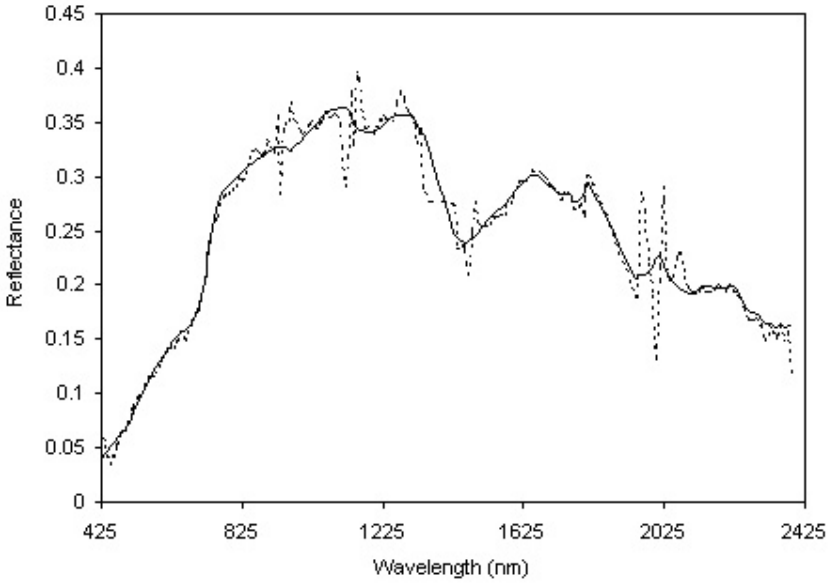

Figure 1.4.7: Fit to Coleambally average data by linear combinations of typical field spectra. Residuals are persistent atmospheric artefacts.

Since these methods tend only to improve the data near to the sites of the field spectra, it can be better to model (say) a regional average by combinations of typical spectra. Again, if the residuals are assumed to be persistent 'noise" a correction can be applied.

Figure 1.4.7 is taken from Datt *et al.* (2003) and shows work done during the Coleambally activity (Section 3.2 Coleambally). It shows a fit to the average image spectrum over the Coleambally site by a linear combination of a wide variety of typical field spectra. There are obvious and persistent residuals associated with atmospheric features. Removing the persistent differences does improve the appearance of the spectra – and provides some improvement near 2000 nm[5]. However, to the extent that these persistent features are due to transmission models or the spectral "smile" it is better to pursue better atmospheric corrections if at all possible.

1.4.1.2.6.2 EFFORT, ACORN and FLAASH polishing

The ENVI-based "EFFORT" spectral polishing (Boardman, 1998) generalises the reference spectrum approach by selecting smooth and smoothed spectral features from the image data from which a kind of wavelength dimension "de-striping" is developed. If field spectra are available they can be incorporated as a "reality boost". It is very commonly used for hyperspectral data and can provide very "clean" spectra.

The ENVI standard EFFORT algorithm and variations on it (including the inbuilt EFFORT polishing available in the ACORN™ software) were used by Chewings (Section 3.3 Kunoth), Cudahy (Sections 3.6 Mt Fitton and 3.7 Panorama), Huntington and Quigley (Section 5.2 The Geoscientific Data Buy) and Held (Section 5.3 Land-Cover Data Buys) as part of their standard pre-processing methods. For example, Figure 5.3.1 in the report by Held (Section 5.3 Land-Cover Data Buys) shows the performance of EFFORT smoothing on a well-defined green sugar cane spectrum.

The FLAASH software also has in-built smoothing for a similar purpose which involves spectral smoothing and "spike" removal rather than reference spectra. Its application certainly improves the appearance of the spectra.

1.4.1.2.6.3 MNF Smoothing

Datt *et al.* (2003 and Section 3.2 Coleambally) used "MNF smoothing" to improve a specific SWIR index. In this approach, MNF bands with (very) low SNR are removed and the data reconstructed only from those with high SNR. If used carefully, (including removing streaks before this is done) the spectral integrity of the data is not significantly affected. The Figure 3.2.8 of Section 3.2 shows a very clear improvement in the SWIR spectrum through this method and makes the use of a derivative based index effective in a way it would not otherwise have been if the data had not been modified.

1.4.1.2.6.4 Band Selection

Datt *et al.* (2003 and Section 3.2 Coleambally) also recommended general band selection as a generic "feature selection" method to improve the results of applications processing (such as classification and spectral matching) by not using potentially noisy

[5] The effect seems to be landcover dependent and so no general post-processing method like the ones described here will fully remove it.

bands. Figure 1.4.8 is repeated from Datt *et al.* (2003) and shows regions of the spectrum where it is likely that atmospheric correction will leave residuals and variations that can "swamp" the information the bands could provide. These regions are also the most sensitive to image "smile" effects on atmospheric correction.

To identify the bands to avoid, Figure 1.4.8 should be used together with Figure 1.4.4, which shows regions that will likely have low SNR in Hyperion due to low spectral sensitivity of the instrument. Low values in both plots equates to a stable band. Based on such considerations it has been proposed that somewhere between 150 and 170 of the Hyperion bands from among both the VNIR and SWIR arrays provide the most stable candidate bands. For example, Coops (Section 3.1 Tumbarumba) reduced the bands used to 162 to provide stability in his forestry application. The Landsat 7 ETM+ bands also lie in the stable areas.

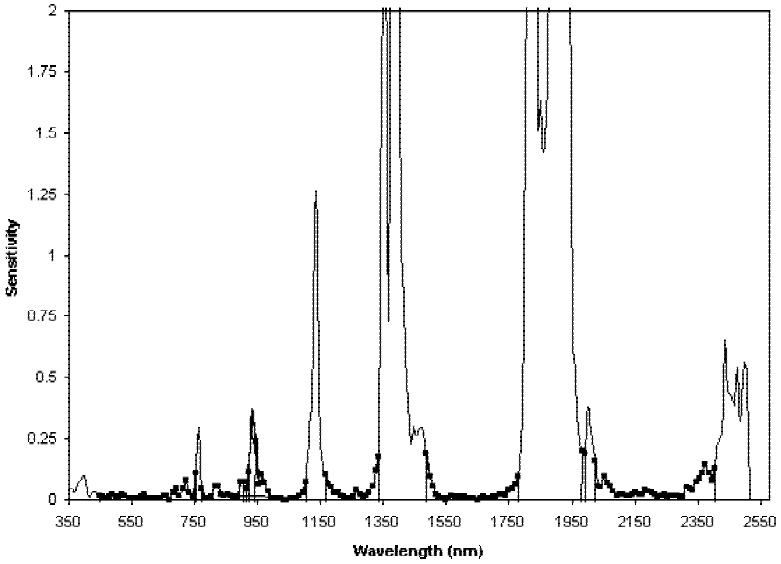

Figure 1.4.8: Stable and unstable areas for atmospheric correction. High values are unstable. Low values are separated from atmospheric features and "stable".

1.4.1.2.6.5Applications oriented smoothing

The main problem with all of the smoothing methods that have been described is that if they are applied generally they can produce smoothed, but biased, spectra and may also remove or lose finer spectral features that are in noisy areas of the spectrum but not impossible to identify and resolve. As a general conclusion it is reasonable to state that none of these methods should be applied unless it is done with a specific application in mind and the trade-off between bias and variance should clearly be evaluated in terms of the objectives of the analysis and the products being sought.

Band selection provides a good example. It is possible to remove some of the bands (even before atmospheric correction) as they have no ground information. The two areas of strong atmospheric water absorption centred on 1400 nm and 1800 nm create bands of this kind. Some imaging spectrometers (such as the HyMap™ scanner, see Section 4.2, HyMap™ airborne Hyperspectral data base) do not sense any data from these areas. Beyond that, however, it is clear that removing the "unstable" bands provides good-

looking spectra. Nonetheless, for a specific application, even noisy bands may need to be retained if they contain vital spectral features. In that case it is the analysis that needs to take account of the noise and define how it should be handled rather than general band selection criteria or by using general spectral "smoothing" that removes the variation near to the important features.

An example of how smoothing can be made a part of the application is in the derivation of indices, such as vegetation indices. Rather than undertake general "EFFORT" type smoothing it is possible to use smoothed (or "regularised") indices. Derivatives of local (and possibly regularised) polynomials that are fitted to the spectrum by least squares in a spectral window are examples of this approach. The window width can be increased to combat the noise level but if it becomes too wide the bias will be too high. The practical situation therefore requires trading off variance and bias separately for each index and region of the spectrum. The extra work can be worth the (lower case) effort.

Because of this it seems better to class the noise reduction and smoothing described in this Section as part of Hyperion applications processing rather than pre-processing. How it fits into the processing of operational hyperspectral sensors in the future still needs some careful thought and decisions and is not independent of the perceived primary applications for the data. We will therefore assume that pre-processing and some decisions about spectral smoothing have been established and focus on the important applications carried out at the Australian sites.

1.4.2 Applications performance

The Australian approach to the EO-1 experiment involved some specialist sites for calibration and validation and considerable research into pre-processing. However, both sites and the motives for the effort invested in pre-processing normally had an application oriented basis. Following the work of the SVT and the early experience of the Extended Mission (in which EO-1 became semi-operational with the transfer of operations to the USGS) it was clear that there are many useful ongoing applications that can be served by Hyperion and many more that will be served by its successors.

The applications described in this report have been grouped under five major categories:

- Agriculture;
- Mining;
- Forestry;
- Coastal and inland waters; and
- Rangelands.

These represent the focus of work that was done at the Australian sites but also cover most of the immediate and future markets for airborne and spaceborne hyperspectral data.

1.4.2.1 Agriculture

The main applications areas involving agriculture are covered in the report on the Coleambally irrigated area (Datt *et al.*, Section 3.2 Coleambally) and the report on work in the north Australian Mackay sugarcane region undertaken during the Extended Mission (Held, Section 5.3 Land-Cover Data Buys). Both of these activities found that pre-processing as described in the above Sections was essential. They have also established that provided such pre-processing is undertaken, there are many potential applications for agriculture from space based hyperspectral information.

The scientists involved at Coleambally (Datt *et al.*, Section 3.2 Coleambally) made a very careful assessment of the pre-processing needs. Their work (see Datt *et al.*, 2003) and software developed for their processing needs and as training tools for the EOC Hyperion Workshop have been used by a number of others for agricultural applications. The scientists working at Coleambally also took on the major task of creating a geometrically accurate, co-registered, spectral reflectance time series for two growing seasons. To allow this to happen, NASA agreed to schedule regular acquisitions of the site that resulted in Coleambally providing the densest and most extensive time series of any of the EO-1 applications sites up until this time.

The provision of accurately co-registered Hyperion, ALI and Landsat data over two growing seasons as atmospherically corrected reflectance data has entailed a great deal of effort and located (and resolved) many issues and difficulties along the way. Its existence shows what is possible and for future missions the task will be to streamline the provision of such data. Space platforms clearly have many advantages for strategic monitoring of agriculture throughout the world. However, they share these advantages with multispectral sensors such as Landsat and ALI (see Liang *et al.*, 2003 for a discussion of ALI improvements over Landsat using the Coleambally site). The key issue to resolve from the data was whether the hyperspectral data provided significant and unique advantages to the time series.

Hyperspectral data can clearly "split" the Landsat/ALI bands and resolve finer spectral features. Based on this Hyperspectral data clearly provide the opportunity to derive many more indices or indicators of crop condition. For example, red-edge methods (described in Section 3.2 Coleambally) based on high spectral resolution can be derived successfully and consistently from Hyperion and match the results obtained from both field spectra and airborne HyMap™ data. The capacity to match Hyperion, airborne and field spectra is key to obtaining value from space data. This is because soil and crop nitrogen, water and fertilizer use efficiency are already measured using laboratory spectra in the NIR/SWIR and extensions to field measurements and airborne platforms are well advanced. The consistency therefore opens up opportunities for mapping nitrogen as well as stress, leaf health and LAI to a level not possible with Landsat or ALI. It is possible because it can be done with the laboratory, ground and airborne hyperspectral data.

Table 1.4-1 has been repeated here from the Coleambally Section 3.2 and lists some of the commonly used and spectrally "hot" regions where finer detail can be readily exploited by hyperspectral sensors – in the laboratory, in the field, from the air or from space for agricultural applications. The match between Hyperion and the near-ground data following effective pre-processing opens many of these regions to space based

mapping. The only limitation is the SNR and other performance factors of the current instrument.

Table 1.4-1 Common spectral features for crops and soils

General Spectral Region (nm)	Indication
400 to 700	PAR region – photosynthetic pigments for species and health
680	Chlorophyll absorption – health and (potential) yield
700 to 750	Red Edge (Chlorophyll and green biomass)
Near 980 and 1200	Liquid Water (leaf) features
1080 to 1170	Liquid Water Inflection feature
1700 to 1780	Leaf Waxes and Oils
2100	Cellulose
2100 to 2300	Soil properties (clays)
2280 to 2290	Nitrogen / Protein

The major current difficulties in applying the indices with Hyperion are:

- The poor performance (SNR, array effects and dynamic range) below about 500 nm and above about 900 nm in the VNIR;
- Low SNR in the two SWIR windows and lack of information above about 2300nm;
- Unstable spectra near to the water absorption areas following atmospheric correction (especially in the instrumental overlap between the arrays near 950 nm and the environmental overlap between water vapour and CO_2 absorption near 2000 nm).

It is therefore important to ensure that future satellite based hyperspectral sensors take into account the needs of agricultural applications if this situation is to improve.

In addition to applications based on established indices, it has been found that a number of weeds can be identified using hyperspectral data due to the way they exploit the crop environment, interact with the crops and to the different combinations of pigments involved in the exploitation. Held (Held, Section 5.3 Land-Cover Data Buys) describes how “Orange rust” seems to be detectable from spectral methods and how the mapping can be achieved at the Hyperion spatial scale. These conclusions also depend on effective pre-processing to achieve consistent results from Hyperion and ground-based survey. Targeted investigations – involving airborne and ground-based spectral studies – can increase the suite of potential applications in specific crop or weed identification in readiness for future missions.

1.4.2.2 Mining

The applications to mining have come principally from the experiences described by Cudahy *et al.* (Section 3.6 Mt Fitton), Cudahy and Quigley (Section 3.7 Panorama) and Huntington and Quigley (Section 5.2 The Geoscientific Data Buy).

The Mount Fitton site (Section 3.6 Mt Fitton) was used primarily for testing and instrument assessment. Its contributions to this area have already been described. However, its role also led to significant outcomes for mineral applications. The pre-launch estimates for the SNR in the SWIR were pessimistic and it was always thought to be a difficult problem for Hyperion to map minerals or use any of the bands in the SWIR window between 2000 and 2500 nm to locate mineral species and map concentrations. At Mount Fitton Cudahy *et al.* determined that *with appropriate pre-processing* and good environmental conditions, mineral spectral signatures can be identified in the SWIR. They reported that dolomite, magnesite, talc, chlorite, tremolite and muscovite could be distinguished and that the white mica shift of up to 12 nm around the 2200nm absorption feature could be measured, reflecting the variation in aluminium cation substitution with iron/magnesium.

Based on the Mount Fitton findings, Cudahy used the Panorama site (Section 3.7 Panorama) to compare Hyperion and HyMap mapping and the application of the processing to currently active areas of exploration. In a report to the SVT, Cudahy concluded that (given appropriate pre-processing):

- Hyperion can be mineralogically interpreted;
- It can be used to generate coherent mineral maps;
- It can map subtle chemical-spectral shifts;
- It is consistent with field and airborne data;
- It allows the mapping of hydrothermal alteration systems.

However, it was equally clear that poor SNR at wavelengths greater than 2300nm impedes the reliable detection of many useful mineral suites[6]. This provided a major limitation for Hyperion mineral mapping applications.

Huntington and Quigley (Section 5.2 The Geoscientific Data Buy) report on a pilot "operational" use of Hyperion data to deliver products to mining and geological users. This occurred as part of the Extended Mission. There were pertinent experiences from their work that complement the scientific findings of Cudahy. Some have been discussed previously but the following are worth quoting in the context of this summary:

- "Hyperion data are not yet adequate to reliably and routinely map minerals whose diagnostic features are beyond 2300 nm, where the signal quality drops-off substantially. Exceptions to this have been demonstrated for bright and very strong absorbing minerals, such as talc, where these are very well exposed, and also other situations where rocks and minerals form large areas from which average signatures can be computed that reduce noise levels".

- "There is an "optimum" hyperspectral scene for geological use. It is often heard that geologists just need any scene, as the geology never changes. This is a fallacy, as it is the *expression* of that geology that changes with season, ground cover, lighting conditions and atmospheric conditions. Service providers therefore need to be aware of user needs for this optimum scene in their scheduling and business transactions."

[6] [Hyperion SWIR array responsivity drops away quickly after 2300 nm as shown in Figure 1.4.4 as does atmospheric stability as shown in Figure 1.4.8 (ED)]

Despite the limitations, the mineral processing reported in this document and in the paper by Kruse *et al.* (2003) in the EO-1 Special Issue, provide clear evidence that mineral mapping from a space platform and with an instrument of sufficient SNR and performance will capture a significant market and meet important world-wide exploration goals for the mining industry. It is a major application area for the future.

1.4.2.3 Forestry

The primary example of a direct application to the Forestry industry was provided by the work carried out at the Tumbarumba site (Coops, Section 3.1 Tumbarumba). The site is located in an operating forestry region with a diverse mix of plantations and native forests. For the industry a key issue is forest health and current and future forest productivity. Any information that remote sensing can provide to improve these assessments is welcome.

Landsat data have provided a base for time series of site LAI and has provided valuable input to forest growth models (Landsberg *et al.*, 2001). However, based on the EO-1 activity of the NASA SVT and the Australian work, Coops and others (Coops *et al.*, 2003 and Coops, Section 3.1 Tumbarumba) have shown how there is added capacity in Hyperspectral data, including both HyMap™ airborne data and Hyperion space based data, to develop predictive maps of leaf nitrogen concentration. The relationships used at Tumbarumba were developed using regression between image and sampled leaf nitrogen data combined with image pre-processing and partial least squares (PLS, Coops *et al.*, 2003). PLS is an exploratory method and can provide both predictive equations and an analysis of the causes and correlates in the relationship.

Coops (Section 3.1 Tumbarumba) has concluded from his analysis that the relationships mapped were due at least in part to correlations between nitrogen and chlorophyll and were therefore partly direct chlorophyll relationships - especially in the VNIR. However, Coops and others have clearly shown by their work that estimates of canopy nitrogen over large spatial areas are possible using hyperspectral data. A major challenge is how to develop generic equations that can be applied without image calibration. Effective image normalisation by pre-processing and atmospheric correction seems promising but speciation and structure have been judged likely to be the main problems (see Section 3.1 Tumbarumba).

Due to low Hyperion SNR and residual atmospheric correction effects, the SWIR window between 1900 nm and 2300 nm was not found to be as useful as was hoped but it could be in a future instrument with better SNR performance. However, the 1500 nm to 1720 nm window did provide significant extra value from the use of hyperspectral data and may provide more direct relationships with nitrogen than data in the visible region.

The forest environment can be very variable and its variation can affect the degree to which results obtained by any remote sensing mapping can be extended. Situations where the LAI is low and where native forests are being measured are much more difficult to assess than plantations – which are more like agricultural applications than they are like those of mapping native forests. Since plantations are becoming the most common type of commercial forest and a major area of forestry applications this may not be a great problem. From the work at Tumbarumba it seems likely that stable

equations and estimates of leaf nitrogen concentrations may be possible for mono-specific plantations with application to mapping commercial forests at a regional scale.

1.4.2.4 Coastal and inland waters

Hyperion was not expected to deliver applications from water-covered areas due to limitations imposed by modifications for EO-1 and the lower SNR performance that was expected from them. However, Hyperion data have proved to have useful applications and be effective at mapping water properties and benthic materials in coastal, inland and shallow water environments. The waters in these areas are not as "dark" as the deeper ocean water and involve important areas where environment and development often collide.

The Australian contributions came from various areas with varying objectives. As part of a large and ongoing area of remote sensing activity, acquisitions were made over Moreton Bay, a large Bay near Brisbane, Queensland (Brando and Dekker, Section 3.4 Moreton Bay) where oceanic, coastal and estuarine interactions are complex and where there are many pressures on the healthy functioning of the Bay with issues of competing uses and viewpoints.

Brando and Dekker (Section 3.4) found they needed to invest a great deal of time into Hyperion data pre-processing before they were able to map concentrations of water constituents. Many of their experiences and findings have already been reported in Sections 1.4.1.2.2 (Streaking/striping) and 1.4.1.2.3 (Other array and digitisation effects over water). The limitations they encountered in using the data were frustrating and the suggestions previously made will need to be taken into account if a future sensor is to address their area of applications in the way they would wish.

However, based on their work at Moreton Bay, Brando and Dekker (Section 3.4) concluded that *given effective pre-processing*, Hyperion data can be used with physical radiative transfer modelling to map optical water quality concentrations of coloured dissolved organic matter, chlorophyll and total suspended matter (i.e. tripton) simultaneously in the complex waters of estuarine and coastal systems. They found (see Section 3.4.5 Quantitative products) that the retrieved concentrations were comparable with those estimated from field data.

The findings of these scientists in the VNIR were as significant and unexpected as the findings made by the mineral exploration scientists such as Cudahy (Section 3.6 Mt Fitton) in the SWIR. They point to an area of immediate application and value that would follow the deployment of a space hyperspectral instrument with some if its specifications more suitable to the application. These needs have already been listed in Sections 1.4.1.2.2 and 1.4.1.2.3.

Other applications were reported by Kutser (Sections 2.4 Lake Argyle and 3.5 Cape Tribulation – Coral Reef Studies). In one case, Kutser undertook to relate the field measured and image sensed signature variations of a large inland water body (Lake Argyle) to its primary driver of suspended sediment or turbidity. The Lake is turbid and so the signal level was quite high. Nevertheless, he again concluded that although mapping turbidity based on a physical model was possible and successful it was only so after adequate attention was paid to the noise in the data – to the pre-processing. His

approach was interesting being a classification-based method where classes are defined from model cases calibrated to the environmental conditions at the time.

Kutser also applied his approach to the problem of mapping different reef substrates and the depth to the substrate from Hyperion data. If the water properties can be estimated from deep-water areas, which the above work at Moreton Bay and Lake Argyle suggests is feasible, then classes based on different substrates as measured in the field and at different depths can be used as candidate categories and mapped from Hyperion. Kutser (Section 3.5 Cape Tribulation – Coral Reef Studies) shows great promise for reef mapping to a significantly increased level of substrate definition by Hyperion compared with current sensors mapping at the same scale – in particular Landsat ETM+.

Coral reefs form a widely distributed and largely inaccessible target for mapping and monitoring. Ground based survey is time-consuming and expensive; airborne remote sensing data are also expensive so that space based data have a clear platform advantage. From a cost and coverage point of view, Landsat data would provide a very good alternative to airborne and ground based if it could map to a suitable level. However, mapping of coral reef substrates has proved hard enough from airborne data and Landsat ETM cannot map beyond the level of Major Geomorphological Zones (MGZs) possibly with some added separation of general substrate categories such as sand and coral.

The results obtained by Kutser (Section 3.5) suggest that Hyperspectral data can map and separate substrates and depths in a way that Landsat data cannot and also that Hyperion in its current form can provide valuable maps of coral reef environments in at least the top 5m (and potentially more) of the reef area. None the less, the constant theme of this section is not too far away. These results only come as a result of overcoming the noise. *The pre-processing needs are as before and also the specific residual effects that affect water covered areas need to be addressed*. In the future, if coral reefs are seen as a major application then it should also be served by careful sensor design and specification along the lines suggested in Section 1.4.1 (Instrument performance and pre-processing).

In terms of the remaining noise, Kutser (Section 3.5) suggested a novel approach in which SNR was maintained and error contained rather than enhanced or spread through the processing by comparing modelled spectra at the sensor (top-of-atmosphere) with the Hyperion data. His success points to ways of extracting information from noisy data that may have a wider application.

1.4.2.5 Rangelands

The Kunoth site provided very interesting results of value for rangelands mapping. At Kunoth the issue being addressed is large area mapping and monitoring (e.g. of biodiversity) but involving “low value” land. Successful methods need to be low cost to be practicable but the high spatial variability often demands higher sampling to achieve accuracy.

Chewings and Bastin (Section 3.3 Kunoth) report that categories such as fraction of cover of green and dry vegetation, soil, litter and shadow have been successfully mapped by 1m video data. However, such data are expensive and time consuming to

collect and process. Landsat at 30m is useful and at a good scale for the application but cannot resolve the components to a level needed for the research and environmental monitoring. The report by Chewings and Bastin (Section 3.3 Kunoth) showed how Hyperion enabled spectral unmixing (using standard unmixing methods developed by the minerals industry) of 30 m pixel data to provide accurate and useful mixture maps involving categories such as "Photo-synthetic Vegetation' (PV), "Non-Photo-synthetic Vegetation" (NPV) and soil to be accurately unmixed and achieve a comparable accuracy with the same (general) categories mapped from airborne 1m video data.

This application is very interesting as it shows how spectral and spatial resolution can be "traded". The lower spatial resolution provides an appropriate scale for low-cost monitoring and provides the only practical approach in rangelands. The hyperspectral data allows the mixing due to the larger pixel to be resolved into useful components. The high but correlated spatial variation and this result suggests that there may be an optimum mapping scale but that it may depend on the capacity to unmix the data using higher spectral resolution data.

1.4.3 Future Opportunities for sensors and applications

It is important to keep in mind that Hyperion was an experiment that pioneered space based hyperspectral data acquisition. It had limitations, but the limitations can also provide important lessons for future sensors and future applications of space-based hyperspectral data.

In the discussions of Hyperion noise and the need to pre-process the data at the Australian sites there were some common themes. These included low SNR, poorer performance of the array materials in the regions below 500 nm, between 950 and 1000 nm and above 2300 nm, pushbroom effects (including streaking and residual dark correction effects) that need to be eliminated or accurately modelled and the need to upgrade atmospheric correction software to take full advantage of the new situation. However, there were also recommendations that were emphasised by and even specific to the applications themselves. This implies that future sensor design and specification needs to be defined and developed with the target applications and target markets in mind so that the best choices can be made for later processing to products.

There seems little doubt that the technology already exists to overcome all of the problems found in the Hyperion applications. High SNR, high precision of FPA alignment, flexible pointing, accurate geometry and stable and accurate calibration are all within engineering capability. What is still needed, however, is a set of clear specifications for an instrument from among the many possible choices that can be made.

The needs of different applications addressed at the Australian sites have been outlined in the preceding sections. However, it is unlikely that any single instrument can serve the needs of all the current applications – let alone future applications. In this situation the balance of the choices may need to be weighted to the potential markets for the products and by the maturity of the processing and delivery associated with different applications.

Based on the experience of the EO-1 mission, an attempt was made by scientists working at the Australian sites to develop a "map" to the current market for hyperspectral data and the most advanced initial applications on which a design could be based. This is presented here in Table 1.4-2 under the same main applications headings:

- Agriculture
- Mining
- Forestry
- Coastal waters (including Reefs)
- Rangelends

In each of these cases, the likely processing steps that will provide the products users need are either known or feasible from current research. However, they are not all "operational" in a commercial sense. The development of weightings based on potential market, capacity to bring the products to an operational stage and cost of implementing the associated sensor specifications may provide a way to balance the choices for a future space based sensor.

The combination needed for the market to support future sensors is:

- The market must exist;
- The data and the processing must be able to solve the problems;
- The solutions must be able to be delivered to users in their timeframe and in a way they can use.

These requirements take us beyond the specifics of sensor design and algorithm development but also provide the framework in which they must be viewed in the development of future systems. A complete solution is likely to involve much more than a satellite based sensor or group of sensors by themselves and include airborne data and involvement in and of specific industries and their needs. In the development of an industry that provides data interpretation and products there are many aspects. Providing sophisticated users and researchers with advanced tools is vital. Locking away knowledge can be fatal.

However, it is also important to keep in mind that the largest market will almost certainly be to non-specialist users. The existence of an industry providing this market with timely, high quality products and reliable service and support provides a solid base for the "food chain" that can support the future of the amazing technology and excellent research and applications that are on display in the following Sections of this Report.

Table 1.4-2 **Potential Application Areas for Hyperion Data and Future Hyperspectral Missions.**

Market	Current Site(s)	Application	Customers	Outcome
Agriculture	Coleambally Irrigation Area	Irrigated rice, corn, soy, sorghum and other crops (eg wheat)	Precision farming Rice Cooperative Growers Associations	Yield prediction Crop health Weeds and pests
	Cape Tribulation	Sugar cane	Sugar Mills Growers Associations Producers	Yield prediction Crop health Weeds and pests
Mining	Mt Fitton & Panorama	Exploration World wide	Mining companies R&D Agencies	Mineral maps Strategic exploration
	Kakadu NT Brukunga (SA) Goldsworthy (WA)	Mine site Environments	Mining Companies R&D Agencies	Time series of rehabilitation Certification
Forestry	Tumbarumba	Sustainable forest management; Carbon accounting	State forests, forest industry Government Agencies	Nitrogen/ productivity
	Cape Tribulation	Tropical rainforest productivity and environment	Environmental agencies Tropical foresters	Rainforest production & mapping Environmental monitoring
Coastal Waters	Moreton Bay	Seagrass mapping, water quality, coral reefs, estuarine turbidity	State and National Agencies Off-shore exploration environment	Water quality Benthic maps Reef health Logistics and environmental monitoring
Rangelands	Kunoth	Environmental monitoring, Biodiversity	State and National Agencies, NGOs	Large area mapping of habitats for low cost and high discrimination

1.4.4 Summary of the outcomes of the activity

The research by the SVT, to which the Australian scientists added significantly, achieved important improvements in the original Level 1 data quality of all the instruments and established a number of recommended pathways to process Level 1 data for applications. If the current Level 1B1 (USGS Level 1R) Hyperion data are used and the recommended pathways followed then it has been found that given appropriate environmental conditions, the instruments on EO-1 and the advanced experiments have met or exceeded operational expectations. In the specific case of Hyperion its applications to areas such as agriculture, mineral exploration, forestry, coastal waters and coral reefs and rangelands have generally exceeded expectations.

The instrument was, however, specifically an advanced technology experiment and not as an operational instrument. The performance of the Hyperion instrument was always less than its engineers would have wished, but the opportunity to meet narrow time constraints and add a hyperspectral instrument to EO-1 using components meant as back-ups to the previous Lewis sensor was too good to pass up. It was very good for us all that they did not. The applications performance has been good but it has also demonstrated the need for and value of having improved SNR in a future space hyperspectral instrument. At the same time it has, through the successful applications such as those outlined in Sections 2 and 3, demonstrated the value of developing and realising such future space missions. If, or rather when, they occur it is clear that some of the issues described above – such as the spectral smile – can be overcome. Others – such as image streaking – need careful attention if similar pushbroom technology is to be used.

A major technical outcome of the Hyperion experiment has been the demonstration that it is possible to launch and validate a well-calibrated instrument and to refine its calibration in space using combinations of calibration approaches such as solar, lunar, lamp and panel methods. This, together with advances in software, has resulted in atmospheric correction of space based hyperspectral data becoming well defined and standard in most cases. The provision of such stable and well-calibrated data with higher SNR will only improve this situation.

From the presentations in the following Sections it is clear that, working closely as part of the NASA SVT, the Australians contributed significantly to the evaluation of the instruments, to improvements in the data processing and to development of recommendations for post-Level 1R processing that have made the data from EO-1 suitable for a range of applications. This led to the current Extended Mission and the semi-operational provision of EO-1 data to the world through the USGS. In the future, the Australian scientists look to build on the increased US/Australian collaboration that has developed during the SVT phase and the excellent experiences of working with the SVT members (Figure 1.4.1) and to continue to develop the international network it has initiated.

Figure 1.4.1: Steve Ungar, NASA Chief EO-1 Mission Scientist and some of the "young turks" at an EO-1 SVT Meeting.

This opportunity of continued collaboration specifically includes the potential to develop a collaborative southern hemisphere activity. There have been important collaborations in calibration & validation, agricultural applications, forest health, mineral exploration and rangelands studies. The use of Australian sites as complementary southern hemisphere study areas will be just as important – if not more important – in the applications phase as it was in the technology evaluation phase. We have welcomed the potential for NASA to build on its investment in EO-1 and in the SVT as a major resource to bring the current data into operational use in applications and prepare the way for the more advanced sensors that the technology experiments will bring about. We look forward to the opportunity of being part of that activity.

1.5 References

IEEE Special Issue on the Earth Observing 1 Mission

[The following set of references occur in the "Special Issue on the Earth Observing 1 (EO-1) Mission"**,** *IEEE - Transactions on Geoscience and Remote Sensing*, **41**(6), June 2003.]

Brando, V.E. and A.G. Dekker. "Satellite hyperspectral remote sensing for estimating estuarine and coastal water quality." pp. 1378-1387.

Cairns, B., B.E. Carlson, R. Ying, A.A. Lacis and V. Oinas. "Atmospheric correction and its application to an analysis of Hyperion data." pp. 1232-1245.

Coops, N.C., Smith, M.L., Martin, M.M, Ollinger, S. "Prediction of Eucalypt Foliage Nitrogen Content from Satellite Derived Hyperspectral Data." pp. 1338-1346.

Datt, B., T.R. McVicar, T.G. Van Niel, D.L.B. Jupp, J.S. Pearlman. "Pre-processing EO-1 Hyperion Hyperspectral Data to Support the Application of Agricultural Indices." pp. 1246-1259.

Goetz, A.F.H., B.C. Kindel, M. Ferri and Z. Qu. "HATCH: results from simulated radiances, AVIRIS and Hyperion." pp. 1246-1259.

Kruse, F.A., J.W. Boardman and J. Huntington. "Comparison of airborne hyperspectral data and EO-1 Hyperion for mineral mapping." pp. 1388-1400.

Liang, S. Fang H. L., Thorp L., Kaul, M., Van Niel, T.G., McVicar, T. R., Pearlman J. S., Walthall, C. L., Daughtry, C. S. T., and Huemmrich, F. "Estimation of land surface broadband albedos and leaf area index from EO-1 ALI data and validation." pp. 1260-1267.

Pearlman, Jay S., Pamela S. Barry, Carol C. Segal, John Shepanski, Debra Beiso, and Stephen L. Carman. "Hyperion, a Space-Based Imaging Spectrometer." pp. 1160-1173.

Qu, Z., B.C. Kindel and A.F.H. Goetz. "The High Accuracy Atmospheric Correction for Hyperspectral Data (HATCH) Model". pp. 1123-1231.

Ungar, Stephen G., Jay S. Pearlman, Jeffrey A. Mendenhall, and Dennis Reuter. "Overview of the Earth Observing One (EO-1) Mission." pp. 1149-1159.

Other References Cited

Adler-Golden, S.M., M.W. Matthew, L.S. Bernstein, R.Y. Levine, A. Berk, S.C. Richtsmeier, P.K. Acharya, G.P. Anderson, G. Felde, J. Gardner, M. Hoke, L.S. Jeong, B. Pukall, J. Mello, A. Ratkowski and H.-H. Burke (1999). Atmospheric correction for short-wave spectral imagery based on MODTRAN4. *Proceedings of the SPIE*, Imaging Spectrometry V, Vol. **3753**, 61-69.

Boardman, J.W. (1998) Post-ATREM Polishing of AVIRIS Apparent Reflectance Data using EFFORT: a Lesson in Accuracy versus Precision*, Summaries of the Seventh JPL Airborne Earth Science Workshop,* JPL Publication 97-21, Vol. 1, p. 53.

Cooley, T.W., G. Anderson, G. W. Felde, M. L. Hoke, and A. J. Ratkowski (2002). FLAASH, a MODTRAN-4 based atmospheric correction algorithm, its application and validation. *Proc. Int. Geoscience and Remote Sensing Symp. (IGARSS'02)*, Toronto, Canada, III: pp.1414-1418.

Goetz, A.F.H., G. Vane, J. Solomon and B.N. Rock (1985). Imaging spectrometry for Earth remote sensing. *Science*, vol. **228**, 1147-1153.

Goetz, A.F.H. and K.B. Heidebrecht (1996). Full-scene, subnanometer HYDICE wavelength calibration. *Proceedings of the SPIE*, **2821**, 85-92.

Green, A.A., M. Berman, P. Switzer, and M. D.Craig, (1988). A transformation for ordering multispectral data in terms of image quality with implications for noise removal. *IEEE Transactions on Geoscience and Remote Sensing*, **26(1),** 65-74.

Horn, B.K.P. and R.J. Woodham (1979). Destriping Landsat MSS images by histogram modification. *Computer Graphics and Image Processing*, **10**, 69-83.

Jupp, D.L.B., B. Datt, T. R. McVicar, T. G. Van Niel, J. S. Pearlman, J. Lovell, and E. A. King (2002). Improving the Analysis of Hyperion Red Edge Index from an Agricultural area. *Proceedings of the SPIE*, Vol. **4898**, 78-92.

Landsberg, J.J., R.H. Waring and N.C. Coops (2001). Performance of the forest productivity model 3-PG applied to a wide range of forest types. Model structure, calibration and sensitivity analysis. *Forest Ecology and Management*, **172**, 199-214.

Liao, L., Jarecke, P., Gleichauf, D. and Hedman, T. (2000). Performance characterization of the Hyperion imaging spectrometer instrument. *Proceedings of the SPIE*, Vol. **4135**, 264-275.

Matthew, M.W., Adler-Golden, S.M., Berk, S.C. Richtsmeier, R.Y. Levine, L.S. Bernstein, Acharya, G.P. Anderson, G. Felde, J. Gardner, M. Hoke, L.S. A. Ratkowski, H.-H. Burke, R.D. Kaiser and D.P. Miller (2000). Status of atmospheric correction using a MODTRAN4-based algorithm. *Proceedings of the SPIE*, Algorithms for Multispectral, Hyperspectral and Ultraspectral Imagery VI, Vol. **4049**, .

Vermote, E.F., D. Tanre, J.L. Deuze, M. Herman and J-J. Morcrette (1997). Second simulation of the satellite signal in the solar spectrum, 6S: an overview. *IEEE Transactions on Geoscience and Remote Sensing*, **35**(3), 675-686.

2 CALIBRATION AND VALIDATION SITES & FINDINGS

2.1 Introduction

Three of the sites (Lake Frome, Uardry and Lake Argyle) were designated specifically as Calibration and Validation sites. In the selection of these sites, the emphasis was on (where possible) uniform land covers, stable conditions, logistical support and associated continuously recording instrumentation and prior field campaigns. The Coleambally site, discussed previously for its significant agricultural time series and applications, also provided a valuable site for geometric studies and sensor inter-comparisons. The studies carried out here were made possible by the well-surveyed field boundaries and roads and the large uniform fields that cover the site.

Lake Frome is a large salt lake (playa) in the north of South Australia. It has a high visible region reflectance (about 70% when dry) with little fall-off in the blue end of the signature. It is ideal for VNIR instruments. Unfortunately, the year of intensive effort (2001) was a wet year and the lake surface had too much associated moisture for the SWIR region (which has high water absorption) to provide effective calibration for an instrument with the SNR of Hyperion. However, Lake Frome provided a very important support function for TRW in the early phase of the Checkout that occurred in the Northern Hemisphere winter. The lake has been imaged in more recent times following a drying period and is being used to study calibration stability and VNIR "smile".

Uardry (near Hay in NSW and close to the Coleambally site) is a prairie site that has been used for AVHRR and MODIS calibration and validation as well as surface radiation balance (SRB) studies. It is located at 14°24'S and 145°18'E. The site is maintained by Fred Prata, Bob Cechet and Graham Rutter of CSIRO. As well as EO-1, data was available for the site from DATM and HyMap scanners, various satellites (AATSR, MODIS, ASTER), tower based surface radiation balance (SRB) and meteorological data and site BRDF measurements. The site was also used in the early checkout period to refine the initial TRW calibrations.

Lake Argyle is an extensive man-made lake in northern Australia. It was planned to provide a dark target to complement Lake Frome and which could be used in the winter period in Australia for calibration. There is an AeroNet CIMEL (maintained by CSIRO) located there and a field campaign was carried out. Studies of the darker end of the calibration for Hyperion have been carried out but reporting has not yet been finalised. There were extensive water quality data and water reflectance obtained and we have therefore provided a report on the completed analysis of Lake Argyle as an inland water body.

2.2 Lake Frome

Locating Sites on (the Salt) Lake Frome in northern South Australia

Site Information:

Site P/Co-Investigator(s): Dean Graetz, Susan Campbell, Edward King, Jenny Lovell David Jupp (CSIRO EOC), Jay Pearlman, Pamela Barry & Peter Jarecke (TRW Inc)
Site Name: Lake Frome
Type of measurement: Surface reflectance
Measurement devices: ASD FR (400-2500 nm)
Dates of acquisition: December 17-20, 2000
Latitude: 30º 51' S
Longitude: 139º 45' E
Elevation: sea level
Surface type: Salt Lake
General atmospheric conditions: Clear
Other satellite data: Landsat ETM+, ALI, AVHRR
Comments: Meteorological data were recorded during the field campaign and Hyperion overpasses on December 20, 2000 and January 5, 2001.
Contact email: Susan.Campbell@csiro.au

Report prepared by: Susan Campbell & David L B Jupp
CSIRO EOC

2.2.1 *Introduction*

CSIRO EOC carried out a field validation campaign between December 17 and 20, 2000 at Lake Frome (see Figure 2.2.1 & Figure 2.2.2) in coordination with an early Hyperion data collect on December 20, 2000. This day was less than perfect so images were also collected on January 5 and 21, 2001 and used in its place. Landsat 7 ETM+ and Advanced Land Imager (ALI) data were also collected at the same time for analysis and comparison. The objective of the field mission was to validate and evaluate the Hyperion and other EO-1 sensors in the early check-out period. Since the northern hemi-sphere was in the depths of winter in December 2000 it was necessary to find and use suitable sites in the southern hemi-sphere.

Lake Frome was judged to be an ideal site as the Hyperion ground track aligns with a well-established and persistent salt track well away from edge effects and where the surface is uniform and flat. In the period leading up to the EO-1 mission the Lake had been dry for an extended period and Landsat images showed it to be extremely bright in the visible region to the extent that the Hi-gain mode was purposely only activated when the Landsat track was south of Lake Frome.

Figure 2.2.1: Landsat Image of Lake Frome – a salt lake in northern South Australia.

Vicarious calibration, in which ground measured data are used to assess the calibration of space data, provides a unique opportunity to investigate the characteristics of the instrument from a position that is user and end-use oriented. However, because of the variability of atmospheric and environmental conditions, the process has to involve extensive ground truth and careful coordination with spacecraft mission operations to coordinate the time of data collection of the spacecraft with the ground truth measurements. It also demands the

collection of sufficient ground information to characterise the site and the atmosphere at the time of the acquisition. The desired result is a direct comparison of the top of atmosphere (TOA) measurements made by the instrument with the TOA predictions based on the independently measured ground spectral reflectance measurements and propagation through a predicted atmosphere using a radiative transfer model that incorporates ground based ancillary atmospheric data (such as visibility and water vapour).

The purpose of the first visit to Lake Frome in December 2000 was to model the TOA radiances from the field measurements of surface reflectance at the time of Hyperion overpass and the ancillary data. The data were acquired soon after the launch of Hyperion as part of the early and vital check-out of the instrument by the instrument team and were provided in an un-calibrated form to maximise the independence of the evaluation. In the end, the TOA radiances were estimated by the CSIRO team for the January 5th 2001 overpass assuming surface reflectance was stable and persistent but the mission served its purpose well and played a significant part in making Hyperion data ready by the end of the check-out period for provision to the NASA Science Validation Team.

Figure 2.2.2(a) (Above) Location of Lake Frome in Northern South Australia

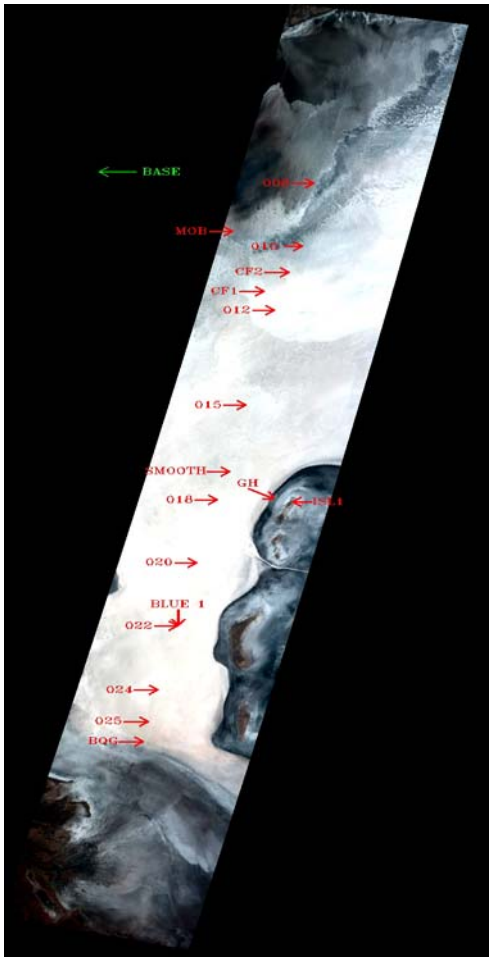

Figure 2.2.2(b) (To Right) Lake Frome image taken by Hyperion on the January 5, 2001 overpass showing field sites along the bright strip.

The Lake Frome site data were also used to check for sensor uniformity (both for sensor calibration in-equalities and scene dependent effects) and to test the accuracy of geo-locating the Hyperion image with the physical sites where the measurements were made. Descriptions of these tests and the uniformity of the sites over regions comparable with the ground sample distance (GSD, approximately 30 m for Hyperion) of the instrument during the campaign can be found in the paper by Campbell *et al.* (2001).

This report describes the early ground truth campaign and the resulting comparison between the predicted and measured TOA radiances. As stated above, these studies were carried out soon after EO-1 launch and provided valuable support to the instrument checkout and validation prior to the release of data in early 2001. It was, in fact, the first vicarious calibration test for Hyperion post-launch and provided very welcome confirmation of excellent calibration performance from the sensor. Lake Frome is also providing an excellent site to support on-going work to characterise the cross-track "smile" effect due to its having a section of the complete Hyperion swath within a relatively uniform area of salt and a very good characterisation of the reflectance of the salt surface based on (at this time) two major field campaigns to the Lake.

2.2.2 Lake Frome ground truth data collection

Lake Frome is located in the north east of South Australia (Figure 2.2.2(a)) and is a large, normally dry salt lake (playa). The centre of the playa is approximately at 30°51'S and 139°45'E. The mission was well supported by atmospheric measurements from the CIMEL site at Tinga Tingana and the ABoM radiosonde site at Woomera. Both of these locations are marked on Figure 2.2.2(a). It also has excellent supporting logistics at the Arkaroola resort which is close to the Lake access.

The Lake is very bright when dry with visible region reflectance being over 70%. However, moisture decreases the SWIR reflectance very significantly and this will be addressed later in this report. Figure 2.2.2(b) is an image of the January 5th 2001 Hyperion acquisition over the Lake Frome area showing the field sites. The sites fall on a path along the centre region of the Hyperion swath.

Figure 2.2.3: Lack of "hotspot" halo around aircraft shadow indicates flat smooth but diffuse texture. However, there is a pattern of "mottles" to take into account.

The Lake was judged to have good surface homogeneity and texture and was hard enough for Quad-bikes to access the central area and carry people and equipment out to the sites. The environment was harsh and great care was taken to avoid possible problems for staff out on the Lake. The surface texture was also good from a radiative point of view. An aerial survey showed it to be primarily smooth as indicated by lack of a distinct "hotspot" halo around the aircraft shadow (Figure 2.2.3) but it did have a pattern of small circular features (called "mottles" during the field survey) that were assessed carefully at each site.

Meteorological data were collected during the mission using a portable weather station and a Yankee Environmental Systems multi-frequency shadow-band radiometer (MFR) operating at the lakeshore. Data were also acquired for every acquisition of the EO-1 data from Bureau of Meteorology radiosondes launched from Woomera (250 km west of Lake Frome, see Figure 2.2.2(a)) and the CIMEL sun photometer located at another CSIRO field site at Tinga Tingana 150 km to the north of the lake.

2.2.2.1 Reflectance Measurements

Spectral reflectance measurements were made with an Analytical Spectral Devices (ASD) Field Spec spectroradiometer at a range of ground sites as shown in Figure 2.2.4. A GER spectroradiometer was also used but its data were not judged to be as good as the ASD.

Figure 2.2.4: Field work at Lake Frome illustrating high surface reflectance and site homogeneity (The field record later won a photo competition prize!).

The measurements during the first field mission were made over specified ground blocks to account for spatial variation and the mean signatures were established. The measurements were referenced to a standard Spectralon panel. However, since field staff had to carry and operate the ASD the design was fairly limited. At a second (later) field mission, a more extensive methodology was developed using an ASD mounted on a quad-bike and

establishing reflectance in a grid at each site. This more advanced methodology was later also used at the Coleambally site.

A brief description of some of the sites that were measured during the first field mission is included in Table 4.2.1. Sites 018, 020, 022 and 024 were used for the initial comparison with Hyperion measurements on behalf of TRW. The "Island" soil site and the wetter Site 8 are included here for comparison.

Table 4.2.1: Sites characterised at Lake Frome

Site	Surface Description	Latitude	Longitude
018	Uniform Salt	-30.80	139.68
020	Uniform Salt	-30.83	139.67
022	Mixed Salt and Mottle	-30.87	139.66
024	Uniform Salt	-30.90	139.65
008	Salt Graded to Ooze	-30.63	139.73
Island	Soil	-30.80	139.71

During the first field mission, because the ASD was carried by field personnel, the sites were only sampled using a central cluster of points that was augmented by local transects of about 100m to characterise the spatial (co-)variance and to produce an effective mean site signature at the scale of the Hyperion GSD. However, the initial measurements showed such high uniformity at each site and this design was judged adequate for the purposes of the first mission. Salt and mud samples at the sites from both at and below the surface and also in nearby wetter areas were also collected for laboratory characterisation.

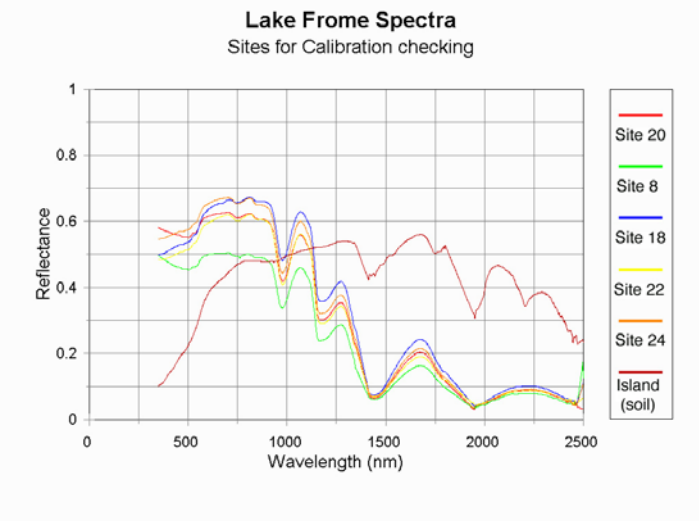

Figure 2.2.5: ASD Spectra recorded at field sites shown in Figure 2.2.2(b). Spectra have been linearly interpolated over regions of strong atmospheric water vapour absorption

Figure 2.2.5 shows some mean reflectance spectra for the main calibration field sites as well as Site 8 and the "Island" soil site. These spectra have been linearly interpolated across the main water absorption bands as the ASD spectra are very noisy in these regions. The form of the spectrum is very similar at all the salt sites. Variation is mostly related to the thickness of the salt crust (a thin crust allows the underlying mud to influence the spectrum – mostly at the

blue end) and the amount of liquid water present in the salt matrix. The liquid water is indicated by a clear "water" absorption effect in the data. As discussed later, the pure dry salt matrix is spectrally flat and nearly "white".

The soil signature was taken on the loess islands around the Lake. The soil is fine textured and quite dark in the visible. However, its reflectance in the SWIR is very high and it would provide an excellent base for SWIR assessment. If Lake Frome is used in the future a parallel "track" of soil sites will be set up and monitored in addition to the salt track.

The full extent of the spatial variation of the surface and its components is being studied in on-going work using a range of data available for Lake Frome including Hyperion, ALI, HyMap airborne hyperspectral and Landsat ETM data. One outcome has been from an initial study of the effects of wetting on the salt signatures. Figure 2.2.6 shows a sequence of signatures (normalised to a panel but not corrected for panel conditions) ranging from "dry" (dried in a microwave oven) to wet (saturated).

The microwave was not sufficient to drive off the bound water but it is clear that more extensive drying would result in a base dry salt signature that is very bright and spectrally flat. Although the work is still preliminary, it has suggested that the amount of water may be determined spectrally through well-chosen ratios and then used to obtain the absolute reflectance from the wetting series without the need for fieldwork. Certainly, a Principal Components Analysis shows that the sequence of data has two "dimensions" of base salt and water effects. This idea, which depends on the main central area at Lake Frome maintaining its "purity", is being assessed against a time series of Frome images.

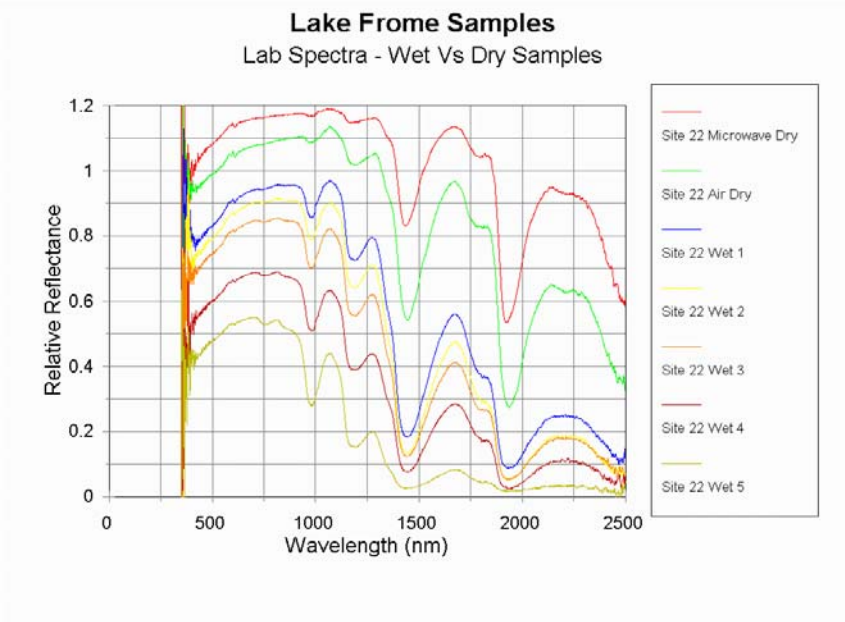

Figure 2.2.6: A sequence of salt samples with different level of wetting showing the two-component spectral variation. Work is continuing to assess its use for time series calibration.

2.2.2.2 Navigation Accuracy Assessment

The utility of the field measurements is crucially dependent on their accurate location (and re-location) on the Lake and in the image data. The GPS readings taken at all sample positions provided an accurate base of geo-located data and so it was necessary to also establish accurate image geo-location.

A set of ground control points (GCPs) was identified in both the image of Hyperion Band 22 (568 nm) and an accurately geo-rectified Landsat ETM+ image (acquired on January 21, 2001) in its (green) Band 3. Analysis of the data fit by different orders of polynomial was based on predictive error and showed that a bi-linear transformation was adequate and possibly best among various orders of model. This model allows for shifts in x and y, separate changes of scale in x and y, image skew, rotation and an x-y interaction term. The statistical significance of the x-y interaction term may indicate that there was a projective geometrical effect in the Hyperion image at the surface. This is likely to have greater significance at other sites since Lake Frome was imaged at near nadir view.

The main characteristics of the pixel geometry as determined from this model is summarised in Table 4.2.2.

TABLE 4.2.2 Hyperion Geometric Characteristics

Pixel-X	30.646 m
Pixel-Y	30.528 m
Rotation	-12.38°
Skew	0.006°

EO-1 has a specific yaw to compensate for the Earth rotation skew. It seems to have been very effective. The pixel shape was also very close to square in this model. The predictive error for the VNIR sensor was 15 metres in x and 20 metres in y. This close registration and the uniformity of much of the Lake Frome site therefore means we can identify the spectra of pixels relating to the ground sites with considerable confidence.

The GCPs were also independently identified in band 94 of the Hyperion image (1084 nm) to test the alignment of the VNIR and SWIR spectrometers that make up the Hyperion instrument. These share the same focal plane but have different read-out properties. Based on predictive errors, the data for each spectrometer were again well modelled by a bi-linear transformation. However, offsets of approximately one pixel in x and a fraction of a pixel in y were noted between the VNIR and SWIR sensors. The magnitude of the offset varied between about 1.0 and 1.2 pixels across the 256-element array. This finding, in fact, confirmed what the TRW checkout team had suspected from pre-launch testing and this and other studies eventually resulted in a standard correction being implemented for the different geometries of the VNIR and SWIR in the later Level 1B release of the Hyperion data.

2.2.2.3 Atmospheric Modelling

Two sources of measured atmospheric data were available. One was CIMEL data taken at Tinga Tingana (a site established in 1998 in central Australia to study aerosols) that could be used to provide estimates of aerosol optical depths and water vapour at that site. The other was the Woomera meteorological station, which is located about 200 km west of the lake (see

Figure 2.2.2(a)) and provides daily radiosondes. The radiosonde data were used to obtain lapse rates for the pressure, temperature and water vapour profiles. These measurements were modified where necessary by using the historical atmospheric statistics for the region to provide stable lapse rates that should be applicable at Lake Frome. A general idea of the total column ozone was available from the GOME satellite data.

The CIMEL data were used to infer integrated atmospheric properties such as the angstrom coefficient of the extinction. The most important parameters of the local visibility and total column water vapour at Lake Frome were not, however, easy to establish for the acquisitions taken later than the field work. Comparisons between the total column water vapour as measured by the MFR at Lake Frome, the value that best predicted the LICOR irradiance data, the Woomera Radiosonde and the CIMEL total water vapour estimate at Tinga Tingana at the time of the field work seemed to show the Lake Frome site tended to have a greater water vapour loading than the others. This relationship was used in the estimation of TOA radiance.

2.2.2.4 Top of the atmosphere radiance comparison

As the EO-1 mission started, CSIRO worked to provide timely feedback on the Hyperion calibration. The Lake Frome data were used with an atmospheric model to compare the estimated at-sensor radiance with un-calibrated Level 1 data. A simple radiative transfer model was used for the initial investigation since the necessary outputs were easy to obtain and it was able to be optimised to the field data that was taken. The estimate (Figure 2.2.7) of the "calibration" (ratio of the estimated radiance to the raw counts) was obtained and compared with the then current curve provided by TRW.

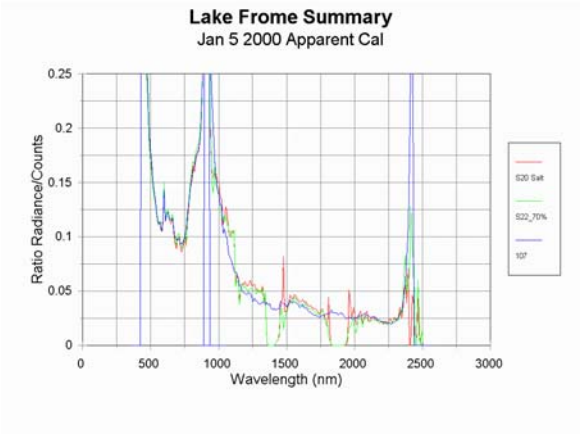

Figure 2.2.7: Early comparison of TRW and vicarious calibration using Lake Frome data

This graph, which provided very welcome confirmation of the post-launch quality of the instrument and its functioning in a working situation, is now largely historical as TRW and CSIRO then proceeded to make considerable efforts to refine the study and look at reasons for the residual discrepancies as well as to undertake many other types of comparisons. However, the basic result that Hyperion was working within a close range of good calibration post-launch provided a major outcome from the Lake Frome mission.

Site 20 showed the best overall agreement between the TOA radiances calculated from ground truth and the Hyperion measurements. **Figure 2.2.8**(a) shows the spectral radiance curves. The agreement is best in the visible and near IR.

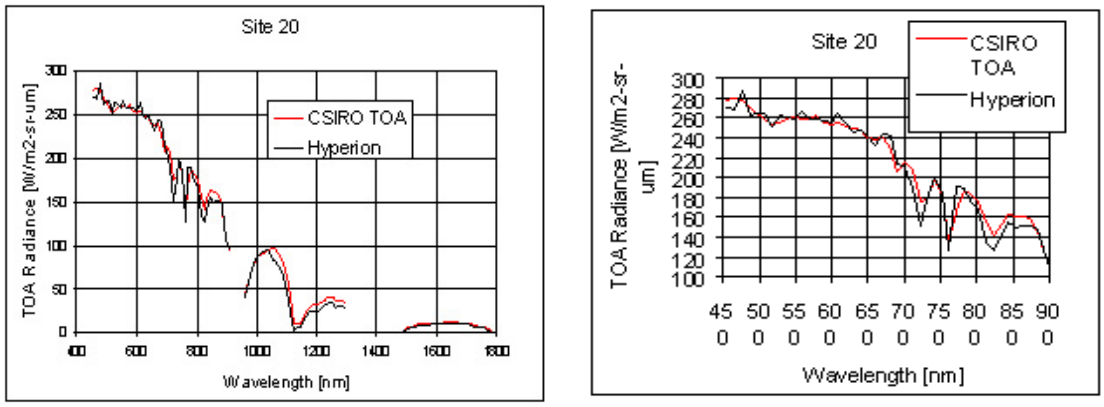

(a) (b)

Figure 2.2.8 (a). Spectral radiance comparisons over the VNIR and SWIR spectral response region of Hyperion. (b) VNIR spectral radiance comparison from Site 20.

As shown in the expanded wavelength scale in **Figure 2.2.8**(b), the mean difference is less than 1.5 % ± 0.5 % from 450 to 900 nm. The CSIRO TOA radiances are 16 % higher than that measured by Hyperion in the SWIR for site 020. The largest differences occur at 715, 760 and 810 nm and in these cases are most likely related to atmospheric correction effects at the spectral features shown in Figure 2.2.7. Otherwise, the general difference ratio ranges from 2 to 10 % throughout the spectral region. In the SWIR, sites 018, 020, and 024 indicate that the TOA model predictions are generally 10 to 25 % higher while site 022 data are lower as shown in **Figure 2.2.8**. The gaps are where water absorption bands affect the data. Corrections for BRDF effects based on view angle and the Standard Spectralon panel SWIR performance would improve the validity of these comparisons.

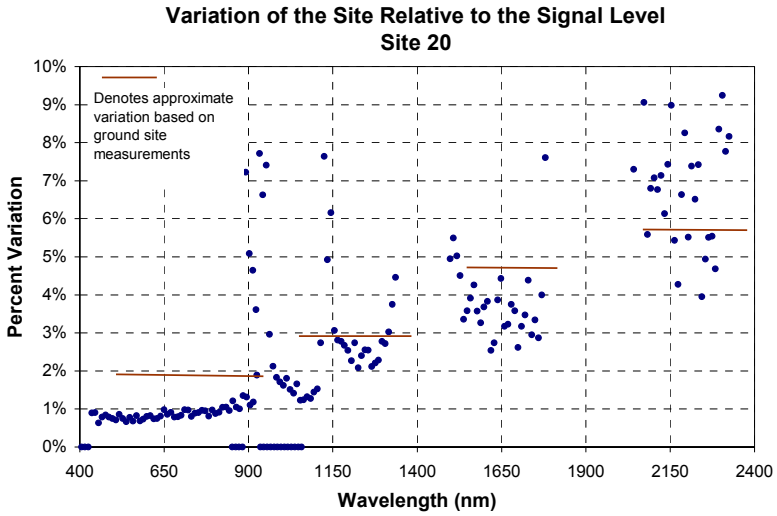

Figure 2.2.9: Coefficient of variation in the Hyperion image around Site 20 (blue dots) plus similar estimates based on the field spectra (brown lines).

A basic limitation on the data in this case was the wetter than normal state of the Lake. This led to the SWIR region being very dark and the data in the SWIR – both from the satellite and at the ground surface – being quite noisy. Figure 2.2.9 shows the coefficient of variation in a neighbourhood of Site 20 from the image and indicates that the coefficient of variation is affected by the instrument sensitivity and SNR but also has an intrinsic behaviour related to the base salt reflectance combined with the solar irradiance. The similar data from the field measurements indicates the base relationship is intrinsic and not instrumental. It would have been better if more sites on the very bright SWIR soil areas (see Figure 2.2.5) that surround Lake Frome had also been measured.

2.2.3 Conclusions from the campaigns

The Lake Frome field campaign in December 2000 was the first time the lake had been visited for a ground based spectral measurement effort. Despite the extreme nature of the environment it was highly successful. A second mission to the lake was made in September 2001 but due to the wet year experienced in 2001 the data were valuable to characterise the Lake but the overpass was not a success for calibration and validation. The lake surface has, however, now been well characterised and the range of target sites has been extended for future EO-1 data collection. Data from the Lake Frome site are available as part of the EO-1 mission and can be found at http://www.eoc.csiro.au under Hyperspectral/Australian Science Validation Team/Data Collections. The site provides an excellent base with which to cross-compare Landsat ETM, ALI and Hyperion and compare their performance with that of other polar orbiting satellites of varying resolution and scale, such as AVHRR, MODIS, ATSR2 and SPOT Vegetation. In recent times a series of images has been acquired following a drying period. These will be processed for testing calibration stability.

While some site spectra in the first exercise provided a very accurate match with the Hyperion data, at others there were variations between the Hyperion data and site measurements that may have a range of causes. Among these is the surface BRDF which it was intended that we measure but is still not completely determined. The HyMap data will provide more insight into this factor. Visual assessment as in Figure 2.2.3 indicates the BRDF of the lake is likely to be stable and able to be characterised. The combination of field and laboratory measurements allowed TRW to quickly confirm that their calibrations were generally within about 5-10% in the VNIR and perhaps similar in the SWIR. The low reflectance of the Lake Frome salt in the SWIR prevented precise conclusions in that region. The wetter-than-normal conditions in the first year of the EO-1 mission contributed to the low environmental SNR in the SWIR region.

On the basis of this work, TRW used the solar calibration to improve uniformity and absolute corrections so that the Level 1 products that were released were of high quality when the data were first delivered to members of the SVT. In the first year of the campaign, results from a range of sites and using a number of sensors were used to define a major correction to the overall calibration. This was implemented in late 2001 to bring Hyperion into alignment with standard choices of solar constant, Landsat ETM and ALI. However, the absolute calibration is certainly still being discussed.

2.2.4 Acknowledgements

Staff from TRW Inc. provided data, responsive help and were a wonderful group to work with. NASA provided access to the Hyperion data, CSIRO Land & Water supported field campaigns with their ASD and staff support including the important role of Guy Byrne in the missions, the CSIRO EOC funded the field missions, the Australian Bureau of Meteorology provided extra radiosonde data for Woomera and the Arkaroola resort provided great interest, help beyond normal hosting and their wonderful surroundings (Figure 2.2.10).

Figure 2.2.10: The road to Arkaroola Resort – Flinders Ranges, northern South Australia

2.2.5 References

S. Campbell, J. Lovell, D.L.B. Jupp, R.D. Graetz, P. Clancy, P. Jarecke, J. Pearlman (2001). The Lake Frome Field Campaign in support of Hyperion Instrument calibration and validation, *IGARSS'01 Special Session 40*, SS40MO, paper 1675.

Graetz, R.D., Campbell, S., Lovell, J., King, E. & Byrne, G. (in preparation). Lake Frome, Australia: A site for vicarious calibration of broadband and narrow band sensors.

Barry, P.S., Jarecke, P., Pearlman, J, Jupp, D, Lovell, J, Campbell, S. (2001). Use of Lake Frome Ground Truth Campaign as a Cross-Calibration of the Hyperion Instrument. *IGARSS'01 Special Session 40*, paper 1780.

2.3 Uardry

Field Crew at the Uardry site near Hay, taken from the 15m tower

Site P/Co-Investigator(s): Fred Prata
Site Name: Uardry (near Hay, New South Wales).
Type of measurement: Short- and long-wave radiation, albedo, surface temperature, aerosol optical depth, surface meteorology
Measurement devices: Pyranometers (5), pyrgeometers (3), infrared radiometers (4), shadowband radiometer (1), surface meteorological instruments, portable radiosonde, 15 m observation tower.
Dates of acquisition: Continuous.
Target acquisition date: 9 January, 2001.
Latitude: 34.392 S
Longitude: 145.304 E
Elevation: 110 m
Surface type: Mitchell grass and bare soil (red cracking clay)
General atmospheric conditions: Generally clean atmosphere, optical depth (500 nm) < 0.1, low rainfall (<350 mm annually). No industrial pollution sources, occasional smoke from stubble burning and large distant bushfires.
Other satellite data: Cal/val site for MODIS/ASTER, ATSR-2/AATSR, GLI (NASDA)
Comments: Instruments in continuous operation since 1993. Well-characterised field site with copious data available. Good uniformity at scales from 10 m to 10 km.
Contact email: Fred.Prata@csiro.au

2.3.1 Introduction and Objectives

On January 9, 2001, EO-1 passed over the Uardry field site, near Hay in NSW, Australia. Hyperion was programmed to acquire an image around 10 AEST (11 am local summer time and close to 00 UT on the boundary between January 8 and January 9) and one minute after the Landsat-7 overpass. The uncorrected Hyperion data for the site are shown in Figure 2.3.1.

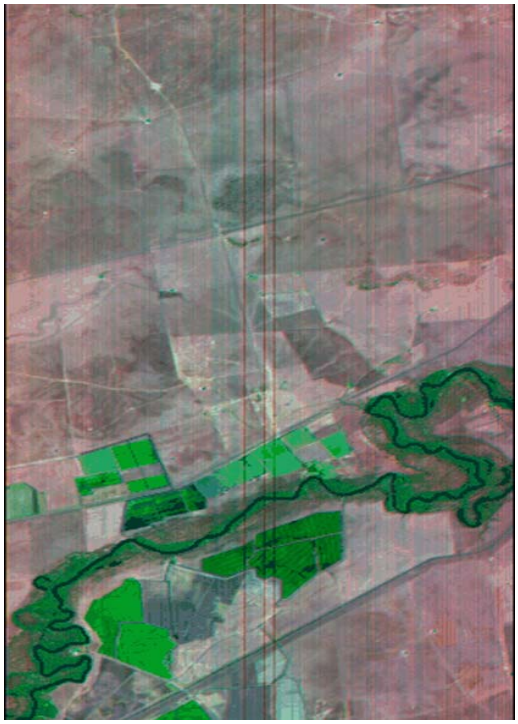

Figure 2.3.1 Early check-out phase of EO-1 mission - Hyperion Image of the Uardry site – January 9 2001 (Uncorrected data).

A team of scientists from CSIRO visited the Uardry site to undertake a careful calibration and validation study and acquired the following data:

- A set of ground-based spectral reflectance measurements at the site;
- Aerosol optical depth information;
- Atmospheric temperature and moisture profiles (radiosonde)
- Radiation data;
- Visual and digital camera measurements of the clear sky;
- Landsat and MODIS data were also collected for this exercise.

The aim of the data collection was to provide important vicarious calibration and validation information for the early check-out period of operation of the Hyperion mission. This activity, and others at Lake Frome and Mt Fitton in South Australia (reported separately) provided vital information at a time when the northern hemisphere was in the depths of winter. A template for the scientific rationale and methodology supporting the field work may be found in the published paper by Prata and Grant (1998).

2.3.2 The Uardry field site

Uardry (34.392 S, 145.304 E, 110m) is a large sheep station situated on the largest plain (prarie) in Australia–the Hay plain. The climate is temperate with most rain falling in the winter months from June to October, but with quite low rainfall totals of around 300 mm annually. The landcover consists primarily of perennial Mitchell grass used for sheep and cattle grazing. The soil is a red-coloured cracking clay. There are few trees and no industry within 200 km of the field site. Skies are generally clean–aerosols arise mainly from smoke particles from bush fires and burning-off episodes, but there are occasional periods of wind blown dust from inland desert sources. The site has been used as a cal/val target for many space and air-borne sensors and has been operational for about 10 years. Time series data of surface radiative fluxes and meteorological parameters such as air temperature, wind speed and humidity are routinely collected both from ground level instrumentation and from levels on a 15m tower that has been constructed at the site. More details of the field site may be found in Prata (1994).

2.3.3 Instrumentation

Instruments are permanently deployed at the field site and collect data in an autonomous fashion. The site uses a distributed network of field instruments to acquire radiation measurements from the surface and sky. The principle measurements pertain to the thermal infrared region, but shortwave (broadband, hemispheric) data from upward- and downward-looking pyranometers are also acquired. The data are relayed to a central computer and stored on disk for later processing. Site visits to download the data and to make routine instrument checks are carried out at roughly 1–2 month intervals.

Table 2.3-1 Instruments and measurements made at Uardry field site on 9 January, 2001.

Instrument	Measurement	Units
CCD Spectrometer	Reflectance	%
MFRSR	Aerosol optical depth	–
Pyranometers	Solar irradiance	W m^{-2}
Pyrgeometers	Thermal irradiance	W m^{-2}
Radiosonde	Temperature profile	K
Radiosonde	Relative humidity	%
GPS	Latitude & Longitude	S, E
Radiometers	Surface radiometric temperature	K

In addition to the routine suite of measurements made at Uardry, a portable radiosonde unit was used for this mission to measure atmospheric profiles of temperature and moisture and a CCD spectrometer was deployed to collect spectral reflectance data. A computer controlled GPS unit was used to log the positions of the reflectance measurements. Table 2.3-1 lists the instruments and measurements made during the field experiment.

The CSIDAT-2 instrumentation (a system for continuously logging site parameters including albedo and components of the surface radiation balance) was also operating during the experiment. Table 2.3-2 lists the parameters and the locations where they were measured at Uardry.

Table 2.3-2 Routine data collected at the Uardry field site and their locations. T_g is ground temperature, T_a is air-temperature, RH is relative humidity, U is wind speed PAR is Photosynthetically Available Radiation, I_S is shortwave irradiance, I^S is shortwave exitance, I_L is longwave irradiance, I^L is longwave exitance, P_S is surface pressure. Repeated parameters represent a cluster of measurements.

Site No.	Parameters	Longitude	Latitude
00 (Central)	T_g T_g T_g T_g	145°18.28'E	34°23.50'S
00 (Central)	T_a (2 m) T_a (15 m)	145°18.28'E	34°23.50'S
00 (Central)	RH (2 m) RH (15 m)	145°18.28'E	34°23.50'S
00 (Central)	I_s I^s	145°18.28'E	34°23.50'S
00 (Central)	I_L I^L	145°18.28'E	34°23.50'S
00 (Central)	U P_S	145°18.28'E	34°23.50'S
01 (N250)	T_g T_g T_g T_g	145°18.30'E	34°23.35'S
02 (N500)	T_g T_g T_a I_s	145°18.33'E	34°23.27'S
03 (W250)	T_g T_g T_g T_g	145°18.11'E	34°23.50'S
04 (S250)	T_g T_g T_g I_s	145°18.21'E	34°23.66'S
05 (E500)	T_g T_g T_g I_s	145°18.53'E	34°23.53'S
06 (S500)	T_g T_g T_a U	145°18.18'E	34°23.76'S
07 (W500)	T_g T_g T_g I_s	145°17.97'E	34°23.45'S
08 (E250)	T_g T_g T_g PAR	145°18.42'E	34°23.50'S

2.3.4 Data-sets

2.3.4.1 A note on time

For various reasons the data contained in this report use two different conventions for time. These are:

1. Universal time (UT) or Greenwich Mean Time (GMT). The GPS uses UT and the recorded spectra were tagged to this time using the GPS.

2. Local time (LT) or Australian Eastern Standard Time (AEST). AEST=UT+10 hours. Data from the CSIDAT-2 system and the digital camera use this time.

Note that Australian summer time was in force during the field work and this was the time used for synchronising the field work. Australian summer time=UT+11 hours.

2.3.4.2 Reflectance measurements

Reflectance measurements were made using a LasTek triple CCD spectrometer model S1000. The spectrometer and computer were mounted inside a vehicle and a specially constructed boom with fibre-optic mounting was used to position the fibres to view the surface at nadir from a height of about 2 m. The vehicle was driven across the field site, traversing from each of the satellite sites towards the central site and then two other legs were conducted along the dirt road and from the eastern most site (E500) to the northern most site (N500) along a near constant bearing of 290° to N. GPS readings were taken every 2 s and logged on a separate computer. The spectrometer was shaded and maintained at a near constant air temperature while taking the measurements.

The spectrometer operates over three separate intervals: 200–575 nm (the master channel), 360–850 nm (slave 01 channel), and 530–1000 nm (slave 02 channel). The spectral resolution of the measurements is between 0.5 and 1 nm, but subsequent processing of the data resamples the reflectances at 1 nm intervals starting from 350 nm and ending at 950 nm. Prior to and during the field measurements, it was noticed that slave 02 channel was rather noisy, particularly at longer wavelengths. The reason for this is unknown, but is under investigation.

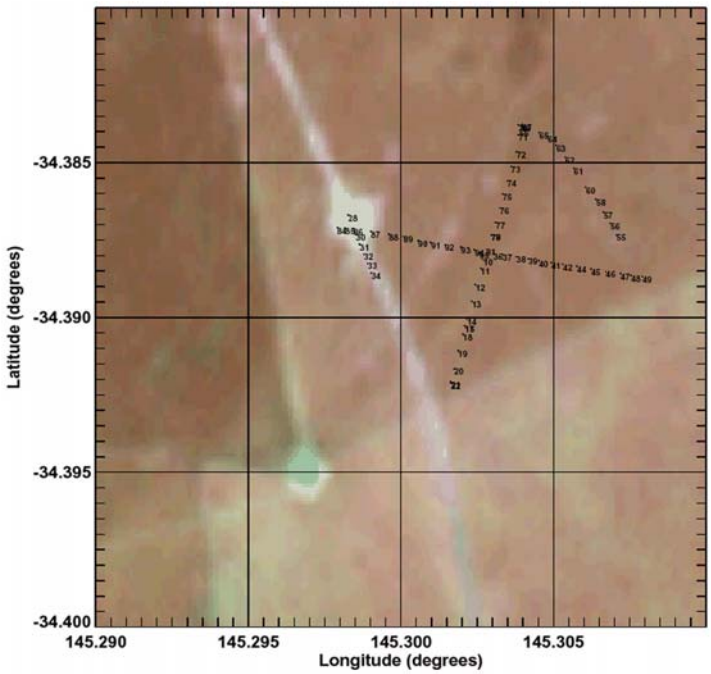

Figure 2.3.2. Landsat-7 image obtained on 7 January 2000 showing locations where spectra were acquired during the field experiment of 9 January 2001. The vegetation state was similar on both dates.

In all, about 300 individual spectra were acquired. The pattern of measurements is shown in Figure 2.3.2. Each number identifies the corresponding spectrum file using the convention: s*2_digit number*.dat, e.g. s11.dat. All of the spectra are archived and available as listed in the Appendix.

Each sample spectrum was acquired with 10 ms integration time and 100 samples were averaged to provide the final spectrum. Thus each spectrum was acquired in about 1 s. Higher integration times tended to saturate the detector under these quite high solar illumination conditions, while lower values tended to be noisier. Every 4–6 data acquisitions, a white panel measurement was made by placing a flat plate covered with A3-size Reflex photocopy paper below the CCD mount. The Reflex plate was used in place of a Spectralon panel, which was unavailable for this experiment. The plate provided a measurement of the spectral solar irradiance within less than 5 minutes of the corresponding sample measurement and using the same illumination and viewing geometry. The Reflex plate was covered when not being used to prevent dirt damaging the surface. The plate had been used in a previous experiment (ACEX, see Prata and Grant, 1998) and its reflectance has been measured with respect to a spectralon panel.

The background image shown in Figure 2.3.2 is a Landsat-7 ETM+ image acquired around the same date as the Hyperion data acquisition, but one year earlier. This image was used as the basis for deciding which parts of the field site reflectance measurements should be made. Essentially at this time of year the vegetation has dried out and is yellow in colour. The height of the vegetation varied from 20 cm to as high as 60 cm in places. Bare soil was noticeable in places around the site, particularly at the eastern edge near the main road. Good representative spectra of the bare soil were obtained by acquiring a transect along the road. Figure 2.3.3 shows photographs of the grass and bare soil at the site.

(a) (b)

Figure 2.3.3 (a) Photograph of a grass site at Uardry. (b) Photograph of the bare soil on the dirt road at Uardry.

2.3.4.3 Radiosonde measurements

Three radiosondes were launched at the site on 9 January at 0830 AEST, 1003 AEST and 1239 AEST. All three flights were successful. Conditions during launch were quite windy with a strong surface wind from WSW. This wind direction seemed to persist up to 850 mb before visual sighting of the balloon made it difficult to ascertain wind direction. The profiles show an inversion around 850–800 mb and some upper level dry regions. The total precipitable water calculated for each flight is 5.23 cm and 4.55 cm (0239 UT). This water vapour amount is quite high for the region and is due to the elevated surface inversion between 1 and 2.5 km above the ground. Despite the high water vapour content, there was no cloud formation.

2.3.4.4 Surface meteorological measurements

Data from the CSIDAT-2 system were downloaded and are provided in analysed files. The data-set consists of:

- Surface pressure (mb) at approximately 2 min intervals
- Air temperature (K) at 2 m at approximately 2 min intervals
- Relative humidity (%) at 2 m at approximately 2 min intervals
- Air temperature (K) at 15 m at approximately 2 min intervals
- Relative humidity (%) at 15 m at approximately 2 min intervals
- Surface (ground) radiometric temperature (K) at approximately 2 min intervals

2.3.4.5 Ancillary data

2.3.4.5.1 Sun's position

Numerical values of the position of the sun at Uardry on 9 January 2001 from 0900 AEST to 1500 AEST are given in Table 2.3-3 every 2 minutes.

Table 2.3-3 The Sun position at Uardry on 9 January 2001. The solar zenith angle is "zen" and the azimuth from North is "azim". Angles are in degrees. Times are Australian Eastern Standard Time (AEST).

Time	zen	azim	Time	zen	azim	Time	zen	azim
09:30	34.20	78.92	09:50	30.18	74.59	10:10	26.26	69.39
09:32	33.79	78.52	09:52	29.78	74.12	10:12	25.87	68.81
09:34	33.39	78.11	09:54	29.39	73.64	10:14	25.49	68.21
09:36	32.98	77.70	09:56	28.99	73.14	10:16	25.10	67.60
09:38	32.58	77.28	09:58	28.60	72.64	10:18	24.72	66.97
09:40	32.18	76.85	10:00	28.20	72.12	10:20	24.34	66.33
09:42	31.78	76.41	10:02	27.81	71.60	10:22	23.97	65.68
09:44	31.38	75.97	10:04	27.42	71.07	10:24	23.59	65.00
09:46	30.98	75.52	10:06	27.03	70.52	10:26	23.22	64.31
09:48	30.58	75.06	10:08	26.64	69.96	10:28	22.85	63.61

2.3.4.5.2 Total column ozone

Strong ozone absorption bands occur at wavelengths below 300 nm in the Hartley-Huggins bands and weaker absorption occurs within a broad band ranging from just above 400 nm to beyond 800 nm–the so-called Chappuis bands. Since most of the ozone lies above in the stratosphere, the Hartley-Huggins bands are responsible for removing most of the sunlight below 300 nm (the solar blind region). The Chappuis bands occur at the peak of solar spectrum and so are important for atmospheric correction of hyperspectral data.

Ozone profile data were not measured at the Uardry site and there are few ground-based ozone measurements made in Australia. There are satellites that can provide instantaneous total column ozone at regional spatial scales (100–300 km). GOME on board the ERS-2 satellite is a spectrometer designed to provide total column ozone and some profile information. For our purposes we have obtained the 'fast delivery product' from the web site operated by KNMI and sponsored by ESA. The URL is: http://www.knmi.nl/gome_fd/. The ozone amount given for 00 UT on 9 January 2001 at 34.3 S, 145.4 E is 275.8 DU. (Dobson units).

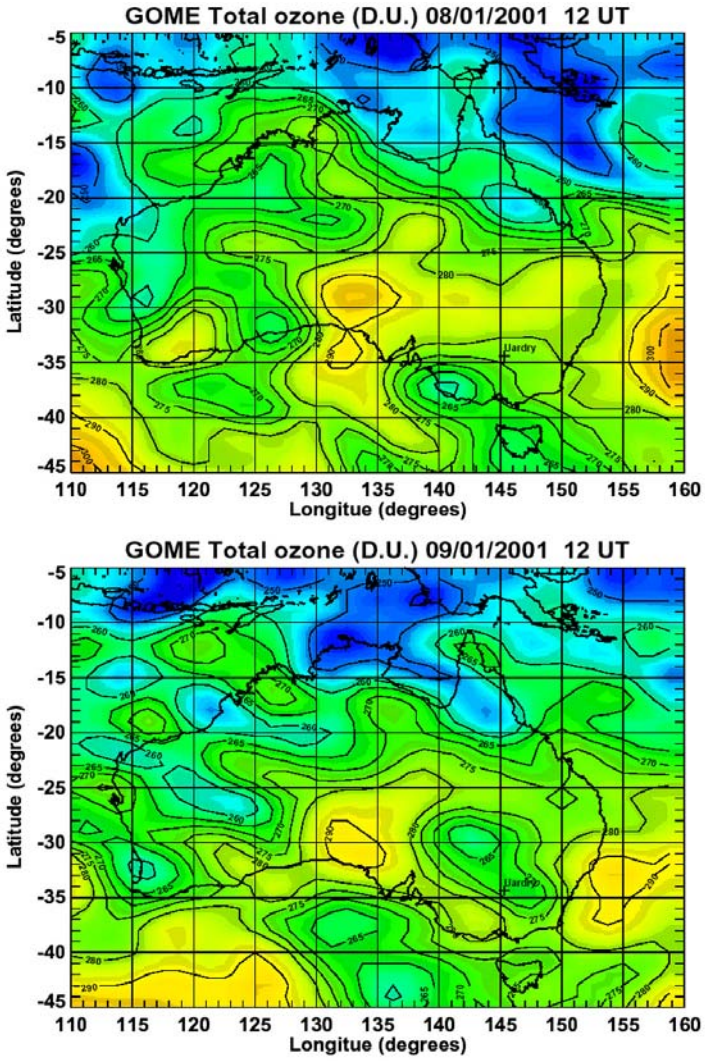

Figure 2.3.4 Assimilated GOME total ozone (Dobson units, DU.)
(a) for 8 January 2001 at 12 UT; (b) for 9 January 2001 at 12 UT

Figure 2.3.4 shows the total ozone derived from a global circulation model assimilating GOME radiances for 8 January (upper panel) and 9 January (lower panel), both at 12 UT. These maps suggest that at the scale of the GOME measurements, the ozone distribution was fairly uniform over Uardry between 8–9 January.

2.3.5 Results

2.3.5.1 Hyperion spectra comparison

The data used in this evaluation were provided directly by TRW and were in an early Level-1 stage of development of the processing chain and calibration of the arrays. The tests described here were focussed on the VNIR sensor and there was no extra pre-processing done to remove remaining image artifacts or other data noise. All comparisons were made directly with no local modifications to the data.

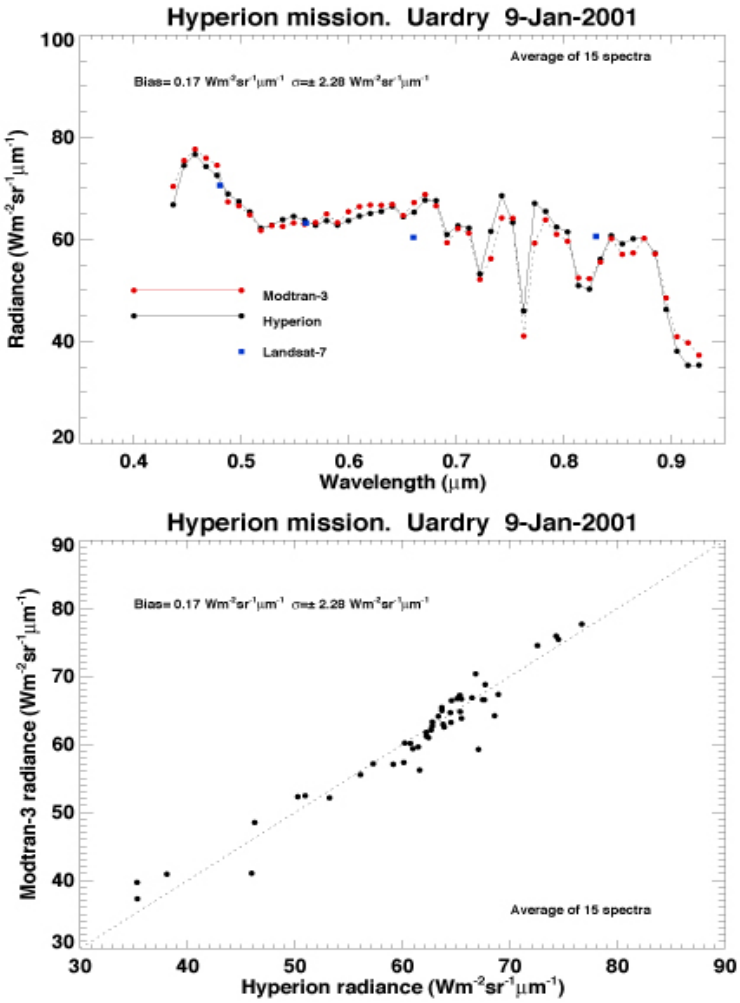

Figure 2.3.5 Modelled top-of-the-atmosphere radiance and Hyperion measured radiances for (a) the spectral region 400-900 nm and (b) as a scatter plot of modelled vs. measured radiances.

At the time of the exercise, investigations using a range of calibration sources (sun, moon, vicarious, on-board lamp) were being used for uniformity correction and absolute calibration improvements. These were subsequently available to the SVT in the Level 1A and higher Level products. A range of these effects can be seen in the Hyperion image at the beginning of this report (Figure 2.3.1).

The methodology used to analyse the Hyperion and other satellite data-sets follows that of Prata and Grant (1998). The ground-based spectra and atmospheric measurements are used in a detailed radiative transfer model (MODTRAN 3) to estimate the top-of-the-atmosphere radiances for each sensor. The modelling depends on the viewing geometry and input data, while the sensor data is crucially dependent on calibration as well as precise knowledge of its viewing parameters. Since the atmospheric conditions are benign, any intercomparison differences are largely due to errors in input data and/or imprecise knowledge of the sensor characteristics. The main result is shown in Figure 2.3.5.

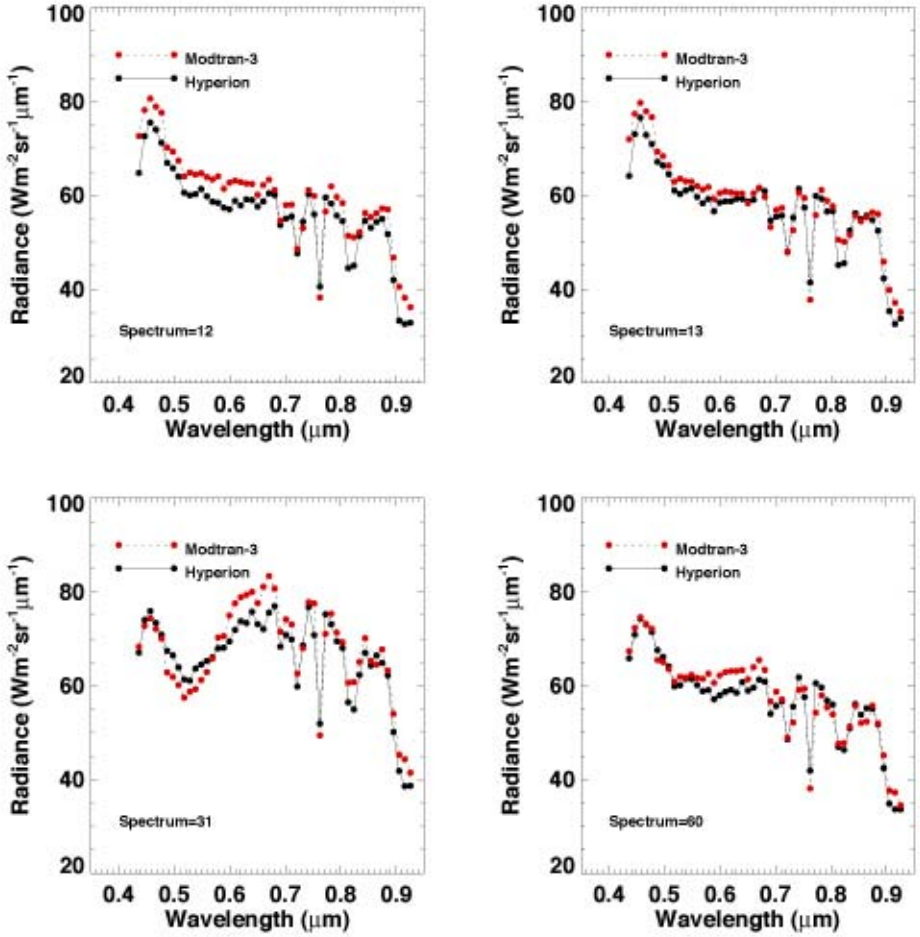

Figure 2.3.6 Comparison of Hyperion spectra with individual ground-based spectra at the Uardry field site.

Figure 2.3.5 shows the Hyperion spectral measurements (400–900 nm) and the MODTRAN modelling estimates obtained from atmospheric data and the average of 15 ground-based spectra. The bias and standard deviation were found to be 0.17 and 2.3 W m^{-2} sr^{-1} m^{-1}, respectively. Figure 2.3.5 also shows a scatter plot of these results with a 1-1 line added. While these results are good, comparisons with individual spectra are not as good, but perhaps this is to be expected given the surface variability at the site and the different fields-of-view of the ground-based and space-based sensors. Figure 2.3.6 illustrates results for individual spectra.

2.3.5.2 MODIS and Landsat wide-band intercomparisons

Data from MODIS (250 m pixels) and Landsat 7 ETM+ were also used to compare with the field data. Figure 2.3.7(a) shows a comparison for a predominantly grass site and Figure 2.3.7(b) shows the result for a predominantly bare site.

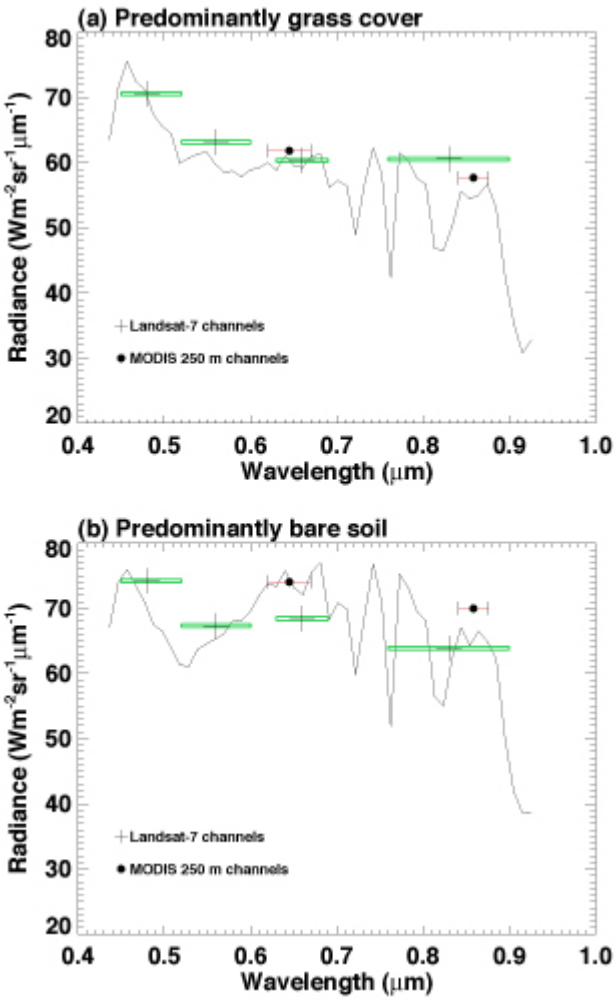

Figure 2.3.7 (a) MODIS and Landsat 7 ETM+ wide-band measurements and modelled radiances at a grass site. (b) As for (a) but at a bare soil site.

For the grass site Landsat and MODIS overestimate the radiances in all bands, while for the bare soil site the results are more variable. The channels at around 600 nm appear to agree well for both sensors compared to the MODTRAN modelling for the grass site, while for the bare site Landsat 7 underestimates the radiances. The sample of measurements is not large enough to make firm conclusions about these sensors, but it appears that both MODIS and Landsat are within 3-6 % of the modelled at-sensor radiances.

2.3.5.3 Hyperion atmospheric correction

Given the good results obtained with the MODTRAN modelling for the Hyperion spectra between 400–900 nm, an attempt was made to perform an atmospheric correction of the data and then compare the reflectances directly with the ground-based spectra. The result for two surfaces (and Hyperion only for a water surface) is shown in Figure 2.3.8.

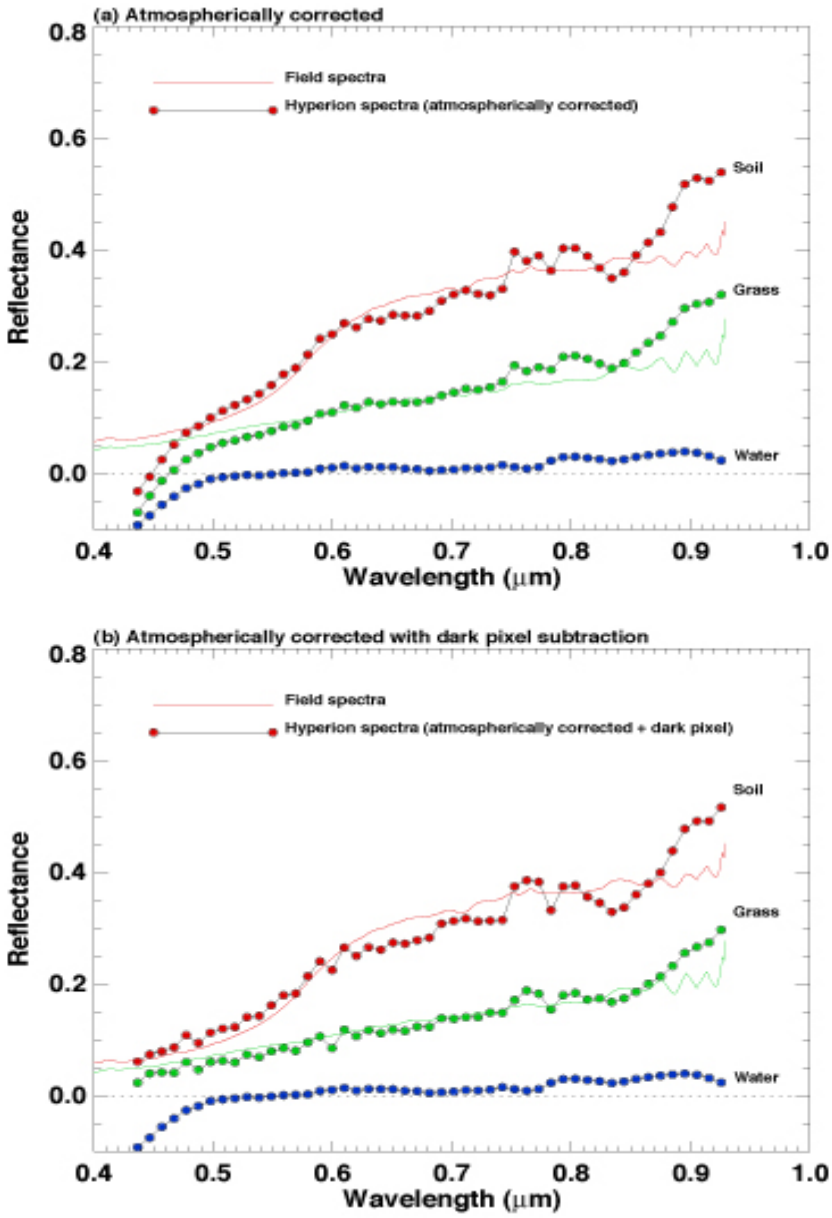

Figure 2.3.8 (a) Hyperion and ground-based reflectance measurements for two surfaces and Hyperion measurements over water. Hyperion data have been atmospherically corrected. (b) As for (a) but with a ``dark'' pixel subtraction procedure applied.

Again the comparison appears quite good, except below 500 nm where the Hyperion data appear to significantly overestimate the reflectance of both surfaces and in water vapour bands which indicate the atmospheric water vapour could have been modified for improved ground spectra. The problem below 500 nm could have been due to poor modelling but was certainly compounded by calibration errors on Hyperion.

[The blue-end (less than 500 nm) calibration was significantly improved for later data releases on the basis of check-out studies such as this one but it has remained an area of some concern in Hyperion data. *Editor's Comment*.]

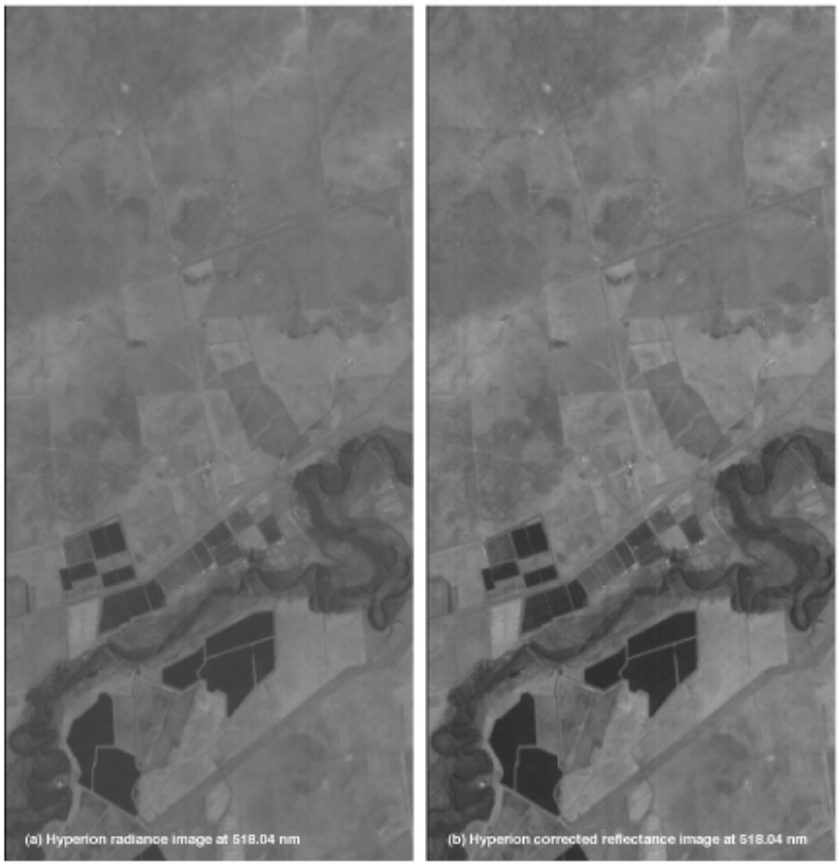

Figure 2.3.9 Uncorrected (a) and atmospherically corrected (b) Hyperion image data of the Uardry field site and environs.

An apparent improvement can be made by performing a 'dark' pixel correction. This is done by subtracting out a constant reflectance based on the darkest pixel in the scene (in this case a river water pixel). The results of doing this correction are shown in Figure 2.3.8(b). Finally, a comparison of an atmospherically corrected and uncorrected Hyperion scene is given in Figure 2.3.9. The corrected image Figure 2.3.9(b) appears to be a little sharper, as might be expected.

2.3.6 Conclusions

A detailed field experiment at a grassland site in Australia has verified that the Hyperion sensor is operating within its specification over the wavelength region 400–900 nm. The bias and standard deviation of the top-of-the-atmosphere radiances within this spectral region are indistinguishable from the anticipated modelling and instrument errors. Good results were obtained through intercomparisons with MODIS and Landsat, suggesting that Hyperion is at least as well calibrated as these sensors. The modelling results suggested that below 480 nm there may be a problem with the Hyperion calibration. This was confirmed by other studies and the calibration (and dark correction) was improved by TRW before data were released to the SVT. However, as noted previously, it remains an area in Hyperion where there may still be improvements to be made. The relatively aerosol-free and cloudless atmosphere

(approaching a Rayleigh atmosphere) at the Australian field site does not challenge the efficacy of the modelling and so we suggest that these results provide an excellent benchmark for gauging Hyperion performance. A list of the data available from the field work and a means for obtaining the data are given in the Appendix.

2.3.7 References

Jupp, D. L. B, 2000: The evaluation of Hyperion performance at Australian hyperspectral calibration and validation sites, *EO-1 Evaluation and Validation* **NRA-99-OES-01**, NASA, Office of Earth Science, Washington, DC 20546, 28pp.

Prata, A. J., and I. F. Grant, 1998: Shortwave calibration of ATSR-2 at Australian land sites, *Proc. of EUROPTO Conf. on Sensors, Systems, and Next-Generation Satellites II*, Barcelona, Spain, 21-24 September, 1998, *SPIE* **3498**, 266–276.

Prata, A. J., Grant, I. F., Cechet, R. P., and Rutter, G. F., 1998: Five years of shortwave radiation budget measurements at a continental land site in southeastern Australia, *J. Geophys. Res.*, **103**(D20), 26,093–26,106.

Prata, A. J., 1994: Validation data for land surface temperature determination from satellites, *Tech. Paper* **33**, 36 pp., CSIRO Div. of Atmospheric Research, Aspendale, Vic., Australia.

2.3.8 Appendix: Available Data Sets for the Uardry experiment

All of the data acquired during this field experiment have been written to CD-ROM and can be acquired by email request to: fred.prata@csiro.au. The data are in ascii and are self-contained. The files are:

1. Spectral data

There are 67 files of spectral reflectance data. Each file is in ASCII. The first line provides a time (UT) and location (latitude and longitude) from the GPS. There follows two columns of wavelength (nm) and reflectance (0–1) values starting at 350 nm and ending at 950 nm in 1 nm intervals.

2. Solar radiation data

The solar radiation data measured from the tower at Uardry are contained in a single ascii file: **solar_data.dat**. There are four columns: Time (hours) Time (minutes) S S. The times are AEST and the irradiances (S is the surface-leaving flux density; S is the incoming solar flux density) are in W m^{-2}.

3. Radiosonde profiles

Radiosonde data are in two ascii files: **us010109002.up, us010109003.up**. Each file consists of 7 columns of data. There is a line of text indicating time of launch, location and the number of records in the file. The columns: Time since start (seconds), Height (km) ,

Pressure (mb) Temperature (C), Vapour Pressure (mb), Relative Humidity (%) and Dew Point Temperature (C).

4. Surface meteorological data

These data are contained in two ascii files:

1.**met_data01.dat** contains time (hrs, min, sec), air temperature at 2 m (K, Ta) and surface temperature (K, Tg).
2. **met_data02.dat** contains time (hrs, min), relative humidity (%) at 2 m (RH2), air temperature (K) at 15 m (RH15), surface pressure (mb, Ps).

2.4 Lake Argyle

Lake Argyle, Kimberley region, north Western Australia

Site Information:

Site P/Co-Investigator(s): Edward King, Susan Campbell, Jenny Lovell, Dean Graetz, Tiit Kutser
Site Name: Lake Argyle
Type of measurement: Surface (water) reflectance
Measurement devices: ASD FR (400-2500 nm)
Type of measurement: In-water spectral profile
Measurement devices: HydroScat, HydroRad
Dates of acquisition: July 16-24, 2001
Latitude: 16º 17'S
Longitude: 128º 41'E
Elevation: 90 m
Surface type: Fresh water
General atmospheric conditions: Clear at Hyperion overpass, some cloud during reflectance measurements on preceding days
Other satellite data: Landsat, ALI, AVHRR
Comments:
Contact email: Edward.King@csiro.au

Report provided by: Edward King & Jenny Lovell
CSIRO EOC

2.4.1 Introduction & Objectives

Lake Argyle is a large (1000 square km) man-made lake in the Kimberley region of northern Australia. It has an associated agricultural region as well as tourism and recreation as uses. Its use as a dark target of satellite calibration has been suggested on a number of occasions and this was investigated for the purposes of the EO-1 mission as well as others of interest to the scientists who visited the area.

Lake Argyle provides a dark target in contrast to Lake Frome (bright target) and has a continuously reading CIMEL aerosol and atmosphere monitoring station in place (Figure 2.4.1) as well as a Nephelometer. Two simultaneous experiments were conducted during the period July 16 to 24, 2001. The objective of the first experiment was to compare the effectiveness of two algorithms for correcting for the influence of aerosols on AVHRR data. The aerosol loading over Lake Argyle in July varies on a daily basis with plumes and sheets of smoke from local and distant biomass burning moving SE-NW across the lake.

Figure 2.4.1 CIMEL being serviced at Lake Argyle during field campaign

The second objective was to measure the apparent optical properties of the lake, and to relate these to Hyperion data from an overpass on July 22. These results and some initial findings using Hyperion data are reported below. Surface radiance of the Lake was measured with a boat-mounted ASD spectroradiometer along six transects, including one aligned with the Hyperion strip. The ASD was mounted approximately 2 m above the water surface and a 1º foreoptic was used. Radiance measurements were made of water and sky consecutively at 30º from vertical along with reference measurements of a Spectralon panel so that reflectance could be measured free of sky reflections from the water surface. Three in-water instruments were also used to measure profiles and surface and bottom reflectance. The in-water measurements were made near the centre of the Hyperion scene at the time of the July 22 overpass. Water samples were taken for analysis of dissolved organic matter, chlorophyll and total suspended matter.

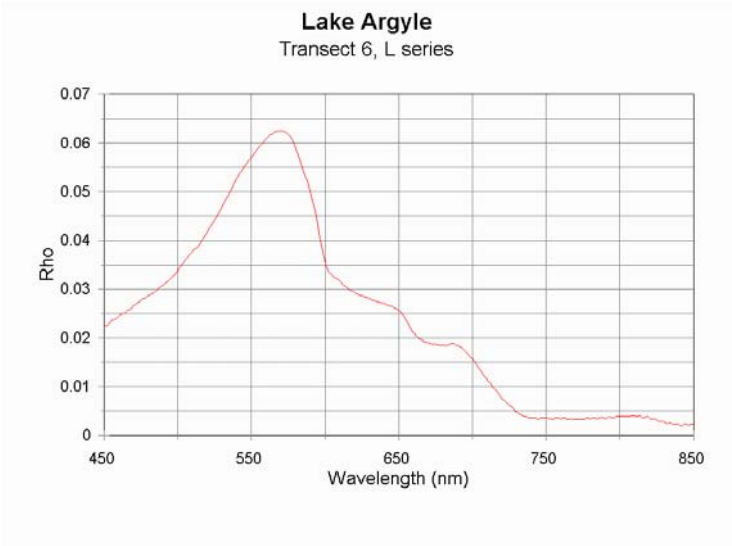

Figure 2.4.2: Average reflectance corrected for sky reflections along Transect 6 of lake Argyle as support for Hyperion calibration and water modelling.

In addition to the spectral measurements, YES MFR shadow band radiometer, LiCor spectroradiometer (total and diffuse irradiance), Exotech radiometers, fish-eye sky camera and weather station (dry bulb air temperature, relative humidity, solar irradiance, wind speed and direction) instruments were operated on the lakeshore from July 16 to 24. The data from this site are still being processed but will be made available to investigators as they become available. The CIMEL data can be accessed via the AERONET web site.

2.4.2 Apparent optical properties of Lake Argyle

2.4.2.1 Introduction

Bio-optical measurements were carried out on Lake Argyle simultaneously with the Hyperion image acquisition on July 22, 2001 in three locations along the Hyperion track. Spectral downwelling irradiance and upwelling radiance just above the water surface and at depths down to 6-7 m were measured with a HydroRad-2. The backscattering coefficient of the water mass was estimated using a HydroScat-6 instrument. Concentrations of chlorophyll-a and other phytoplankton pigments were measured from the water samples using HPLC. The concentration of total suspended solids (TSS) as well as absorption by coloured dissolved organic matter (CDOM) phytoplankton and detritus were also measured from the water samples.

The concentration of chlorophyll-a varied between 2.26 and 3.13 µg/L between the three measurement stations. The pigment composition of the phytoplankton indicated that although levels were generally low, cyanobacteria were the dominating group of the algae present with some presence of diatoms, chlorophytes and cryptophytes. The amount of CDOM was also relatively stable in the lake. Absorption by CDOM at 380 nm varied between 0.819 and 0.885 m^{-1}. The biggest variation was found in the concentration of TSS. The concentration of suspended solids was relatively stable and between 1.8 and 2.2 mg/L in the central part of the lake, but rose to 4.6 mg/L in the shallower southern end of the lake. This may be due to re-

suspension through wind stirring in the shallow part of the lake or river discharge or both. The main inflow into the Lake Argyle is at the southern end.

2.4.2.2 Image processing and classification

The image acquired on July 22, 2001 was cloud free (see Figure 2.4.3). Atmospheric correction to surface reflectance of a pre-processed and locally de-streaked image (as described in Datt *et al.*, 2003) was performed using Modtran 4 with input visibility and water vapour information from the CIMEL instrument that was located at Lake Argyle at the time of the experiment. Attempts to use ACORN and FLAASH atmospheric correction packages were not successful due to the effects of the large body of water on their automatic algorithms. Special issues in the pre-processing that are needed for dark targets such as lakes were also an issue and will be discussed later.

A semi-analytical bio-optical model (Kutser *et al.*, 2001) was used to study the variation seen in the Hyperion image and the results obtained by processing Hyperion data. The model simulations indicated that the variation in amount of phytoplankton observed in the field would not have a significant influence on water reflectance spectra. One of the reasons is the relatively strong absorption by CDOM in the shorter wavelengths that masks the influence of phytoplankton on the reflectance spectra. On the other hand, while the effect of CDOM on the signature is significant, the variation in the amount of CDOM observed in the field is too small to cause significant differences in the reflectance spectra across the lake.

Modelling results confirmed that the concentration of TSS is the dominating factor in the shape of the water spectrum in Lake Argyle as also indicated by the field spectra such as the transect 6 of Figure 2.4.2. In some places, the highest TSS values are very likely due to a component of lake bottom reflectance in the measured signal rather than a very high amount of re-suspended sediments in the water. However, it is difficult to estimate the extent of the influence of the lake bottom on the measured signal since we do not have reflectance spectra of the sediments present in the coastal areas of Lake Argyle.

A spectral library was created using the bio-optical model as a means to map the amount of TSS in Lake Argyle. The chlorophyll-a concentration was fixed at 2.8 µg/L, absorption by CDOM at 380 nm was fixed to 0.84 m^{-1}, and TSS concentrations of 1, 2, 4, 8, 16, 32, 64, and 128 mg/L were used. These spectra were used as templates with the Spectral Angle Mapper (SAM) classifier to allocate water areas to the different categories.

The classification results are shown on Figure 2.4.4 and Figure 2.4.5. The difference between the results is due to the greater level of pre-processing done for Figure 2.4.5 to account for the residual dark current artefacts that occur in water covered areas and clearly observed in Figure 2.4.4 (which had only standard pre-processing) as discussed below.

Figure 2.4.3 Pseudo-true-colour Hyperion image of Lake Argyle acquired in July 22, 2001

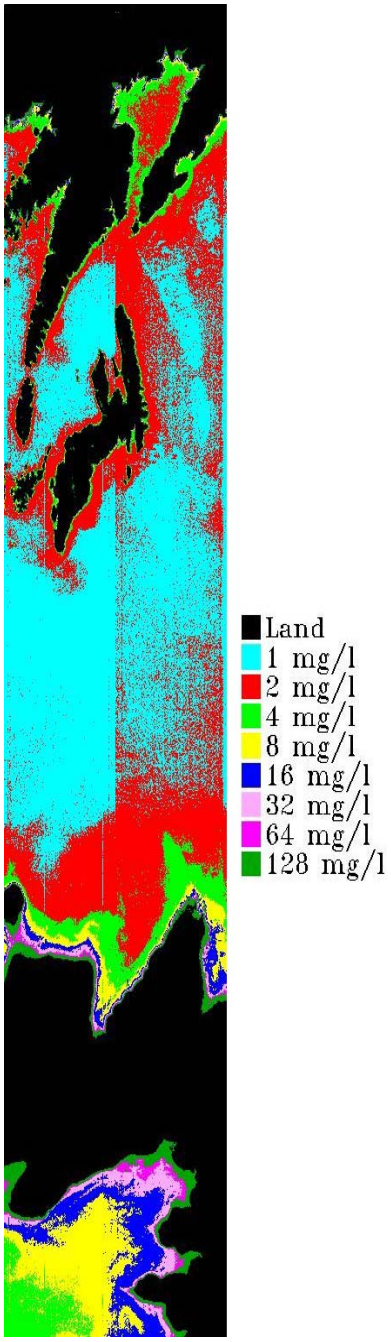

Figure 2.4.4 Map of total suspended solids obtained from the Hyperion image using simulated spectral library and a physics-based method

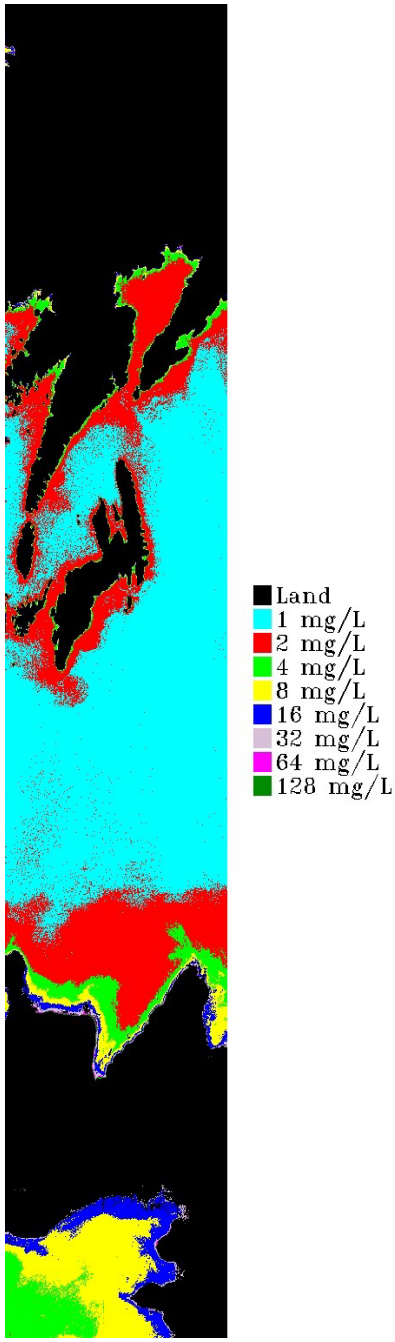

Figure 2.4.5 Map of suspended sediments carried out in the same way as Figure 2.4.4 but with the image pre-processed to remove residual sensor array effects.

The classification results fit quite well with our field data. The direct comparison is shown in Table 2.4-1 for the three measuring stations - one in the shallow southern part of the lake and the other two in the central part of the lake.

Table 2.4-1: Comparison of TSS concentration estimated from the Hyperion image with that derived from water analysis.

Location	Hyperion TSS estimate	TSS sample measured
South, shallow water	4 mg/L	4.6 mg/L
Centre, deep water	1 mg/L	1.8 mg/L
Centre, deep water	2 mg/L	2.2 mg/L

2.4.2.3 Special Pre-Processing of the Argyle Image

The effects that appeared in the classification shown in Figure 2.4.4 prompted a closer analysis of the noise structure over the water areas at Lake Argyle. The image had been subject to standard pre-processing to remove bad pixels, outliers and major "streaking" effects as described in Datt *et al.* (2003). However, over water targets this is not enough and the de-streaking could reduce the image quality unless great care was taken.

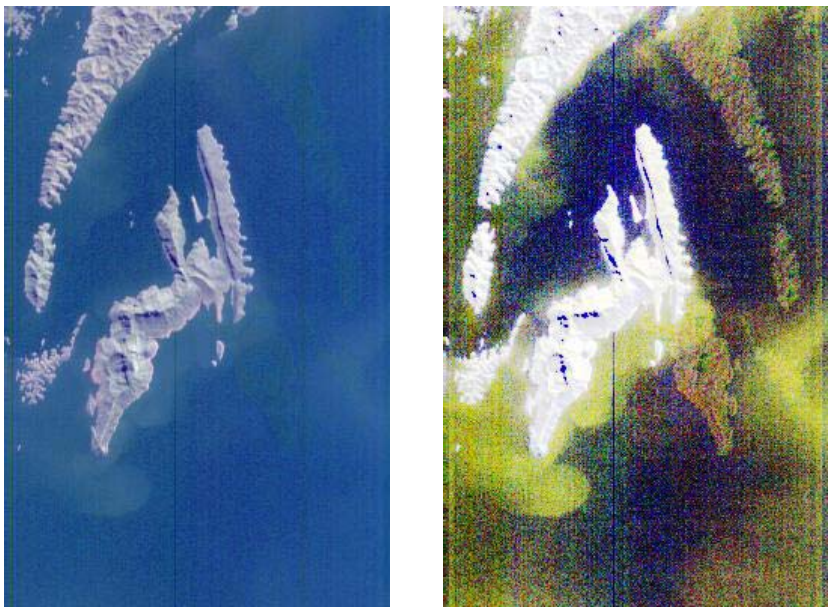

(a) (b)

Figure 2.4.6 (a) General view of a water covered area at Lake Argyle with no pre-processing. (b) Image enhanced by equalisation using bands 17, 18 and 52 to show the "mirror" effect or "ghost" of bright targets.

Figure 2.4.6 shows a subset of the image selected to investigate the effects. Figure 2.4.6 (a) is a colour balanced image to show the normal appearance and extent of the subset while in Figure 2.4.6 (b) the image has been heavily enhanced by histogram equalisation to show how a bright headland and a bright island have been "mirrored" as "ghosts" across the central pixel 128 of the 256 pixels of the image. The effect is quite small but degree of enhancement in this image is due both to the use of histogram equalisation and to the choice of bands (17, 18 and 52) on the two sides the central band 35 of the 70 band VNIR array in Hyperion.

Below this band the ghost increases the brightness of the water while above it the ghost reduces the water brightness.

Figure 2.4.7 shows the same subset with band selections for (a) of Bands 33, 34 and 35 enhanced by equalising within the "zoom" window near the centre of the image in the deep water and for (b) of Bands 36, 37 and 38 enhanced the same way.

(a) (b)

Figure 2.4.7 (a) Enhanced images of Bands 33, 34 and 35. (b) Enhanced image of Bands 36, 37 and 38

The opposite effects of the ghost are seen here but there are also clear imbalances generally between two sides of the central pixel and across the divide at band 35. A number of these effects are seen in the initial classification shown in Figure 2.4.4.

Some reasons for these effects can be found in Pearlman *et al.* (2003). The VNIR array of Hyperion (the first 70 bands) is divided into four quadrants corresponding to Bands 1-35and 36-70 and pixels 1-128 and 129-256. The noise and dark current properties of the quadrants are slightly different at a level that it was assumed was corrected by the dark current correction described in the reference. However, it is clear that over darker water areas where the signal and noise levels are not as well separated as they are in most land images that there is a residual imprint of this array structure that can affect image classification.

The residual imbalances across the image (between pixels 1-128 and 129-256) can also be affected and enhanced by image "smile" (Pearlman *et al.*, 2003) and the best way to reduce the effect in the current case was to use the de-streaking tool used in the standard processing (Datt *et al.*, 2003) to use an offset balancing so that the vertical column mean of pixels within a band where only water is covered become the same. While this may not be applicable where significant gradients exist in an image it has reduced the array effects to below the noise threshold affecting the classification. More work is to be done to find a general solution to this problem.

2.4.2.4 Conclusions

Provided the water areas of the image were also pre-processed to remove artefacts due to detector imbalance and residual dark current effects, the shape and magnitude of atmospherically corrected Hyperion spectra were reliable and fit well with the field data. It was difficult to estimate the suitability of Hyperion for mapping the amount of CDOM and phytoplankton in lakes since concentrations of those substances were low and relatively stable over the lake and the amount of CDOM masked the influence of phytoplankton on the water colour spectra. Variability in the amount of suspended solids was the dominating factor causing variance in Hyperion spectra. A map of the TSS obtained from the Hyperion image gave reliable estimations of TSS concentrations.

There are clearly significant residual dark current and other array effects that need to be corrected in water covered target areas. For example, the mirror or "ghosting" effect across the Hyperion image seen here is common in coastal and other water covered areas where high contrasts exist near the water. The mirror images of the bright targets (such as a peninsula or island) are seen in pseudo-true-colour image, classification results and in ratio images when the ratios are across the divide between bands 35 and 36. The edge between the "true image" and "mirror image" across the two sides of the VNIR array (first 128 pixels and the second 128 pixels) is clearly seen in clearer water (i.e. low reflectance) areas in the classification image of Figure 2.4.4. This effect has been significantly improved by the pre-processing described and work should be done in the future to establish the best ways to overcome them in general processing of water covered targets.

2.4.2.5 References

Datt, B., McVicar, T.R., Van Niel, T.G., Jupp, D.L.B. and Pearlman, J.S. (2003). Pre-processing EO-1 Hyperion hyperspectral data to support the application of agricultural indexes. *IEEE Transactions on Geoscience and Remote Sensing*, vol. **41**(6), 1246-1259.

Kutser T., A. Herlevi, K. Kallio and H. Arst (2001). A hyperspectral model for the interpretation of passive optical remote sensing data from turbid lakes. *The Science of the Total Environment*, **268,** 47-58.

Pearlman, J.S., Barry, P.S., Segal, C.C., Shepanski, J., Beiso, D. and Carman, S.L. (2003). Hyperion, a space-based imaging spectrometer. *IEEE Transactions on Geoscience and Remote Sensing*, vol. **41**(6), 1160-1173.

3 APPLICATIONS SITES & FINDINGS

3.1 Tumbarumba

Site Information:

Site P/Co-Investigator(s): Nicholas Coops, Mary Martin, Marie-Louise Smith and Alex Held
Site Name: Tumbarumba
Type of measurement: Leaf reflectance, leaf biochemistry, forest inventory data, fluxes of carbon, water and energy, plus meteorological data at time of overpass.
Measurement device: ASD FR (400 nm - 2500 nm)
Dates of acquisition: 25th December 2000, 1st April 2001, 19th May 2001
Latitude: S 35º 45'
Longitude: E 148º 15'
Elevation: 1200m
Surface type: Forestry (Eucalyptus, Radiata Pine, pastures, summer crops, lake, riparian vegetation)
General atmospheric conditions: Clear -to- partial clouds
Other satellite data: Landsat ETM, Limited IKONOS
Comments: 5m HyMap data and CASI-2 airborne data are also available. Project is collaboration between CSIRO and University of New Hampshire and United States Forest Service.
Contact email: Nicholas.coops@csiro.au

Report prepared by: Nicholas Coops
CSIRO Forests & Forest Products

3.1.1 Introduction & Objectives

The Tumbarumba field site in South-East Australia is the focus of recent studies as part of CSIRO's ongoing soil and forest productivity project (see **http://www.ffp.csiro.au/nfm/mdp/**). The Tumbarumba study area is adjacent to the Snowy Mountains in southern New South Wales and covers 50,000 ha. Altitude varies from 400 m in the north-east to a maximum of 1438 m at Granite Mountain. It has a cool to cold moist sub-alpine climate with a mean annual rainfall of 680-1800 mm, with most of the area receiving approximately 1400 mm. As part of ongoing projects, the area has been extensively studied and modelled using forest growth and process based models driven in part by remote sensing inputs, to predict and assess native eucalypt forest productivity. Research has also focused on development of a GIS-based spatial soil model including development of soil fertility and soil water holding capacity indices that are integrated within a spatially disaggregated forest growth model. The region is shown in Figure 3.1.1

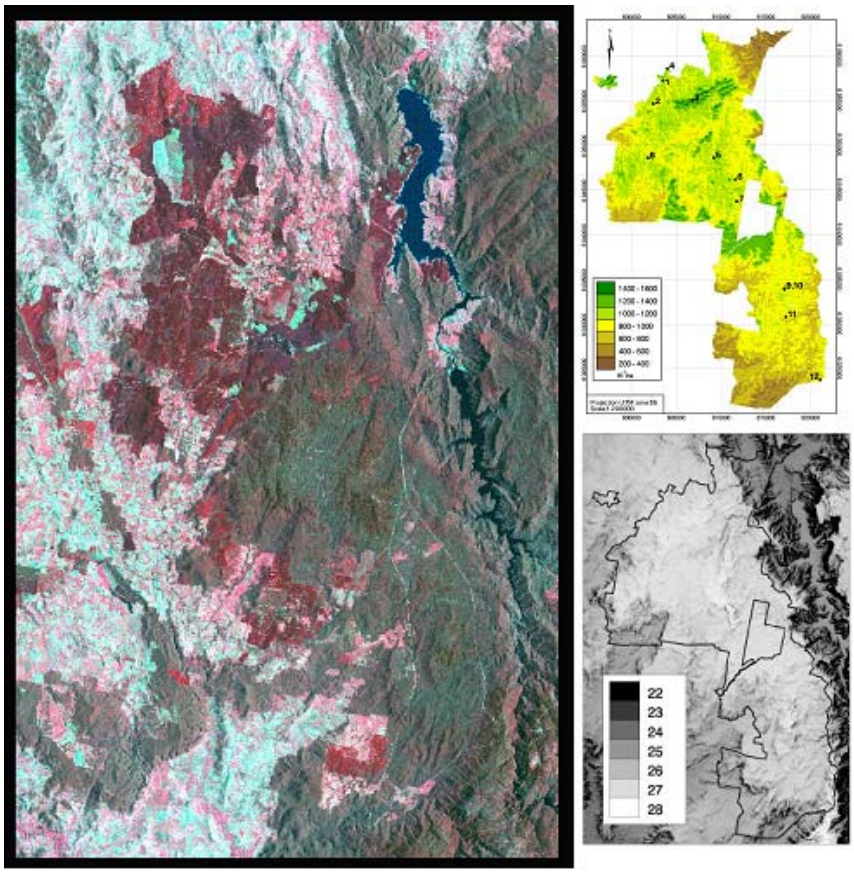

Figure 3.1.1: Landsat 7 ETM+ image of the Tumbarumba area and maps of the forestry areas

As part of the validation of the earth observing capability of EO-1, this site has ongoing programs of research directed at the potential for remote estimation of forest canopy properties including Leaf Area Index (LAI) and foliar chemistry in conjunction with ongoing measurements of forest productivity. This site allowed researchers to evaluate the capacity of the Hyperion sensor on EO-1 to predict concentrations of canopy nitrogen for a range of eucalyptus species in Australia.

A total of 14 plots were located within the study area covering the full range of eucalypt species present. For determination of leaf-level foliar chemistry, leaf samples were taken as shown in Figure 3.1.2, then taken to the laboratory where they were dried and ground through a mesh sieve and wet leaf chemistry was undertaken to extract nitrogen (N) and other nutrient concentrations. Plot level whole canopy biochemistry concentrations (such as N in g N of foliar biomass) were calculated as the mean of the foliar N concentration for individual species in each plot weighed by the fraction of canopy foliar mass per species. Canopy total leaf area was estimated using a camera-based point quadrat sampling technique, hemispherical photography and a LICOR 2000 instrument (Coops *et al.*, 2004).

Figure 3.1.2 Collecting leaf samples (a) Getting base material (b) Selecting samples

The overall objectives of the work carried out at Tumbarumba during the EO-1 mission were to investigate the capacity of ground-based, air and satellite based spectral measurements to estimate eucalypt canopy pigment and bio-chemistry concentrations at the leaf, canopy and forest stand scale. This report focuses on the prediction of foliar biochemistry at the forest stand scale using imagery obtained from the HYPERION sensor on EO-1, in particular nitrogen and phosphors predictions. In addition the use of multiple forest sites around the world allows ongoing work to assess the extent to which these estimates can provide robust and accurate predictions of forest canopy condition and growth in context with other biomes and functional types.

3.1.2 Hyperion Data Processing

A cloud-free, good quality, Hyperion scene was acquired over the Tumbarumba site on the 1st April 2001. Level 1A Hyperion imagery contains both systematic and random noise, such as "bad" pixels, vertical striping and atmospheric effects which are different for Hyperion's two spectrometers. Removing or minimising these effects is not trivial and a number of papers in the IEEE Special Issue on EO-1[7] describe methods such as fixing bad and outlier pixels, local de-striping and atmospheric correction smoothing to obtain improved results. In this paper the HYPERION imagery was pre-processed within the ENVI image analysis software package (RSI 2001) using a series of pre-processing routines developed by CSIRO (listed and discussed in detail by Datt *et al.*, 2003). The pixel shift between the VNIR and

[7] "Special Issue on the Earth Observing 1 (EO-1) Mission"**,** *IEEE - Transactions on Geoscience and Remote Sensing*, **41**(6), June 2003.

SWIR spectral planes, which was not corrected in Level 1A data, was corrected using routines developed by McVicar *et al.* (2003) and Lawrence Ong (GSFC, Pers. Comm.). Visual inspection of Hyperion data especially in the SWIR bands showed a number of bands with varying balance between the vertical columns in the along track direction of the data. Such along-track effects are common in push-broom systems and are known as "streaks". These streaks were treated as scene-dependent and were corrected using a statistical balancing using the means and variances of the columns of the data image. A linear approach was used that balanced the complete image mean and standard deviation for each column and each channel (Jenny Lovell, CSIRO EOC, Pers. Comm.; Datt and Jupp, 2002). This approach is similar to methods described and analysed by Cudahy *et al.* (2001) and in the section on Mount Fitton in this report. Wavelengths that covered major absorption bands and were significantly affected by water vapour were removed from further processing reducing the data set to 162 spectral channels. These ranged from 446 – 2406 nm and were rescaled to calibrated radiance ($Wm^{-2}sr^{-1}\mu m^{-1}$). The imagery was atmospherically corrected using the ACORN Atmospheric correction package (http://www.aigllc.com/acorn/intro.asp) and the co-registered arrays were rectified to Australian Map Grid (AMG) coordinate systems to within 0.5 pixel (15 m) accuracy using six carefully selected ground control points. In this way, Hyperion average reflectance spectra could be obtained for the sampling sites providing spectra as shown in Figure 3.1.3.

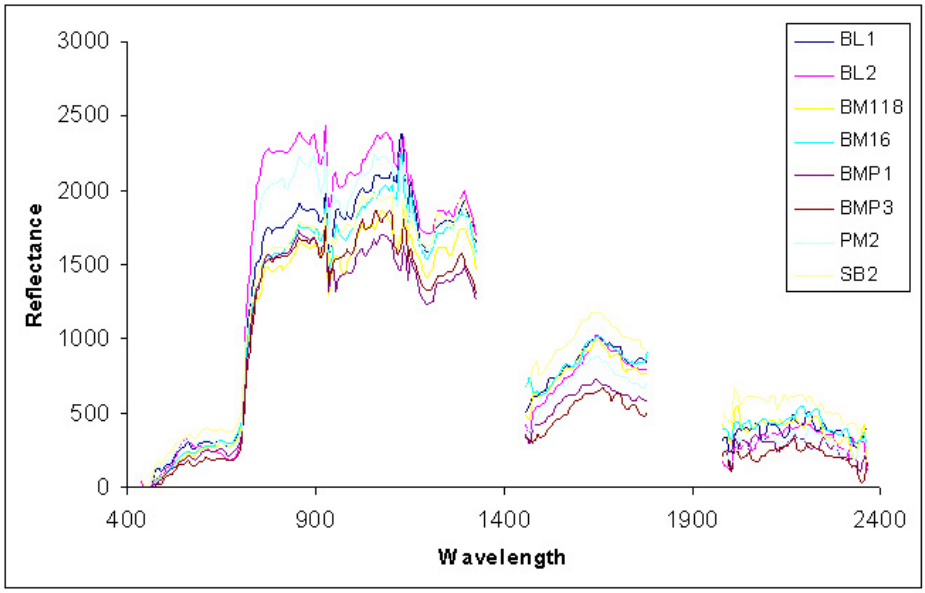

Figure 3.1.3: Average reflectance spectra for Tumbarumba sites based on corrected Hyperion data

Prior to analysis the derived Hyperion reflectance spectra were transformed to absorbance (A) where A = log10 (1/r) and a simple derivative transformation was applied. A Partial Least Squares (PLS) regression method was used for analysis which allows the full spectrum to be reduced or represented by a series of independent variables, or latent factors, which are extracted from a spectra and leaf biochemistry matrix (Shenk and Westerhaus 1991; Smith *et al.*, 2001). From these, regression coefficients are developed for each wavelength that are directly related to the biochemical concentration of interest, while at the same time describing the spectral variation most relevant to the variation in the chemistry data.

A number of models were developed from Hyperion reflectance, absorbance and derivative transformations using partial least squares regression. The most significant calibration model predicted N with a correlation coefficient r = 0.9 (82% variance explained) and a validation r^2 = 0.62 (P < 0.01). Figure 3.1.4 shows the predicted versus observed %N using the PLS absorbance model for both the calibration and validation values.

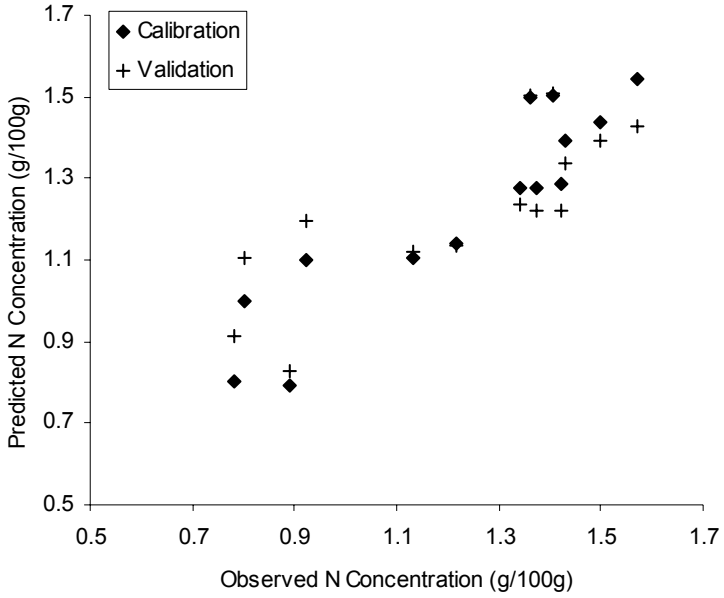

Figure 3.1.4 Predicted versus observed %N using the PLS absorbance model.

The standard error of the estimate of foliar N was 0.16 % equating to 13% of the mean observed %N at the site. Figure 3.1.5 shows the Earth Observing-1 Hyperion image acquired at Tumbarumba (Bago-Maragle State Forest), Australia on 1st April 2001. The image is a greyscale of the 803 nm wavelength reflectance and Figure 3.1.6 presents the spatial prediction of foliar % N (0 – 2%) based on the absorbance model.

3.1.3 Conclusions

The challenge to extrapolate from leaf level biochemistry to canopy and ultimately forest stands is an important one for the remote sensing community. The limited availability and difficulty of obtaining co-incident eucalypt leaf chemistry, whole fresh leaf NIR spectra and airborne reflectance data has previously limited this application to geographically small areas and single mission analysis. The advent of the Hyperion sensor with its space-based platform allows imagery to be acquired and processed over much larger areas as well as to cover many different forest and vegetation communities at the same time. This application of imaging spectrometry indicates that estimates of canopy nitrogen concentrations over large spatial areas are possible. However, the complex speciation of the eucalyptus genus can make the development of generic equations relating spectra to canopy and/or leaf biochemistry difficult. The extent to which the estimates described here can provide robust and accurate predictions of forest canopy condition and growth is the subject of ongoing research and similar studies worldwide will allow these findings to be placed in context with other biomes and functional types. To support ongoing research, data from the Tumbarumba site have been

made available at http://www.eoc.csiro.au under Hyperspectral/Australian Science Validation Team/Data Collections.

3.1.4 Acknowledgements

The Tumbarumba team acknowledges staff at the CSIRO EOC (David Jupp, Jill Huntington, Ray Merton, Bisun Datt, Jenny Lovell) as well as Steve Ungar (NASA) and Jay and Françoise Pearlman (TRW Inc.) whose efforts made this joint research program possible. In addition we acknowledge Tom Van Niel, Tim McVicar and Steve Dury for help with data processing. We also acknowledge the considerable research effort already undertaken by staff at the Tumbarumba long-term forestry site. The joint Australian / US collaboration was made possible by travel grants from CSIRO EOC, CSIRO FFP and the Organisation Economic Cooperation and Development (OECD) Co-operative Research Program. We thank the directors of these programs for their interest and enthusiasm in this research.

3.1.5 References

Cudahy, T., Hewson, R., Huntington, J., Quigley, M., Barry, P. (2001). The performance of the satellite-borne Hyperion hyperspectral VNIR-SWIR imaging system for mineral mapping at Mount Fitton, South Australia. In *Proceedings IEEE International Geoscience and Remote Sensing Symposium*, (CDROM) Sydney, 9-13th July. I: 314-316.

B. Datt, and D.L.B Jupp (2002). Hyperion Data Processing Workshop: Hands-on Processing Instructions. CSIRO Earth Observation Centre, 2002.

Datt, B., McVicar, T.R., Van Niel, T., Jupp, D.L.B., and Pearlman, J. (2003). Pre-processing EO-1 Hyperion hyperspectral data to support the application of agricultural indices. *IEEE Transactions on Geoscience and Remote Sensing,* **41**(6), 1246-1259.

McVicar, T.R., Van Niel, T.G., Jupp, D.L.B. (2003). Geometric validation of Hyperion data acquired by Earth Observing 1 satellite at Coleambally Irrigation Area. CSIRO Land and Water Technical Report 46/01.

RSI (Research Systems Incorporated) (2001). ENVI Version 3.5 October 8, 2001. 4990 Pearl East Circle, Boulder, CO 80301, USA. http://www.ResearchSystems.com/envi

Shenk, J. and Westerhaus, M. (1991). Population structuring of near infrared spectra and modified partial least squares regression. *Crop Science*, **31**: 1548-1555.

Smith, M.L., Ollinger, S.V., Martin, M.E., Aber, J.D., Hallett, R.A., and Goodale, C.J. (2001). Direct prediction of above ground forest productivity by hyperspectral remote sensing of canopy nitrogen. *Ecol. Appl.* **12**:1286-1302.

3.1.6 Publications & Presentations

3.1.6.1 Journal Papers

Coops, N.C., Dury, S., Smith, M.L., Martin, M.M. and Ollinger, S. (2002). Comparison of Green Leaf Eucalypt Spectra using Spectral Decomposition. *Australian Journal of Botany,* **50**, 567 – 576.

Coops, N.C., Smith, M.L., Martin, M.M. and Ollinger, S. (2003). Prediction of Eucalypt Foliage Nitrogen Content from Satellite Derived Hyperspectral Data. *IEEE Transactions on Geoscience and Remote Sensing,* **41**(6), 1338-1346.

Coops, N.C., Smith, M.L., Jacobsen, K.L., Martin, M. and Ollinger, S. (2004). Estimation of plant and leaf area index using three techniques in a mature native eucalypt canopy. *Austral Ecology*, **29**(3), 332 – 341.

3.1.6.2 Conference & Workshop Papers

Coops, N.C., Smith, M.L., Martin, M.M., Ollinger, S.V., Held, A.H. and Dury, S. (2001). Assessing the Performance of Hyperion in Relation to Eucalypt Biochemistry: Preliminary Project Design and Specifications. Proc. IGARSS'2001, Sydney, Australia, July, 2001. Paper: I: 311-313

Coops, N.C., Smith, M.L., Martin, M.M., Ollinger, S.V. and Held, A.H. (2002). Predicting Eucalypt Biochemistry from Hyperion and HyMap Imagery Proc. IGARSS'2002, Toronto, Canada. 24 - 29th June. Paper: 03-06-09.20

3.1.6.3 Media Reports

Forests a blaze of colour from space Date: 03/07/01, Ref 2001/54 **,** http://www.csiro.au/index.asp?type=mediaRelease&id=PrsatelliteA

CSIRO Media: May 2001. A satellite eying our forests. (Available on CD from CSIRO National Science radio).

ABC National Radio (South Australia) 10th March 2001.

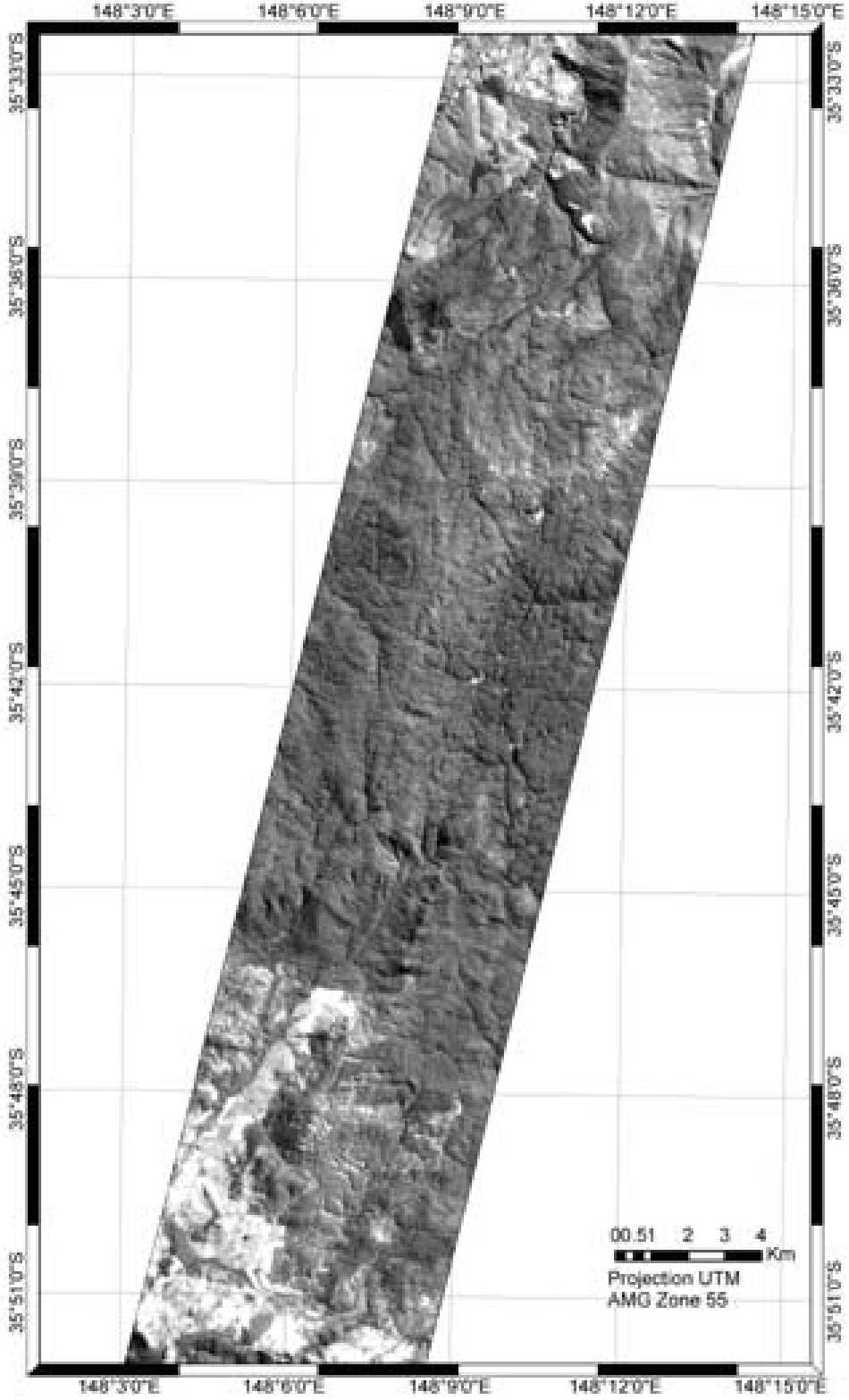

Figure 3.1.5 EO-1 Hyperion image acquired at Tumbarumba (Bago-Maragle State Forest), Australia on 1st April 2001. The image is a greyscale of the 803 nm wavelength reflectance.

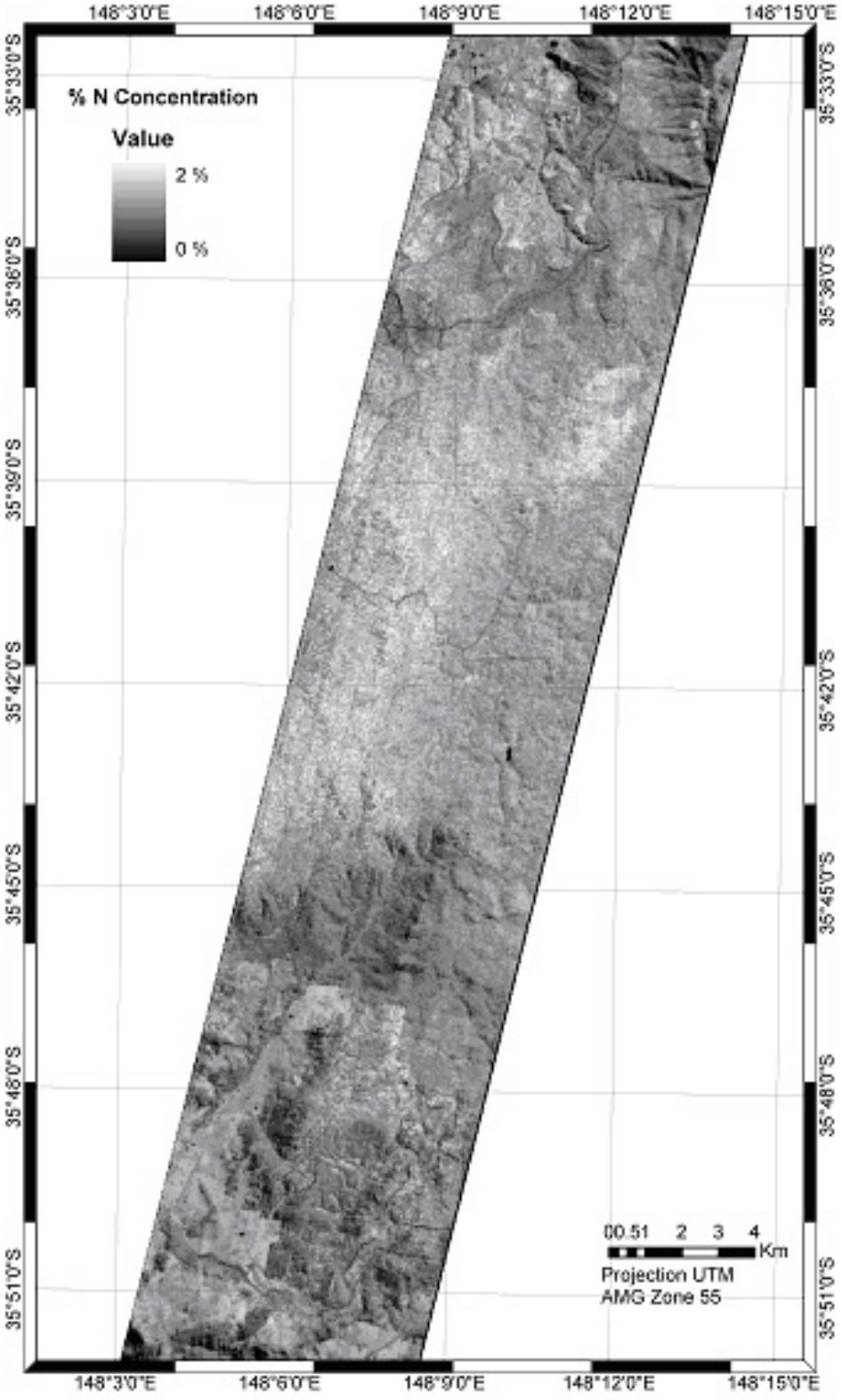

Figure 3.1.6 Spatial prediction of foliar % N (0 – 2%) based on the absorbance model.

3.2 Coleambally

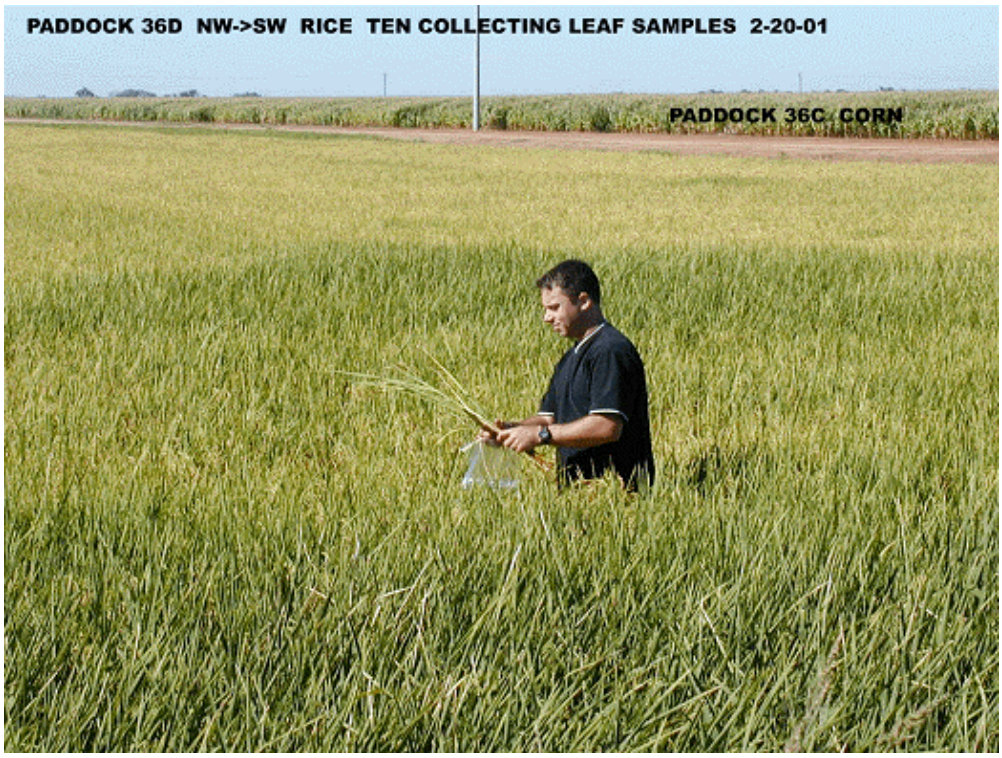

Site Information:

Site P/Co-Investigator(s): Tim McVicar, Tom Van Niel, Jay Pearlman, Bisun Datt & David Jupp
Site Name: Coleambally
Type of measurement: Ground reflectance
Measurement device: ASD FR (400 - 2500 nm)
Dates of acquisition: March 7 2001, January 12, 13, 14, 15 2002, February 13 2002.
Latitude: -34.8012 (34° 48' 4.32" S)
Longitude: 146.0136 (146° 0' 48.96" E)
Elevation: 120 m above mean sea level, with a slope of near 0° (for most purposes CIA can be considered to be “pan flat”)
Surface type: Agriculture (irrigated) Summer Crops are rice, corn, soybeans and sorghum
General atmospheric conditions: Most acquisitions clear
Other satellite data: Landsat 7, TERRA (Modis and ASTER), SAC-C
Comments: Extensive Field Data, HyMap airborne images (two missions) and GIS data sets.
Contact email: tim.mcvicar@csiro.au

Report provided by: Bisun Datt, Tim McVicar & Tom Van Niel

3.2.1 Introduction & Objectives

Australian government agencies, private companies and farmers engaged in agricultural management and food production have been using satellite-based remote sensing products to acquire information such as cropped area estimates, crop type, (inter-)regional effects of weather and yield estimates for at least the last 20 years. The type of information most useful to them has, however, been somewhat restricted for various reasons including limitations of past technology, the small number of fixed broad spectral bands available for analysis, coarse spatial resolution, inadequate repeat cycles of data-gathering and long delivery times for processed data. Many of these limitations are being overcome as currently available satellite based sensor technology improves and ground support and data use becomes more sophisticated. However, the EO-1 Hyperion hyperspectral spectrometer has provided an added opportunity to investigate whether spaceborne hyperspectral data can overcome some of the limitations due to the coarser spectral and spatial resolutions of the satellite data currently available to agriculturalists.

Research at the laboratory and field scales in recent years has established that hyperspectral sensors can provide valuable added spectral discrimination and information through their ability to resolve the broader bands of currently operational systems such as Landsat into a large number of fine bands and access finer spectral features that relate strongly to crop condition. The capacity to provide such spectral information remotely has, until recently, only been available from airborne systems such as the Australian HyMap™ airborne scanner. Airborne systems provide information at different time and spatial scales from spaceborne systems and, in particular, it is costly to use airborne data to acquire repetitive, multi-date regional scale data for general monitoring. Airborne systems are ideal for targeted and time specific (tactical) applications but space platforms can provide advantages of repeatability of data gathering and the ability to cover large areas in a consistent way for routine monitoring and surveillance.

Investigations of these potential advantages have been pursued in Australia in the Coleambally Irrigation Area. The main objectives of the present study have been to:

1. Perform geometric validation of the Hyperion sensor;
2. Develop methods for data pre-processing and noise reduction appropriate for agricultural areas;
3. Atmospherically correct Hyperion images and validate results using ground reflectance data;
4. Assess the consistency between spectral indices derived from Hyperion and ground based reflectance data;
5. Develop a time series of Hyperion reflectance data;
6. Establish the benefits obtainable for hyperspectral time series relative to equivalent series of multispectral data.

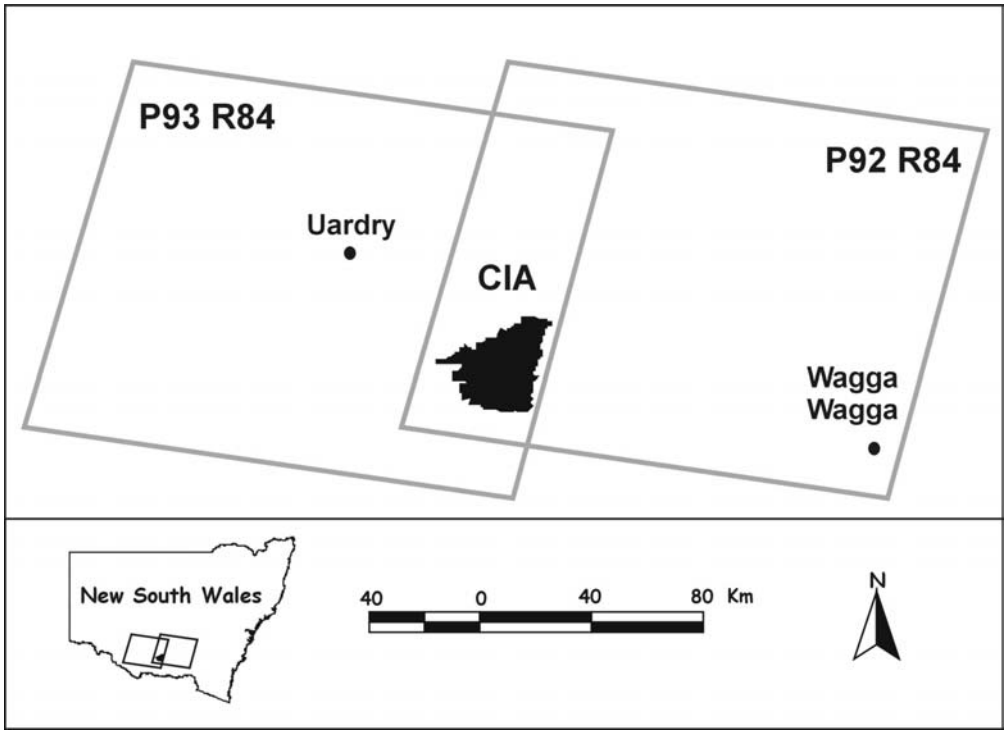

Figure 3.2.1 The CIA falls completely within two Landsat ETM+ scenes, allowing for an 8-day repeat cycle.

3.2.2 The Coleambally Site

The Coleambally Irrigation Area (CIA) in New South Wales, Australia, is a large (95,000 hectares) agricultural area that contains more than 500 farms. The CIA is flat and is covered by large, uniform fields of a number of crop types as well as a range of associated landcovers. The crops grown in this area include a number of strains of rice as well as corn, soybeans, and sorghum. In addition, there are large fallow fields that provide opportunities for calibration. The area falls entirely within the overlap area of two Landsat Enhanced Thematic Mapper (ETM+) scenes making it possible to acquire both Landsat and Hyperion imagery on an eight-day repeat cycle (see Figure 3.2.1).

A time series of cloud-free 12 Hyperion images of the area was acquired over the 2001-2002 Southern Hemisphere summer growing season (Figure 3.2.2). Field visits for on-site ground sampling were carried out several times during the growing season to validate spectral signatures received from Hyperion and collect ancillary information for data interpretation. In addition, data from the HyMap™ airborne hyperspectral imaging spectrometer at 5 meters spatial resolution was acquired on two occasions (December 8, 2000 and January 12, 2002) to provide reference high resolution and high quality hyperspectral data for significant areas of the CIA. To establish an accurate geographic base for the data acquired, use was made of a high-resolution digital air photo mosaic that is acquired over the CIA every January (Figure 3.2.3).

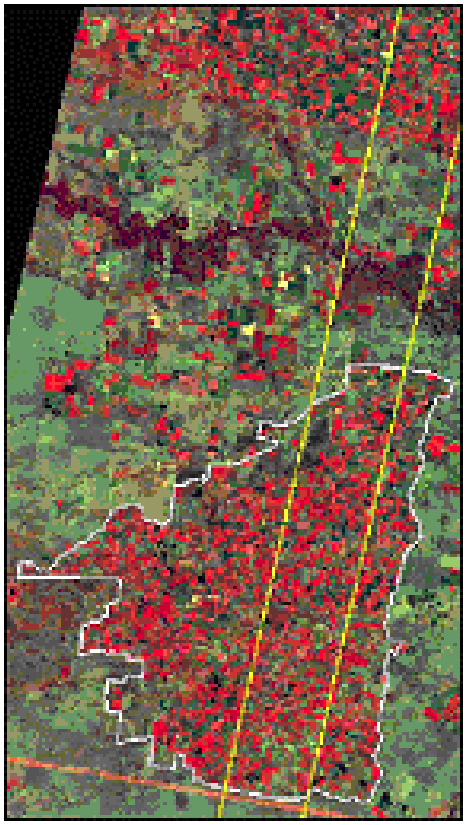

Figure 3.2.2 Site of Hyperion image acquisitions on ETM background. Yellow lines show the Hyperion track.

Figure 3.2.3 High resolution digital air photo acquired in January 2001 to support the 2000/2001 summer (Southern Hemisphere) growing season

In this study, a systematic set of processing steps has been developed and applied to all of the data to reduce the effects of noise in Hyperion data and in order to produce a consistent time series of measurements that may be valuable for farm management. Such measurements include crop leaf area index, percent canopy cover, chlorophyll and nitrogen content, water content, grain yield, etc. The measurements are currently being based on indices that have

been found from laboratory and airborne studies to be useful in this task. The outcomes and conclusions from this study have been described in Datt *et al.* (2003). The study has also included the provision of publicly available data that may be used for future instrument validation efforts and crop identification (see http://www.eoc.csiro.au under Hyperspectral/Australian Science Validation Team/Data Collections).

3.2.3 Hyperion Data Pre-Processing

Operational geometric correction methods were developed using Hyperion images acquired in the 2001/2 growing season. When the study commenced, the Hyperion and other sensors on EO-1 were still undergoing evaluation and testing. A study of the geometry and capacity for accurate geo-rectification of Hyperion data was undertaken and reported in McVicar *et al.* (2001). The study showed that Hyperion geometry was very stable and relatively uncomplicated being able to be registered to the map base with minimal complexity in the distortion functions used. While the study was progressing, tests were undertaken to establish effective methods for aligning the VNIR and SWIR arrays, which were systematically offset due to the data read-out process. Using two bands (Band 57 from the VNIR array and Band 78 from the SWIR array) comparisons indicated that the uncorrected arrays certainly had a consistent mis-alignment but that proposed processing introduced for the Level 1B1 data had excellent VNIR and SWIR co-registration. On the basis of this study the complete time series has been registered to fractional pixel accuracy between every image pair and to an accurate geodetic base.

The data were delivered as calibrated radiance at sensor. As the EO-1 mission was experimental, the base data processing was improved over the mission due to the work being done by members of the Science Validation Team, including the Australian members. However, a number of data noise sources have remained in the Hyperion data and must be processed using scene-dependent and often application dependent methods. One of these is the existence of very different pixels or "outliers" that do not seem to have a systematic cause but must be located and removed by software on a scene-dependent basis. Most users have needed to use such "spike removal" so that further processing does not make the problems worse by "spreading" bad data values.

Two more systematic sources of noise that also remain in Hyperion data when it is delivered to users are vertical streaking and spectral "smile". Vertical streaking is a residual calibration imbalance that is not consistent and persistent enough to be handled by the standard calibration steps that were carefully "trained" using the solar calibration with very good effect. The remaining effect are found to be different in structure between the VNIR and SWIR arrays and generally need to be overcome by some form of balancing or equalisation of the statistics of the vertical columns of data from the same image pixel as a scene-dependent pre-processing step.

Good streaking noise reduction can often be obtained by (for example) equalizing column means and variances. Figure 3.2.4 shows MNF (Minimum Noise Fraction) Bands 1 and 15 before and after de-streaking by equalising all of the column means and variances to the global mean and variance in each band. The result seems very good.

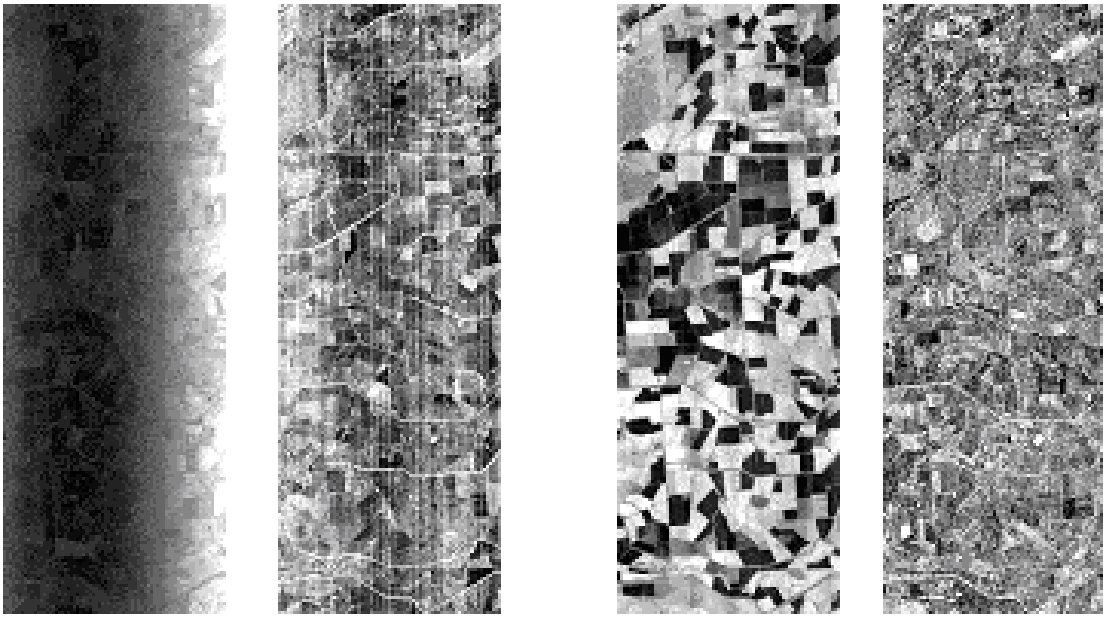

MNF 1 MNF 15 MNF 1 MNF 15

(a) Original Data (b) Globally De-Streaked Data

Figure 3.2.4 MNF Bands 1 and 15 (a) before and (b) after Global de-streaking.

However, due to the scene and landcover dependent nature of the effects – as well as the different properties of the streaking in the VNIR and SWIR data - a number of variations on this simple column equalising needed to be developed for the Coleambally data series. These are described in detail in Datt *et al.* (2003) and include pre-processing to remove outliers and the use of more "local" equalisation methods in the presence of trends in landcover radiance.

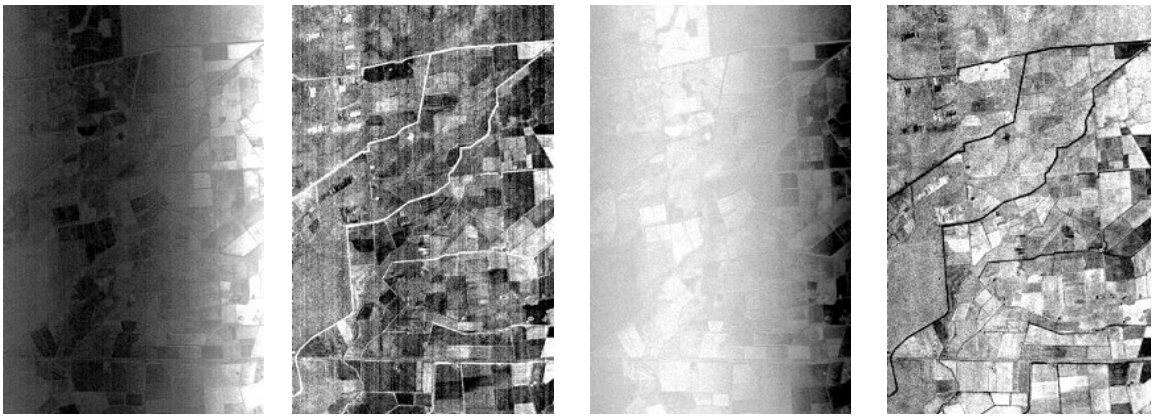

MNF 1 MNF 15 MNF 1 MNF 15

(a) Original Data (b) Locally De-Streaked Data

Figure 3.2.5 MNF Bands 1 and 15 (a) before and (b) after Local de-streaking.

Figure 3.2.5 shows the results from using the local statistics to remove the streaks. In this case the MNF-1 still shows a systematic effect that will be discussed below but the MNF-15 is clear of streaks. The differences and benefits of the methods can be clearly illustrated by looking at the MNF transform of the difference images between the original data and the two

approaches to the de-streaking. The use of the MNF transform highlights the noise effects removed as well as any systematic residuals.

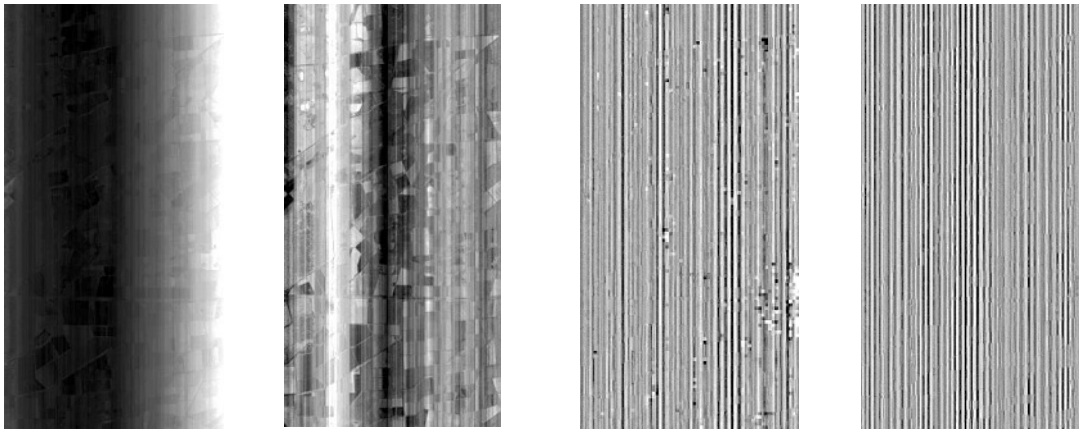

MNF 1 MNF 2 MNF 1 MNF 2

(a) Global De-Streaking Difference Image (b) Local De-Streaking Difference Image

Figure 3.2.6 MNF Bands 1 and 2 (a) for the Global difference and (b) the Local difference showing how Global balancing removes both "smile" and spatial information.

Figure 3.2.6 shows how the residuals of the globally de-streaked data contain the systematic effect that may not be good to have in the data but is not a streaking effect as well as effects due to the spatial distribution of fields with different levels of brightness. These systematic effects are image information and not noise. On the other hand, all of the residuals following local de-streaking are streaks. Difficulties still exist when the streaking occurs in "blocks". This occurs both in the VNIR and SWIR but is more common in the SWIR. Then, as described in Datt *et al.* (2003a) the decision must be how to balance local and global effects.

The spectral/spatial effect of spectral "smile" in Hyperion data has been illustrated clearly in Figure 3.2.4(a) and Figure 3.2.5 where the systematic brightening or darkening at the edge of the scene has been caused by the fact that in a given band, and especially in the VNIR array, the central wavelength of the band varies systematically across the array (from pixel 1 to pixel 256). The effect has been discussed and evaluated for agricultural time series in Jupp *et al.* (2002, 2003) where the nature of the effect is described and its impact on indices evaluated. The effect is very small in the SWIR but it can affect the red edge area in the VNIR that is important for agricultural monitoring. Hence, a first order correction was developed and implemented that has reduced the effect in the red-edge statistics to a level satisfactory for the work intended at Coleambally.

To provide a consistent data series of apparent surface reflectance, the Hyperion data also require atmospheric correction, particularly in regard to spatial and temporal variations in atmospheric water vapour and aerosols as expressed by the atmospheric visibility at the time of the acquisition. The HATCH (Goetz *et al.*, 2002), FLAASH (Cooley *et al.*, 2002), and ACORN™ (http://www.aigllc.com/acorn/intro.asp) atmospheric correction programs were used as they adjust the correction for the amount of water vapour in each pixel. It was found by systematic study for which Coleambally was well suited that all of these methods provided satisfactory normalisation for the time series data (see Figure 3.2.7). However, in all cases some residual noise effects remain that need to be addressed when a series of indices is developed for specific applications. This requires that extra application-specific data

cleaning, noise accounting and feature selection be performed as described in Datt *et al.* (2003a).

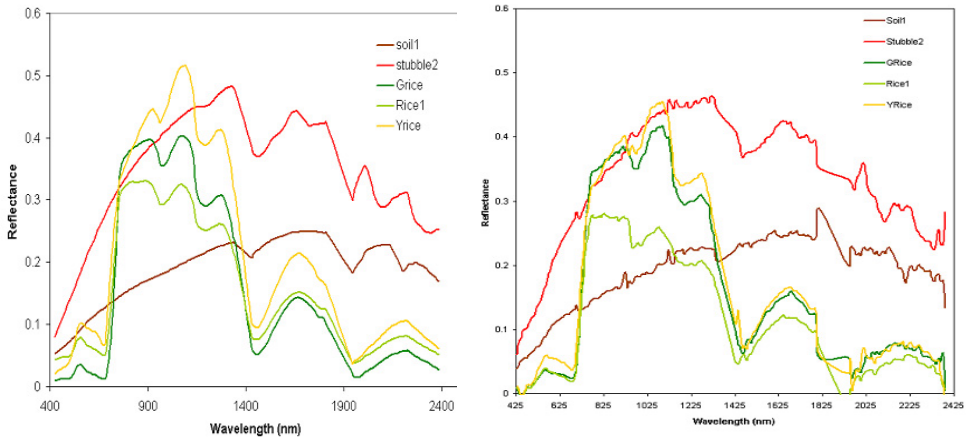

Figure 3.2.7: (a) ASD Field spectra at sites in the CIA compared (b) with estimates based on processed Hyperion data.

The acquisition of a time series of images over two crop growing seasons has produced a large volume of data that has required pre-processing of the kind described here before it can be used to accurately and consistently measure soil and crop constituents. One way to organize the massive data volume is to synthesise or "bin" the Hyperion spectral bands into synthetic Advanced Land Imager (ALI) or ETM+ bands and process the synthetic data into major land cover types. Since atmospheric correction may already have been applied at the fine spectral level in Hyperion data, the binned estimates of reflectance in ALI and ETM+ bands generally exhibit a higher SNR than the ALI and ETM+ data acquired by the respective instruments. Stratification of Hyperion data into synthetic broad bands can thereby allow consistent comparison between fine spectral data and currently available broadband data as well as effective selection of sensor characteristics and associated indices in future remote sensing missions.

3.2.4 Indices for agricultural performance

The applications based work being undertaken has made use of a range of indices that have been used at other sites and in continuing work at Coleambally to measure yield, stress, crop health, crop condition (such as nitrogen content), water content and cover. The indices are transformations, including ratios, derivatives and other mathematical functions that enhance spectral features associated with absorption and (sometimes) scattering. They provide enhancements and feature selection for classification and also inputs to regression and other models relating to quantities such as chlorophyll, liquid water or proteins that are important measurements of crop health. In many cases, they are already the basis of operational laboratory-based methods for taking these measurements. In such cases, remote sensing is seen as taking an established procedure from the laboratory into the air and on to a space platform. A more complete discussion of the indices being investigated at Coleambally can be found in Datt *et al.* (2003a).

To illustrate the benefits of the pre-processing, the major such spectral regions providing the opportunities for the work are briefly summarized in Table 3.2-1.

Table 3.2-1 Common spectral features for crops and soils

General Spectral Region (nm)	Indication
400 to 700	PAR region – photosynthetic pigments
680	Chlorophyll absorption
700 to 750	Red Edge (Chlorophyll)
Near 980 and 1200	Liquid water Absorption
1080 to 1170	Liquid Water Inflection
1700 to 1780	Various Leaf Waxes and Oils
2100	Cellulose
2100 to 2300	Soil properties (clays)
2280 to 2290	Nitrogen / Protein

The value of indices based on these particular spectral regions (such as the derivatives and other enhancements mentioned above) is well established from airborne remote sensing and through the use of hand-held spectrometers as well as laboratory studies. The capacity for Hyperion data to measure the indices from space has been assessed and it has been found that many of the indices based on spectral features like those displayed by the spectra in Figure 3.2.7 can be successfully extracted provided the data are pre-processed using methods as outlined above.

For example, one of the indices assessed in this study was the soil clay index, measured as the area of the clay absorption feature at 2203 nm. This feature is clearly identifiable in four of the spectra (the soil spectra) in Figure 3.2.7 and is a feature of the kind of soils common in the Coleambally region and in the areas where cropping is best located. The plots in Figure 3.2.8 show the improvement in the correlation between the soil clay index values derived from ground based ASD data and Hyperion reflectance before and after standard pre-processing and an additional noise reduction due to "MNF smoothing". The MNF smoothing was found to be most effective in the SWIR data region and consisted of removing MNF components of small magnitude from the data in MNF space and "rotating" the transformed data back into the space of the original data. It is necessary to remove the streaking effect before this action to ensure its best effects on image data quality. For other features it may be better to use other approaches – such as smoothed derivatives. Some different approaches taken for various other indices are outlined in Datt *et al.* (2003a).

If the data are effectively pre-processed and atmospherically corrected then data series consistent with those obtained from airborne instruments can be derived (albeit with lower SNR) from the space data. However, an extensive time series such as that obtained from EO-1 would be prohibitively expensive if obtained through airborne data acquisition. Acquiring airborne data would need some specific "trigger" of value to the farmers to activate a mission and analyse the detailed data it can provide. It is possible that routine and strategic space-based data acquisition can be used to provide such "triggers" to activate tactical airborne and ground based missions which thereby combine the benefits of both platforms.

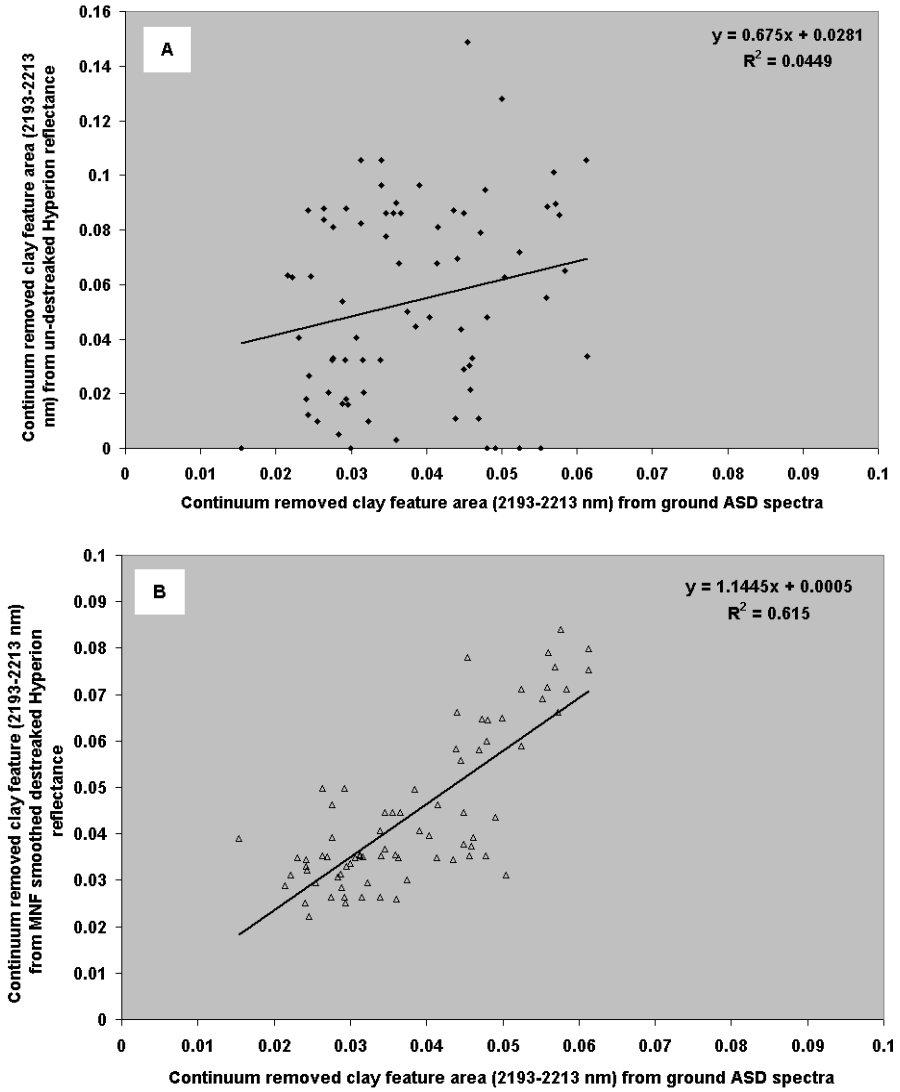

Figure 3.2.8: ASD clay index vs clay index from: (A) un-destreaked Hyperion reflectance, and (B) destreaked, MNF smoothed Hyperion reflectance.

3.2.5 Conclusions

This investigation undertaken at Coleambally over the period of the investigation of EO-1 mission performance by the Science Validation Team has demonstrated effective methods of image pre-processing and noise-reduction resulting in the production of a normalised time series of Hyperion images. The normalisation provides consistent apparent surface reflectance data for input to agricultural index mapping and is a crucial step to the routine provision of reflectance data suitable for agricultural applications. The study has demonstrated how time series of space data from anywhere in the world may be processed for similar purposes. Following this level of processing, the benefits of hyperspectral data processing for agriculture are being assessed with the aim of applying them at a broad scale and for regional surveys and preliminary findings for this time series are outlined in Datt *et al.* (2003b). Satellite data do not displace the need for information that can be acquired in detail on the ground or acquired by airborne scanners but they can provide complementary, repeatable and worldwide regional scale information at affordable costs.

3.2.6 References

A. F. H. Goetz, Z. Qu, B. Kindel, and M. Ferri (2002). Atmospheric correction of Hyperion data and techniques for dynamic scene correction. In *Proc. Int. Geoscience and Remote Sensing Symp. (IGARSS'02)*, Toronto, Canada, III: pp.1408-1410, 2002.

T. W. Cooley, G. Anderson, G. W. Felde, M. L. Hoke, and A. J. Ratkowski (2002). FLAASH, a MODTRAN-4 based atmospheric correction algorithm, its application and validation. In *Proc. Int. Geoscience and Remote Sensing Symp. (IGARSS'02)*, Toronto, Canada, III: pp.1414-1418, 2002.

3.2.7 Publications & Presentations

3.2.7.1 Journal Papers

Datt, B., McVicar, T.R., Van Niel, T.G., Jupp, D.L.B. and Pearlman, J.S. (2003a). Pre-processing EO-1 Hyperion hyperspectral data to support the application of agricultural indexes. *IEEE Transactions on Geoscience and Remote Sensing*, vol. **41**(6), 1246-1259.

Jupp, D.L.B., Datt, B., McVicar, T.R., Van Niel, T.G., Pearlman, J.S., Lovell, J. and King, E.G. (2003). Improving the Analysis of Hyperion Red Edge Index from an Agricultural Area. (for) Society of Photo-Optical Instrumentation Engineers (SPIE), *Journal of Optical Engineering*. (In Review).

Liang, S. Fang H. L., Thorp L., Kaul, M., Van Niel, T.G., McVicar, T. R., Pearlman J. S., Walthall, C. L., Daughtry, C. S. T., and Huemmrich, F. (2003). Estimation of land surface broadband albedos and leaf area index from EO-1 ALI data and validation. *IEEE Transactions on Geoscience and Remote Sensing*. **41**(6), 1260-1267.

3.2.7.2 Peer Reviewed Technical Reports

McVicar, T.R., Van Niel, T.G. and Jupp, D.L.B. (2001). Geometric Validation of Hyperion Data acquired by Earth Observing 1 Satellite at Coleambally Irrigation Area. CSIRO Land and Water Technical Report 46/01.

3.2.7.3 Conference & Workshop Papers

Datt, B., Jupp, D.L. B., McVicar, T. R., Van Niel, T. G., and Pearlman, J. S. (2003b). Time Series Analysis of EO-1Hyperion Data for Yield Estimation at an Agricultural Site. *Proceedings of the International Geoscience and Remote Sensing Symposium*, Toulouse, France 21-25 July.

Jupp, D.L.B., Datt, B., McVicar, T.R., Van Niel, T.G., Pearlman, J.S., Lovell, J. and King, E.G. (2002). Improving the Analysis of Hyperion Red Edge Index. *Proceedings of the SPIE*, Vol. **4898**, 78-92.

McVicar, T.R., Van Niel, T.G., Jupp, D.L.B. and Edge, F. (2002). Remote Sensing Research at Coleambally Irrigation Area. *ACRES Update*, Geoscience Australia. Issue 26, September 2002, 5-8. With accompanying A3 poster.

Pearlman, J.S., McVicar, T.R., Van Niel, T.G., Jupp, D.L.B., Datt, B., Campbell, S.K., Lovell, J.L., Mitchell, R.M., Barry, P. and Liang, S. (2002). Assessing the Value of a Time Series of EO-1 Data for Coleambally Irrigation Area. *Proceedings of the International Geoscience and Remote Sensing Symposium*, Toronto, July 2002.

Van Niel, T.G., McVicar, T.R., Campbell, S.K., Liang, S., Kaul, M., Pearlman, J.S., Clancy, P., and Segal, C. (2001). The Coleambally Agricultural Component of Hyperion Instrument Validation. *Proceedings of the International Geoscience and Remote Sensing Symposium*, Sydney, July 2001.

Liang, S., Fang, H., Kaul, M., Van Niel, T.G., McVicar, T.R., Campbell, S.K., Walthall, C., Daughtry, C. and Pearlman, J. (2001). Land Surface Bio/Geophysical Variable Estimation for EO-1 Data and Validation. *Proceedings of the International Geoscience and Remote Sensing Symposium*, Sydney, July 2001.

B. Datt, D.L.B. Jupp, T. R. McVicar, T.G. Van Niel, J. Lovell, S. Campbell (2002). Spectral Feature Analysis of Crop, Soil and Stubble Using Hyperion and HyMap Data. *Proceedings of the 11th Australasian Remote Sensing and Photogrammetry Conference*, Brisbane, Australia, 2002.

3.2.7.4 Posters

McVicar, T.R., Van Niel, T.G. and Campbell, S.K. (2002). Coleambally Irrigation Area: A Time Series Remote Sensing Site. Presented at the *11th Australasian Remote Sensing and Photogrammetry Conference*, 2-6 September, Brisbane.

Van Niel, T.G., McVicar, T.R. and Edge, F. (2002). Coleambally Irrigation Area, Riverina District, New South Wales. *ACRES Update*, Geoscience Australia. Issue 26, September 2002, A-3 poster.

3.2.7.5 Media Interactions

McVicar, T.R. ABC Radio Wagga Wagga NSW “NASA and Coleambally Irrigation Area” September 5, 2001.

McVicar, T.R. The Weekend Australian “NASA helps beat salinity” September 1-2, 2001, pp 22.

3.3 Kunoth

Kunoth Paddock, Central Australia.

Site P/Co-Investigator(s): Vanessa Chewings
Site Name: Kunoth
Type of measurement (1): Hyperion, ALI
Dates of acquisitions: Dec 2000 – Oct 2001.
Type of measurement (2): Cover and cover type
Measurement device: wheel point
Dates of acquisitions: May 29, 2001
Type of measurement (3): Airborne video transects. 4 transects at 0.2m pixel resolution. 1 transect at 0.5m, 2 transects at 1.0m, 2 transects at 1.7m.
Measurement device: DMSV airborne video 450, 550, 650, 770nm
Dates of acquisitions: May 9, 2001
Type of measurement (4): Ground reflectance
Measurement device: GER 3700.
Dates of acquisition: October 11-16, 2000
Latitude: -23° 33'
Longitude: 133° 34'
Elevation: 700m
Surface type: semi-arid rangelands containing floodplain, open woodland, acacia shrubland.
General atmospheric conditions: Clear
Other satellite data: Multitemporal Landsat 1972 – 2002, SPOT PAN, JERS-1.
Other airborne: Daedelus 1997, HyMap 1998, AIRSAR/TOPSAR 1993, 2000, Master 2001.

Comments:
Contact email: Vanessa.Chewings@csiro.au

Report by:
Vanessa Chewings, Gary Bastin and Janine Kinloch.
CSIRO Sustainable Ecosystems, Centre for Arid Zone Research.

3.3.1 Introduction & Objectives

The Kunoth arid zone application site has high spatial variability of landscape types and vegetation cover. Principal landscapes include grassland, open woodland, floodplain and Acacia shrubland, as shown in the photograph at the start of this report. The interest of the Centre for Arid Zone Research is in the potential of hyperspectral remote sensing to improve understanding of "landscape integrity" as a potentially useful surrogate of biodiversity status in the rangelands (Ludwig *et al.* in press). We use landscape integrity as an integrating concept for landscape function (the extent to which scarce rain-water and plant nutrient resources are retained *in situ*), extent of nutrient cycling and habitat quality (in terms of vegetation composition and structure). High spatial resolution remote sensing such as aerial videography has a demonstrated role for monitoring landscape leakiness (Ludwig *et al.* 2002, Bastin *et al.* 2002). With the opportunity provided by Hyperion data, we have extended this work to test the potential of hyperspectral satellite data to provide suitable information about resource retention and habitat structure at larger scales but with sub-pixel resolution.

Objectives

- Explore data techniques for analysing hyperspectral imagery.
- Test our ability to discriminate levels of soil and the main cover components (trees and shrubs, green vegetation, dry vegetation, litter and shadow) within 30 m Hyperion pixels using spectral unmixing techniques.
- Compare unmixed fractions of soil and vegetation cover within Hyperion pixels to equivalent areas measured with the wheelpoint or aerial videography classified to distinguish similar components.

3.3.2 Site & seasonal conditions

Kunoth Paddock is 160 km^2 in area located 45 km north west of Alice Springs (paddock centred on 23^o 32' S, 133^o 34' E). It is one of several large paddocks on Hamilton Downs station, a commercial beef growing enterprise. Kunoth paddock has considerable landscape diversity including floodplains, grassland, mulga (Acacia) shrubland and open woodland (Figure 3.3.1, Low *et al.* 1978). The site had been used in a number of previous remote-sensing projects; e.g. describing soil erosion processes (Pickup and Nelson 1984), modelling cattle grazing distribution (Pickup and Chewings 1988) and assessing the impact of grazing (Chewings *et al.* 1998).

The climate is arid with generally low but highly variable rainfall. Although the long-term average rainfall is 268 mm, 360 mm was recorded at Alice Springs between October 2000 and April 2001, the period of active vegetation growth associated with our investigation of Hyperion imagery. This and the preceding summer of above average rainfall had produced an abundance of pasture growth with relatively high cover present on much of the area.

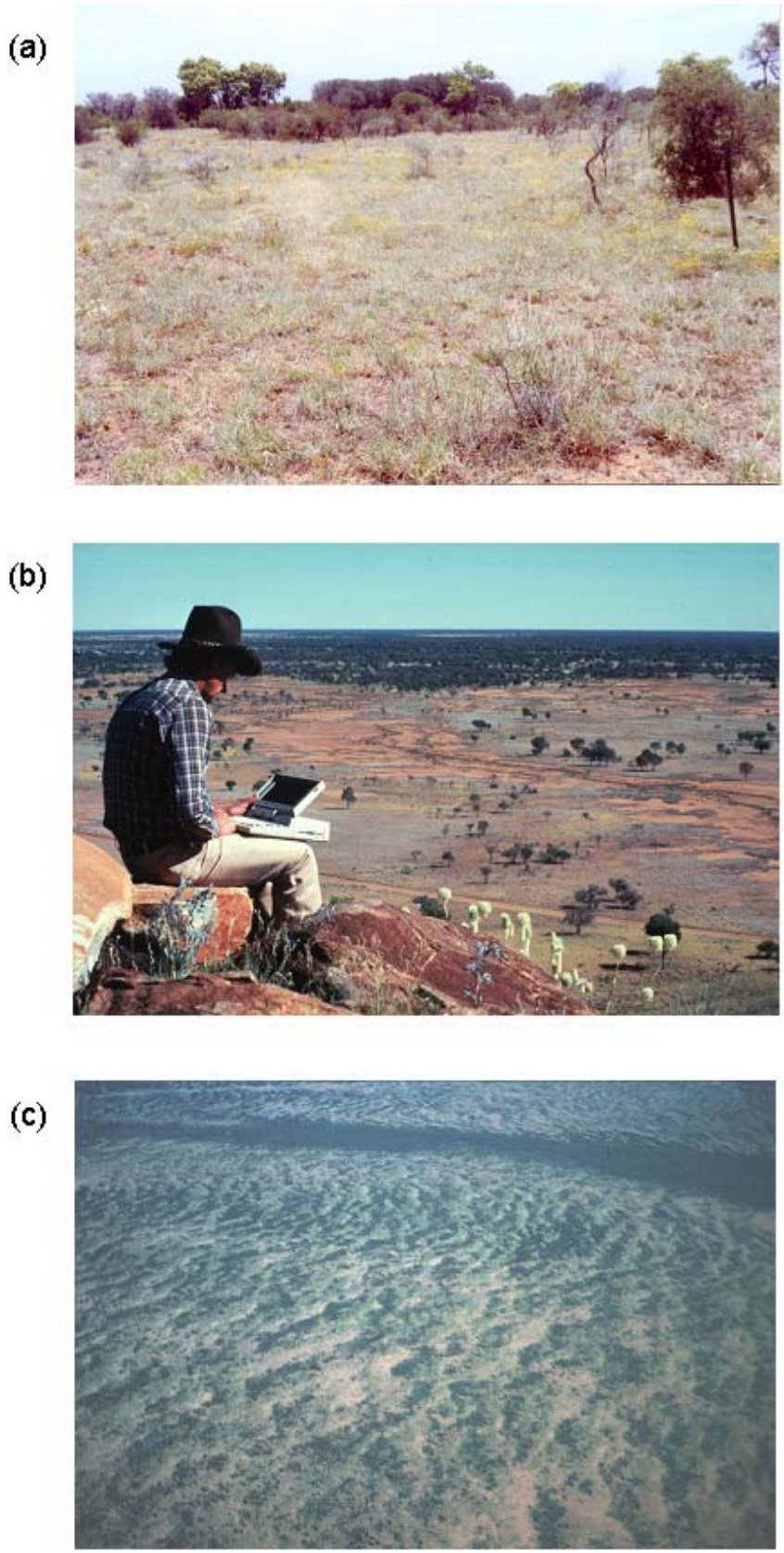

Figure 3.3.1: Example images of landscapes analysed with Hyperion and video imagery: (a) open woodland, (b) floodplain and (c) groved mulga. Photos from the CAZR collection, CSIRO, Alice Springs.

3.3.3 Methods

Hyperion images

A number of scenes from the Hyperion and ALI instruments on board the EO-1 platform were acquired over the Kunoth site during the instrument test phase in 2001. These images provided a north-south swath through the centre of the paddock (Figure 3.3.2). Results reported here are derived from images acquired on February 26, 2001 (herbage layer photosynthetically active) and August 4, 2001 (herbage layer senescent).

We used a combination of ground data and aerial videography to interpret and validate analyses of the Hyperion imagery.

Ground data

Ground data consisted of a limited set of field spectra collected with a GER 3700 (Geophysical Environmental Research, Inc.) spectroradiometer and cover measurements made with a wheelpoint device. The GER 3700 has 650 narrow spectral bands between 330 nm and 2500 nm. Spectral data were acquired on an opportunistic basis during October 2000 and measurements were not repeated during the test phase of Hyperion because of logistics and limited access to a suitable instrument. The dominant grasses, forbs, shrubs and soils were sampled at 11 sites and where possible, sampling covered the different phenological states from actively growing (green) to senescent (litter). These field spectra were used to guide selection of spectral signatures of relatively "pure" features within the Hyperion imagery. These and other Kunoth data have also been made available as part of the EO-1 mission and can be found at http://www.eoc.csiro.au under Hyperspectral/Australian Science Validation Team/Data Collections.

The extent of bare soil and vegetation components (litter, grasses, forbs and woody species) was measured in May 2001 using a wheelpoint device with 1000 points in each of four 1-Ha sites. These sites were located in an area of reasonably homogenous open woodland (Figure 3.3.1(a) and Figure 3.3.2). The species-level data were grouped to match the cover types discriminated by mixture analysis of the Hyperion imagery. The aggregated ground data were then used to validate the within-pixel cover components obtained from unmixing Hyperion imagery.

Aerial videography

Digital aerial video images at a range of pixel sizes (0.2 – 1.7 m) were acquired at various locations within the area covered by Hyperion images. The analyses reported here are for a flight transect of 1-m pixel size acquired along the central portion of the Hyperion imagery in May 2001 (Figure 3.3.2). Imagery was acquired with a Specterra Systems Digital Multi-Spectral Video System (DMSV, details of the system and image correction procedures in Pickup *et al.* 1995a & b). Multi-spectral capacity is provided by four 25 nm bandwidth interference filters centred on 450 nm, 550 nm, 650 nm and 770 nm. Images were corrected for spatial and spectral lens distortion and used to create a mosaic in the AMG coordinate system. The mosaic was classified into broad components of soil, green and dry herbage (mainly grasses), litter, trees and shrubs, and shadow using established techniques of

sequential image classification (Pickup *et al.* 2000).

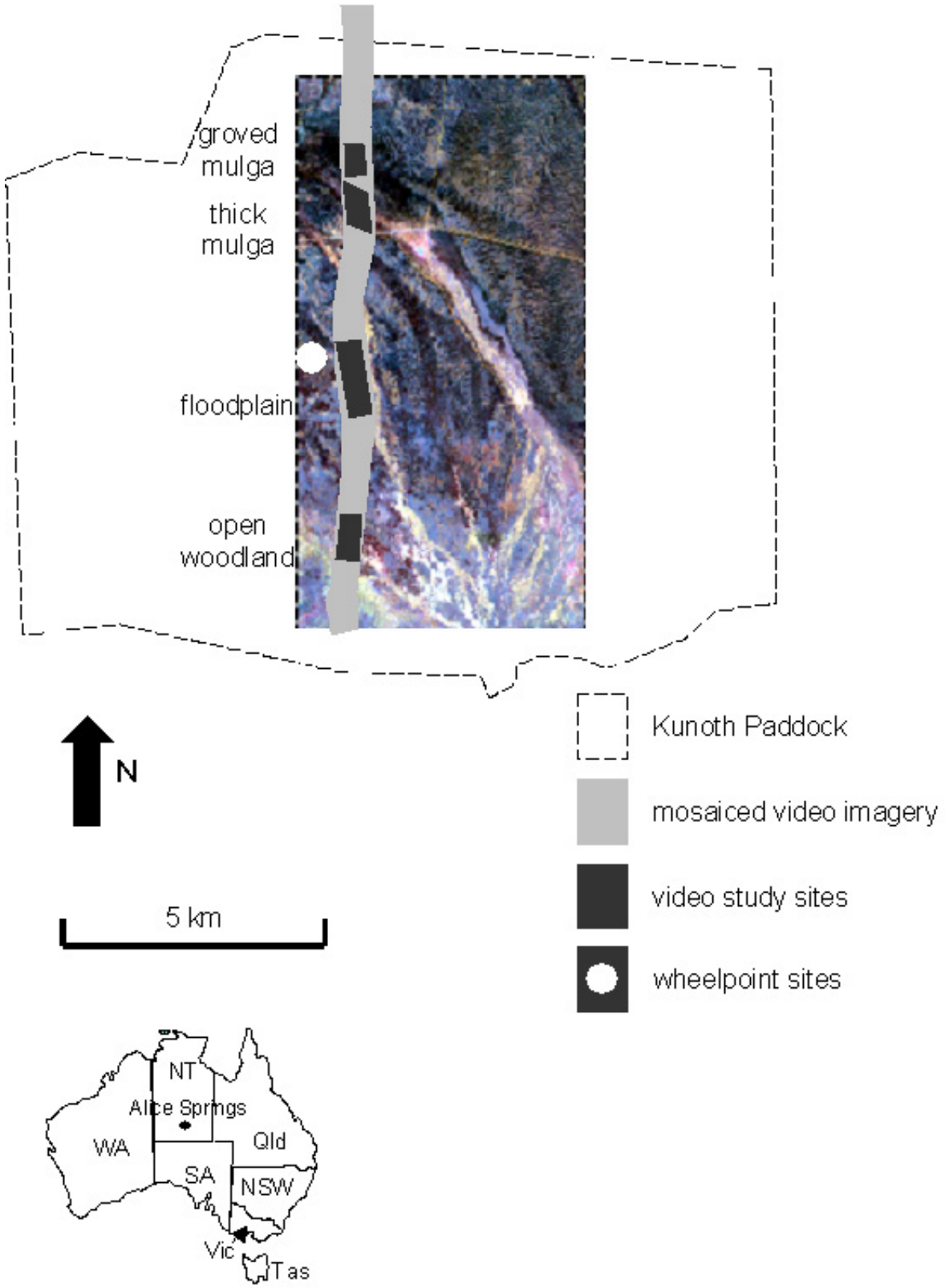

Figure 3.3.2: Location of mosaiced 1 m aerial videography with respect to the August 2001 Hyperion satellite image of Kunoth Paddock, central Australia. Also shown is the general location of wheelpoint measurements and where classified aerial videography was used to validate results obtained from unmixing of the Hyperion image.

Reasonably uniform areas of floodplain, open woodland, groved mulga and dense mulga (Table 3.3-1, Figure 3.3.1 and Figure 3.3.2) were selected from the mosaiced video imagery for comparison with a Hyperion overpass representing similar vegetation conditions (4th August 2001). The number of 1-m^2 video pixels of each classified cover type within corresponding 30 m Hyperion pixels of the four sites was calculated and compared with the fractional cover types of unmixed Hyperion pixels.

Due to a variety of factors it was not possible for the Hyperion imagery, aerial videography and field spectra to be acquired at the same time. Vegetation was green at the time of the February Hyperion image acquisition. However subsequent dry seasonal conditions and minimal grazing pressure from cattle and kangaroos meant that the herbage layer was little changed in the three months between acquisition of the wheelpoint data and video imagery in May 2001 and the August Hyperion image, the main results presented here.

3.3.4 EO-1 Data Processing

Two main approaches have been used to explore the potential for Hyperion imagery to provide information that could be useful for biodiversity surrogates. Techniques tested include indices based on the 'red-edge' feature of photosynthetic vegetation (680 nm to 760 nm) and unmixing techniques to produce abundance fractions of components of interest.

The Hyperion images acquired on February 26, 2001 and August 4, 2001 were processed by TRW to Level 1 (February) and Level 1_A (August). Several pre-processing routines developed by CSIRO were applied including a 'de-streaking' routine. CSIRO colleagues used ACORN software (ACORN 2001) to correct the imagery for atmospheric effects and convert it to apparent surface reflectance. The images were then registered to a map base.

Spectral indices

A number of vegetation indices have been developed for use with broad band, and more recently narrow band, sensors. These are usually based on data from the red and near-infrared spectrum. For this exploratory study we calculated vegetation indices which Merton (1998) found to be useful for comparing vegetation stress in a range of vegetation communities through time. These included the traditional NDVI based on bands at 672 nm and 834 nm, a modified NDVI based on bands found to be useful for analysing plant geochemistry changes, a red-edge vegetation stress index, moisture stress indices based on the 850 nm cellular feature and water features, and the slope of the red edge at the inflection point.

Table 3.3-1 Area and description of sites selected from the mosaiced transect of 1 m aerial videography to validate MTMF unmixing of the August 4, 2001 Hyperion image.

Site	Size	Landform	Soil	Vegetation
Floodplain	66.51 Ha	Level to very gently sloping	Active floodplains – duplex (red-brown sandy loam over clay loam) or scalded (reddish to bright clay loam subsoil exposed) Adjacent to active floodplain – gradational (red-brown sandy loam over sandy clay loam)	Active floodplain – generally treeless. Scattered cottonbush (*Maireana aphylla*) and other low shrubs. Perennial grasses in run-on depressions. Elsewhere, annual grasses and forbs. Adjacent to active floodplain – scattered trees and shrubs (whitewood – *Atalaya hemiglauca*, ironwood – *Acacia estrophiolata*, *Hakea* spp.) with mainly annual grasses and forbs.
Open Woodland	35.01 Ha	Level plains	Gradational – red-brown sandy loam over sandy clay loam	Scattered to clumped trees and shrubs (whitewood, supplejack – *Ventilago viminalis*, ironwood, mulga – *Acacia aneura*, witchetty bush – *Acacia kempeana*, *Hakea* spp., *Senna* spp.) with mainly annual grasses and forbs (mulga grass – *Aristida contorta*, woollyoat & oat grasses – *Enneapogon* spp., copperburrs – *Sclerolaena* spp.). Perennial grasses adjacent to larger trees and in small depressions.
Groved Mulga	21.06 Ha	Level plains – banded mulga (grove) in very slight depressions	Red earth – red sandy clay loam	Groves – banded mulga with perennial grasses Intergroves – slightly elevated (run-off) areas with scattered mulga, witchetty bush and shrubs (*Senna* and *Eremophila* spp.). Perennial grasses (mainly woollybut – *Eragrostis eriopoda*) with annual grasses (mulga grass) and forbs (copperburrs).
Dense Mulga	33.21 Ha	Floodout or broad drainage depression	Red earth – red sandy clay loam and clay loam	Very dense mulga with scattered ironwood. Sparse grasses and forbs because of dense tree cover.

Spectral mixture analysis

Several approaches to spectral mixture analysis implemented in the ENVI software package (RSI Inc. 2000) were tested including Linear Unmixing, Mixture-Tuned Matched Filter (MTMF) and Spectral Angle Mapper (SAM) procedures. We found MTMF analysis to produce the most robust results so this report focuses on those results. Endmembers and target spectra were determined using several procedures including common indices (e.g. NDVI to identify the greenest pixels) and a combination of minimum noise fraction (MNF) transformation followed by pixel purity index (PPI) and n-dimensional visualization to find the most extreme pixels in the n-dimensional image dataspace (Boardman *et al.* 1995). Pixel cover fractions were then produced by applying a MTMF process to MNF transformed imagery using the most suitable image spectra.

To avoid co-registration problems between the VISNIR and SWIR arrays, only data from the VISNIR array were used.

3.3.5 Results

Field and multi-date image spectra

Although sampling of vegetation and soil spectra with the GER was limited and not coincident with acquisition of Hyperion images, the data from both sources suggested that the field spectra should usefully guide selection of relatively pure training spectra from the Hyperion imagery (Chewings *et al.* 2002, Figure 3.3.3). We recognise here that at 30 m pixel size, no image spectra can be absolutely pure. However, we have adopted the pragmatic approach of image analysis based on image spectra because of lack of field spectra, noise in the available GER spectral data and the need to calibrate field and image spectra.

Distinction is made between photosynthetic (PV) and non-photosynthetic (NPV) vegetation components. We use PVg when referring to green grass and shrubs with green canopies such as whitewood (*Atalaya hemiglauca*) and PVm for shrubs with grey foliage such as mulga (*Acacia aneura*). NPV includes standing dry grass and litter while NPVs refers to sparse dry vegetation.

All spectra shown in Figure 3.3.3 are mean curves for several samples. Both the GER and Hyperion instruments show similar reflectance curves for soil, with a mainly increasing trend from 450 nm to around 2060 nm through the visible, near infrared and SWIR regions. The red-edge feature between 680 nm and 760 nm (i.e. centred on the red/NIR boundary) is apparent in both the field spectra and the Hyperion data of photosynthetic vegetation (PV samples). The PV sample for the February image has much higher reflectance in the NIR region than the August sample, and is most similar to the GER PVg spectra. The samples of non-photosynthetic vegetation (NPV) show a gradual increase in reflectance over the visible-near infrared region.

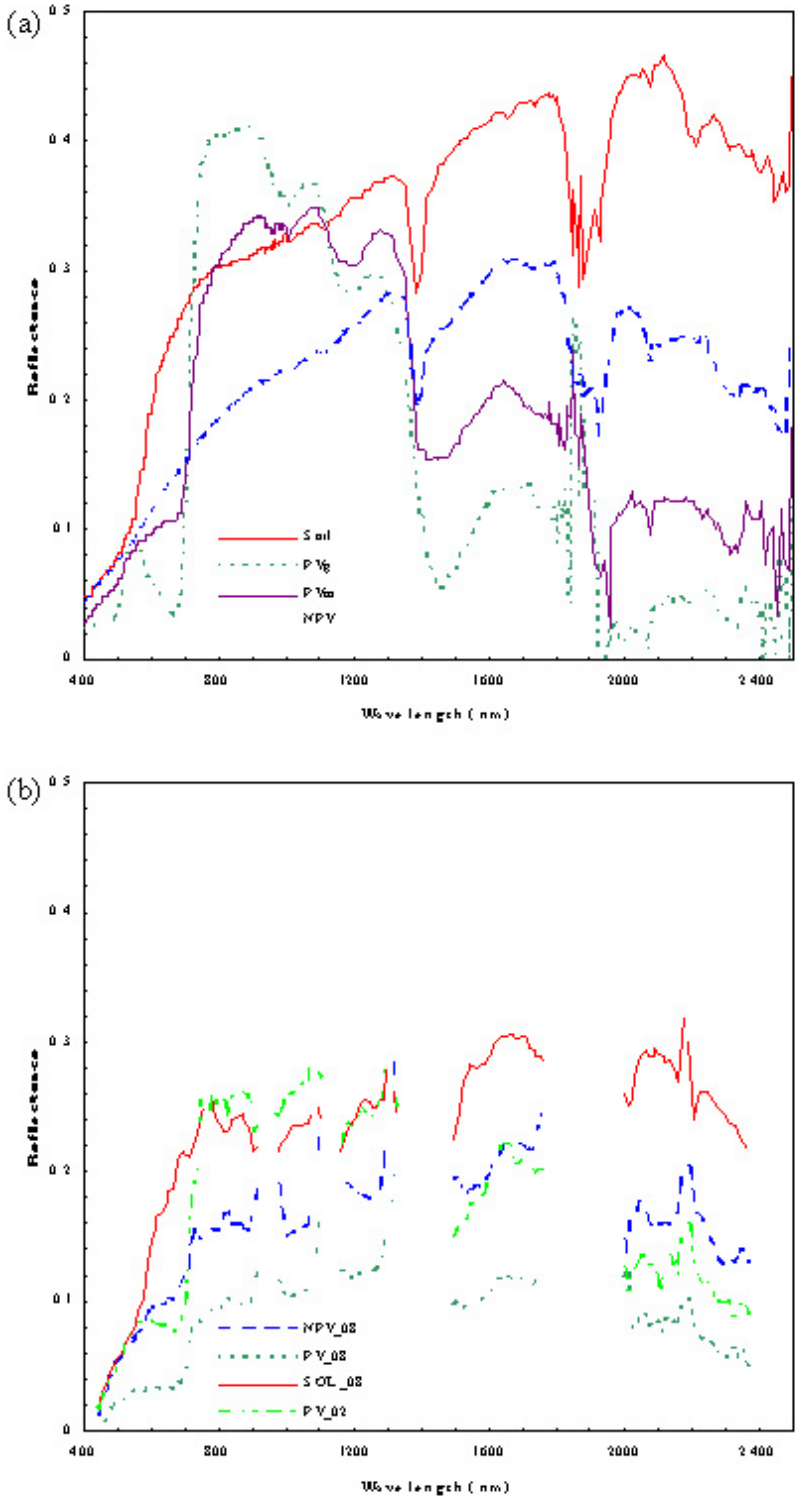

Figure 3.3.3: Example spectra for Kunoth Paddock: (a) field spectra acquired with the GER 3700 spectroradiometer and (b) Hyperion image spectra extracted from, and averaged across, representative pixels in the February and August 2001 images. Further explanation is available in Chewings *et al.* (2003).

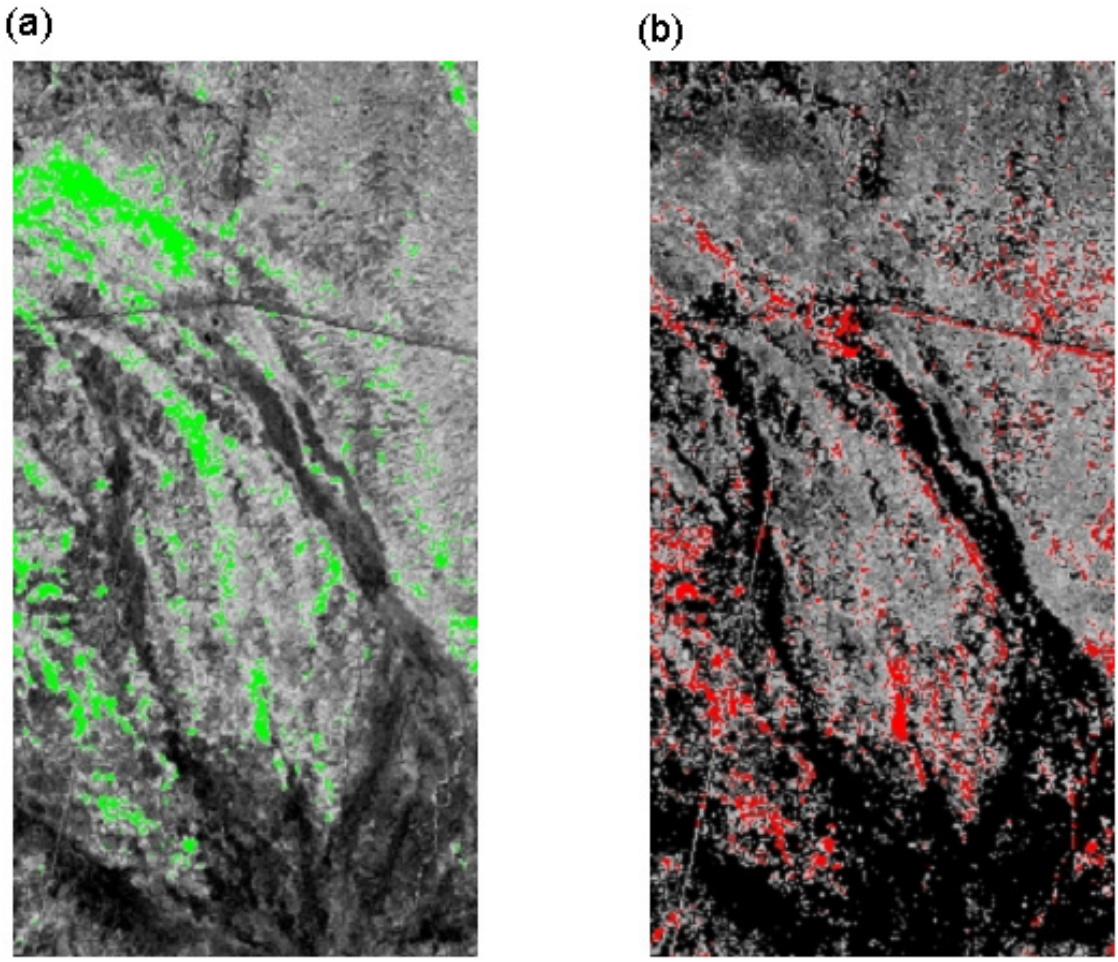

Figure 3.3.4: Indices derived using the August Hyperion image: (a) NDVI image with areas containing the highest 1% of NDVI values shown in green and (b) image showing the slope of the red-edge inflection point for each pixel (pixels with the highest 1% of values shown in red).

Spectral indices

The spatial patterning of NDVI and an index based on the slope of the red edge is shown in Figure 3.3.4. In both cases, highest values occur along the main drainage features where there are clusters of tree canopies. Highest values for the index derived using the slope of the red edge appear to be consistent with the distribution of shrubs with green canopies such as whitewood (*Atalaya hemiglauca*) and ironwood (*Acacia estrophiolata*), whereas the NDVI image is also picking up large areas of mulga.

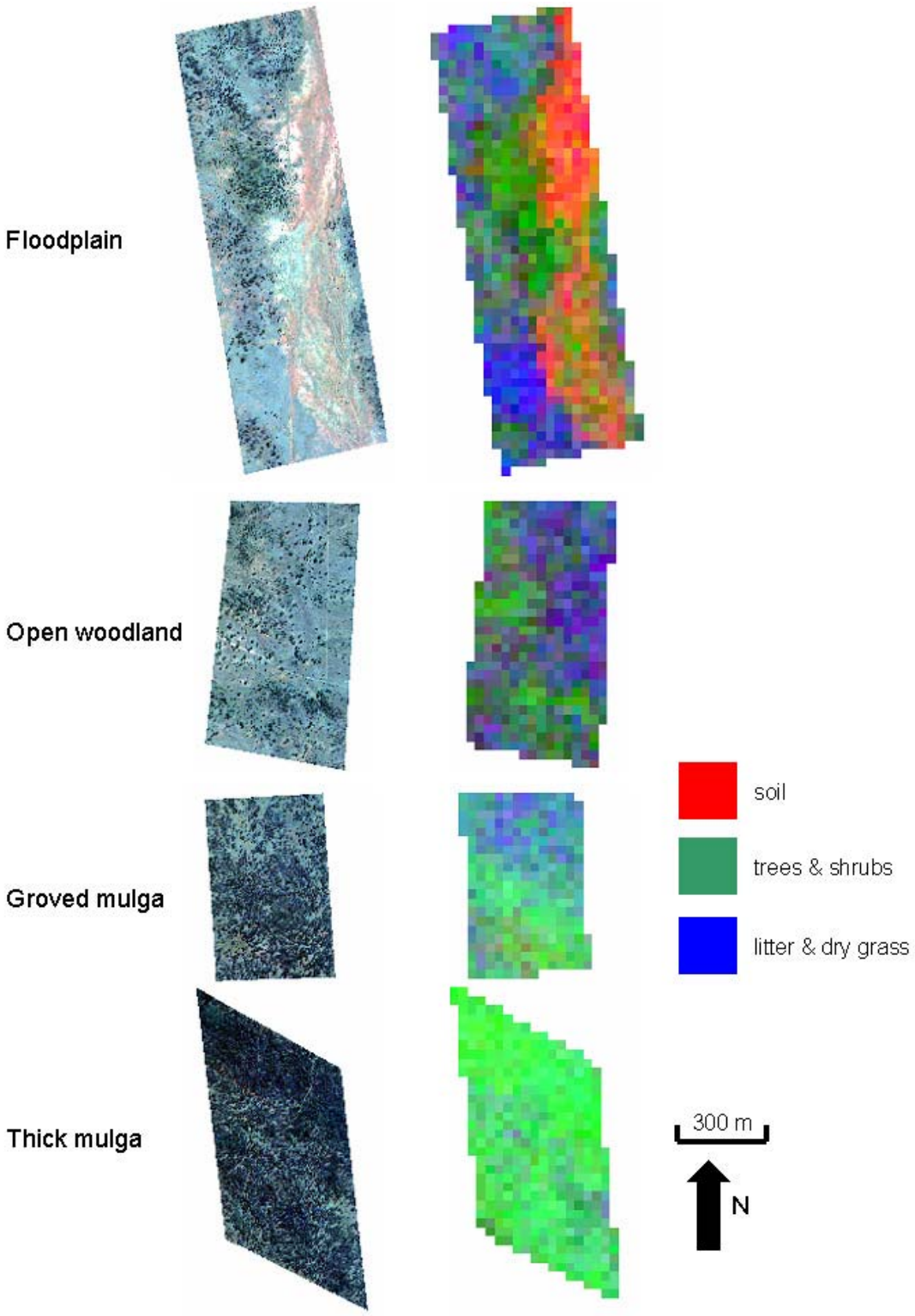

Figure 3.3.5: True-colour aerial video images of four study sites (left column) and corresponding cover fractions of soil, woody vegetation and dry grass-litter obtained from mixture-tuned matched filtering analysis of Hyperion imagery. Note that the woody vegetation cover fraction includes shadow as a component.

Mixture-Tuned Matched Filter (MTMF) analysis

Unmixing the August Hyperion image with MTMF into components of soil, woody vegetation, litter and dry grass showed good visual correspondence with corresponding areas of higher spatial resolution aerial videography (Figure 3.3.5). The floodplain site has predominantly bare soil exposed in the eastern side of the video imagery with the dominance of bare soil increasing towards the north of the image. Patches of grassland (showing as light blue due to the dominance of litter and dry grass) and woodland (darker speckle of tree canopies) occur in the west and far southeastern portion of the video image. The equivalent area of unmixed Hyperion imagery has corresponding high fractional cover of soil in the east, with this component having maximum values in the northeast and central southern parts of the image and decreasing in the southeast. Litter and dry grass dominate towards the southwest and in the northwest corner and there is high fractional cover of trees and shrubs in the central portion and far south west of the image. Elsewhere, mixed proportions of ground and upper storey vegetation occur (e.g. central northern and western edges) with other small areas where the soil signal contributes significantly.

Video imagery of the open woodland site shows mainly litter and dry grass in the central and northeastern portions and far southwest. Clumps of woody vegetation occur through the southern and western parts of the image. Small areas of soil are also visible in the western half of the image. The corresponding area of unmixed Hyperion imagery shows dominance of litter and dry grass in the central and northeastern parts and woody vegetation in the central western and southern areas. The pink-mauve colours of scattered pixels towards the western and southern edges indicate where the soil signal is contributing through the litter and dry grass.

Mulga sites at the bottom of Figure 3.3.5 have much higher vegetation cover, almost exclusively trees and shrubs on the thick mulga site. The higher density of trees also means that these two sites have a considerable shadow component within pixels, not accounted for in these simple visual displays. Litter and mulga dominate in the larger intergroves (open areas) of the central northern portion of the groved mulga site. The pale green-light yellow colouring of some pixels in the southern half of this site indicate mixed soil and woody cover fractions.

Trees on the floodplain and open woodland landscapes have two different canopy colours, typically “green” (PVg in Figure 3.3.3) or darker “olive-green” as characterised by mulga (PVm, Figure 3.3.3). We extended our testing of MTMF analysis to determine the extent to which we could discriminate these two canopy types. The fractional cover of “green” tree canopies within Hyperion pixels for the floodplain site is shown in shades of green in Figure 3.3.6(c), the brighter the level of green, the higher the fractional cover of this canopy type within pixels. Fractional cover of darker “mulga-like” canopies is shown in shades of red. Increasing intensity of yellow means higher fractional cover of both “green” and “mulga-like” canopies. Mapped pixels show as generally darker areas in a true-colour representation of the Hyperion image (Figure 3.3.6(b)). Comparison of the same (mapped) pixels with the raw (true-colour) aerial video (Figure 3.3.6(a)) shows reasonable spatial correspondence – although the threshold used (positive values of “green” and “mulga-like” canopies) suggests that some mapped pixels on the eroded floodplain have very little woody cover. Similar

visual correspondence was obtained for tree canopies on the Open Woodland site (image area not shown).

Wheelpoint data

The four 1-Ha sites measured with the wheelpoint generally had little bare soil exposed due to recent good rainfall (Figure 3.3.7(a)). Although soil MTMF fractional-cover values were small (close to zero for "Hyp Soil1" and negative for "Hyp Soil2") indicating that site areas had a relatively poor match with the two selected "purest" soil spectra, there was quite good correspondence between wheelpoint cover and MTMF values for the better soil signature ("Hyp Soil1"). This suggests that these soil spectra may be reliably indicating the proportional amount of bare soil within pixels for this area of open woodland. It was difficult to spectrally distinguish litter and dry grass as measured with the wheelpoint so these two cover types were combined. They comprised the dominant cover component across sites in terms of both the wheelpoint data and degree of match with the spectra of "purest" litter and dry grass pixels (Figure 3.3.7(b)).

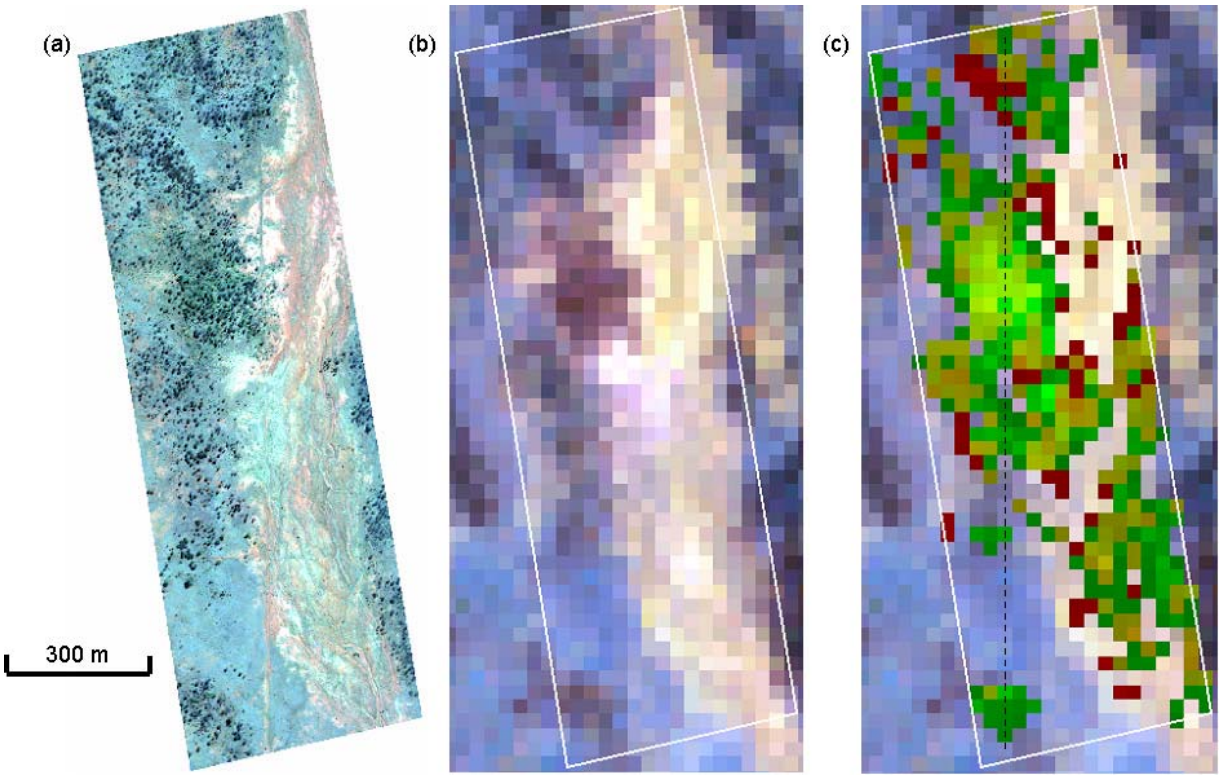

Figure 3.3.6: Floodplain site: (a) true-colour video image (1 m pixel size), (b) true-colour Hyperion image (30 m pixel size) and (c) positive MTMF values of "green" tree canopy (shown in shades of green) and "mulga-like" canopy (shown in shades of red) overlaid on the Hyperion image. The dashed line (panel c) shows the location of pixel values graphed in Figure 3.3.8.

There was reasonable correspondence in relative proportions across sites as measured with the wheelpoint and distinguished with MTMF analysis. All four sites had sparse woody cover and matched (i.e. MTMF) values for the two spectra selected to best represent different tree canopies were negative (Figure 3.3.7(c)). However, the wheelpoint data suggested that differences in these negative values among sites may indicate some degree of separation in fractional woody cover. For example, Site OW1

had the lowest measured woody cover and the most negative fractional covers for the "mulga" and "green tree" canopy types. Site OW2 had higher measured woody cover and slightly better degree of match with both canopy spectra. Site OW4 had more canopy cover than OW3 and the mulga cover fraction also reflected this increase.

In summary, the four open woodland sites measured with the wheelpoint were dominated by dry grass and litter in May 2001. MTMF analysis of Hyperion imagery acquired in early August showed that the same cover fraction dominated on the four site areas and that both data types showed the same relative differences amongst sites. Extent of bare soil was relatively minor reducing the degree of match with the most appropriate soil spectra but again, MTMF analysis differentiated proportional differences in amount of bare soil amongst sites.

Classified aerial videography

The spatial complexity of landscapes within Kunoth Paddock meant that it was difficult to verify the results of hyperspectral remote sensing analyses using just conventional ground-based measurement. Consequently, we used classified aerial videography to scale up interpretations and validation of MTMF analyses made on the August Hyperion image. Visual comparison of the floodplain site is presented above. In the following section we use a line transect of pixel values across the Floodplain site to graphically demonstrate relationships between the MTMF (Hyperion) and classified (video) datasets. Here, the classified video data are blocked to the 30 m pixel size of Hyperion. That is, each Hyperion MTMF pixel value has a corresponding set of 900 1-m^2 video pixels classified into various cover types. We then present a Table of correlation values (Table 3.3-2) to show levels of agreement over the entire area of each video test site.

There was generally good spatial correspondence between fractional cover levels within Hyperion pixels and the number of classified video pixels along a line transect on the Floodplain site purposely selected to intersect patches of high and low woody cover (Figure 3.3.8). The positioning of this transect away from bare eroded soil meant that the number of 1-m^2 video pixels classified as soil (or mostly bare) within corresponding Hyperion pixels was low (Figure 3.3.8(a)). MTMF fractional cover values were also low. Where soil was exposed, the peaks in Hyperion MTMF and classified video generally coincided. Peaks in litter (which included dry grasses) were offset to soil and again, there was good agreement in values along the length of the selected transect (Figure 3.3.8(b)). The considerable ground cover amongst the patches of woody vegetation on this intact area of floodplain produced MTMF values approaching one and classified video proportions approaching 100% of the area of individual Hyperion pixels. Again there was reasonable agreement between the two datasets in levels of woody cover (Figure 3.3.8(c)). Maximum fractional cover of woody vegetation coincided with troughs in the cover of bare soil and litter. At this location, video pixels classified as woody vegetation filled half the area of each Hyperion pixel.

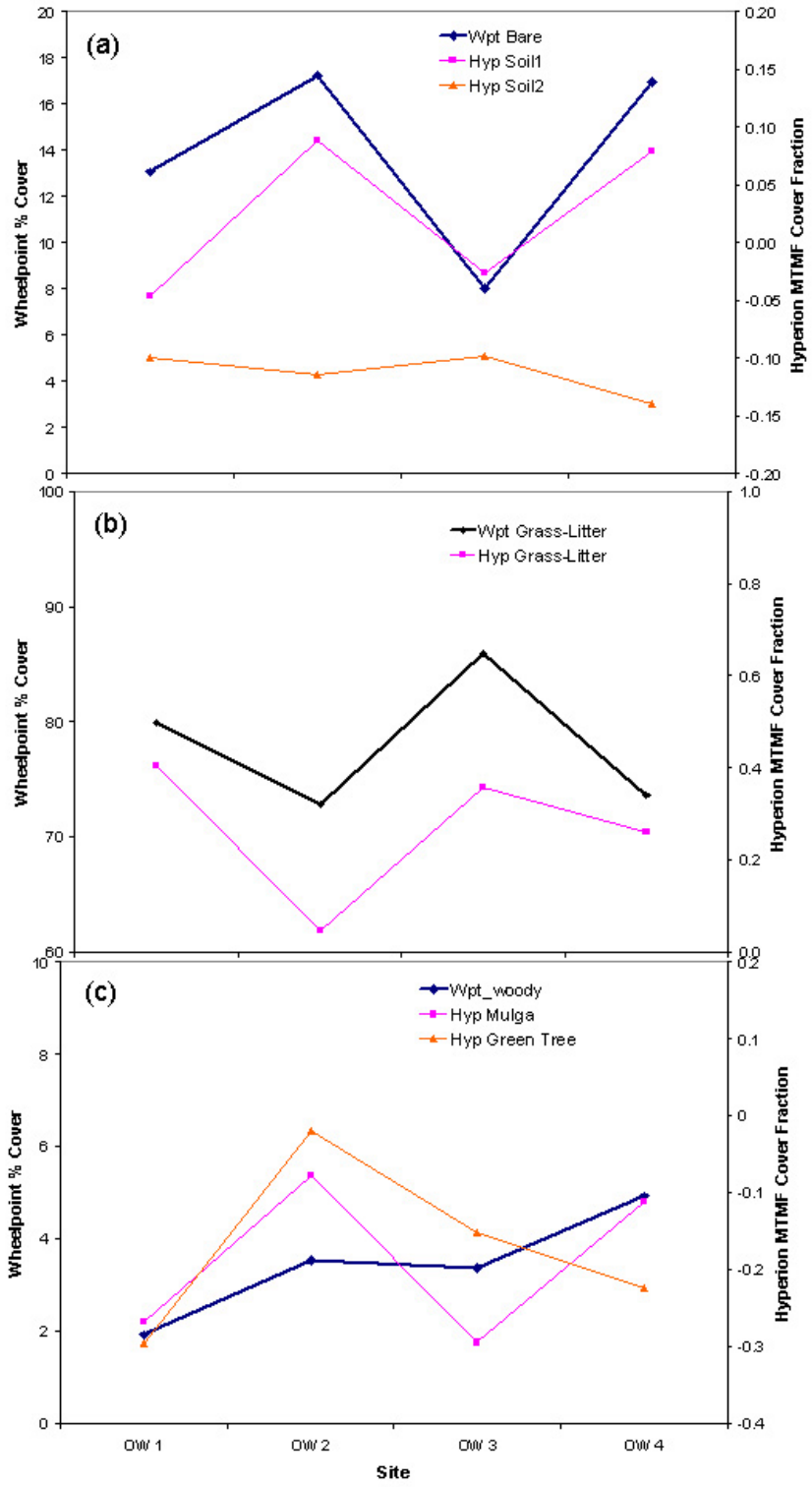

Figure 3.3.7: Comparisons of cover levels measured at four 1 Ha sites with the wheelpoint in May 2001 and fractional cover components derived by MTMF analysis of corresponding pixels in the August 2001 Hyperion image.

The floodplain and open woodland sites had higher levels of agreement between Hyperion fractional cover levels (produced by MTMF) and classified video than the two mulga sites (Table 3.3-2). For example, correlations between the separately derived estimates of soil and dry grass – litter cover fractions on the Floodplain site were >0.7.

Soil and dry grass – litter were inversely correlated (r = -0.785). The Open Woodland site had moderately strong associations between woody vegetation characterised by "green tree" type canopies and shadow. Soil was also well correlated on this site. Dry grass and litter was inversely correlated with the "green tree" type and shadow. Video pixels classified as shadow were moderately well correlated with MTMF fractional cover of the two woody types ("mulga" and "green tree") and shadow for the Groved Mulga site. There was also reasonable positive agreement for the separately derived category of "dry grass – litter". The only notable correlations for the Thick Mulga site were for the mulga canopy type. The dominance of mulga (and associated shadow) on this site probably accounted for unremarkable correlations between other cover types.

Table 3.3-2. Correlations between the number of classified 1-m2 pixels of various cover types in each 900-m2 Hyperion pixel and corresponding Hyperion MTMF cover fractions for the four landscape test sites shown in Figure 3.3.2. Figures in bold indicate a correlation >0.6.

Floodplain: n = 739 pixels, area = 66.51 Ha					
Classified aerial videography	Hyperion image – MTMF cover fraction				
	soil	dry grass - litter	woody vegetation		shadow
			mulga type	green tree type	
soil	**0.898**	-0.481	-0.035	-0.224	-0.402
dry grass-litter	**-0.785**	**0.712**	-0.309	-0.150	0.075
trees and shrubs	-0.502	-0.005	0.297	0.545	**0.635**
shadow	-0.411	-0.049	0.275	0.487	0.582
Open Woodland: n = 389 pixels, area = 35.01 Ha					
soil	**0.689**	-0.166	0.145	-0.132	-0.129
dry grass-litter	0.451	0.564	0.557	**-0.766**	**-0.689**
trees and shrubs	-0.478	-0.555	0.555	**0.757**	**0.685**
shadow	-0.454	-0.470	0.500	**0.688**	**0.602**
Groved Mulga: n = 234 pixels, area = 21.06 Ha					
soil	0.239	-0.067	0.034	0.071	0.047
dry grass-litter	-0.085	**0.626**	**-0.709**	-0.597	-0.519
trees and shrubs	-0.067	-0.036	0.550	0.297	0.260
shadow	0.236	**-0.726**	**0.604**	**0.764**	**0.664**
Thick Mulga: n = 369 pixels, area = 33.21 Ha					
soil	0.149	0.233	**-0.604**	-0.216	-0.091
dry grass-litter	0.067	0.415	**-0.699**	-0.273	-0.203
trees and shrubs	-0.115	0.107	-0.111	-0.126	-0.093
shadow	-0.004	-0.422	**0.695**	0.344	0.238

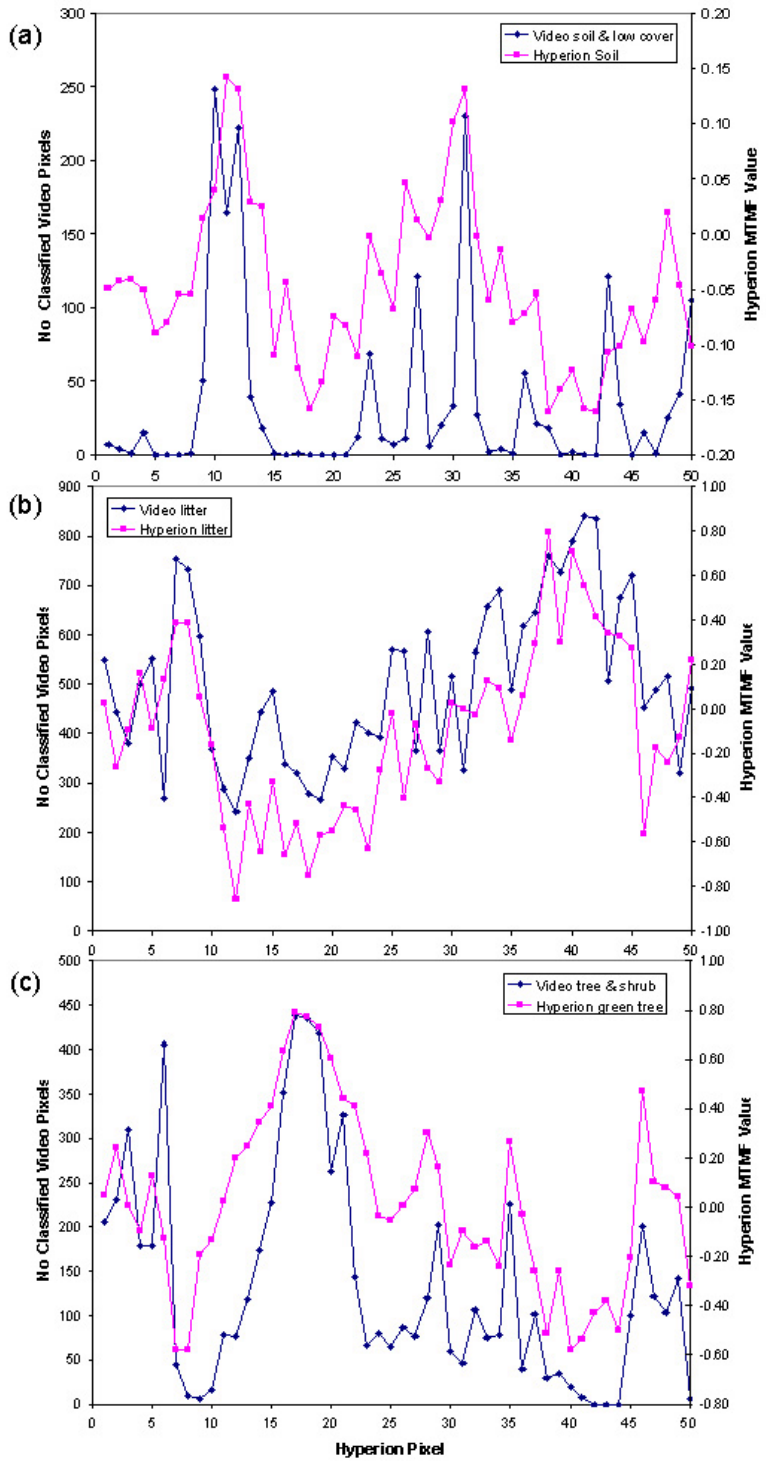

Figure 3.3.8: Proportional cover values extracted with a line traversing classified aerial videography and mixture-tuned matched filtering analysis of Hyperion imagery for the Floodplain site: (a) soil, (b) dry grass and litter and (c) woody vegetation. The transect location is shown in Figure 3.3.6(c). Proportional cover from aerial videography is the percentage of classified 1-m2 pixels of the indicated cover type within corresponding 900-m2 Hyperion pixels.

Two factors contributed to the strength, or otherwise, of spatial correlations. The large difference in pixel size meant that it was difficult to obtain perfect alignment between

the two datasets with this problem compounded by the roll and yaw of the aircraft platform used to acquire aerial videography. Thus, any spatial misalignment would have affected comparisons. The other difficulty was in spectrally defining "shadow". It was not possible to definitively separate shadow from darker tree canopies in the video classification procedure. Nor were we able to obtain a sufficiently "pure" spectra for shadow from the Hyperion image. Thus, as the cover of mulga-type canopies increased within Hyperion pixels, the confidence in separating mulga from shadow using both MTMF and classification decreased.

3.3.6 Discussion

Our first objective with the Kunoth Hyperion test site was a learning exercise; to become familiar with satellite hyperspectral data, techniques for data standardisation and analysis. A primary interest in terms of analysis was to explore the potential of Hyperion imagery to contribute to monitoring of biodiversity in the rangelands. Based on our experience with Landsat data (e.g. grazing gradient techniques for monitoring land degradation, Pickup *et al.* 1994, Bastin *et al.* 1993), we anticipated that hyperspectral data could make an important contribution through their potential to inform about components of cover within pixels. As part of this process, we needed to become familiar with different unmixing techniques. Our experience to date with both airborne (HyMap) and satellite (Hyperion) hyperspectral imagery is that unmixing is not a simple process (Chewings *et al.* 2000, 2002).

A paper by Okin *et al.* (2001) provides an overview of research using AVIRIS imagery and spectral mixture analyses techniques in arid and semi-arid environments. The authors list some of the factors that make quantitative retrieval of information about vegetation type, cover and biomass difficult in these environments. These include bright soil backgrounds, the potential for non linear mixing due to multiple scattering of light rays, many plants often lacking a strong red edge, high spectral variability within shrubs of the same species and open shrub canopies. Some of these technical difficulties may also explain our difficulty in accurately unmixing cover components across a range of vegetation types.

Rigorous approaches to unmixing pixel spectra into cover components have generally involved matching comprehensive field spectra to hyperspectral data (e.g. Asner and Lobel 2000). In this study, we lacked field spectra coincident with the acquisition of each image date. Given the availability of relevant spectra, there is still the scaling issue of relating diverse "pure" spectra to the many surface features that may be contributing to the sensor reflectance of 900 m^2 Hyperion pixels. Of concern is the conclusion by Okin *et al.* (2001) that "in areas of low vegetation cover, multiple endmember spectral mixture analysis of imaging spectrometer data using full-range field reflectance spectra is not able to provide reliable retrievals of vegetation type when covers are below at least 30%".

In Chewings *et al.* (2002) we discuss our experiences using linear unmixing techniques in a spatially variable landscape. A number of the linear unmixing and matched filtering tests yielded similar results and produced credible images of fractional cover. However we concluded that due to inherent spectral variability within the landscape, it was not a simple procedure to find a few image 'endmembers' which would satisfactorily produce abundance images for the components we were interested in. Subsequent work, reported

here, used Mixture-Tuned Matched Filter (MTMF) techniques with improved results, possibly because the technique allowed us to focus on a range of components of interest.

We found that MTMF has some potential for discriminating fractional cover levels within-pixels. This accords with the experience of Dehaan and Taylor (2003) who used MTMF analysis of HyMap imagery to derive spectral endmembers as indicators of salinisation. Available Hyperion images, and particularly the August 2001 dry period image, have provided us with the opportunity to expand our image processing and interpretation skills.

Initial attempts to calibrate the GER spectra and the image spectra were problematic, so we did not pursue that work. Instead, we used the available field spectra, public spectral libraries and the remote sensing literature to guide selection of image spectra that formed the basis of MTMF analysis. For single dates, MNF transformed images and n-dimensional viewing techniques provided additional tools for identifying components of interest. We recognise that image spectra derived from 30 m pixels cannot be pure. For example, the spectra of "litter – dry grass" pixels would inevitably have included a contribution from soil while the "green tree" spectra would have contained elements of shadow, litter and small amounts of herbage close to tree canopies. However, the results obtained here suggest that carefully selected image spectra may provide a pragmatic solution to the lack of a sophisticated and expensive instrument for acquiring field spectra.

The spatial complexity of Kunoth Paddock meant that it would be difficult to collect sufficient field data to adequately verify the results of image analysis. Instead we initially sampled a restricted and relatively uniform area of the Open Woodland landscape type with the wheelpoint and compared these cover data to cover fractions unmixed from corresponding Hyperion pixels. The results obtained (Figure 3.3.7) indicated that both the ground data and MTMF analysis characterised similarities (and differences) in cover amongst sites in broadly the same way. From there, we used aerial videography to upscale validation of hyperspectral image analysis across larger areas of more complex landscapes. We need to expand this testing but the results obtained thus far (Figure 3.3.8) indicate reasonable levels of agreement between video images classified into broad cover components and corresponding cover fractions discriminated with Hyperion pixels using MTMF analysis.

3.3.7 Conclusions

Access to Hyperion images acquired over the Kunoth test site have allowed us to expand our image processing and interpretation skills, particularly in discriminating levels of fractional cover within-pixels. Digital video images classified into similar cover components were integral to validating the results of hyperspectral image analysis across reasonably large areas of spatially heterogeneous landscapes. Our results indicate some potential to unmix dry-period Hyperion imagery into sub-pixel fractional components of cover. An expanded ability to do this accurately over large areas should contribute to monitoring of the integrity of rangeland landscapes, particularly by allowing upscaling of an existing technique for indicating landscape leakiness (Ludwig *et al.*, 2002). Further development of the ability to discriminate broadly different tree canopies within 30 m pixels, such as the "green tree" and "mulga" types demonstrated here, should have useful application for monitoring elements of biodiversity.

3.3.8 Other activities

We were pleased to be able to show the Kunoth site to several delegates following IGARSS 2001 in Sydney. Visitors included Jay Pearlman (formerly TRW) and Melba Crawford (University of Texas at Austin). The ALI imagery acquired during the EO-1 passes provides a valuable record of local conditions during 2001 after exceptionally good rainfall over a larger area than covered by the Hyperion imagery. Maps were produced for the Alice Springs community using ALI imagery from February 2001, which showed actively growing areas of vegetation. Most of these areas represent buffel grass, an introduced grass which has an impact on the biodiversity of the area and which contributed to several intense fires during 2001. The ALI images acquired throughout 2001 clearly show the extent of some of these fires.

3.3.9 Acknowledgements

This work was undertaken as part of a collaborative EO-1 science validation program of CSIRO EOC and NASA. David Jupp (EOC) arranged the acquisition of Hyperion imagery. Researchers from the University of Texas provided technical advice. We thank the owner (Andrew Miller) and manager (Jamie Evans) of Hamilton Downs station for allowing us to work in Kunoth Paddock. Main photo: Kunoth Paddock, Central Australia.

3.3.10 References

ACORN (2001). ACORN User's Guide Version 3.12, Analytical Imaging and Geophysics LLC. Boulder, Colorado, USA.

Asner, G.P. and Lobel, D.B. (2000). A biogeophysical approach for automated SWIR unmixing of soils and vegetation. *Remote Sensing of Environment*, **74**, 99-112.

Bastin, G. N., Ludwig, J. A., Eager, R. W., Chewings, V. H. and Liedloff, A. C. (2002). Indicators of landscape function: comparing patchiness metrics using remotely-sensed data from rangelands. *Ecological Indicators*, **1**, 247-260.

Bastin, G.N., Pickup, G., Chewings, V.H. and Pearce, G. (1993). Land degradation assessment in central Australia using a grazing gradient method. *Rangeland Journal*, **15**, 190-216.

Boardman, J.W., Kruse, F.A. and Green, R.O. (1995). Mapping target signatures via partial unmixing of AVIRIS data. *Summaries, 5th JPL Airborne Earth Science Workshop, JPL Publication* 95-1, **1**:23-26.

Chewings, V. H., Bastin, G. N., Pearce, G. and Pickup, G. (1998). *Remote sensing of Central Australian Deserts*. Interactive CD-ROM. CSIRO Wildlife and Ecology, Alice Springs, Australia.

Chewings, V. H., Pickup, G., Bastin, G. N. and Pearce, G. (2000). The potential for hyperspectral data mapping in Australian arid zone vegetation. *Proceedings of 10th*

Australasian Remote Sensing & Photogrammetry Conference, August 21-25, Adelaide, 2000. (Proceedings published on CD-ROM.)

Chewings, V.H., Bastin. G.N., Crawford, M.M. and Kinloch, J.E. (2002). Characterisation of Vegetation Components in the Australian Arid Zone using EO-1 Hyperion imagery. *Proceedings of 11th Australasian Remote Sensing & Photogrammetry Conference,* Brisbane, 634-646. (Proceedings published on CD-ROM.)

Dehaan, R. and Taylor, G.R. (2003). Image-derived spectral endmembers as indicators of salinisation. *International Journal of Remote Sensing*, **24**, 775-794.

Low, W.A. (Ed.), (1978). *The Physical and Biological Features of Kunoth Paddock in Central Australia*. CSIRO Division of Land Resources Management Technical Paper No. 4. 137 p.

Ludwig, J.A., Eager, R.W., Bastin, G.N., Chewings, V.H. and Liedloff, A.C. (2002). A leakiness index for assessing landscape function using remote sensing. *Landscape Ecology*, **17**, 157-171.

Ludwig, J. A.; Tongway, D. J.; Bastin, G. N., and James, C. D. (2004). Monitoring Ecological Indicators of Rangeland Functional Integrity and Their Relation to Biodiversity at Local to Regional Scales. *Austral Ecology*, **29**(1), 108-120.

Merton, R.N. (1998). *Multi-temporal analysis of community scale vegetation stress with imaging spectroscopy*. Phd Thesis. University of Auckland, New Zealand. 490p.

Okin, G.S., Roberts, D.A., Murray, B. and Okin, W.J. (2001). Practical limits on hyperspectral vegetation discrimination in arid and semiarid environments. *Remote Sensing of Environment*, **77**, 212-225.

Pickup, G., Bastin, G.N. and Chewings, V.H. (2000). Measuring rangeland vegetation with high resolution airborne videography in the blue-near infrared spectral region. *International Journal of Remote Sensing*, **21**, 339-351.

Pickup, G., Bastin, G.N. and Chewings, V.H. (1994). Remote sensing-based condition assessment procedures for nonequilbrium rangelands under large-scale commercial grazing. *Ecological Application*, **4**, 497-517.

Pickup, G., Chewings, V.H. and Pearce, G. (1995a). Procedures for correcting high resolution airborne video imagery. *International Journal of Remote Sensing*, **16**, 1647-1662.

Pickup, G., Bastin, G.N., Chewings, V.H. and Pearce, G. (1995b). Correction and classification procedures for assessing rangeland vegetation cover with airborne video data. *Procs. 15th Biennial Workshop on Videography and Colour Photography in Resource Assessment*, Terre Haute, Indiana, 305-314.

Pickup, G. and Chewings, V. H. (1988). Estimating the distribution of grazing and patterns of cattle movement in a large arid-zone paddock - an approach using

animal distribution models and Landsat imagery. *International Journal of Remote Sensing*, **9**, 1469-1490.

Pickup, G. and Nelson, D.J. (1984). Use of Landsat radiance parameters to distinguish soil erosion, stability and deposition in arid central Australia. *Remote Sensing of Environment*, **16**, 195-209.

RSI Inc. (2000). *The ENvironment for Visualizing Images (ENVI) Manual*. Research Systems Inc. (RSI), Lafayette, CO., USA.

3.4 Moreton Bay

Landsat Image of Moreton Bay, near Brisbane, Queensland, Australia

Site P/Co-Investigator(s): Vittorio Brando, Arnold Dekker
Site Name: Moreton Bay
Latitude: 27.112 S
Longitude: 153.168 E
Elevation: 0 m
Surface type: Coastal waters
General atmospheric conditions: cloud free on almost all the dates, on the exact location
Other satellite data: Landsat7 ETM, Modis
Comments:
Contact email: vittorio.brando@csiro.au

Report by Vittorio Brando & Arnold Dekker
CSIRO Land & Water

3.4.1 Introduction & Objectives

During the SVT Southern Hemisphere campaign, six Hyperion and ALI images of Moreton Bay in southeast Queensland, Australia were acquired from December 2000 to July 2001. Cloud-free data were acquired for Deception Bay (a sub-basin of Moreton Bay) over summer, autumn and winter (12 January 2001, 2 April 2001, 7 July 2001).

The coastal site of Moreton Bay was chosen, as it has been studied extensively and has a number of major active coastal water quality monitoring and management projects. Research groups from the University of Queensland (UQ) and CSIRO Land & Water are cooperatively developing remote sensing solutions to environmental monitoring. This region shows spatial gradients in optical depth, water quality, bathymetry, and substrate composition. A combination of turbid and humic river inputs, as well as the open ocean flushing, determines the water quality of the bay.

Aim of the work was to determine the capacity of Hyperion to estimate concentrations of water quality variables in a coastal environment with a known degree of precision and accuracy.

3.4.2 Calibration & Validation Activities

During each Hyperion overpass a limited set of spectroradiometric measurements and *in situ* sampling was carried out by the University of Queensland in Deception Bay (see Table 3.4-1). Two extensive joint field campaigns were carried out in February 2001 and June 2001 to parameterize a bio-optical model for Moreton Bay for both optically deep and shallow waters (see Figure 3.4.1).

Figure 3.4.1: Field work in support of Hyperion missions on Moreton Bay

Table 3.4-1 In situ sampling concurrent with the Hyperion imagery acquisition

Dates of acquisition	Type of measurement:	Device
12 January	Water leaving radiance, downwelling irradiance, water column profiles	ASD
1 March	Water leaving radiance, downwelling irradiance, water column profiles	ASD
2 April	Downwelling irradiance	ASD, Ramses
5 June	--	--
21 June	Water leaving radiance, downwelling irradiance, water column profiles	ASD, HydroRAD, RAMSES
7 July	--	--

The field campaign collected inherent and apparent optical properties as well as concentrations of water constituents and substrate reflectances (see Table 3.4-2).

Table 3.4-2 Extensive joint field campaign – measured and estimated parameters

Instrument	Measured parameters	Estimated Parameters	Affiliations
ASD	E_d/L_u	R(0-), R(z), K_d, K_u	UQ- BRG
RAMSES MCC	E_d air		UQ- BRG
RAMSES MCC & MRC	E_d/L_u	R(0-), R(z), K_d, K_u	CLW
Unispec	L_u	R(0-), R(z), K_u	CLW
Licor	E_d	R(0-), R(z), K_d,	CLW
HydroScat 6	b_{bp} (140^o)	$b_{b\,TR}(\lambda)$, $b_{b\,CHL}(\lambda)$	CLW
PSICAM	$a_{tot}(\lambda)$,$a_{CDOM}(\lambda)$	$a_{\,TR}(\lambda)$, $a_{\,CHL}(\lambda)$	CLW
Turbidity-meter	b_b (90^o)	NTU	EHMP
Secchi Disc			CLW, UQ-MB
CTD	Temp, Salinity		EHMP
Water samples	Chl-a, TSS		UQ-MB, EHMP

Affiliations: CLW: CSIRO Land &Water; UQ- BRG: University of Queensland Biophysical Remote Sensing Group; UQ- MB: University of Queensland, Marine Botany; EHMP: Ecological Health Monitoring Program.

3.4.3 Atmospheric Correction Procedures

The dedicated "coastal **W**aters and **O**cean **M**ODTRAN-4 **B**ased **AT**mospheric correction" ("c-WOMBAT-c") procedure was developed in this work to perform atmospheric and air water interface corrections to a high degree of accuracy. The "c-WOMBAT-c" procedure was implemented in IDL/ENVI® and includes an air/water interface following De Haan *et al.* (1996, 1997). The procedure consists of: i) a three step atmospheric inversion from at-sensor-radiance to apparent reflectance (De Haan *et*

al., 1997; Adler-Golden et al 1998) and ii) a two-step inversion of the air-water interface from apparent reflectance to subsurface irradiance reflectance (De Haan *et al.*, 1997). "c-WOMBAT-c" applies a full MODTRAN-4 atmosphere parameterisation and characterization to run the inversion. Adjacency effects in the imagery were corrected for using a spatially averaged radiance image generated by convolving the radiance imagery with a one square kilometre spatial weighting function reflectance (De Haan *et al.*, 1996; Adler-Golden *et al.*, 1998).

The atmospheric parameterisation for the 12th January 2001 image was based on radio-sonde data to estimate the atmospheric column contents and the actual and 24 hour average wind speed and TOMS data for estimating ozone content. The atmospheric correction was validated by comparing the reflectance just below the water surface (R(0–)) extracted from the 12th January Hyperion imagery to the R(0–) measured *in situ* at the time of the overpass using an ASD FieldSpec spectrometer equipped with a submersible optical fiber (see Figure 3.4.2).

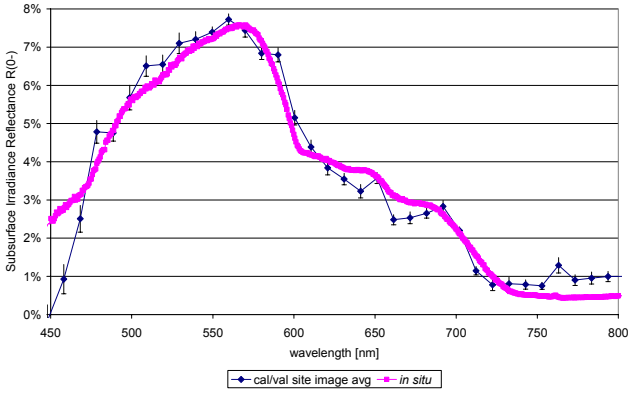

Figure 3.4.2 Validation of atmospheric correction. Comparison of the R(0̃) calculated for Hyperion imagery with the R(0̃) measured in situ at the time of the overpass.

3.4.4 Methods for Quantitative products retrieval

Using inherent and apparent optical properties as input to an analytical optical model, it was possible to simulate the effect on R(0–) of any range of water quality variable concentrations, such as coloured dissolved organic matter (CDOM), chlorophyll (CHL) and suspended matter (as tripton, TR) present at the time of a Hyperion overpass (provided the specific inherent optical properties do not vary significantly). By inverting this analytical model it becomes possible to determine the capacity of Hyperion to estimate concentrations of water quality variables. A full description of the analytical model and of the implementation of the model inversion on the Hyperion imagery is given in Brando & Dekker (2003).

The precision and accuracy of these estimates are a function of the sensitivity of Hyperion, of the pre-processing and of the (inversion of the) analytical model. For example, the Hyperion data has remaining array effects which act as "noise" in the model inversion. These include vertical (column) stripes and subtle imbalances that are in evidence over darker water targets and may be residual dark current effects. Figure

3.4.3(a) shows an example of these effects over a later Hyperion image of "homogeneous" ocean on July 7 2001. Figure 3.4.3(b) shows the result of pre-processing by balancing the column means with additive corrections. Both the column stripes and the distinct differences between the first 128 and the second 128 pixels of the 256 pixel Hyperion line are removed.

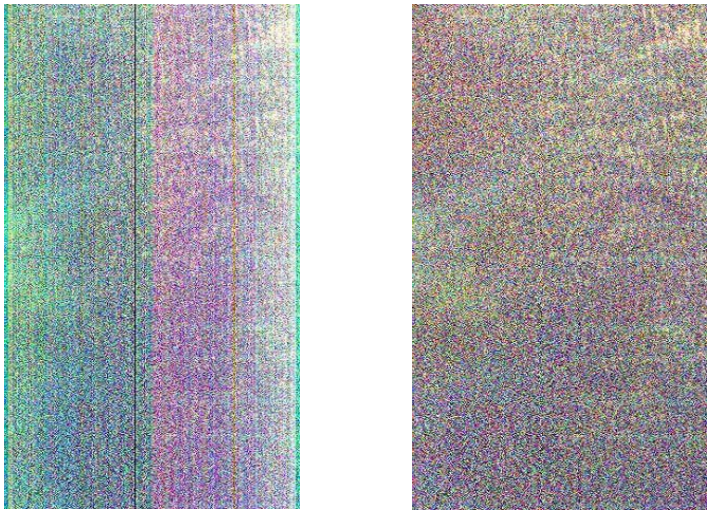

(a) (b)

Figure 3.4.3 Homogeneous ocean before (a) and after (b) detector (column) balancing by additive correction to overall mean. (a) shows residual array effects and column striping.

If this sample-based correction is applied to all of the data of July 7 2001 (Figure 3.4.4(a)) the result is as shown in Figure 3.4.4(b). The image in (b) still does show some residual effects but they are very small compared with the uncorrected image. These and other approaches to the noise in Hyperion are essential for effective modelling.

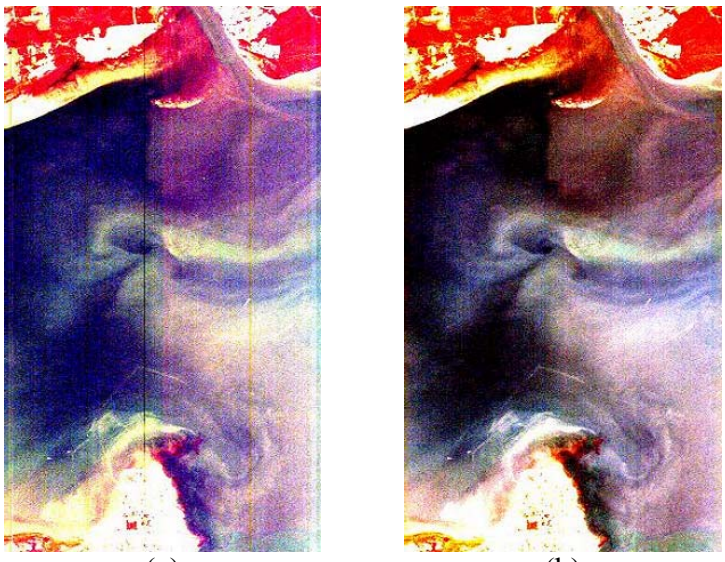

(a) (b)

Figure 3.4.4 Deception Bay on July 7 2001 before (a) and after (b) detector (column) balancing using statistics developed over the homogeneous ocean.

3.4.5 Quantitative products

A matrix inversion method (MIM) was applied successfully for the first time to satellite hyperspectral imagery. Since the MIM encompasses the simultaneous retrieval of all constituent concentrations it automatically accounts for the complex interaction of the constituents with light in water, as it doesn't simplify the non-linearity of the analytical model for R(0-). To achieve an adequate environmental dynamic range of the imagery for optical water quality remote sensing purposes a 5x5 low-pass filter was applied on the R(0–) image.

Figure 3.4.5 shows the products retrieved inverting the (5x5 low pass) filtered R(0–) Hyperion imagery of Deception Bay of January 12th 2001. The pseudo true colour image (Figure 3.4.5 a), shows a re-suspension eddy in the centre of the bay due to the anticlockwise circulation pattern of the "rising' tide. The water quality of the Deception Bay is determined by interaction of the open ocean waters flushing the bay (from the top right corner) with the turbid and humic Caboulture River input (off the south-west corner of the Hyperion image, but clearly visible in the Landsat 7 TM image acquired within 1 minute from Hyperion) in the lower left corner.

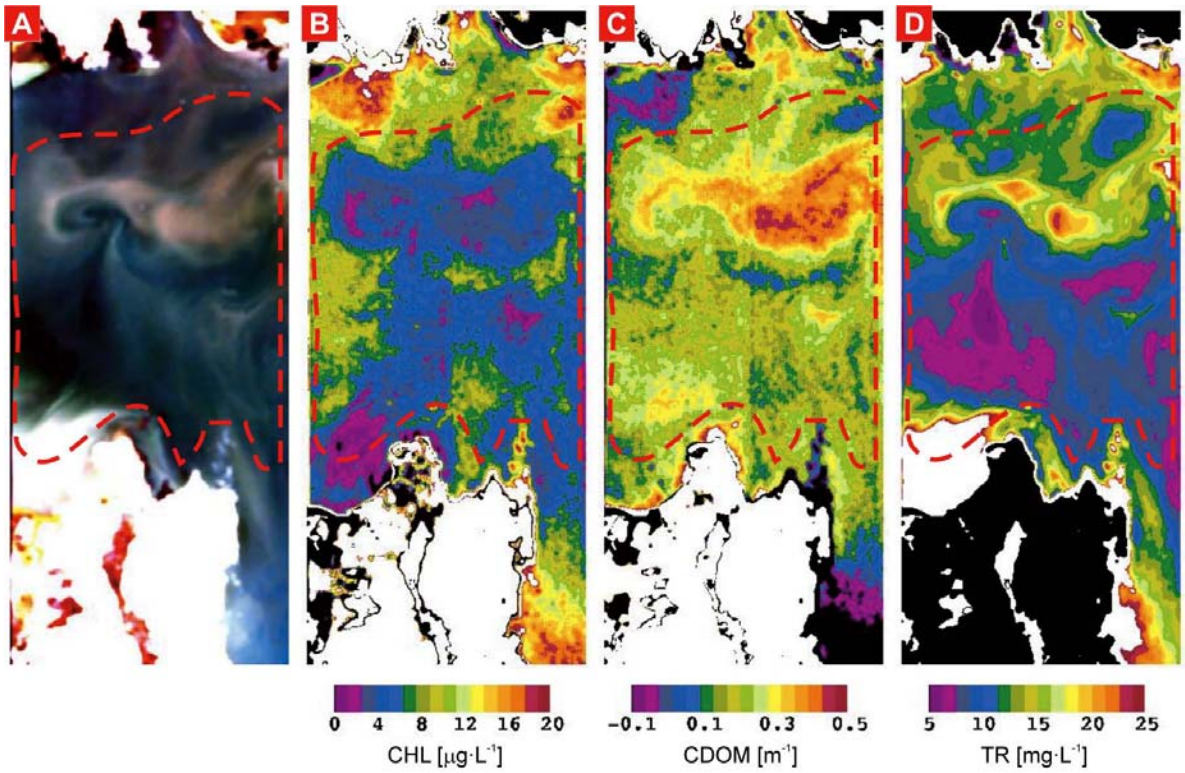

Figure 3.4.5. a) 5x5 low pass filtered subsurface irradiance reflectance Hyperion imagery of Deception Bay January 12th 2001and the MIM retrieved concentrations for b) CHL, c) CDOM, d) TR. The dashed red line delimits the cloud free and optically deep water region

The chlorophyll map (Figure 3.4.5 b) shows four areas almost uniform in values while the CDOM and Tripton images (Figure 3.4.5 c&d) show high concentration likely to be caused by sediment re-suspension due to the tidal eddy in the central part of the bay. The tripton image reaches the maximum concentration values in the lower left corner

where a sediment re-suspension due to the tidal pattern is visible in the pseudo true colour image (Figure 3.4.2(a).

The resulting water quality product maps are within the range of values measured by the ongoing monitoring programs in Moreton Bay (Ecological Health Monitoring Program, EHMP) (where EHMP sampled for CHL) and within *in situ* measurements for CDOM (see Table 3.4-3). CHL and TR are in the range of those measured in Deception Bay on February 14th 2001 when CHL and TSS was estimated along the Deception Bay coastline and the Caboulture River estuary as part of a joint exercise within the Hyperion EO-1 cal/val activities. The difference in tidal condition and time of the day will influence these results.

Table 3.4-3. Concentration ranges for optical water quality variables estimated in situ and retrieved with MIM from cloud free and optically deep water Hyperion data.

	Date	Min	Max	Mean	Stdev
CHL (EHMP) [µg·L-1]	10-Jan	1.4	4.4	2.5	0.9
CHL (EHMP) [µg·L-1]	14-Feb	0.97	19.91	3.47	4.9
CHL (MIM Hyperion) [µg·L-1]	12-Jan	0.47	18.92	6.05	2.32
CDOM (CLW) [m-1]	14-Feb	0.13	0.75	-	-
CDOM (MIM Hyperion) [m-1]	12-Jan	-0.08	0.55	0.22	0.10
TSS (EHMP) [mg·L-1]	14-Feb	3.4	46.3	8.69	11.24
Tripton (MIM Hyperion) [mg·L-1]	12-Jan	6.23	39.61	11.73	3.70

3.4.6 Conclusions

Hyperion imagery, after pre-processing and noise reduction strategies, can be used to map optical water quality concentrations of coloured dissolved organic matter, chlorophyll and total suspended matter (as tripton) simultaneously in the complex waters of estuarine and coastal systems. Retrieved concentrations of CHL, CDOM and TR were comparable to those estimated on the field in the days of the overpass.

3.4.7 Acknowledgments

This work was supported in part by the CSIRO Earth Observation Center and by the Cooperative Research Center for Coastal Zone, Estuary and Waterways Management. The Hyperion data were collected by NASA and processed by TRW for the evaluation of the experimental sensors on the New Millennium EO-1 mission. Data were provided to CSIRO through its membership of the EO-1 Science Validation Team (SVT).
None of these results would have been possible without the contributions of the University of Queensland Marine Botany and Biophysical Remote Research groups (Stuart Phinn, Chris Roelfsema, Peter Scarth, Josh Rapp, Jason Scriffignano) and the infrastructural support the Centre of Marine Studies at UQ. The authors thank Eva Abal and Paul Maxwell for the access to the EHMP water quality variables concentrations dataset, and Janet Anstee and Nicole Pinnel of CSIRO Land & Water for the field and lab support.

3.4.8 References

S. B. Adler-Golden, A. Bernstein, L. S. Richtsmeier (1998). Flaash, A Modtran4 Atmospheric Correction Package for Hyperspectral Data Retrievals and Simulations. Presented at AVIRIS Workshop, Pasadena, 1998.

J. F. De Haan and J. M. M. Kokke (1996). Remote sensing algorithm development Toolkit I: Operationalization of atmospheric correction methods for tidal and inland waters. BCRS, Delft BCRS 96-16, 1996.

J. F. De Haan, J. M. M. Kokke, H. J. Hoogenboom, and A. G. Dekker (1997). An integrated toolbox for processing and analysis of remote sensing data of inland and coastal waters-atmospheric correction. Presented at Fourth International Conference: Remote Sensing for Marine and Coastal Environments, Michigan, USA, 1997.

3.4.9 Publications & Presentations

3.4.9.1 Journal Papers

V.E. Brando and A.G. Dekker (2003). Satellite hyperspectral remote sensing for estimating estuarine and coastal water quality. *IEEE - Transactions on Geoscience and Remote Sensing*, **41** (6), pp 1378- 1387.

A.G. Dekker, V.E. Brando, N. Pinnel, A. Held (2002). HYPERION: the first imaging spectrometer from space: also suitable for inland and coastal water observations. *Backscatter magazine (http://www.waterobserver.org/backscatter/issue-02-winter.html),* 2002.

3.4.9.2 Conference Proceedings

A.G. Dekker, V.E. Brando, J.M. Anstee, N. Pinnel, A. Held, "Preliminary Assessment of the performance of Hyperion in Coastal waters. Cal/Val activities in Moreton Bay, Queensland, Australia," *Proceedings of International Geoscience and Remote Sensing Symposium (IGARSS'01)*, Sydney, Australia, 2001.

V.E. Brando, A.G. Dekker, and J.M. Anstee, "Estuarine Hyperspectral Remote Sensing from Space: Case Study Moreton Bay," *Proceedings of the 11th Australasian Remote Sensing and Photogrammetry Conference*, Brisbane, Australia, 2002.

3.4.9.3 CSIRO EOC Annual Science Meetings

A.G. Dekker, V.E. Brando, J.M. Anstee, N. Pinnel and A. Held, "Preliminary assessment of the performance of Hyperion in coastal waters. Cal/Val activities in Moreton Bay, Queensland, Australia," C*SIRO EOC Annual Science Meeting*, Canberra, 2001.

V.E. Brando, A.G. Dekker and J.M. Anstee. “Satellite hyperspectral remote sensing for estimating estuarine and coastal water quality,” C*SIRO EOC Annual Science Meeting*, Canberra, 2002”

3.4.9.4 SVT Meetings

A.G. Dekker, V. E. Brando, J.M. Anstee, N. Pinnel, A. Held, “Preliminary assessment of the performance of Hyperion in coastal waters. Cal/ Val activities in Moreton Bay, Queensland, Australia,” *EO-1 SVT Meeting*, Tuscon, May 2001.

V. E. Brando, A. G. Dekker, J.M. Anstee, N. Pinnel, A. Held. “Preliminary multitemporal assessment of the performance of Hyperion in coastal waters. Cal/ Val activities in Moreton, Bay, Queensland, Australia,” *EO-1 SVT Meeting*, Buenos Aires, 6-8 November, 2001.

V.E. Brando, A.G. Dekker, J.M. Anstee. “Satellite hyperspectral remote sensing for estimating estuarine and coastal water quality. Results of the Australian Science Validation Team for assessing Hyperion for coastal remote sensing,” *EO-1 SVT Meeting*, Hilo, Hawaii, November, 2002

3.5 Cape Tribulation – Coral Reef Studies

Offshore from Cape Tribulation

Site Information:

Site P/Co-Investigator(s): Tiit Kutser, David Jupp
Site Name: Cape Tribulation
General location: North Queensland, Australia
Type of measurement: Video transects to map coral reef habitat types, inherent optical water properties
Measurement device: Hydroscat-6, GER
Dates of acquisition: March 3, March 19, May 6, Sept. 11, Sept. 27 Oct. 13 2001
Latitude: -16.11
Longitude: 145.441
Elevation: 0 m
Surface type: Coral reef
General atmospheric conditions: Cloudy to heavy cloud
Other satellite data: Landsat ETM
Comments: Some HyMap and casi-2 data available at other locations
Contact email: David.Jupp@csiro.au

Report prepared by: Tiit Kutser
CSIRO EOC

3.5.1 Introduction & Objectives

Most of the Hyperion images acquired above Cape Tribulation were cloudy or partly cloudy. However, three images (March 3, March 19 and October 13, 2001) were suitable for coral reef research as most of the Cairns Reef area was cloud free. A field trip was organized to Cairns Reef in September 10-12, 2001 to collect data about inherent optical water properties in the area and to map benthic habitat. Australian Institute of Marine Sciences (AIMS) diving teams carried out ground truthing measurements on September 12, 2001. Most of the work was carried out as replicated video transects with timed, parallel swims, by two videographers 10m apart for approximately 5 minutes each, which equates to an area of approximately 500 m^2. Water samples were taken from the surface layer in three locations. Concentration of total suspended solids, chlorophyll a and some other pigments were measured from the water samples. Absorption by coloured dissolved organic matter (CDOM), phytoplankton, and detritus was also measured. Vertical profiles of the backscattering coefficients were measured *in situ* with a HydroScat-6. Reflectance of a few substrates was measured using a GER spectrometer (Figure 3.5.1).

Figure 3.5.1: Attaching video camera to sensor head of the underwater hyperspectral radiometer.

The primary objective of the study was to estimate the suitability of Hyperion for providing reliable data from the water environment, especially for mapping the shallow water benthic habitat in coral reefs. Hyperion is the first civilian hyperspectral sensor in space and has the advantages of a space platform for global, repeat coverage. Its data have allowed us to test a novel, physics-based approach to interpreting the data and to estimate advantages of hyperspectral versus multispectral data even given the lower expected SNR of the Hyperion sensor in a low signal water covered environment.

3.5.2 Hyperion data processing

Atmospheric correction of Hyperion images was carried out using the ENVI FLAASH module. The FLAASH module incorporates MODTRAN 4 radiation transfer code with the standard MODTRAN atmosphere and aerosol types to calculate a solution for each image. Settings for a tropical atmosphere and marine aerosols were used in FLAASH to correct the images. Clouds and cloud shadows were manually masked out in all images.

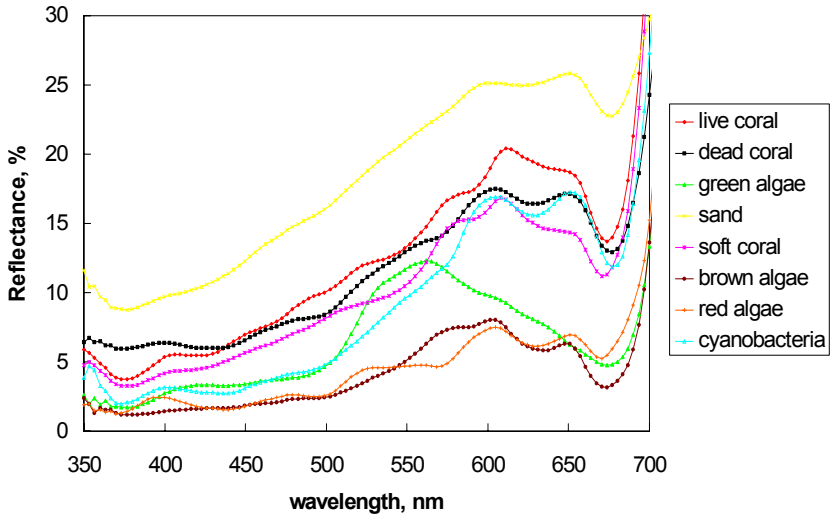

Figure 3.5.2 Typical *In situ* measured radiance reflectance spectra used in the modelling

Extensive fieldwork had been carried out in the mid-section of the Great Barrier Reef (GBR) of Australia in 1999 within the framework of a CSIRO-AIMS Coral Reef Project. The aim of the project was to study spectral signatures of different coral reef habitats and the resolvability of the habitats by remote sensing instruments with high spectral resolution. The spectral library obtained (Figure 3.5.2) enabled us to use a physics-based approach to interpret Hyperion data. Radiative transfer models together with spectral libraries of the reflectance of benthic substrates and the optical properties of the water column and atmosphere were used to model reflectance spectra above the water and also at the sensor altitude. The reflectance just above the water surface was calculated using the Hydrolight 4.1 (Sequoia Scientific) radiative transfer model placing different substrates in waters with variable depth (1-15 m with 1 m step, 20 m and 25 m) and specific optical properties for the water mass. A deep-water reflectance spectrum was simulated with the same optical water properties. The just above water surface reflectance library was used to interpret atmospherically corrected Hyperion images.

A second hyperspectral library (Kutser *et al.*, 2000; Kutser and Jupp, 2003) was created from the first by modelling radiance above the atmosphere. An in-house atmospheric model similar to MODTRAN 3.7 was used to calculate the radiance spectra at the sensor altitude. This spectral library was then used to interpret the Hyperion radiance images. Both spectral libraries were converted to Hyperion equivalent bands by multiplying the modelled spectra (with 1 nm resolution) with the normalized spectral response functions of the Hyperion bands and then integrating over each band.

Modern image processing software packages (such as Research Systems Inc. ENVI) include several procedures to produce classification maps given a spectral library of end-members - or "pure" examples of substrates. We have used the Spectral Angle Mapper (SAM). SAM is a spectral classification that uses an n-dimensional angle to match pixels to reference spectra. The algorithm determines the spectral similarity between two spectra by calculating the angle between the spectra, treating them as vectors in a space with dimensionality equal to the number of bands. This technique, when used on calibrated reflectance data, is relatively insensitive to illumination and albedo effects since it is invariant to multiplication of signatures by a constant. It has been found especially useful for spectral libraries taken under variable field and illumination conditions such as occur on reefs. In operation, SAM compares the angle between the end-member spectrum vector and each pixel vector in n-dimensional space and selects the end-members (or mixtures) with minimum angle. Smaller angles represent closer matches to the reference spectrum. Pixels further away than a specified maximum angle threshold in radians are not classified.

The spectral range in the application of the SAM was chosen taking into account substrate properties and Hyperion technical characteristics. In particular, Hyperion data are not calibrated below 430 nm and the effects of the atmosphere are very high below 500 nm. The reflectance values of water targets are normally low and noisy after atmospheric correction at these shorter wavelengths, and in addition the spectral differences between coral reef substrates are low below 500 nm. Therefore we decided not to include bands below 500 nm in the SAM analysis. Almost all coral reef benthic substrates (except sand) have high reflectance in the near-infrared part of spectrum. However, the water-leaving radiance in this part of the spectrum is low due to water absorption. Both models and images showed that there was practically no water-leaving signal at wavelengths greater than 730 nm if the substrates were covered with just 1 meter of water. Using bands that contain mainly noise in a SAM analysis can lead to very poor results and so these data were not included.

First we applied the spectral library of at-sensor radiance spectra with the atmospherically uncorrected radiance images. The benthic substrate classification image is shown in Figure 3.5.3. Each class in this image is a benthic substrate at a certain depth. Our spectral library consists of 137 end-members. 132 of them were found in the image (not all are able to be shown in the legend at one time). Since each of the classes is a substrate at a particular depth the classification map can also be separated into substrate and bathymetry maps. The bathymetry map was obtained from the classification map by changing all substrate types at a certain depth into one colour as shown in Figure 3.5.4(a). Changing every substrate type into one colour independently of the depth at which they occurred gave us the substrate map shown in Figure 3.5.4(b).

We did not carry out any bathymetry measurements in the Cairns Reef. Therefore the only reference we have is a shipping map and dive computer data from locations where the ground truth measurements were carried out. The bathymetry map generated from the Hyperion image (Figure 3.5.4(a)) fits very well with the shipping map. Most of the reef itself in the bathymetry map is in water 1-2 m deep as is the *in situ* data (depending on tide, some of the reef is exposed during very low tides). Steep increases in depth of the reef slope are clearly seen in the Hyperion map and the predicted water depths are located in the right order (not 1m, 2m, 5m, 10m, 7m for example). Even differences between water depths in and outside the lagoon are clearly seen. The water depth in the

lagoon is mainly between 5 m and 15 m according to the shipping map (with a 5m depth contour interval) and between 3 m and 15 m in the Hyperion map. Water depths between the Cairns Reef (horse shoe shaped) and Osterland Reefs (patchy reef in the upper part of the Hyperion image) is greater (27-36 m) than south from the Cairns Reef. This is also seen on the Hyperion bathymetry map in Figure 3.5.4(a). The greatest water depths used in modelling of the spectral libraries were 25 m and optically deep water. In the Hyperion map these depths are in the region where water depths are the deepest according to the shipping map (between 27 m and 36 m). Water depths above the major pinnacles in the lagoon correspond to diver's estimates based on dive computer readings.

3.5.3 Conclusions

Hyperion was not originally expected to provide its best data from water-covered environments. However our results suggest that Hyperion is suitable for mapping coral reef benthic habitats and estimating water depth and is potentially able to do this for coral reefs in many parts of the world.

Mapping of water depth and substrate types simultaneously appears to be possible using hyperspectral Hyperion data and spectral libraries in a wide range of environmental conditions. Both the substrate and bathymetry maps obtained were reliable compared to the limited (vs. size of the image) bathymetry and substrate type information that was collected in situ. The biggest problems occur in the areas where the variations in water depth and substrate type are significant (outer reef slopes) within the pixel size of the instrument.

Hyperion shows significant advantages over multispectral sensors. Differences in reflectance spectra of coral reef benthic habitats that allow the habitats to be optically separable from each other occur in narrow spectral regions. Hyperion spectral resolution is adequate to pick up those differences in shallow waters. This is not possible in the case of multispectral sensors (such as ALI, Landsat and IKONOS). The number of spectral bands available also makes it possible to estimate habitat type and water depth simultaneously. This is not the case when using multispectral sensors that have only three spectral bands in the visible part of spectrum.

3.5.4 Acknowledgements

The AIMS diving team, lead by Ian Miller, carried out extensive ground truthing on Cairns Reef and contributed significantly to this work. Acknowledgements are also due to the participants of the CSIRO-AIMS Coral Reef project John Parslow, Lesley Clementson, William Skirving, Terry Done, Ian Miller, and Mary Wakeford for their contributions. The original photograph at the start of the report was most likely taken by Terry Done.

3.5.5 References

Kutser, T., W. Skirving, J. Parslow, T. Done, L. Clementson, M. Wakeford, and I. Miller. (2000). Hyperspectral detection of coral reef health**.** *Proc. of the 10th Australasian Remote Sensing Conference*, Adelaide, 18 pp., CD-ROM**.**

Kutser, T. and D.L.B. Jupp (2003). *The CSIRO-AIMS Reef Remote Sensing Project*. CSIRO EOC Technical Paper, 2003/, pp.

3.5.6 Publications & Presentations

3.5.6.1 Journal Papers

Kutser T., A.G. Dekker and W. Skirving (2003). Modelling spectral discrimination of Great Barrier Reef benthic communities by remote sensing instruments, *Limnology and Oceanography,* **48**: 497-510.

Kutser T., I. Miller and D.L.B. Jupp (2004). Mapping coral reef benthic substrates using hyperspectral space borne images and spectral libraries. *Remote Sensing of Environment* (submitted).

3.5.6.2 Conference Proceedings

Kutser T, A.G. Dekker, and W. Skirving (2002). Detecting coral reef substrate types by airborne and space borne hyperspectral sensors. *Proceedings of SPIE*, 4544, 93-102.

Kutser T. and D.L.B Jupp (2002). Mapping coral reef benthic habitat with a hyperspectral space borne sensor. Proceedings of Ocean Optics XVI, Santa Fe, CD-ROM.

3.5.6.3 Other publications

Kutser T, (2002). How looks health of coral reefs from space? *Horisont*, **5**, 10-15. (In Estonian).

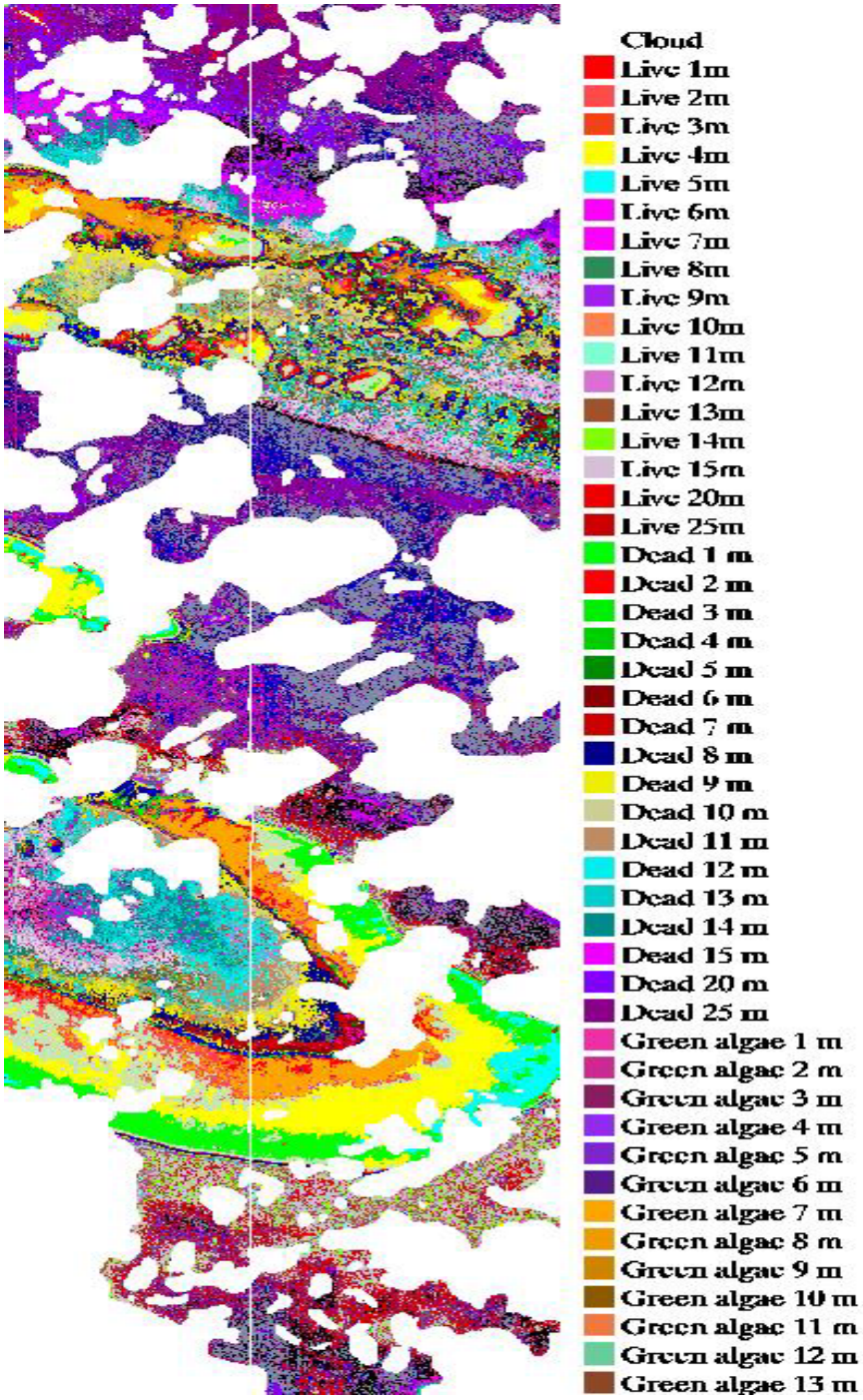

Figure 3.5.3 Substrate type and water depth classification map of Cairns (horse shoe shaped) and Osterland Reefs (patchy reef in the upper part of the image) obtained from Hyperion image acquired on March 19, 2001. Spectral Angle Mapper was applied on the radiance data and the spectral library as radiance at Hyperion altitude was used. Only some of the detected substrate classes are shown in the legend due to technical reasons.

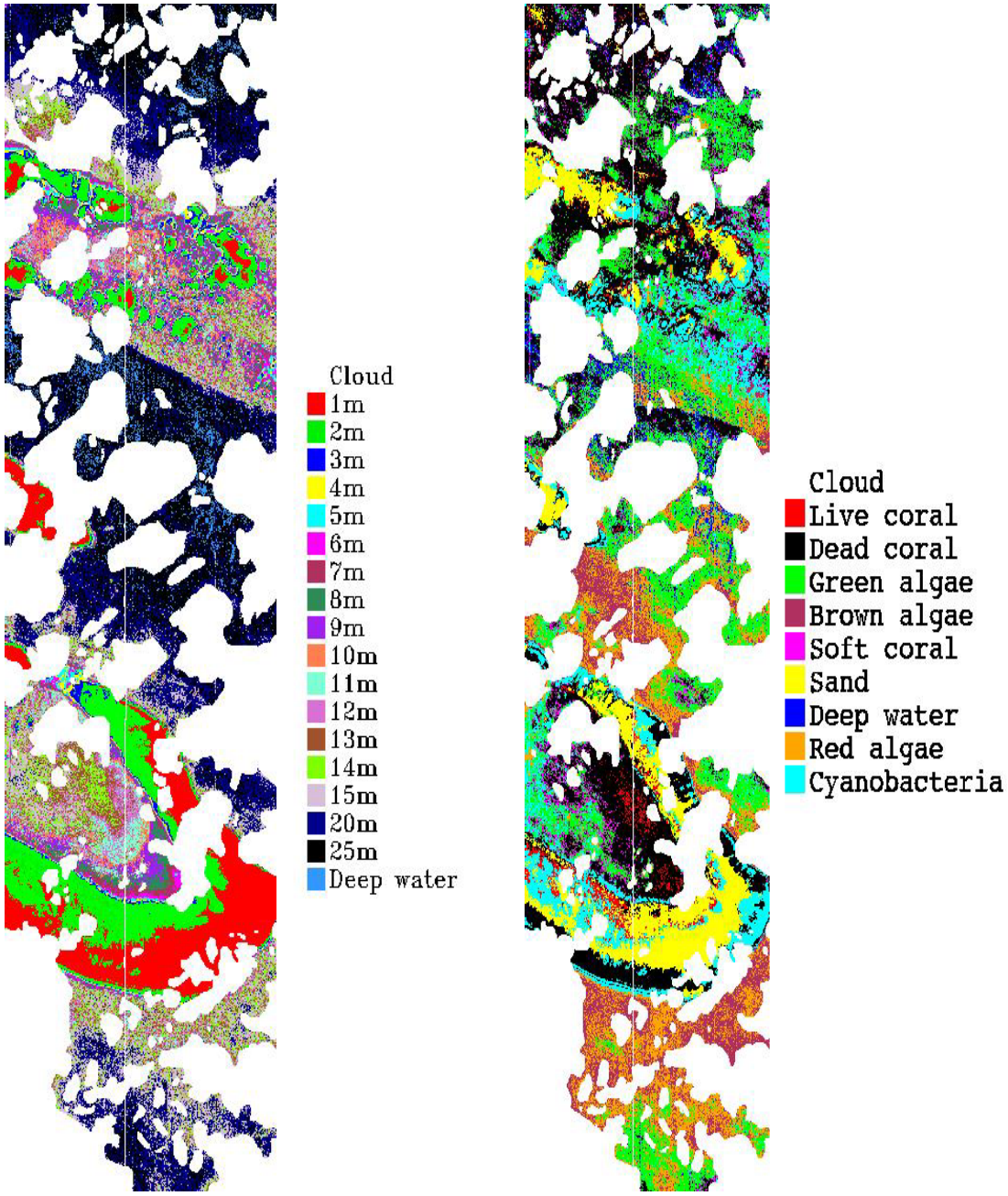

Figure 3.5.4 Bathymetry map (a) and benthic substrate map (b) obtained from the Hyperion classification map shown on Figure 3.5.1.

3.6 Mt Fitton

Natural, well exposed geology at the Mt Fitton site, South Australia

Site P/Co-Investigator(s): Tom Cudahy, Pamela Barry and Jon Huntington
Site Name: Mt Fitton
Type of measurement: radiance at sensor
Dates of acquisition: 27.12.00; 12.01.00; 13.02.01;07.07.01; 25.09.01; 27.10.01
Latitude: 29° 55’ S
Longitude: 139° 25’ E
Elevation: 100m ASL
Surface type: low and sparse vegetation cover (5-15%), relatively fresh rock outcrop
General atmospheric conditions: Clear
Other satellite data: ASTER
Comments: 5m HyMap data also collected (19 September 2000)
Contact email: Thomas.Cudahy@csiro.au

Report by: Tom Cudahy, Melissa Quigley, Pamela Barry and Jon Huntington.
CSIRO Exploration and Mining
Mineral Mapping Technology Group

3.6.1 Introduction & Objectives

Remote hyperspectral sensing for detecting and mapping, often subtle, mineralogical spectral signatures using airborne systems has been operational for a number of years using instruments such as HyMap (see http://www.hyvista.com/). The launch of the EO-1 satellite in November 2000 (see http://eo1.gsfc.nasa.gov/) introduced hyperspectral sensing of the Earth from space through the Hyperion system (Liao *et al.*, 2000; Pearlman *et al.*, 2001).

The Mount Fitton site in the northern Flinders Ranges of South Australia (near both Lake Frome and the CIMEL site at Tinga Tingana) was used extensively in the early check-out period to validate Hyperion's performance. It became clear during this exercise that the capability of Hyperion to provide selected mineral maps under certain circumstances was higher than first anticipated. These and later confirmations of the findings led to the CSIRO Mineral Mapping and Technologies Group (MMTG) facilitating extended data collection, pre-processing and selected product generation for users in several parts of the world.

This Mt Fitton report is divided into two sections to reflect two major sets of objectives. The first describes work that assessed the basic performance of the Hyperion system in space for the purposes of mineral mapping during the early assessment period. The outcomes of that work prompted increased interest amongst geologists. The extent of Hyperion's capability had previously been doubted due to the much lower SNR specification compared with current airborne instruments. High SNR is necessary for effective mineral mapping. The second section reports on activities that investigated the stability of the SWIR module of the sensor array and the implications this had for data processing and mineral mapping. It found that with careful pre-processing, including taking account of the striping artefacts found in Hyperion data, the data were able, under selected circumstances to realise useful and spatially coherent mineral maps. It also found the instrument and its calibration had been effective and stable over the first year.

3.6.2 Study 1 - The Mineral Mapping Performance of Hyperion

3.6.2.1 Background

The first study summarises the results for the Hyperion spectral and geological validation site at Mount Fitton in South Australia (Cudahy *et al.*, 2001), one of three sites chosen by the science team to evaluate Hyperion data for resolving surface spectral signatures throughout the 400 nm to 2500 nm wavelength region in the early phase of the evaluation of the instrument. Success in this endeavour depended on having an instrument with accurate wavelength, radiometric and MTF calibration/characterization and adequate SNR.

Hyperion's SNR was initially thought to be marginal for mineral mapping. The pre-launch specifications quoted SNR for a 60° solar zenith and 30% reflector with results ranging from 190:1 for the visible to 38:1 for the 2100-2150 nm wavelength range in the SWIR. Based on experience with HyMap and AVIRIS this was regarded as inadequate for effective operational and routine mineral exploration across a wide range of environments.

3.6.2.2 Initial Data and Processing

Cloud-free Hyperion data were collected over the Mount Fitton test site in South Australia on the 27th December 2000. Data were provided by TRW as radiance at sensor. Reduction to apparent surface reflectance was achieved using ACORN (see http://www.aigllc.com/acorn/intro.asp), which is a radiative transfer routine based on MODTRAN.

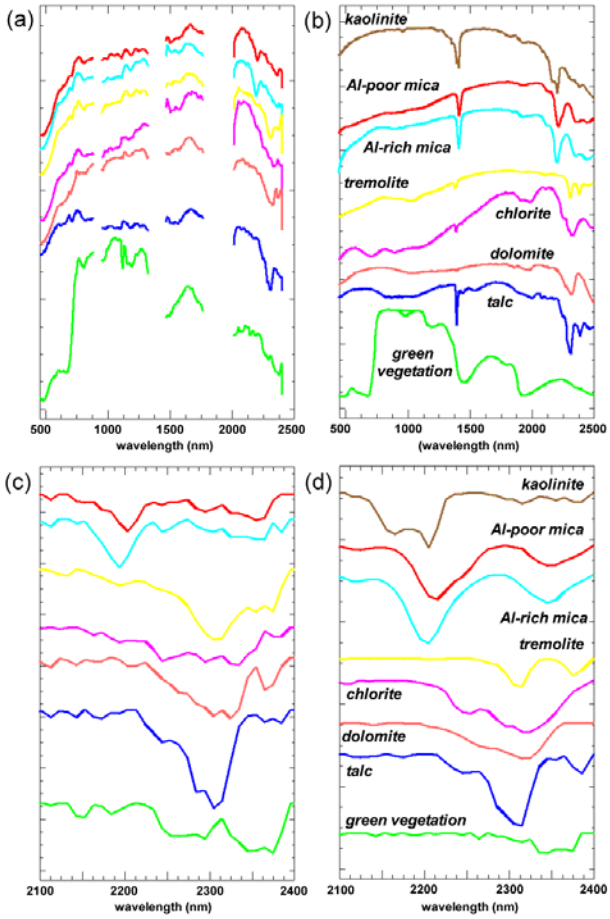

Figure 3.6.1: Stacked spectra offset for clarity (a) Mean Hyperion spectral signatures from selected regions-of-interest (ROI) of the Mount Fitton scene. (b) Selected library mineral and green vegetation spectra from http://speclab.cr.usgs.gov/ convolved to the Hyperion bandpasses. (c) Same as (a) but restricted to the SWIR wavelengths. (d) Same as (b) but restricted to the SWIR wavelengths.

Pixel-based estimates of water vapour are usually measured using the continuum-depths of the 940 and 1140 nm atmospheric water vapour absorption bands. The resultant retrieval of surface radiance thus relied on sufficient spectral resolution of the atmospheric water bands. However, only the 1140 nm band was used in this case because of complications with the detector overlap in the 900 nm region. This may be overcome in the future if cross-calibration in the overlap is improved.

The efficacy of the atmospheric correction was initially assessed through successful recognition of green vegetation spectral signatures along creeks (Figure 3.6.1a and Figure 3.6.1b). The overall shape, including the characteristic NIR plateau between 700 and 1300 nm, as well as absorption bands related to chlorophyll (675 nm) and leaf water (980, 1190, 1450 nm) are clearly evident in the reduced Hyperion data.

Processing of the data was carried out using the ENVI image processing software (see http://www.envi-sw.com/) as well as software developed by CSIRO. Information extraction from the reduced Hyperion data, especially from the SWIR region, involved several processes including extraction of scene spectral endmembers using the MNF, PPI and n-dimensional approach as well as a more targeted spectral parameter approach. Partial unmixing of the data was carried out using the Mixture Tuned Match Filter (MTMF) procedure. This technique maximises the response of the known endmember and suppresses the response of the composite unknown background, thus "matching" the known signature. MTMF products were used to generate thematic mineral maps. A CSIRO procedure based on fitting a 4^{th} order fitted polynomial to mineralogically-diagnostic wavelength ranges was also employed to measure a given absorption's depth, area and wavelength information. This technique provides accurate mineral information because it targets only those wavelengths diagnostic of specific minerals and is not compromised by scene-dependent statistics. All the processed image data were not georeferenced as initial inspection of the geometric fidelity of the data showed it to be good.

3.6.2.3 Geology

The semi-arid Mount Fitton area is located in the northern Flinders Ranges of South Australia, centred at 139° 25' E and 29° 55' S. Local relief is up to 100 m. Infrequent flash flooding has prevented the development of a deep regolith cover, resulting in abundant exposure of relatively fresh outcrop. Vegetation is generally low and sparse (5-15% cover), except along ephemeral drainage.

The geology has been mapped by Coats *et al.* (1969). The published 1:100,000 scale geology map covering the Hyperion overpass of the Mount Fitton talc mines (Figure 3.6.2a) shows the Early Proterozoic Terrapinna Granite, and Late Proterozoic (Adelaidean) sediments of the Umberatana Group, including tillites of the Bolla Bollana Formation, carbonates of the Balcanoona Formation and siltstones and other quartzose sediments of the Amberoona Siltstone, Fortress Hill and other formations. Metamorphic mineralogy is largely controlled by the host rock composition. Calcite within the Balcanoona Formation was converted to dolomite or magnesite, which were altered later during hydrothermal Si metasomatism to locally produce talc (after magnesite), tremolite (after dolomite), quartz, white mica and chlorite.

3.6.2.4 Initial Results

Processing of the 40 SWIR bands between 2000 and 2400 nm for 1000 lines over the Mount Fitton talc mines (Figure 3.6.2b) yielded only 3 MNF bands without apparent instrument noise (primarily column and random noise) and only 10 with spatially varying geological information (with or without noise). Extraction of spectral endmembers from these data using ENVI's 'n-dimensional visualiser' proved difficult with only 3 endmembers clearly distinct in the MNF data cloud. Better results in

collecting different mineralogical spectral signatures were achieved using *a priori* knowledge of the geology (locations of these regions of interest are shown in Figure 3.6.2a). This yielded recognisable average spectral signatures for most of the minerals expected for the area, including dolomite, talc, chlorite, various white micas and possibly tremolite (Figure 3.6.2c & Figure 3.6.1a).

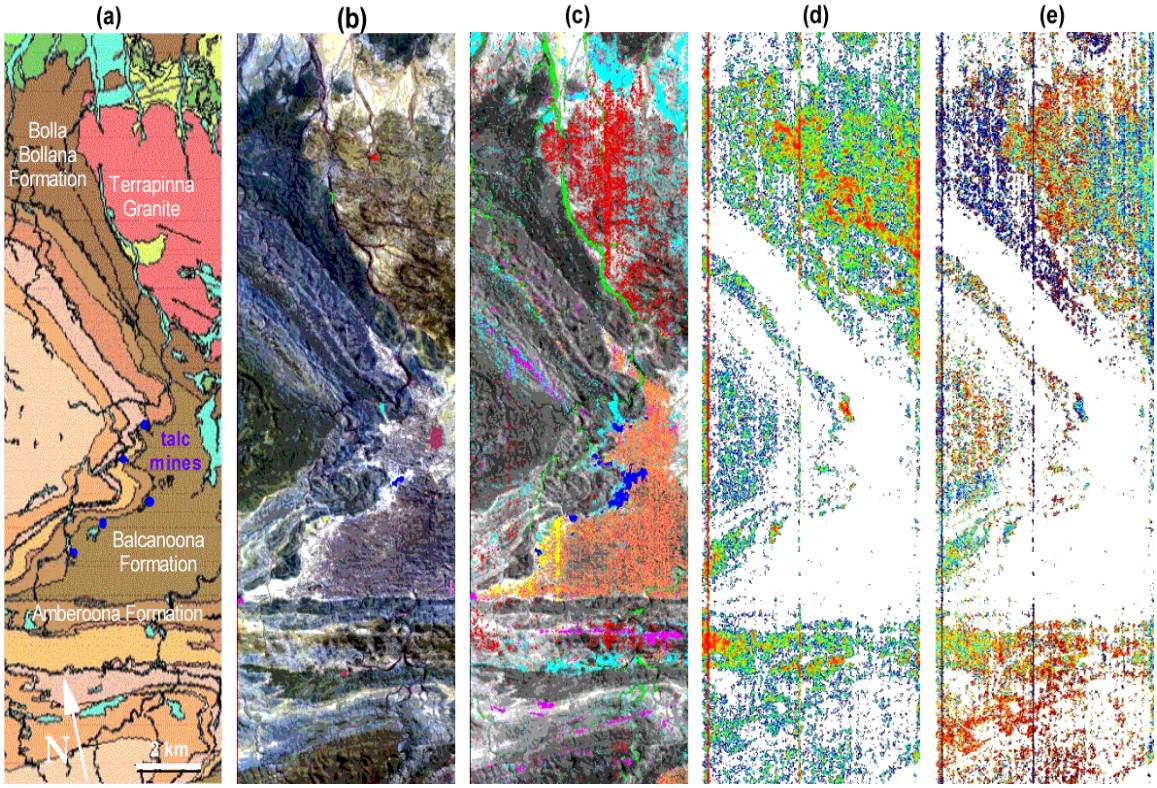

Figure 3.6.2: (a) Published 1:100 000 scale geology Coates *et al.* (1969) of the Mount Fitton test site. (b) Hyperion colour composite image (R: 720 nm; G: 620 nm; B: 550 nm) showing colour-coded regions of interest from which the spectra of Figure 1a were derived. (c) Mineral map derived using MTMF of the spectral endmembers shown in Figure 3.6.1a. The same colour labels apply. (d) The area of the 2200 nm absorption related to the abundance of Al-OH minerals like muscovite (blue:small and red:large). (e) Wavelength of the 2200 nm absorption, which is sensitive to Al-substitution in muscovite, for those pixels with absorption at these wavelengths (shown in (d)). The wavelength range is from 2190 nm (Al-rich mica : dark blue) to 2208 nm (Al-poor mica : red)

The chlorite spectrum shows the characteristic broad ferrous iron absorption centred at 1000 nm similar to that observed in the library chlorite spectrum (Figure 3.6.1b). The SWIR wavelengths of the selected Hyperion mineral spectra (Figure 3.6.1c) show diagnostic absorption bands that allow identification of mineralogy, albeit with spectrally independent noise apparent throughout. For example, the spectrum collected from the talc mine (blue) shows the same deep absorption band at 2310 and accompanying shoulder absorptions at 2290 nm and 2250 nm as the library pure mineral talc spectrum. Chlorite shows a small absorption at 2250 nm (slightly deeper than the noise level), dolomite a broad, left-asymmetric feature centred at 2325 nm and white mica spectra show absorption near 2200 nm. However, all spectra show poorer results at wavelengths greater than 2350 nm, probably because of poorer signal-to-noise.

The Hyperion MTMF-derived mineral map (Figure 3.6.2c) shows spatially coherent mineral distributions consistent with the mapped geology as well as superimposed alteration. For example, the dolomites of the Balcanoona Formation are well mapped, as is the white mica-rich granite. All the open pit talc mines and related processing plant are mapped. The presence of tremolite, chlorite and white mica towards the western part of the Balcanoona Formation has been established previously by field mapping and represents hydrothermal fluid alteration in the carbonate rocks beneath contact with the overlying siltstones of the Amberoona Formation.

The white mica absorption near 2200 nm can vary in wavelength depending on the level of Tschermak substitution $\{Al \Leftrightarrow Si + (Fe^{2+} \pm Mg)\}$. The Hyperion data were processed to deliver images depicting the area and wavelength of the 2200 nm absorption (abundance and Al-chemistry of white mica, respectively) in Figure 3.6.2d and Figure 3.6.2e. These show geologically significant patterns within the granite and quartz-rich sediments and, as expected, essentially absent in the Balcanoona Formation. Note the mapping of Al-poor mica in the Bolla Bollana Formation is not apparent in the MTMF results (Figure 3.6.2c, Figure 3.6.2d, Figure 3.6.2e). This is because white mica in the Bolla Bollana Formation does not have the same overall SWIR spectral character as white mica in the image/ROI endmembers taken from the granite and Amberoona Formation, even though white mica itself is the same. That is, MTMF (and similar endmember-based techniques) is being influenced to a significant extent by non-mica spectral variation that is characteristic of the lithotype of the extracted endember/ROI.

This level of mineral mapping and mineral chemistry mapping based on recognisable mean spectral signatures was clear testament to the success of the satellite-borne Hyperion system and its spectral resolving power for mineral mapping, in bright well-exposed terrains. These encouraging early results were reported by Cudahy *et al.* (2001). However, instrument effects, including column-dependent striping (Figure 3.6.2), were considered as potential problems that needed to be resolved if Hyperion data were to be used more operationally for geological applications. These issues were subsequently addressed in additional work at Mt Fitton, the Panorama site and in studies overseas as well.

3.6.2.5 Follow-on Work at Mt Fitton

Due to deficiencies recognised in Hyperion's initial spectral quality and imagery, the Mineral Mapping and Technology Group (MMTG) at CSIRO Exploration and Mining developed a number of ENVI add-on programs to enhance Hyperion's ability to effectively map surface composition with the intent of 'cleaning' the data to a level that initially improved the coherency of the mineral maps generated by standard methods and additionally made it suitable for input into semi-automatic, in-house developed mineral mapping routines.

As seen above in Figure 3.6.2, the Hyperion scene is heavily influenced by column-striping effects caused by small mis-calibrations of the detector array. Two programs called *Plugger* and *Destripe* were developed (see description under *Geoscientific Databuy*). *Plugger* collects channel and pixel statistics for large blocks of lines in order to identify aberrant detector elements, which are then nulled/replaced. Based on these statistics, *Destripe* then adjusts (gains and/or offsets) the detector element responses to remove the striping effects. A comparison of the original mineral map and the mineral

map from the ‘repaired’ datacube in Figure 3.6.3 highlight the increase in quality of the spatial coherency. More detailed analysis of the problems associated with the calibration of the area array are discussed in Section 1.1.3.1.

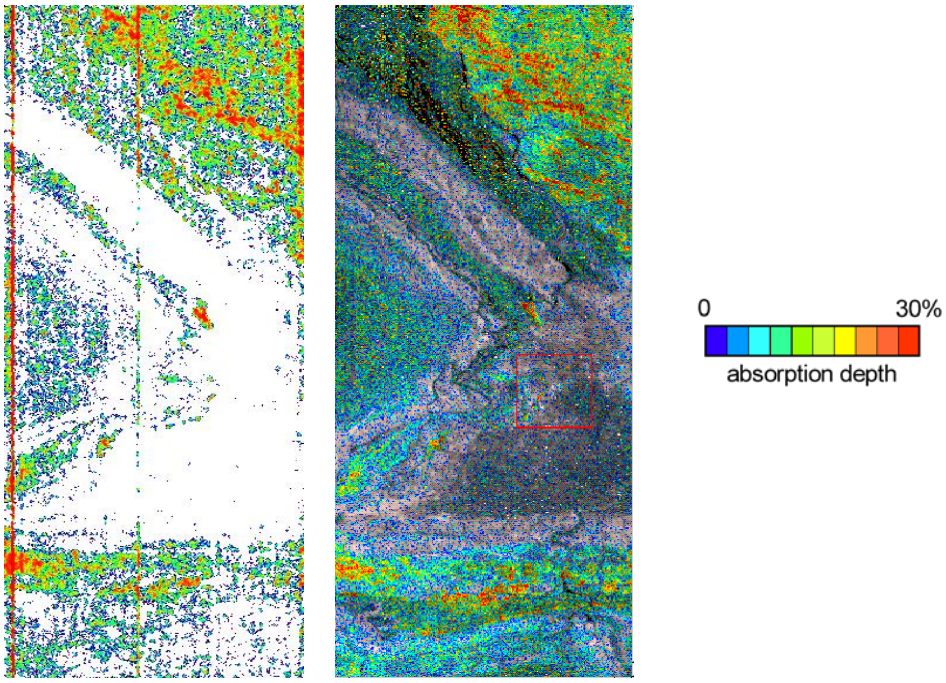

Figure 3.6.3: Comparison of white mica abundance mineral maps from the original datacube (left) and the ‘repaired’ datacube (right).

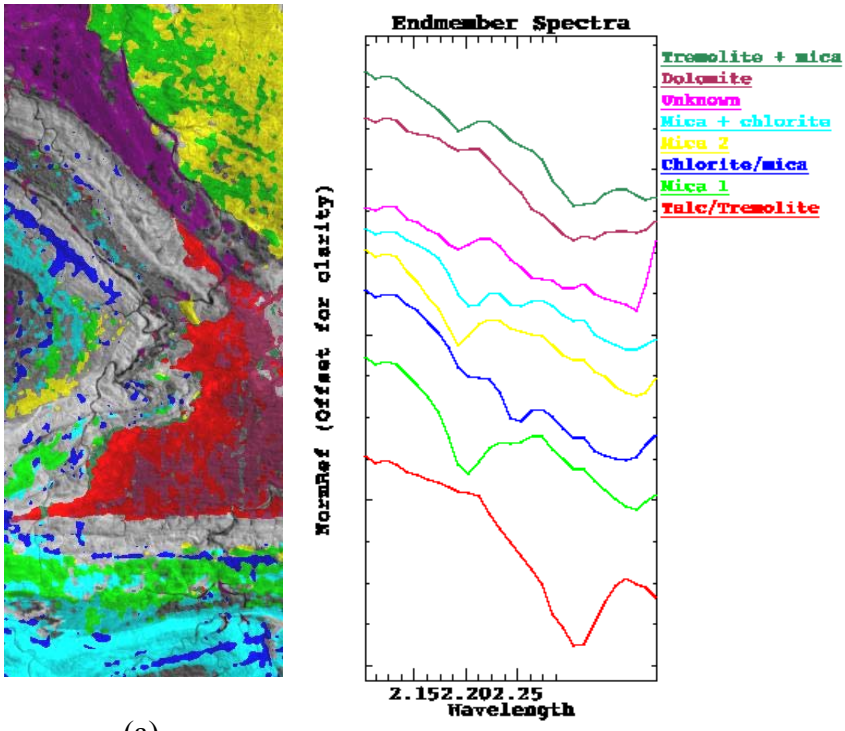

(a) (b)

Figure 3.6.4: Quick-look mineral map (a) and individual scene endmember spectra (b) generated from the repaired and smoothed datacube.

Subsequent "spectrally-sensitive" smoothing of the datacube enabled the datacube to be used as input into semi-automatic mineral mapping programs that created a quick-look mineral map in approximately 30 seconds (Figure 3.6.4). These follow-on studies evaluating the 'repaired' datacubes showed the improved quality of the data that produced more cohesive mineral map products leading to an increase in user confidence of the results and hence increased utility of the data.

3.6.3 Study 2 - Assessment of the stability of the SWIR module

3.6.3.1 Background

To further assess the operational usage of Hyperion data for the extended mission, a series six of Hyperion acquisitions were collected from the Mount Fitton site over a one year period, including dates from winter (low sun angle/insolation) through to summer (high sun angle/insolation). These multi-date imagery were necessary to better characterise the nature of the column striping and to assess the repeatability and stability of Hyperion's SWIR area array and related calibration. These are important issues that impact on the accuracy and reproducibility of any derived surface compositional maps especially as an expanded user role for Hyperion was being considered as part of the extended EO-1 mission (see http://eo1.usgs.gov).

3.6.3.2 Destriping

The first test was to investigate whether the column striping was additive or multiplicative in nature, or a combination of both. Figure 3.6.5e presents an image of a single SWIR band that shows no apparent striping but only relative brightness variations related to different surface types and topographic shading. The column striping can be readily enhanced by normalising out the correlated albedo and topographic illumination as shown by the ratio of two SWIR bands (Figure 3.6.5d). The *Destriping* routine was then applied to the original SWIR radiance at sensor data with adjustments applied using gains (equalise column means by scaling - Figure 3.6.5a), offsets (equalise column means by offsets - Figure 3.6.5b) and gains and offsets (equalise the column variances by scaling and equalise the means through offsets Figure 3.6.5c). All the resultant destriped products show significant improvement in reducing the striping though applying only gains or offsets has residual striping in those columns on the right-hand-side of the image, which changes from high to low along its length depending on pixel albedo. That is bright striping over brighter pixels and dark striping over darker pixels. Similar, though not as complex residual striping occurs over areas of low brightness in other parts of the image.

The presence of a significant additive instrument effect was not anticipated because of the dark current subtraction that is performed, however this additive component may be explained as residual error in the instrument smear, dark current and echo artefact corrections.

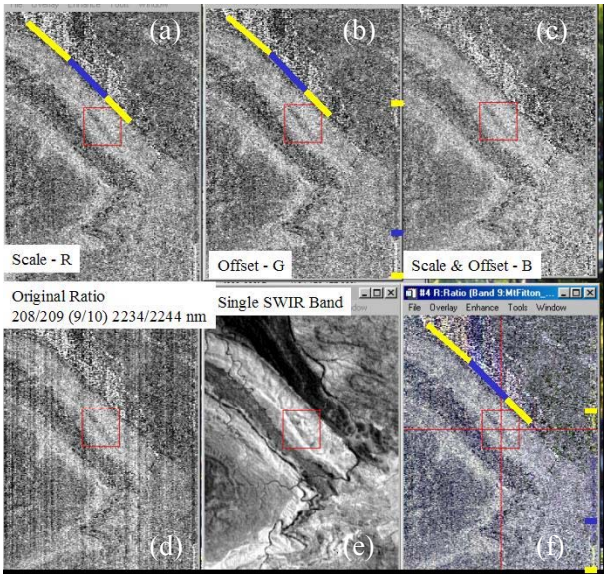

Figure 3.6.5: Nature of column striping (a) Destripe correction using gains. (b) Destripe correction using offsets. (c) Destripe correction using gains and offsets. (d) Ratio of SWIR bands to reveal striping without the Destripe correction. (e) SWIR band at 2244 nm. (f) RGB colour composite of (a), (b) and (c). Blue and yellow colour bars highlight residual striping effects.

The next experiment examined multi-date ratio products with and without destriping to see if the striping was systematic through time or different for each scene (Figure 3.6.6). The red arrows point to column variations visible for all three dates. Due to the repeatable nature of this variation, it is likely that the cause is an error in the calibration file, which can be updated.

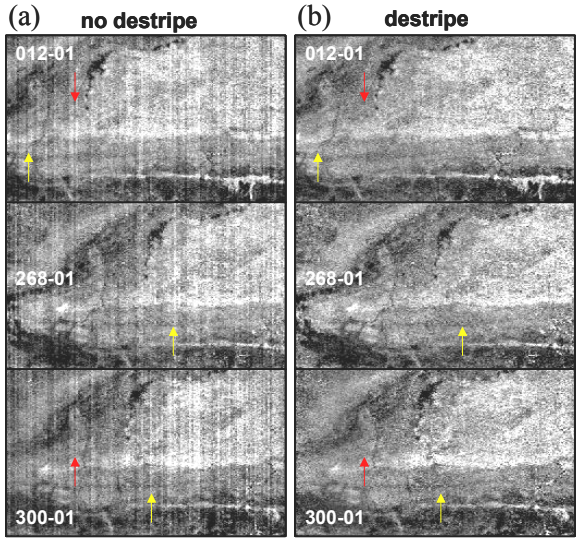

Figure 3.6.6: (a) Hyperion ratio (sum of bands 204-209 divided by band 210) sub-images from three dates (012-01, 268-01, 300-01) exhibiting striping. (b) Destriped image (shift and scale corrected based on 1400 lines for statistics). Examples of systematic inter-scene (red arrows) and scene-dependent (yellow arrows) column striping are shown in (a).

The yellow arrows point to column variations that vary from one collect to the next. It is likely that this type of variation needs to be corrected for by using in-scene techniques.

The third experiment examined the importance of gathering enough lines for the statistics used in *Destripe*. This was particularly important as the size of the standard Hyperion image to be supplied to clients was to be reduced from 6170 lines to 1400 lines with the transfer of operations from TRW to EDC. The critical assumption for successful destriping is that the block of lines for gathering column statistics is sufficiently homogenous across the width of the imagery. That is, a large collection of pixels with strong spectral contrast located preferentially down one section of the image will dominate the column statistics and thus introduce residual error into the destriping. In theory, the more lines gathered the greater the chance that spatially-dependent surface spectral heterogeneity will not compromise the statistics.

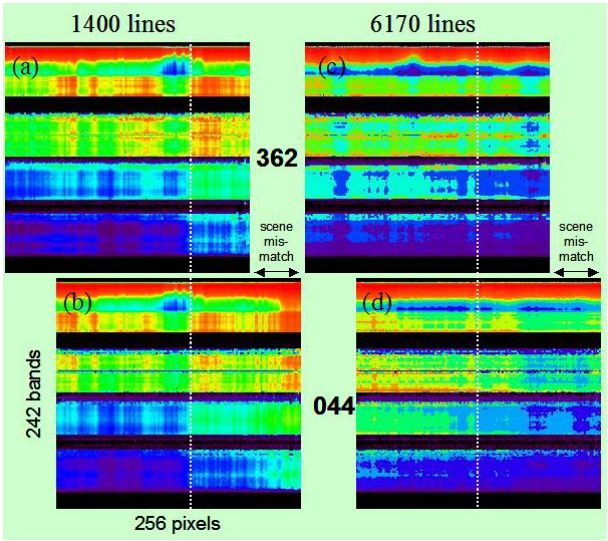

Figure 3.6.7: Hyperion detector area array means for two different dates of imagery but offset in track by only 50 pixels calculated using 1400 lines versus 6170 lines.

Two dates of imagery (named 362 and 044 in Figure 3.6.7) from the Mount Fitton sites were selected. The tracks of these two scenes were offset by approximately 50 pixels and covered well exposed and contrasting geology as shown in Figure 3.6.2. The detector array means, generated using *Plugger*, were calculated for these two dates for 1400 lines and 6170 lines of data. The results (Figure 3.6.7) show that the same spectral variation in the means, albeit offset by 50 pixels, is more prominent in 1400 line data set compared with the 6170 data set. This suggests that it is preferable to use 6170 lines for calculating column statistics to reduce the effects of spatial-spectral heterogeneity.

To further test the importance of sample size when gathering statistics, the spectra of several ROIs from different minerals groups from the same scene 044 used in Figure 3.6.7 and destriped using 1400 and 6170 lines as well as no destriping were compared to see if spectral integrity was being compromised through destriping.

The results (Figure 3.6.8) for talc, dolomite, chlorite and white mica ROIs show generally less than a 1% effect at all wavelengths in the SWIR-2 with or without destriping or with 1400 or 6170 lines used in the statistics. That is, there appears to be little or no compromise on mineral spectral integrity by applying a destriping algorithm to the Hyperion data, even for 1400 lines.

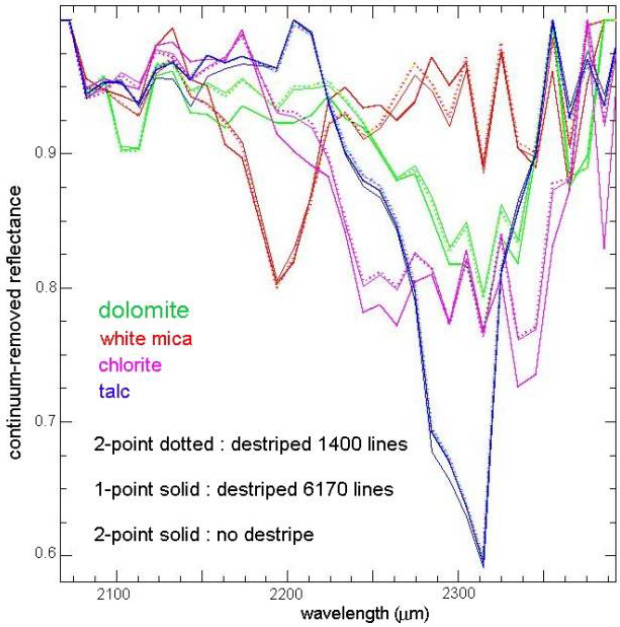

Figure 3.6.8: Various mineral ROI spectra with and without destriping applied with the destriping calculated using 1400 and 6170 lines.

3.6.3.3 Instrument Stability

The next question addressed is whether the Hyperion system is generating the same spectral signature from the same area of ground over time? To help address this question, six scenes of essentially cloud-free Hyperion data were collected for the Mount Fitton test site. The scenes are denoted by the day of the year, and the year of the collect. The data set includes: 362-00; 012-01; 044-01; 188-01; 268-01; and 300-01. Data were provided as Level 1A radiance at sensor for scenes 185 km in length (6700 lines each). No atmospheric correction was applied to the data.

Figure 3.6.9 presents the mean continuum-removed radiance at sensor SWIR-2 spectra collected from each of the 6 dates of Hyperion imagery after destriping (as well as three examples before destriping) for a single region of interest (ROI) of between 40-50 contiguous pixels over an area of white mica alteration (shown in the zoom window of 10). The close similarity of these spectra testifies to spectral stability of Hyperion over the 12 month period examined. It also confirms what little adverse effect the destriping correction has on the spectral integrity of the data for multiple dates of imagery.

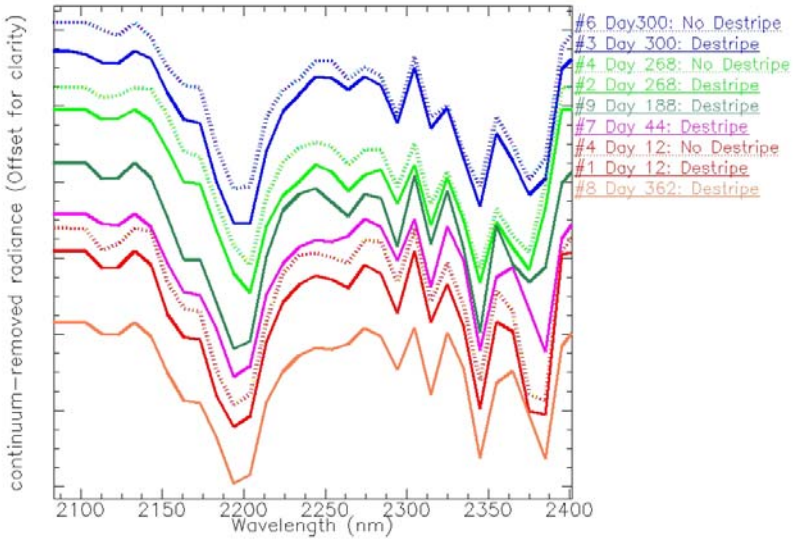

Figure 3.6.9: (a) Stacked ROI pixel mean, continuum-removed radiance at sensor spectra collected from the six dates of Hyperion imagery from a common area of field-verified white mica alteration shown in the zoom window of Figure 1.1.7. The shoulders in these spectra near 2160 nm, that make these spectra look like kaolinite is interpreted to be a noise effect, equivalent in amplitude to other noise spikes in these spectra and points to the ambiguities that can sometimes occur with noisy data.

The effectiveness of the destriping correction and the stability of Hyperion's SWIR-2 calibration on the spatial coherency of derived mineral maps is presented in Figure 3.6.10. The mineral product in this case was a ratio, a sum of bands 207 (2224 nm), 208 (2234 nm) and 209 (2244 nm) over a sum of bands 204 (2193 nm) and 205 (2203 nm), designed to minimize random noise but capture the change in depth of the Al-OH absorption band of white mica centred at 2200 nm. Again, only the radiance at sensor data was used and the same threshold value (0.31) was applied for the resulting ratio image products.

The results (Figure 3.6.10) show the same areas are mapped for each scene. Note that scene 188-01 was taken at low sun angle (late-winter) with half the radiance levels of the other scenes. Nevertheless, it is still producing a coherent mineral map, at least for white mica, similar to all the other dates of imagery. An increased number of isolated pixels (errors of commission) have been captured related to the data approaching the end of the useable SNR levels, especially for lower albedo surfaces.

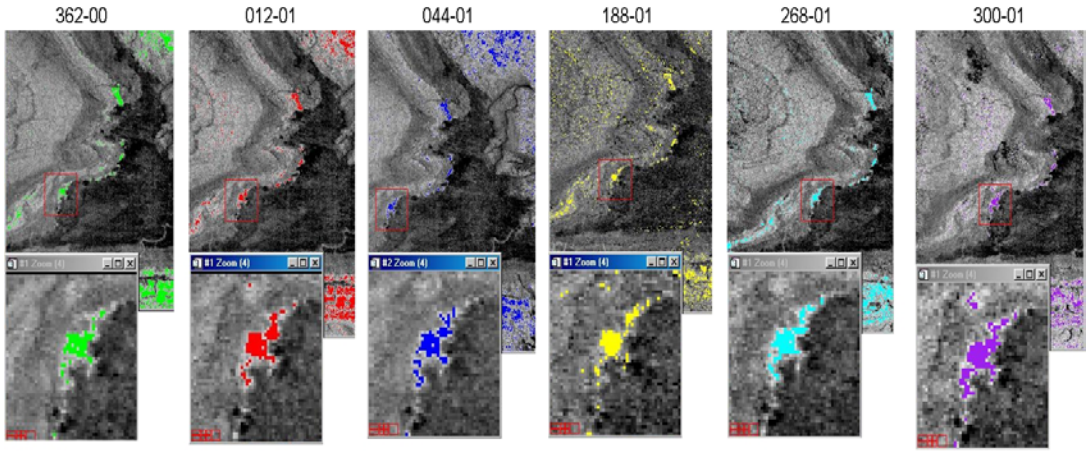

Figure 3.6.10: Six Mt Fitton Hyperion subscenes of destriped SWIR-2 radiance at sensor data with band 208 as the grey-scale background and each date of imagery showing a coloured threshold overlay of a multiband ratio (sum of bands 208 to 210 over the sum of bands 204 to 206), sensitive to white mica abundance (Al-OH absorption at 2200 nm), and then threshold to capture all pixels above a value 0.31 for all images.

3.6.3.4 Conclusions

The results from the two Mt Fitton studies show that a) Hyperion is capable of mineral mapping in a semi-arid terrain with well-exposed, bright, geological outcrop and b) the sensor is temporally stable producing reasonably consistent results from six data collects over twelve months. The best mineral mapping results are for those minerals with diagnostic features at wavelengths <2300 nm as SNR appears to be much better at these wavelengths. That is, poor SNR at wavelengths greater than ~2330 nm[8] impedes the reliable detection of several mineral suites, in particular, minerals with dominant Mg-OH and CO_3 absorption features, common in mafic and ultra-mafic terrains. Higher SNR will also be required for low albedo, high latitude, and more vegetated sites. Furthermore, as non-expert users demand products from automated mineral mapping algorithms, SNR will also have to improve, as these algorithms are currently far less forgiving than human experts and are prone to generating more errors with noisy data.

By the application of a gain and offset correction on a spectral subset of the Mt Fitton Hyperion cube it was shown that the striping effect caused by mis-calibrations in the detector array could be successfully removed, thereby allowing homogenous mineral maps to be produced. The assessment of six white mica maps produced by band ratios from each of the six multi-temporal scenes showed consistent results, verifying Hyperion's performance and high stability over the first twelve months of its operation.

Overall, the evaluation and validation studies conducted at Mt Fitton produced surprisingly good results for the Hyperion experimental hyperspectral sensor considering the low SNR and mis-calibration in the detector array. Spaceborne sensing still has a long way to go for fully operational mineral mapping applications to be comparable to the high quality airborne hyperspectral instruments commercially available today.

[8] [As noted before: Hyperion SWIR array responsivity drops away quickly after 2300 nm as shown in Figure 1.4.4 as does atmospheric stability as shown in Figure 1.4.8 (ED)]

3.6.3.5 Acknowledgements

The people involved at Mt Fitton and in processing its data extended to a wider group than the principal site investigators and included:

T.J. Cudahy
R.D. Hewson
A.P. Rodger
CSIRO Exploration and Mining
Underwood Avenue
Floreat Park, W.A.,
Australia, 6014

J.F. Huntington
M.A. Quigley
P. Mason
CSIRO Exploration and Mining
Delhi Road
North Ryde, N.S.W.,
Australia, 2113

P.S. Barry
J.S. Pearlman
M. Folkman
TRW Space and Electronics Group
One Space Park, R1-1026
Redondo Beach, CA.,
USA, 90278

3.6.3.6 References

R.P. Coats, R.C. Horwitz, A.R. Crawford, B. Campana, B. and D. Thatcher (1969). *1:*125*,000 scale geological map of the Mount Painter Province*. Geological Survey of South Australia.

T.J. Cudahy, R.D. Hewson, M.A. Quigley, J.F. Huntington and P. Barry (2001). The Performance of the Satellite-borne Hyperion Hyperspectral VNIR-SWIR Imaging System for Mineral Mapping at Mount Fitton, South Australia. *Proceedings IGARSS*, Sydney, 9-13 July, .

T.J. Cudahy, P.S. Barry, M.A. Quigley, P. Mason, and J.F. Huntington (2002). Assessment of the stability of Hyperion's SWIR Module for Hyperspectral Mineral Mapping Using Multi-Date Images from Mount Fitton, Australia. *Proceedings IGARSS*, Toronto, 24-28 June, VI: 3504-3506.

J.S. Pearlman, S. Carman, C. Segal, P. Jarecke, P.S. Barry, W. Browne (2001). Overview of the Hyperion Imaging Spectrometer for the NASA EO-1 Mission. *IGARSS Special Session* 40, SS40MO, Paper 1775, 2001.

L. Liao, P. Jarecke, D. Gleichauf and T. Hedman (2000). Performance Characterization of the Hyperion Imaging Spectrometer Instrument. *Proc. of SPIE*, Vol. 4101, pp. 22-26, July 2000.

3.7 Panorama

Panorama Site in Northern Western Australia

Site P/Co-Investigator(s): Tom Cudahy and Pamela Barry
Site Name: Panorama
Type of measurement: radiance at sensor
Dates of acquisition: 30.12.00
Latitude: 21° 12’ S Longitude: 119° 10’ E
Elevation: 250m
Surface type: extensive rock outcrop, vegetation dominated by Spinifex grass
General atmospheric conditions: clear
Other satellite data: Landsat ETM
Comments: 5 m HyMap data collected November 1998
Contact email: Thomas.Cudahy@csiro.au

Reported by: Tom Cudahy
Melissa Quigley
CSIRO Exploration and Mining
Mineral Mapping Technologies Group

3.7.1 Earth magmatic-seawater hydrothermal alteration at Panorama

3.7.1.1 Introduction

The Panorama area, in the Archaean Pilbara Block of Western Australia, provides arguably the world's best example of an exposed volcanic massive sulphide (VMS) hydrothermal alteration system, being relatively unweathered and well exposed in near-complete cross-section over its 6 km depth and 30 km strike length (Brauhart *et al.*, 1998). This 3.24 Ga hydrothermal system is associated with base metal sulphide mineralisation and fossil extremophiles (microbes that live in extreme conditions) in the discharge sites of emanating seawater and/or magmatic fluids (Rasmussen, 2000). Remote mapping of this type of system therefore has implications for both mineral exploration and as an analogue for those seeking suitable sites for early life on Earth and elsewhere.

Previous work (Cudahy *et al.*, 1999; 2000) found that the VMS discharge sites, and indeed much of the alteration associated with the hydrothermal convective system at Panorama, could be mapped using airborne HyMap hyperspectral visible and near infrared to shortwave infrared (VNIR-SWIR) data and provided a complementary and critical data set to conventional mapping methods. Critical amongst the mapped minerals is white mica with its associated Tschermak substitution (Al-⇔[Si+Fe/Mg]), which produces a subtle 10-20 nm shift of the diagnostic 2200 nm Al-OH absorption band (Duke, 1994; Scott and Yang, 1997). Huntington and Boardman *et al.* (1994), using field spectra and Geoscan multispectral scanner data, documented similar wavelength shifts, and spatial variations in white mica aluminium substitution, in very similar rocks from the east Pilbara. In that case, the longer wavelength, Al-poor rocks were associated with mineralised targets.

The objective of this study was to establish whether the space-borne Hyperion data could be applied to map the mineralogy, mineral chemistry and spatial geometry of the Panorama hydrothermal alteration system, thus providing a potential analogue for mapping similar systems elsewhere on Earth and other planetary bodies.

3.7.1.2 Panorama Test Site

The Panorama area is located 100 km SE of Port Hedland in Western Australia centred at approximately 119°10' E and 21°12' S (Figure 3.7.1). Topographic relief is up to 300 m and outcrop exposure is excellent. The region is semi-arid but can experience cyclonic activity in summer, which brings infrequent but heavy rainfall. The vegetation is dominated by spinifex grass with eucalypts and other trees variably developed along the major ephemeral drainage systems. Infrequent fires have left large areas with differing extents of spinifex cover.

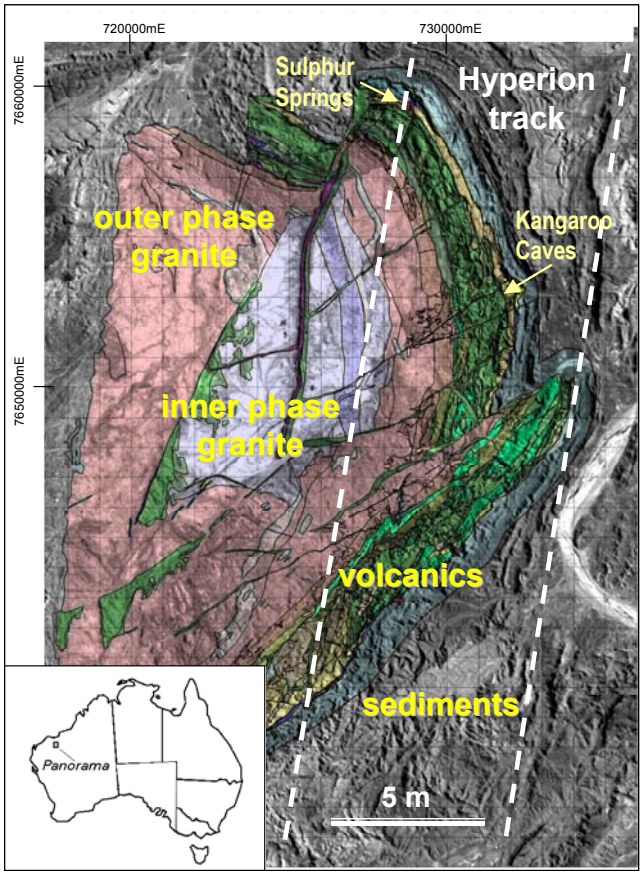

Figure 3.7.1 Geology of the Panorama area (from Brauhart et. al., 1998), superimposed on an orthophoto. The main geological units are shown together with the approximate track of the Hyperion overpass.

The geology of the Panorama area has been well mapped by (Brauhart *et al.*, 1998). The Strelley Succession comprises a high-level hornblende-biotite granite and granophyre, as well as an overlying 2 km thick tholeiitic and calc-alkaline volcanic suite (basalts, andesite, dacite, rhyolite). The Strelley Granite contains two major phases. An outer phase coarse grained, equigranular, hornblende-biotite granite, which changes upward through to finer grained equigranular granite to a fine-grained granophyre, which has a concordant contact with the overlying volcanic strata. An inner phase, porphyritic biotite-hornblende granite has a sharp "intrusive" contact with the outer phase granite. The overlying 1.5 km thick sequence of volcanic rocks (dipping 50° to 60° to the east) comprises a series of submarine tholeiitic volcanic units ranging from basalt to rhyolite. The andesite-basalt and dacite units are dominant in the north whereas rhyolitic flows and volcanic clastic rocks are dominant in the southwest. The change from felsic-dominated to mafic-dominated volcanic rocks is gradational. This sequence is conformably overlain by quartzose turbidites of the Gorge Creek Group (Figure 3.7.1). The so called "marker chert", comprising a laminated black chert, marks the contact between the Strelley Succession and the overlying Gorge Creek Group. This chert horizon is typically less than 5 m thick but thickens (up to 80 m) around the discharge sites, like Kangaroo Caves.

The published hydrothermal alteration mapping of Brauhart *et al.* (1998) comprises: (a) distal feldspar-sericite; (b) intermediate sericite-quartz; and (c) proximal chlorite-quartz-sericite. Chlorite-quartz alteration is mapped generally lower in the volcanic pile and at

the VMS discharge sites like at Kangaroo Caves and Sulphur Springs (Figure 3.7.1 and Figure 3.7.2). Sericite-quartz alteration is generally found in the upper parts of the volcanic pile and in fracture-controlled parts of the underlying outer phase granite. Also, in the granite, quartz-topaz-sericite greisens have developed in places. The published alteration map of Brauhart *et al.* (1998) over the area covered by the Hyperion image is presented in Figure 3.7.2(a).

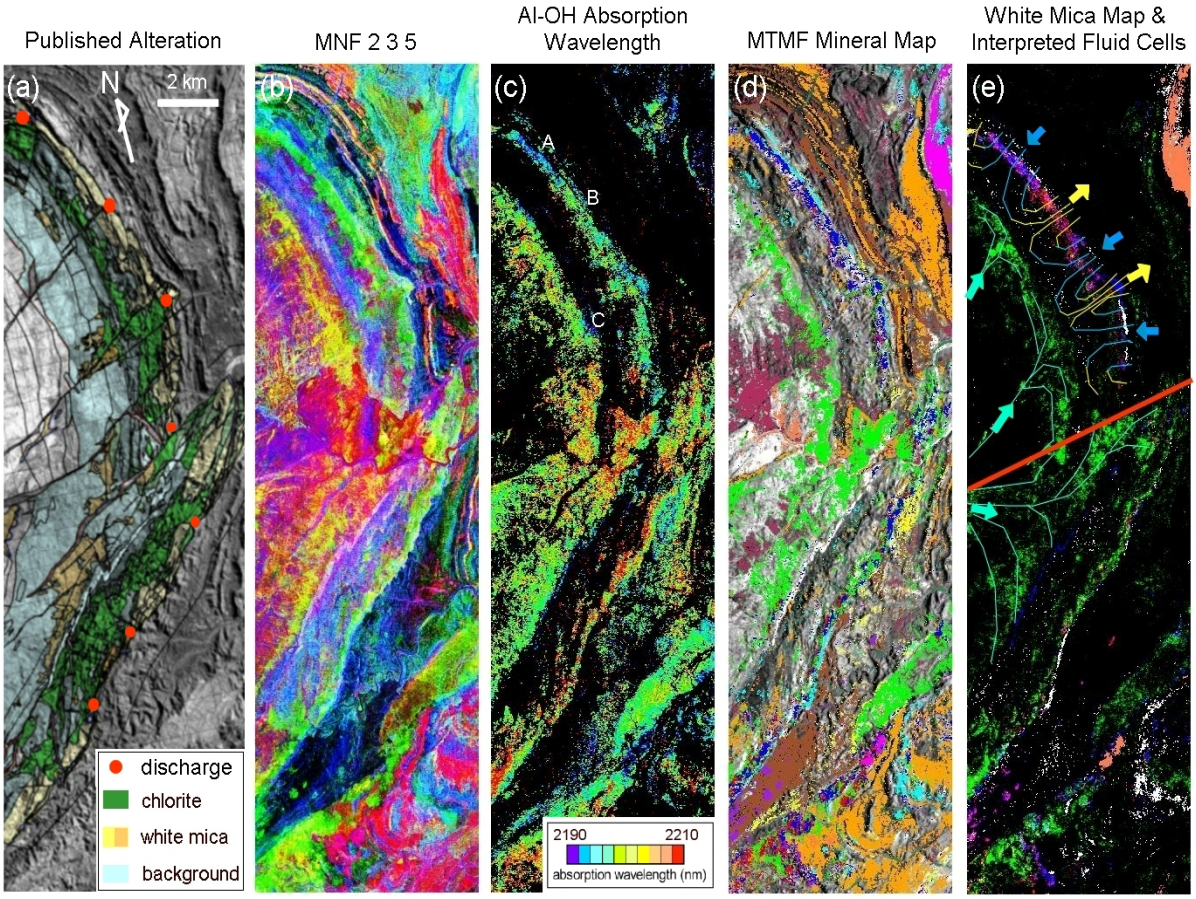

Figure 3.7.2: (a) Published alteration geology of the Panorama area (Brauhart *et al.*, 1998) overlain on a B&W orthoimage covering the Hyperion overpass (b) Hyperion MNF bands 2, 3 and 4 for the 38 input SWIR-2 bands (note that 9 MNF SWIR bands yielded geological information); (c) tracking of Hyperion derived wavelength position of the 2200 nm white mica absorption (d) MTMF mineral map with colours matching the mineral spectra in Figure 3.7.3(b) (e) MTMF mineral abundance map with marker chert (white), pyrophyllite (orange), Al-poor white mica in granite (green), Al-poor white mica in volcanic rocks (red) and Al-rich white mica in volcanic rocks (blue). The interpreted fluid flow pathways are annotated as blue (seawater recharging), yellow (evolved seawater discharging) and green (magmatic) lines. The thick red line shows a major fault (from Cudahy *et al.*, 2002).

The Zn-Cu VMS mineralisation is found at a number of sites close to the marker chert. These include: Sulphur Springs (5.3 Mt @ 6.1% Zn and 2.2% Cu) and Kangaroo Caves (1.7 Mt @ 9.8% Zn and 0.6% Cu), which are the largest known occurrence of VMS mineralisation in the area (Figure 3.7.1).

3.7.1.3 Hyperion Data And Processing

The Hyperion scene, 364-00 (day, year), was provided by TRW as L1A radiance at sensor data. The data was processed as follows:

(a) repair and/or replace bad detector pixels/bands using CSIRO's *Deplugger* and remove the effected of column striping (both a gain and offset correction) as described in the report on the work at Mt Fitton;
(b) atmospheric correction using ACORN (see http://www.aigllc.com/acorn/intro.asp);
(c) EFFORT polishing (involved finding and correcting systematic gain errors);
(d) identification of scene spectral endmembers; and
(e) generation of surface compositional maps using various methods including Mixture Tuned Matched Filtering (MTMF) (see http://www.envi-sw.com) and derivatives of fitted 4th order polynomials to selected wavelength intervals to obtain the wavelengths of the Al-OH absorption feature. This use of polynomials has the effect of reducing the impact of the noisy spectra in this difficult wavelength region.

Airborne HyMap hyperspectral VNIR-SWIR data (at 5 m pixel resolution) and related mineral mapping and field/laboratory results for the Panorama area (Cudahy *et al.*, 1999, 2000) were used for comparison and validation of the processed Hyperion data.

3.7.1.4 Mineral Mapping Results

Particular attention was given to Hyperion's SWIR region (2000-2400 nm) for the spectral analysis as hydrothermal minerals such as white mica and chlorite have diagnostic features within these wavelengths. A selection of scene endmembers is presented in Figure 3.7.3(a) (full spectrum) and Figure 3.7.3(b) (SWIR-2 only) alongside the HyMap endmembers extracted from the same area (Figure 3.7.3(c)). Except for some error in water vapour correction causing systematic error at 960 and 1140 nm, the Hyperion spectra can be used to confidently interpret composition. There is generally good matching between the two data sets, includes different types of white mica (2200 nm absorption), chlorite (2250 absorption) and pyrophyllite (2165 nm absorption). Green vegetation and dry vegetation as well as iron oxides (hematite and hydrated iron oxide) and "aspectral" materials like unaltered granite and marker chert were also extracted. The relatively low SNR of Hyperion in the SWIR does compromise this spectral interpretability except at wavelengths longer than 2300 nm where it is difficult to recognise the diagnostic spectral absorptions of minerals like chlorite/epidote, amphibole and dolomite which are clearly identified in the associated airborne HyMap SWIR endmember spectra shown Figure 3.7.3(c) (Cudahy *et al.*, 1999). Also, topaz with its diagnostic sharp 2070 nm absorption was identified in the HyMap data but was not apparent in the Hyperion data. The reason for this is not clear though is probably related to relatively small depth and narrow width (20 nm) of this topaz band as well as the large pixel size of Hyperion.

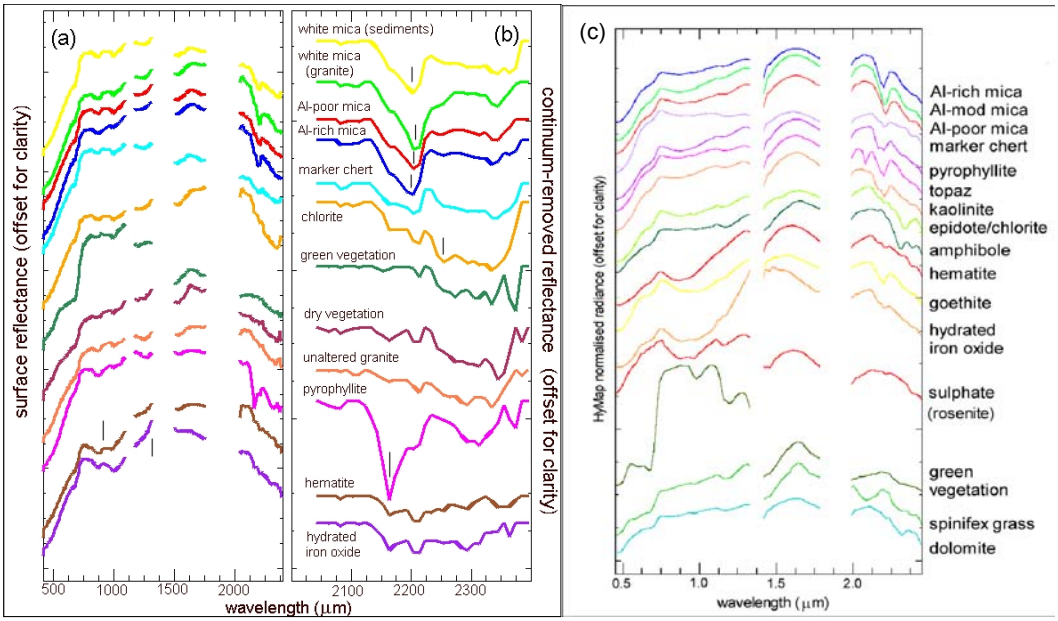

Figure 3.7.3: Stacked (a) full spectrum (surface reflectance) and (b) SWIR-2 (continuum removed surface reflectance) spectra of selected Panorama Hyperion image endmember spectra (c) Airborne HyMap Panorama image endmember spectra from the same area.

One of the critical maps made with the HyMap data for defining the nature and geometry of the Panorama hydrothermal alteration system was measuring and mapping the level of Tschermak substitution in white mica (Cudahy *et al.*, 1999). This measurement is based on tracking the shift in the position of the white mica absorption feature around 2200 nm by up to 20 nm. This shift is also apparent in the Hyperion image endmember Figure 3.7.3 (top four spectra). To evaluate and validate Hyperion's ability to accurately map this 20 nm wavelength shift in the 2200 nm absorption, the 1st derivative was calculated for each pixel that was fitted with a 4th order polynomial for the wavelength segment between 2100 and 2250 nm. This product was first masked to isolate and include only those pixels with significant Al-OH absorption calculated using the depth above a nominated threshold for the same fitted polynomial. A second mask was applied to remove all those with significant kaolinite absorption on the left shoulder of the 2200 nm, which was calculated using a band math operation $[(B_{2133}+B_{2183})/(B_{2163}+B_{2183})]$. This procedure was applied to the Hyperion, HyMap and associated field PIMA data.

The results (Figure 3.7.4) show that the measured wavelength shift in all data sets is 20 nm from 2190 to 2210 nm with the resultant maps showing coherent and geologically interpretable information. Strong correlations in the spatial patterns exist between all the data sets though as expected the Hyperion results are not as detailed given the larger pixel size though they do provide a more regional overview because of its larger spatial coverage compared with the available HyMap data. Important geological features to note include the interpreted seawater recharge sites (blue arrows) where Al-rich white micas (blue tones) are developed in the volcanic rocks. At the interpreted discharge sites, such as those at Kangaroo Caves and Sulphur Springs (Figure 3.7.1), there are developed Al-poor white micas (green-yellow tones) though the most Al-poor micas (longest wavelength 220 nm absorptions) are found further to the south (red tones). This

is an important result as it shows that Hyperion can be used to measure and track subtle 20 nm shift in mineral absorption features using its SWIR-2 module.

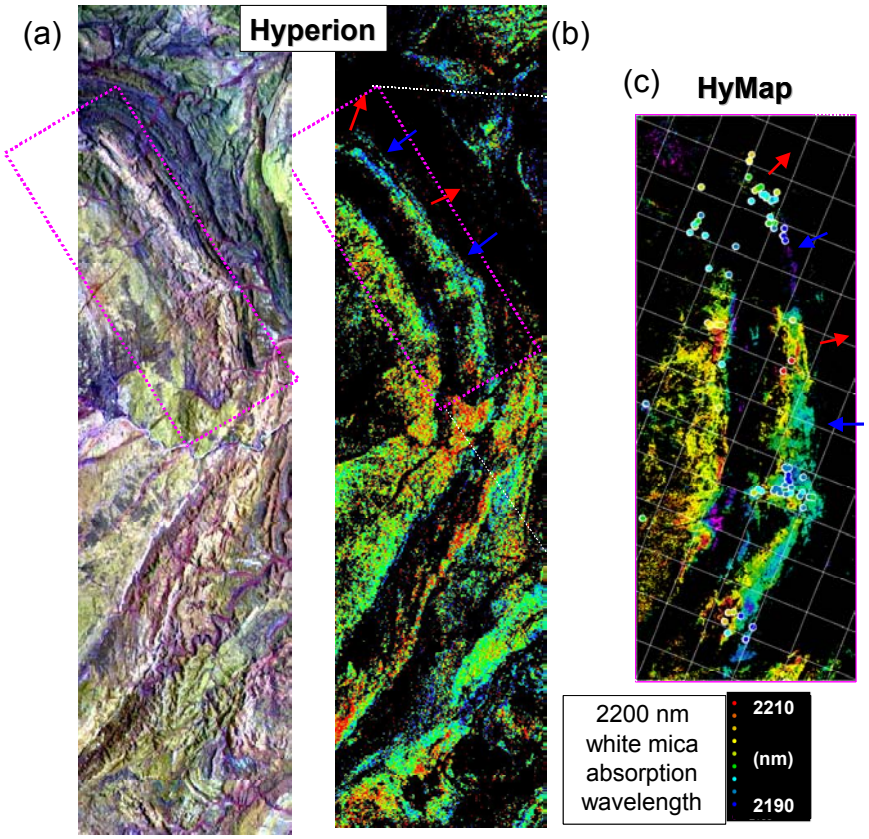

Figure 3.7.4: Tracking the wavelength position of the white mica 2200 nm absorption related to Tschermak substitution. (a) Colour composite RGB image of radiance at sensor channels at 760, 650 and 550 nm for reference. (b) Measurement of the wavelength of the white mica absorption wavelength near 2200 nm from the Hyperion data. (c) Measurement of the wavelength of the white mica absorption wavelength near 2200 nm from the HyMap data and the field data (coloured circles). The 1 km grid is shown on the HyMap image.

The HyMap Panorama study also found it useful using the partial unmixing information extraction available in ENVI, called Mixture Tuned Matched Filtering (MTMF), to generate a map that separates the white mica alteration that developed largely in the granites from the white mica alteration that developed largely in the volcanic rocks. The value of this product is that it can potentially identify areas of alteration in the volcanic rocks that may possess similar alteration signatures to that found in the granites as this may help establish the role of magmatic versus seawater hydrothermal fluids and their interactions.

A Hyperion mineral map generated using MTMF and a selection of the image endmembers in Figure 3.7.3 is presented in Figure 3.7.5. In addition to the mica endmembers, the "marker" chert endmember was also chosen for comparison as this is an important unit for defining the upper boundary of the Panorama hydrothermal alteration system. The resultant mineral theme maps generally show good correlation between the Hyperion and HyMap processed data (Figure 3.7.5(b) and Figure 3.7.5(c)). The thin marker chert that separates the Strelley volcanic rocks and the Gorge Creek

turbidites is mapped in both, especially around the Kangaroo Caves area where it is thickest (up to 80 m wide). It is also mapped at this contact near Sulphur Springs (multiple thin layers as expected) and further to the south.

The white mica information is also well correlated between the two data sets with both largely separating the white mica alteration in the granites (green) from the white mica alteration in the northeastern volcanic rocks (blue-red). The fracture-controlled white mica alteration in the granites is better mapped in the higher spatial resolution HyMap imagery though the major subvertical fracture zones below the interpreted discharge sites (A and B in Figure 3.7.5(b)) can also be mapped by Hyperion. The change from Al-poor (red) to Al-rich (blue) white mica in the volcanic rocks in the northeast is also mapped by Hyperion, which provides evidence for the sites of sweater recharge and hydrothermal discharge. Around Sulphur Springs, the alteration is mapped as yellow in the Hyperion image indicating a mixture of both the granite and Al-poor volcanic rock white mica signatures. A similar response is also found in the processed HyMap data. This observation, combined with a lack of a cracking front below the Sulphur Springs area, which is defined by the intense green coloured fracturing near the contact between the outer phase granite and the overlying volcanic rocks, are evidence for a possible magmatic source contributing to the hydrothermal fluids that were discharged at the Sulphur Springs site.

The Hyperion MTMF results also show that much of the white mica alteration in the volcanic rocks in the south have a similar signature to the altered granites (green colour) and not with the altered volcanic rocks in the north. This could be explained by the greater amount of felsic volcanic rocks in the south compared to the northeast though could also be evidence that the architecture of the convective cells and their sources of hydrothermal fluids in these two regions were different.

Figure 3.7.2(e) provides a possible interpretation of the fluid pathways and convective cells of magmatic (green lines) and seawater (blue and yellow lines) Of note is the clear separation in the nature of the white mica alteration across a major fault (red line) with seawater related white mica alteration developed largely in the volcanic rocks to the north and magmatic related white mica alteration developed to the south. This suggests that the roles of the two fluid sources in the convective system are complex. At any rate, recognition of the hydrothermal discharge sites (yellow arrows) is critical for locating sites of economic base metal sulphide mineralisation and potential sites for early life, especially extremophiles.

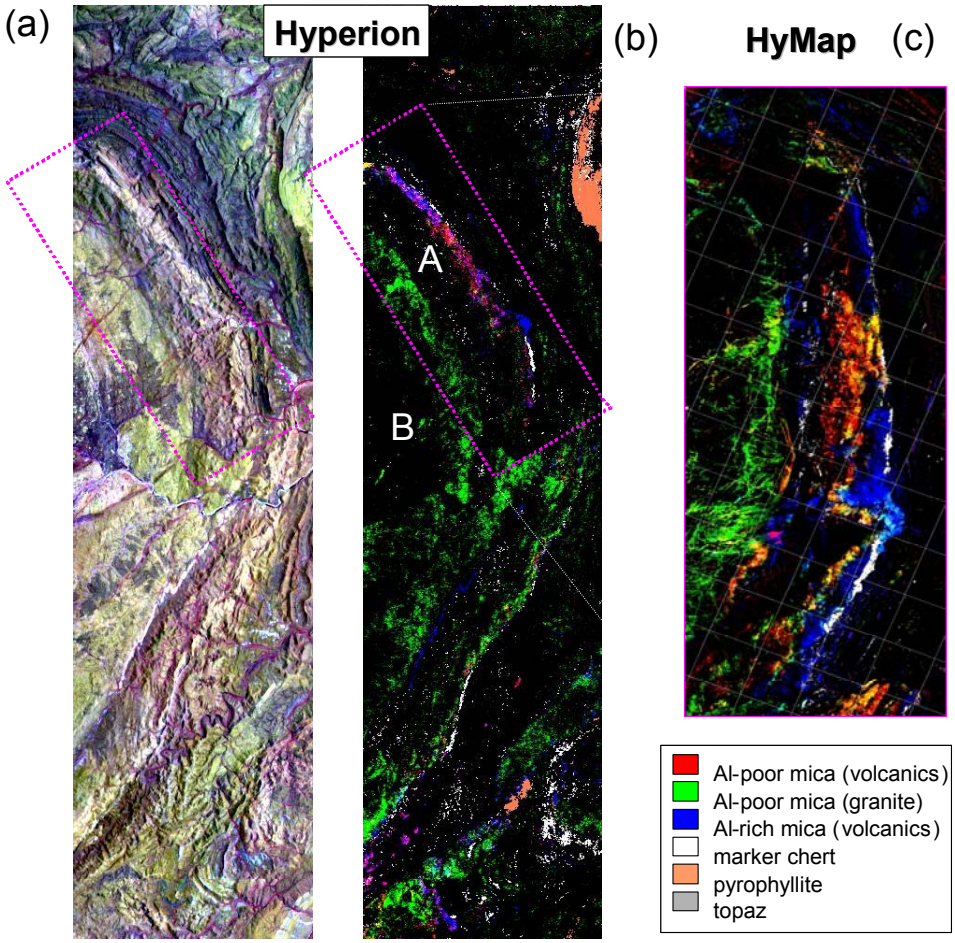

Figure 3.7.5: MTMF mineral maps of the Panorama area. (a) Colour composite RGB image of radiance at sensor channels at 760, 650 and 550 nm. (b) Hyperion MTMF mineral map. (c) HyMap MTMF mineral map. The mineralogical legend for the colours of the images is also presented. The grid shown on the HyMap image is a 1 km grid.

3.7.1.5 Conclusions

The successful launch and operation of the satellite-borne Hyperion hyperspectral VNIR-SWIR system (Pearlman *et al.*, 2001) in November 2000 provided an opportunity to evaluate the space-borne data for mineral exploration applications. This study has demonstrated how the Hyperion data provided excellent results for mapping the mineralogy, mineral chemistry and spatial geometry of the exposed volcanic massive sulphide system at Panorama.

Validation of Hyperion's results was carried out by comparisons with a) published geology for which it showed excellent spatial correlation; b) recently produced HyMap mineral maps which displayed consistent endmember mapping (with the exception of topaz) although with some compromise in spectral shape; and c) field spectra.

Recognition of hydrothermal discharge sites is critical for locating areas of potential economic base metal mineralisation. This case study has shown Hyperion to be successful in accomplishing the task at a regional scale. The success was largely achieved due to image restoration techniques to minimise the impact of noise, as well as

the benefit of the study area's location within a semi-arid environment with relatively unweathered "bright" rocks well exposed over large areas, with critical alteration minerals that contained diagnostic absorption features at wavelengths shorter than 2300 nm, beyond which the Hyperion data becomes much more noisy.

3.7.1.6 Acknowledgements

Carl Brauhart (Sipa Resources) provided some associated sample data and critical geological advice about the Panorama area. Mike Caccetta and Peter Mason provided software engineering and image data handling support.

At this site the primary work was carried out and reported by:

T.J. Cudahy,
CSIRO Exploration and Mining
Underwood Avenue
Floreat Park, W.A., Australia, 6014

P.S. Barry
Raytheon Electronic Systems
2000 E. El Segundo Blvd
El Segundo, CA., USA, 90245

3.7.1.7 References

Brauhart, C.W., D.I Groves, and P. Morant (1998). Regional alteration systems associated with volcanogenic massive sulphide mineralization at Panorama, Pilbara, Western Australia. *Economic Geology*, **93**, 292-302.

Cudahy, T.J., K. Okada, K. Ueda, C.W. Brauhart, P. Morant, D. Huston, T.D. Cocks, J. Wilson, P. Mason, and J.F. Huntington (1999). Mapping the Panorama VMS-style Alteration and Host Rock Mineralogy, Pilbara Block, Using Airborne Hyperspectral VNIR-SWIR Data. *CSIRO Exploration and Mining Report*, 661R, 1999, pp 107.

Cudahy, T.J., K. Okada, & C. Brauhart, 2000. Targeting VMS-style Zn mineralisation at Panorama, Australia, using airborne hyperspectral VNIR-SWIR HyMap data. *ERIM Proceedings of the 14th International Conference on Applied Geologic Remote Sensing*, 6-8 November, Las Vegas, pp. 395-402.

Cudahy T.J., and P.S. Barry (2002). Earth magmatic-seawater hydrothermal alteration revealed through satellite-borne Hyperion imagery at Panorama, Western Australia. *Proceedings IGARSS*, Toronto, 24-28 June, I: 584-586.

Duke, E.F. (1994). Near infrared spectra of muscovite, Tschermak substitution and metamorphic reaction progress: implications for remote sensing. *Geology*, **22**, 621-624.

Huntington, J.F., J.W. Boardman, M.D. Craig, T.J. Munday, and A.R. Gabell, (1994). Mineral Mapping with Spectrally Processed Geoscan MK II Scanner Data, Copper Gorge, Nullagine Western Australia. *CSIRO Division of Exploration and Mining* Report 46R, AMIRA Project P382, July 1994.

Liao, L., P. Jarecke, D. Gleichauf and T. Hedman (2000). Performance Characterization of the Hyperion Imaging Spectrometer Instrument. *Proc. of SPIE*, Vol. 4101, pp. 22-26, July 2000.

Pearlman, J.S., S. Carman, C. Segal, P. Jarecke, P.S. Barry, W. Browne (2001). Overview of the Hyperion Imaging Spectrometer for the NASA EO-1 Mission. *IGARSS Special Session* 40, SS40MO, Paper 1775, 3pp.

Rasmussen, B. 2000. Filamentous microfossils in a 3,235-million-year-old volcanogenic massive sulphide deposit. *Nature*, **405**, pp. 676-679.

Scott, K.M. and K. Yang (1997). Spectral Reflectance Studies of White Micas. *CSIRO Exploration and Mining* Report 439R, AMIRA Project P435, 34pp.

4 MISSION SUPPORT & DATA MANAGEMENT

In addition to the scientific and validation studies, there were also a number of significant activities involving international collaboration, mission support, data acquisition and data management. These were:

Activity	Australian Participant	International Participant
EO-1 Data download	Ian Shepherd and Craig Smith, ACRES, Geoscience Australia	NASA Goddard, USGS
CIMEL sites (4)	Ross Mitchell, CSIRO	NASA Goddard Aeronet
HyMap Data & support	Terry Cocks, ISPL Peter Cocks, HyVista	

Since the commencement of the mission, EO-1 data have been regularly downloaded at the Tasmanian Earth Resources Satellite System (TERSS) X-Band station in Hobart, Tasmania. This activity provided a means for NASA to increase acquisitions over the first year of operation and has continued in collaboration with the USGS during the Extended Mission. The CIMEL sites provided significant atmospheric data for a range of sites and the internationally established HyMap instrument was used for airborne data collection at all of the Australian sites to provide accurate and detailed reference hyperspectral data against which to benchmark the Hyperion data.

TERSS X-Band Site near Hobart, Tasmania, Australia

4.1 ACRES data downlink, data management & outreach activities

4.1.1 EO-1 Mission Support

In mid-1999, staff scientists from NASA and TRW met with ACRES to discuss the possibility of acquiring EO-1 data from the Tasmanian Earth Resources Satellite Station (TERSS) site in Hobart (see http://www.terss.org.au/) to increase the potential number of EO-1 Data Collection Events (DCEs). ACRES saw this as an opportunity to develop technical interactions and improve co-operation between the two countries. Subsequently, ACRES participated in this initiative by upgrading its reception management system and direct ingest system software to handle recording of X-band downlink from the EO-1 satellite. Following successful testing in late 2000, ACRES began acquiring EO-1 data on an operational basis from the Hobart ground station. Up until late 2003 ACRES had acquired about 750 passes, adding on average one pass each day over that time. The data were written to DLT and shipped to GSFC on a weekly basis as the data down linked from the EO-1 data storage system (the WARP) were not necessarily of Australia or sites in the view of the satellite while being tracked by TERSS but rather for scheduled acquisitions from previous orbits. The down linking of data at TERSS allowed NASA to significantly increase data acquisition and also to provide redundancy and data security that they would otherwise not have had.

4.1.2 ACRES provision of imagery from the EO-1 mission.

Early in 2002, ACRES coordinated a bulk purchase of EO-1 data from the United States Geological Survey (USGS) for Australian and overseas users as part of the extended mission. This initial bulk purchase involved acquisitions for a limited time until March 2002. The EO-1 mission was subsequently extended further to mid 2003 and ACRES was able to coordinate the continued supply of EO-1 products to Australian customers through a special arrangement with the USGS. ACRES has facilitated the purchase of over 45 Hyperion and ALI scenes for Australian customers to the end of 2003 as part of the extended mission.

4.1.3 EO-1 Image Data Applications Workshop. 15 March 2002

In order to promote the use of Hyperion and ALI imagery, ACRES and CSIRO co-hosted a one-day EO-1 Hyperion & ALI Information Workshop on 15 March 2002. The Workshop was designed to introduce potential users to hyperspectral imagery in general and provide information about Australian based applications experience and how end users could acquire hyperspectral imagery such as the EO-1 Hyperion data. A number of EO-1 researchers presented their experiences with Hyperion covering Agriculture, Water quality and Forestry. The Workshop was a very successful event with attendance by over 60 participants.

CSIRO also organised a hands-on course in the processing of Hyperion data that attracted 12 people who were taken through the basic steps in Hyperion data structure, processing and manipulation. Both the workshop and the course were aimed at supporting the extended mission among Australian remote sensing data suppliers and users.

4.2 HyMap™ airborne Hyperspectral data base

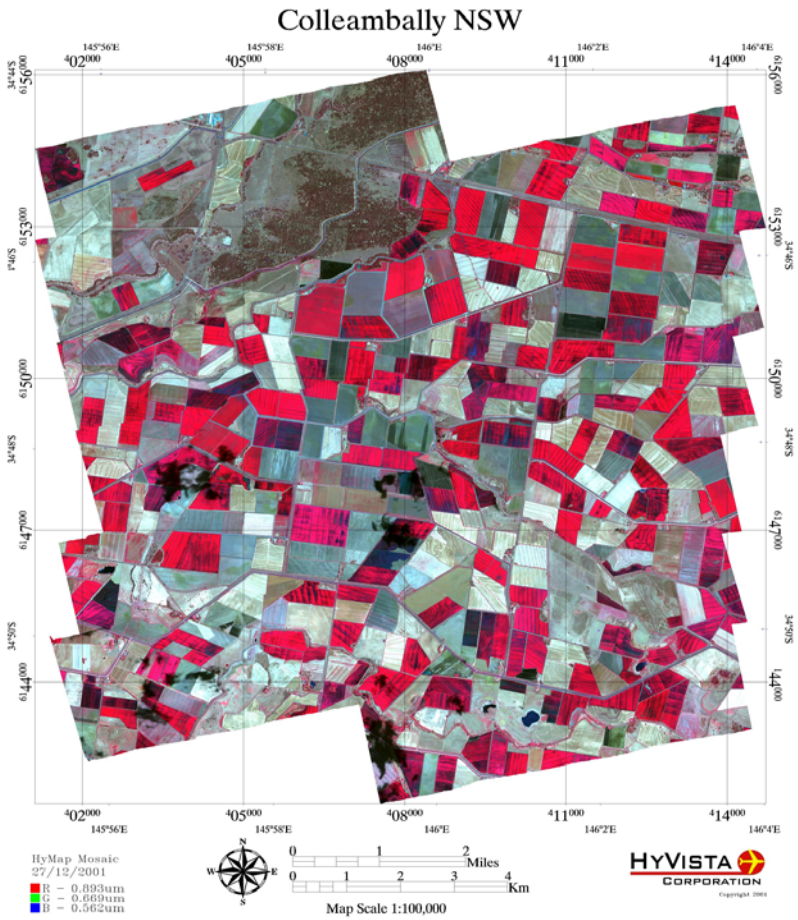

Figure 4.2.1: HyVista delivered HyMap™ airborne scanner mosaic of the Coleambally Irrigation Area. Typical product for EO-1 sites.

Report by: Terry Cocks
Integrated Spectronics Pty Ltd
tdc@intspec.com

4.2.1 Introduction to HyMap™

HyMap™ Scanners are built by Integrated Spectronics Inc. Two are operated in Australia and overseas by HyVista Corp. (http://www.intspec.com/). HyMap™ scanners provide calibrated radiance data of high accuracy and with a high SNR suitable for atmospheric correction to surface reflectance and for demanding applications such as mineral mapping as well as a wide range of environmental applications.

As described in Cocks *et al.* (1998), HyMap™ is one of a range of sensors being developed by Integrated Spectronics Inc that aim to operate within the general specifications listed in Table 4.2-1.

Table 4.2-1 ISPL scanners and HyMap characteristics

Property	General Series specification	HyMap operating characteristics
Spectral regions	**VIS, NIR, SWIR, MWIR, TIR**	**VIS, NIR, SWIR**
Number of channels	100 - 200	126
Spectral bandwidths	10 – 20 nm	
Spatial resolution	2 – 10 m	
Swath width	60 – 70 degrees	
Signal to noise ratio[9]	>500:1	
Operational altitude	2000 – 5000 m AGL	

To achieve the basic specifications of Table 4.2-1, the platform requirements and choices for optics (geometry) for the specific VNIR/SWIR HyMap™ sensor used for EO-1 validation were those listed inTable 4.2-2:

Table 4.2-2 Typical HyMap Operational Parameters	
Platform	Light, twin engined aircraft e.g. Cessna 404, unpressurised
Altitudes	2000 – 5000 m AGL
Ground Speeds	110 – 180 kts
IFOV	2.5 mr along track 2.0 mr across track
FOV	60 degrees (512 pixels)
Swath	2.3 km at 5m IFOV (along track) 4.6 km at 10m IFOV (along track)

HyMap™ sensors are optomechanically scanned systems incorporating spectrographic detector array modules, on-board reference lamp and a shutter synchronised to scan line readouts for dark current monitoring, The fully enclosed optomechanical system views the ground through a window and is mounted in a 3 axis, gyro-stabilised platform. The spectral configuation for the HyMap™ used to collect the EO1 mission data was as shown in Table 4.2-3:

Table 4.2-3 Spectral Configuration			
Module	**Spectral range**	**Bandwidth across module**	**Average sampling interval**
VIS	0.45 – 0.89 um	15 – 16 nm	15 nm
NIR	0.89 – 1.35 um	15 – 16 nm	15 nm
SWIR1	1.40 – 1.80 um	15 – 16 nm	13 nm
SWIR2	1.95 – 2.48 um	18 – 20 nm	17 nm

[9] (30 degrees sun zenith angle, 50% reflectance)

A plot of the bands against a green vegetation spectrum (Cocks *et al.*, 1998) is shown in Figure 4.2.2.

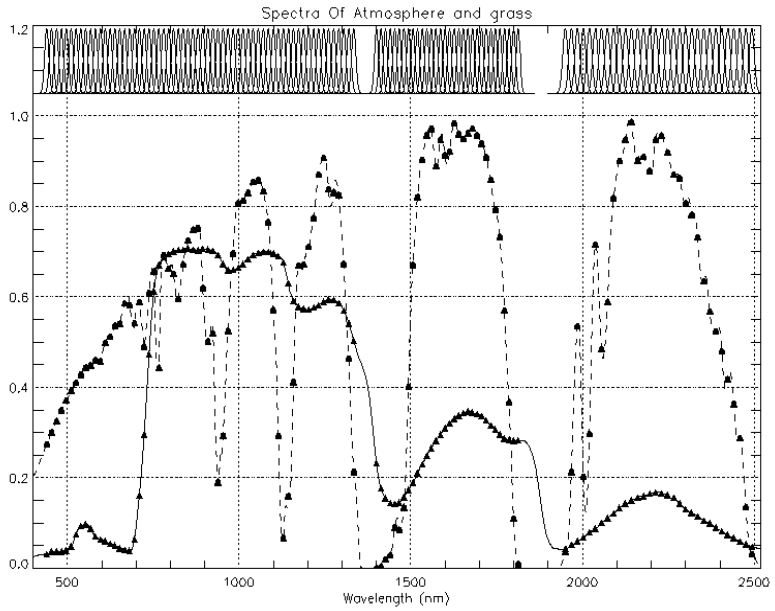

Figure 4.2.2 HyMap spectral coverage and resolution

This figure illustrates how the response of the HyMap™ 126 band system covers the range 0.45 – 2.5 micrometers with band widths in the range 15 – 20 nm. The spectral coverage is contiguous except for regions where the atmosphere is opaque due to strong water absorption bands.

Figure 4.2.3 Cross-calibrating ground based instruments with HyMap™ on board its aircraft platform.

4.2.2 HyMap™ Missions in support of EO-1 validation

HyVista Corporation conducted a number of HyMap™-based airborne missions over the Australian Cal/Val sites in support of EO-1 preparation and as part of the EO-1 SVT mission. CSIRO scientists established good calibrations between their instruments and the airborne scanner and supported all the flights with ground data consisting of relevant spectra and environmental conditions. These field support missions have been described as part of the site reports.

Some HyMap™ images were acquired prior to the EO-1 launch to provide baseline data for the sites and establish design parameters. On other occasions HyMap™ images were acquired that were coincident with EO-1 overpasses. Since HyMap™ operates in a similar wavelength range to Hyperion it provided a baseline of high SNR hyperspectral data for each EO-1 site. HyMap also provides data with excellent geometric properties and accurate geo-location. To minimise distortion induced in the image by aircraft pitch, roll and yaw motions, the HyMap is mounted in a gyro-stabilised platform. Any residual motions are monitored by a 3 axis gyro, 3 axis accelerometer system (IMU – inertial monitoring unit).

Table 4.2-4 HyMap™ Data Collections

EO-1 Site	Number of Missions	Date(s) of Mission
Moreton Bay (1) Logan R.	1	11 Sept. 1998
Moreton Bay (2)	1	11 Sept. 1998
Moreton Bay (3) Pumicestone Passage	1	Nov 1998
Panorama	1	12 Nov 1998
Kunoth (Alice Springs)	1	18 Nov 1998
Uardry (Hay)	1	22 Mar. 2000
Cape Tribulation (cloudy)	1	13 Sept 2000
Kakadu	1 (5m and 3m)	17 Sept. 2000
Mt Fitton	1	19 Sept. 2000
Lake Frome	1	28 Nov. 2000
Coleambally	2	8th Dec. 2000, 12th Jan 2002
Tumbarumba	1	31 Mar 2001

The calibrated data for each site were provided to the site investigators in both geo-referenced and image formats on CD or DVD media with a Data Acquisition Report, the GPS track for reference and ENVI-compatible files such as the geometric lookup table ("glt") file for later more accurate and application specific georectification. All data for the EO-1 mission was sent initially to CSIRO EOC for management and archive. Table 4.2-4 provides a list of HyMap™ images acquired for the sites.

The data were delivered as calibrated hyperspectral data (including band pass functions to people who wished) and also as precision georectified data based on the GPS/INS information collected by the onboard HyVista system. Figure 4.2.4 Shows part of the mosaic of Figure 4.2.1 with GIS information added using the ancillary geographic and geometric information provided by HyVista.

Figure 4.2.4: Detail of Figure 4.2.1 showing co-registration with GIS strings. This was made as part of the Coleambally information system using HyVista provided information.

The HyMap™ system provided a very sound base for comparisons between ground data and Hyperion data as well as independent hyperspectral information for EO-1 related and future research at the sites. These data are not generally available but enquiries can be made through the site PI.

4.2.3 Reference

Cocks, T. R. Jenssen, A. Stewart, I. Wilson and T. Shields, (1998). "The HyMap airborne hyperspectral sensor: the system, calibration and performance." 1st EARSEL Workshop on Imaging Spectroscopy, Zurich, October 1998

4.3 Data and Information Management

4.3.1 Image Data

All EO-1 data for the Australian sites have been received and archived at the CSIRO EOC in Canberra in a well-managed data storage and retrieval area. The data are managed with other EOC data holdings in stable and secure environmental conditions. The data management at the EOC consisted of entering details for each data tape into a database, storing the tapes and sending email notification to co-investigators. Copies of data tapes were then sent to the co-investigators upon request. ALI quick look images of the sites were also provided on a protected area of the EOC website for the co-investigators to browse before requesting copies of data.

Table 4.3-1. Number of Hyperion and ALI images collected for each site.

Site	Hyperion Data (Level 1)	ALI Data (Level 1)
Cape Tribulation	4	6
Kakadu	9	21
Kioloa	1	1
Kunoth	13	20
Lake Argyle	4	6
Lake Frome	11	14
Mayon Volcano	6	12
Moreton bay	6	5
Mt Fitton	6	5
Panorama	4	4
Tumbarumba	7	10
Uardry	2	1
Coleambally	25	26
TOTALS	**92**	**131**

Table 4.3-1 lists the number of ALI and Hyperion images acquired for each site. The Table only lists the Level 1 (including Levels 1, 1A and 1B) data available. The corresponding Level 0 ALI and Hyperion images are also archived at the EOC. We are intending to bring all of the key site and image conjunctions (such as data collected at the time of missions or special time series or applications) to a base of the Level 1B1 in the coming year. We have had significant support and help from NASA Goddard to achieve this for the most important data sites and overpasses. Since the Level 0 data are archived it is possible to re-process any data if further developments are made to the base processing provided software becomes available to take data from Level 0 to the new Level product.

4.3.2 Field and Ancillary Data

Ancillary and collateral data were collected at every site and especially for selected dates of EO-1 acquisitions. At every site, HyMap™ airborne hyperspectral data have been collected and at most sites ground spectra with instruments similar to ASD spectral resolution have been collected. In addition, Landsat ETM+ data were acquired at every site when there was a successful acquisition at the same time as fieldwork.

While access to site data is generally by permission of the site PI, CSIRO has started to make some of the data generally available as a base for future research and teaching. One area where this has been done is through the course notes and CDs of the Hyperion Data Workshop (Datt and Jupp, 2002) where a range of image data have been used as examples and are provided to enable users to undertake essential pre-processing.

In addition, the EOC web site (http://www.eoc.csiro.au under “Hyperspectral”) has a collection of many electronic publications, image data, reports and information and selected site data collections for EO-1 and for other hyperspectral missions. At this time four base ancillary data sets for EO-1 have been collected and made available for:

- Lake Frome
- Coleambally
- Tumbarumba
- Kunoth

The data available are as listed in Table Table 4.3-2.

Table 4.3-2 Data held at CSIRO EOC with public access for selected EO-1 sites

Site	Hymap data	Landsat data	ASD data	Other
Lake Frome	28 Nov.2000	1 Oct. 2000, 15 Sept. 2000 5 Jan. 2001 21 Jan. 2001	16-19 Dec. 2000	GPS, radiosonde, CIMEL sun photometer data
Coleambally	8 Dec. 2000	20 images (Aug. 2000 – May 2001)	7 Mar. 2001	High resolution digital air photos, radiosonde and ground based meteorological data
Tumbarumba	31 Mar.2001	25 Dec 2000	28 Feb. 2001 Leaf Spectra	Hemispherical photography (jpegs); ALI & HyMap Quick looks, Met data
Kunoth	18 Nov.1998		GER spectra - Oct. 11, 16, 23, 2000.	Airborne Video data – May 9 2001. Radiosonde data - 2 Feb.2001, 25 Feb.2001, 3 Mar.2001, 4 Aug. 2001

Data from other sites will be made available when it has been provided to the EOC for that purpose. The Uardry site has a range of data available as listed in the site report (Section 2.3, Uardry, Appendix). People interested should contact the site PI (Dr Fred Prata).

For further information or questions concerning EOC data holdings please make contact as listed under “Contact us” at http://www.eoc.csiro.au.

5 THE EXTENDED MISSION

5.1 The Australian Response & Bulk Order

The EO-1 package of instruments and supporting technology launched in November 2000 had a planned operation of only one year. It was expected that during that time the data collected would be sufficient to demonstrate the various technology experiments being carried out. By September 2001 it was clear that there were many reasons to extend the life of the mission. Among these were:

- The lack of current alternative space borne instruments – especially hyperspectral instruments;
- The fact that many researchers had received insufficient data for their experiments due to cloud cover and other issues;
- The growing interest in the use of EO-1 data for applications and more operational uses.

Funding issues and the growth of the third reason above led NASA to commission a survey of the potential interest among users to purchase data and commission data acquisition for these operational purposes. The survey was collated near the end of September 2001 in time to help with the decision to continue the mission or end it.

The Australian response to the proposal was very positive and supportive. Members of the Australian SVT and others in the remote sensing community established the potential applications for the data. Many of these were already being demonstrated at the SVT experimental sites. They also developed lists of the potential data users in Australia. To increase the awareness of these groups to the EO-1 data and opportunities, they then organised informative workshops and data processing courses. As a result, they were able to develop a large initial data buy on behalf of a wide range of Australian users that became the basis of Australian support for the eventual Extended Mission. The information provided and summaries of the Australian workshops can be found on the CSIRO EOC web area at http://www.eoc.csiro.au under Hyperspectral/EO-1.

The market areas established as those with greatest current maturity and potential were in Agriculture, Forestry, Mining and Coastal Waters. In the analysis carried out, Coastal applications were assumed to include both optical water quality and benthic applications. Benthic applications included shallow water areas such as coral reefs and atolls. Among the responses, that from the Minerals sector was especially strong and CSIRO Mineral Mapping and Technology Group (MMTG) organised a worldwide data buy and included processing and user support in their service. This was a very successful activity and is reported separately below.

The acquisition of EO-1 data continued into 2002 until after discussions and studies, the United States Geological Survey (USGS) decided to take over the operations of the EO-1 mission and offer its data through their distribution system. Over time the USGS operation has become well established and data may be commissioned or acquired from the web site at http://eo1.usgs.gov/ where data in the archive can be located using the standard USGS Earth Explorer system.

In Australia, the good working relationship that ACRES has with the USGS provided local support for data ordering, purchase and acquisition as well as advantages in price and data re-tries (due to cloud cover) based on the extent of the Australian bulk order(s). Since the commencement of the Extended Mission there has been continuing activity from many sources in Australia and, following the failure of OrbView4, NASA and USGS decided to extend the life of EO-1 to fill the gap in access to space based hyperspectral analysis until new instruments start to come on-line.

5.2 The Geoscientific Data Buy

Reported by: Jon Huntington and Melissa Quigley, CSIRO Exploration & Mining
Email Contacts: Jon.Huntington@csiro.au and Melissa.Quigley@csiro.au

5.2.1 The data buy

Due to the existing science validation relationship and agreements with NASA, the EOC negotiated a "group-shoot" style data-buy with NASA in support of Hyperion's extended mission. This brought significant advantages to many international participants by way of price discounts, centralised common pre-processing, simpler dealings with NASA, and assistance to those users merely interested in the end products, rather than the science.
CSIRO's Mineral Mapping Technologies Group (MMTG) coordinated a Hyperion data-buy directed at the international geoscience community through a project entitled "Geological Evaluation of Hyperion Spaceborne Hyperspectral Data".

In December 2001, specific international mining companies and government mapping agencies were contacted to solicit their interest in acquiring discounted Hyperion data over their nominated sites and to have the data pre-processed and converted to reflectance, and optionally value-added. A favourable response was received from sixteen organisations, including: Falconbridge/Noranda Ltd, BHP Billiton, Sumitomo Metal Mining Co. Ltd., China Aero Geophysical Survey & Remote Sensing Centre, Anglo Gold, Zarcan Minerals Inc., Cameco Corporation, Department of Primary Industries in South Australia (PIRSA), Western Australia's Department of Land Administration (DOLA), Technical University of Clausthal (Germany), DSK (Deutsche Steinkohle), Geological Survey of Denmark and Greenland, British Geological Survey, Finnish Geological Survey, Austrian Geological Survey, and France's Bureau of Natural Resources (BRGM). Orders for a total of 30 data collection events (DCE) were received over a broad cross-section of terrains spanning 14 countries around the world with orders still to be tasked during 2003.

5.2.2 Selected Outcomes

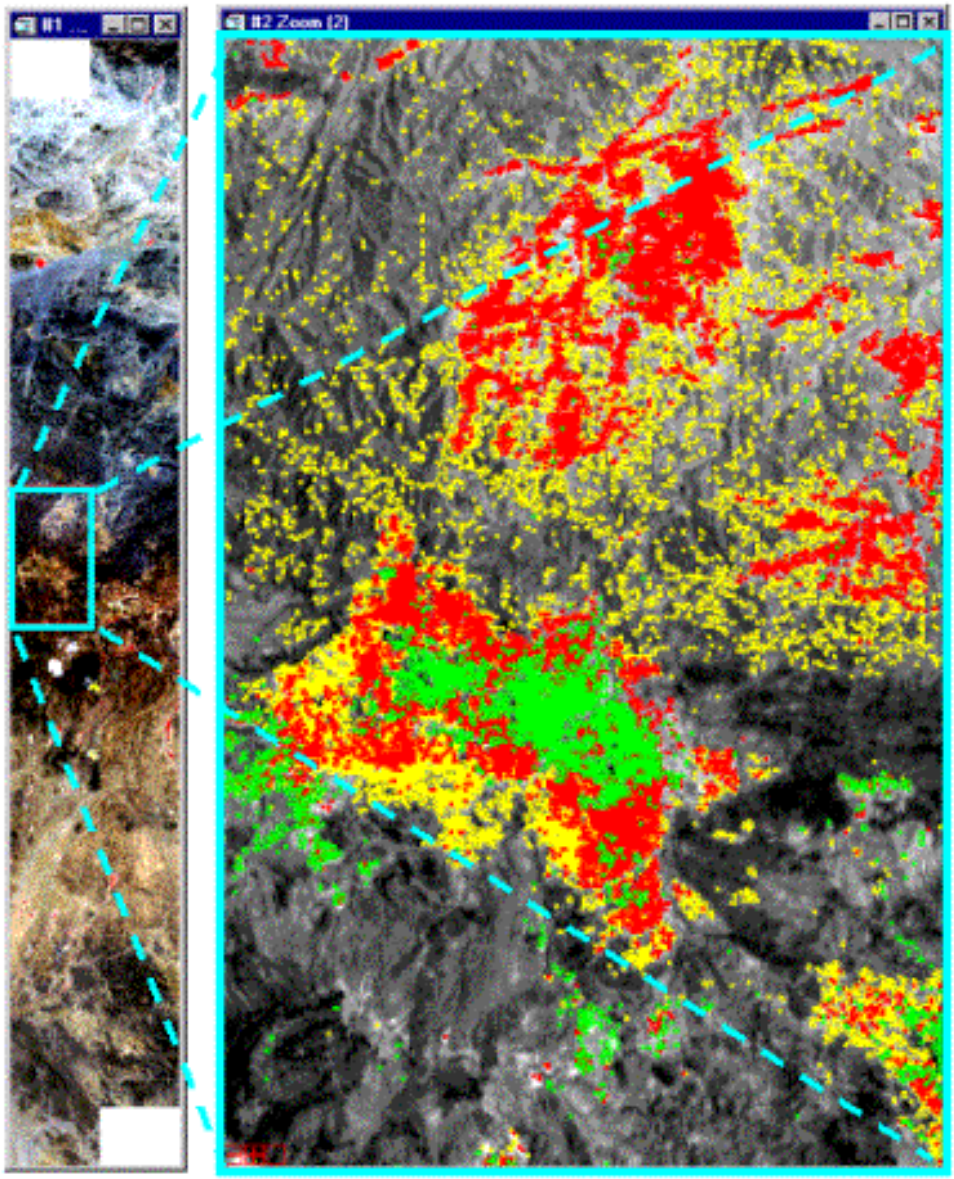

(a) (b)

Figure 5.2.1 (a) CIR mosaic of two Hyperion scenes showing outline of mineral map subset, (b) subset of mineral map showing exploration target (Kaolinite = red, Muscovite = yellow, Alunite = green). Disjointed muscovite (yellow) 'spots' reflect errors of commission resulting from noisy data even after image restoration.

From these investigations it was found that Hyperion data could be useful for certain types of regional mineralogical mapping in selected terrains, such as arid to semi-arid terrains and for large, bright (high albedo) targets, typified by some Cu/Au, Porphyry and Epithermal alteration systems.

One of Hyperion's greatest benefits is the ability to capture data over politically sensitive or logistically challenging terrains, where fieldwork or airborne surveys are not practical, and also where the existing knowledge base is low. The use of hyperspectral

data is not about merely demonstrating in a new way what is already known, but about the creation of new or more detailed knowledge in a cost-effective manner.

A typical case is shown in Figure 5.2.1, a remote, mountainous, third world country with few publicly available, high-quality geological maps. In the mosaic of two runs (each run is 93 km long by 7.5 km wide) one area of zoned muscovite, kaolinite and alunite mineral alteration stands out. This provides an excellent target for more detailed study, either with an airborne hyperspectral scanner, such as HyMap, or on the ground with field-based spectroscopy such as PIMA. This is an example of significant time and cost saving in locating targets worthy of a more detailed mineral exploration study.

The MMTG pre-processing method developed for the "Geological Evaluation of Spaceborne Hyperspectral Data from Hyperion" project involved the use of two software packages, *ENVI 3.5* with the MMTG add-ons for the image processing (masking, plugging, destriping etc) and *ACORN* for the atmospheric correction. The application of the MMTG-created ENVI add-ons *Plugger* and *Destriper* were crucial to effectively rectify inherent noise problems in the data and produce cleaner datacubes, and more recognisable spectra.

The *Plugger* program creates a mask of bad detector cells (including those missed by TRW and the EDC) by checking whether a cell is an outlier, compared to the entire row, using the mean or standard deviation or both (default), then replaces the values of irredeemably bad cells with an interpolated value from the surrounding cells.

The *Destriper* program normalises the column means and is used to repair vertical streaks or stripes caused by a variation in the calibration of the pixels in the cross-track direction where pixels have gains relatively different in effect from their neighbours.

The datacubes were atmospherically corrected using ACORN Version 3 (during February-May 2002) and Version 4 in Mode 1.5 when it became available. The latter incorporated a path radiance option that fine-tuned the spectral fitting of water vapour and liquid water.

The USGS EROS Data Centre (EDC) became responsible for the Level 1 processing from TRW in June 2002. A significant result from this change was the method used to calculate the central wavelength (CWL) and the Full-Width Half-Maximum (FWHM) values. The CWL is simply the central wavelength in a channel width. The FWHM is the distance between the points where the response function falls to half of its maximum value. Hyperion CWL's and FWHM's vary across the 256 pixels/samples in a line. TRW used the CWL and the FWHM from sample 128 as the standard in their header files whilst the EDC adopted the average of the row instead.

TRW's choice of central pixel resulted in the wavelength being accurate for only pixel 128 and showed a spectral smile effect increasing further away from the middle 128 pixel. The EDC's calculated CWL and FWHM values are based on the average of all 256 samples. A spectral comparison of the reflectance data using both sets of header files showed that EDC's method produced a better result with substantially less residual atmospheric artefacts and a less obvious spectral smile. All Hyperion scenes pre-processed after June 2002 showed a significant improvement in the quality of the reflectance spectra due to the new EDC generated header information and the

application of ACORN4 using Mode 1.5 for the atmospheric correction (**Figure 5.2.2**(a) and Figure 5.2.1(b)). The modified procedure corrected sporadic ambiguities regarding mineral identification that are often based on subtle spectral differences and easily impacted by poor quality or incorrectly processed data.

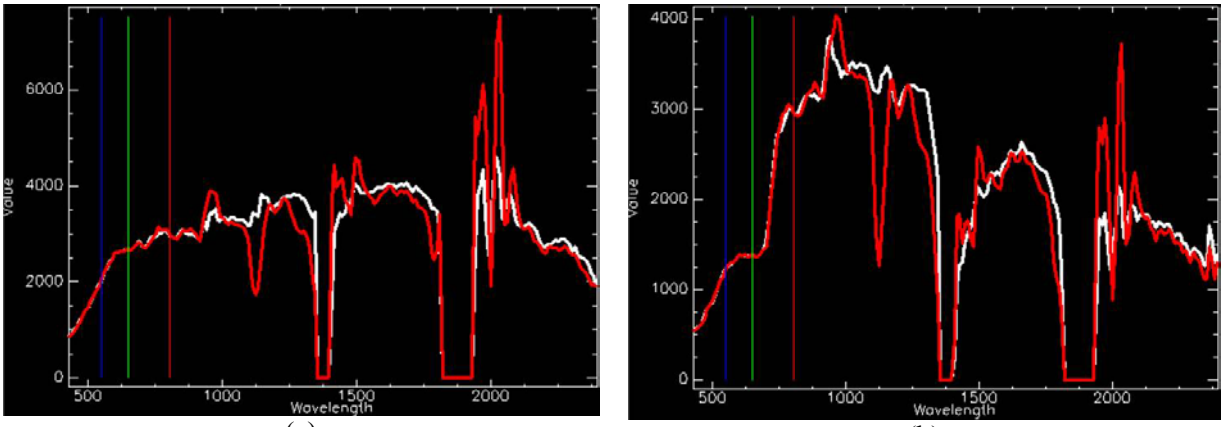

(a) (b)

Figure 5.2.2. Spectral profile comparisons from a single pixel over muscovite (a) and vegetation (b) from reflectance data produced by ACORN4 highlighting the improvement (i.e. fewer atmospheric artifacts) after using the EDC header information (white line) compared to the TRW header information (red line).

5.2.3 Lessons learned from the Geological Applications

Following are some of the lessons learned from the extended mission activity:

- The lack of georeferencing of the Hyperion data, without having to resort to an external reference, is a disadvantage to operational users familiar with integrating data from disparate sources in a GIS, particularly where good quality maps do not exist.

- Hyperion data is not yet adequate for reliably and routinely mapping minerals whose diagnostic features are beyond 2300 nm, where the signal quality drops-off substantially. Exceptions to this have been demonstrated for bright and very strong absorbing minerals, such as talc, where these are very well exposed, and also other situations where rocks and minerals form large areas from which average signatures can be computed that reduce noise levels.

- As with any remote sensing method, its suitability to any particular problem may vary and success in one situation should not be taken as applying everywhere, under all circumstances. For example, in geological studies, vegetation cover and deep surface weathering can reduce the utility of remotely sensed hyperspectral data.

- Spaceborne hyperspectral sensing is complementary to airborne hyperspectral sensing. It is a matter of "horses for courses". For large, regional, "greenfields" surveys spaceborne data, of adequate quality, should be attractive as data analysis becomes simpler. Many problems, however, may require more detail or more sensitivity, than current spaceborne technologies can provide. An ideal, long-term

goal would be to have spaceborne, airborne and field instruments of adequate quality that can be used in concert in a stratified, multi-scale manner.

- Many routine users in the mining sector are specialists in their own fields, not in remote sensing or spectral analysis. These users thus want information products and tools to simply create them, without having to become experts. Such tools are now becoming progressively more automated and the data quality needs to be adequate for these tools to function effectively and produce reliable products. Sensors coming after, and developed from the Hyperion experience, must therefore be considerably more sensitive so that they operate in a wider variety of, progressively more automated, situations.

- Many users have asked why use Hyperion when we have ASTER data? The answer to this is that hyperspectral sensors should be able to map mineral species and fractions of these in mixtures. ASTER is a good mapper of mineral and lithological groups, but can lead to ambiguities in the interpretation of mineral species, particularly if little is known about an area beforehand. Species mapping requires good SNR. Geological users are now learning the value of mapping individual species in building models for more detailed geological understanding.

- There is an "optimum" hyperspectral scene for geological use. It is often heard that geologists just need any scene, as the geology never changes. This is a fallacy, as it is the *expression* of that geology that changes with season, ground cover, lighting conditions and atmospheric conditions. Service providers therefore need to be aware of user needs for this optimum scene in their scheduling and business transactions.

- Operational users, perhaps more so than researchers, operate within strict budget years. Thus market development of "commercial" hyperspectral applications must consider the time taken to provision a budget and gain sign-off, before a survey can be conducted. Often delivery is required very quickly, before the funded project changes its status. If that happens the information may be acquired by some other means, or the tenement may be dropped as the company moves on. Slow delivery will turn-off some users and lead to data never being fully utilised. Successfully delivered and processed high-quality data, however, can save considerable amounts of time and money and define previously unseen targets or competitive value.

5.3 Land-Cover Data Buys

Reported by: Alex Held, CSIRO Land and Water
Contact email: Alex.Held@csiro.au

A number of 'Extended Mission" data buys have been commissioned by various research groups and organisations across Australia directly via the USGS DAAC. Applications undertaken as part of this activity by CSIRO include agriculture (sugarcane), as well as natural and managed pasture mapping in the states of Victoria and Western Australia. In addition, Hyperion data collections have been attempted over sub-Antarctic islands with limited success due to excessive cloud cover at times. Most of these investigators have ordered their data directly, but are benefiting from the relationship developed between ACRES and USGS and from collaboration with

Australian SVT members. Many users also acquired valuable experience from attending the "Hyperion Data Processing Workshop", given by the CSIRO Earth Observation Centre in Canberra. As an example of the increasing research, a PhD. degree study is currently underway by Susanne Thulin (Royal Melbourne Institute of Technology) to evaluate the use of Hyperion data for mapping grassland diversity and dairy pasture quality in the state of Victoria.

Another application – 'Sugarcane Condition Mapping' has been undertaken by Alex Held (CSIRO), Armando Apan (University of Southern Queensland) and Stuart Phinn (University of Queensland). This crop is primarily grown in sub-tropical and tropical areas of the state of Queensland and near the Ord River in the north of Western Australia. Pests, diseases and stresses due to low water and low nutrient levels, have in the past seriously affected sugarcane yields; therefore disease management is seen as important in maintaining the competitive advantage of the sugar industry.

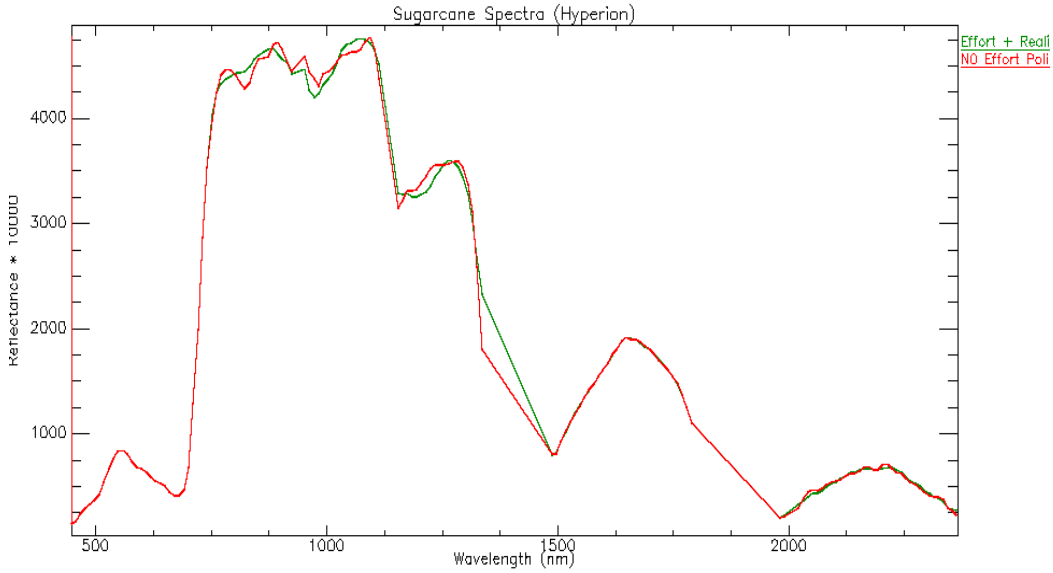

Figure 5.3.1. Comparison of spectra for a sugarcane field after atmospheric correction with (green line) and without (red line) 'EFFORT" and "Reality-Boost Spectra' polishing applied within the ACORN™ software.

To date, other broadband sensor systems have not been able to accurately map the presence of diseases like "Orange Rust". Thus one aim of the study was to examine the potential of Hyperion imagery to detect the incidence of sugarcane 'orange rust' disease, in addition to development of methodologies for nutrient status mapping and variety discrimination, using primarily biophysical mapping approaches. During an initial phase of this project, the objectives have been to develop a very rapid, index-based processing methodology that could produce the relevant information with limited pre-processing required. This included the development of a consistent and high quality atmospheric correction methodology and use of spectral vegetation indices (SVIs) to gain insights on the relationship between sugarcane orange rust disease and changes on the biochemical component of the crop.

The study area selected for this work is in the Mackay sugarcane-growing region in Queensland, which is the largest sugar-producing area in Australia. A Hyperion image was acquired on 2 April 2002, and delivered as Level 1B_1 data in scaled radiance

units. To facilitate the development of indices, these values were converted to apparent surface reflectance using ACORN 4.10 software (Analytical Imaging and Geophysics LLC, 2002). Prior to this conversion, the following pre-processing steps were implemented: *re-calibration, band selection, de-streaking* and *removal of bad pixels* (Datt, *et al.*, 2003; Apan and Held, 2002; Apan *et al.*, 2004).

A maximum noise fraction (MNF) transformation smoothing was applied to the post-atmospheric correction reflectance image to minimise uncorrelated spatial noise. The output image was further processed by applying the *Empirical Flat Field Optimal Reflectance Transformation* (EFFORT, Boardman, 1998) polishing technique (Figure 5.3.1).

Field measurements include detailed ASD FR reflectance measurements of sugarcane leaves and whole canopy, in conjunction with detailed tissue sampling for nutrient and pigment analysis. A comprehensive GIS database has been made available by Mackay Sugar, which contains information on the different planning dates, varieties and agronomic practices in the region. This database is being used for training and verification of the ongoing spectral analysis.

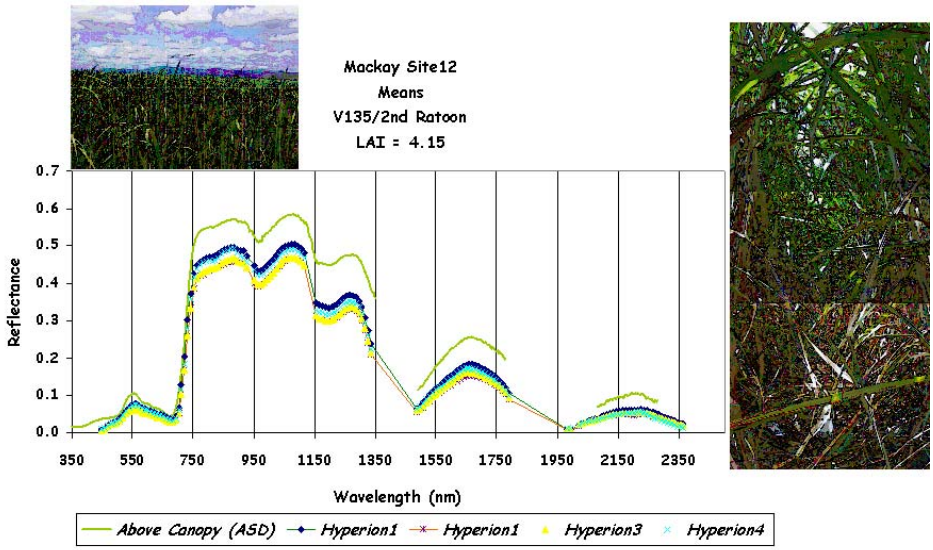

Figure 5.3.2. Comparison of ASD FR spectrum collected over a full cover sugarcane canopy in Mackay (March 2002), and three different individual pixel spectra extracted from Hyperion reflectance data over closed-canopy sugarcane fields.

The resulting reflectance image is of very high quality when compared against ground spectral measurements (Figure 5.3.2). The resulting image is being used to derive a range of spectral indices that have been correlated to variations in the crop's foliar chemistry and potentially associated with the incidence of "Orange Rust" or other stress factors.

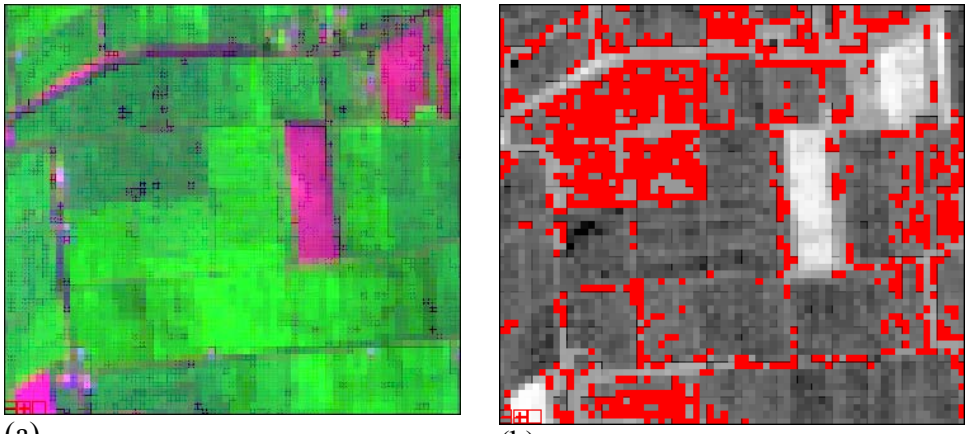

(a) (b)

Figure 5.3.3. (a) True colour RGB of a subsection of the Mackay Hyperion image showing various sugarcane fields. (b) Preliminary results of "Orange Rust" disease detection (red pixels), using a range of spectral indexes.

Initial mapping results (Figure 5.3.3), with narrow band indices derived from the Hyperion image data were able to discriminate sugarcane crops severely affected by orange rust disease from non-diseased areas. The indices developed used spectral bands that are known to be sensitive to changes in leaf pigments, internal leaf structure and moisture content. Work is underway to develop robust methodologies for assessing the crop's nutrient status and for varietal mapping, and is due to be reported at a special session of the Agronomy Society of America meetings in Colorado, November 2003.

References

Apan, A. and Held, A. (2000) Mapping of sugarcane biophysical variables with Hyperion imaging spectrometer on the NASA EO-1 Mission. *Final EO-1 SVT Meeting*, Hawaii, November 2002.

Apan, A., Held, A., Phinn, S, and Markley, J. (accepted 2004) Detecting Sugarcane 'Orange Rust' Disease Using EO-1 Hyperion Hyperspectral Imagery, *International Journal of Remote Sensing*.

Boardman, J.W. (1998) Post-ATREM Polishing of AVIRIS Apparent Reflectance Data using EFFORT: a Lesson in Accuracy versus Precision*, Summaries of the Seventh JPL Airborne Earth Science Workshop,* JPL Publication 97-21, Vol. 1, p. 53.

Datt, B., T.R. McVicar, T.G. Van Niel, D.L.B. Jupp & J.S. Pearlman, (2003). "Pre-processing EO-1 Hyperion Hyperspectral Data to Support the Application of Agricultural Indices," *IEEE Transactions on Geoscience and Remote Sensing,* **41**(6), 1246-1259.

6 CONCLUSIONS & RECOMMENDATIONS

6.1 The Completed SVT Mission

Australian scientists have participated energetically in the EO-1 mission with its focus on new technology evaluation and inter-comparisons. The diverse sites across the continent and a solid program of field and airborne supporting data collection have led to a wide range of outcomes for Calibration & Validation studies, base data processing (including atmospheric correction) and the capability of the sensors on-board to meet the needs for a range of applications.

In addition, EO-1 has been tested against a range of applications for spectral data and found, despite its experimental nature and purpose, to be already a highly valuable tool for applications from the space environment. These have been described in the site reports of this document. Each site has a specific area of application to demonstrate and all have had significant success to their aims. To be effective in applications the data need, however, to be processed beyond Level 1B and the experience of the SVT and the Australian contributions have provided a processing framework on which such operational applications may be built.

The main benefit of the mission that has arisen from the work presented here has been the opportunity to observe and work with hyperspectral data in a space environment and with a space perspective. The Hyperion sensor was never specified to the level that might be flown for an operational mission. Its role was to be part of the overall technology experiment. In doing this it surprised many but has also demonstrated how future operational sensors will need much higher SNR and possibly finer spatial resolution to fully meet the needs of users. The Hyperion mission has added a large amount of information to support the development of such sensors.

6.2 The Extended Mission

The benefits that reside in the EO-1 sensors for operational analysis of the earth surface led to the extended mission. Australian scientists also responded enthusiastically to the NASA/USGS extended mission. They promoted and collected a significant bulk data purchase to ensure that EO-1 data reach as many new researchers and applied users of remote sensing as possible. The Australian Centre for Remote Sensing (ACRES) worked closely with USGS and continued data acquisition when required. CSIRO EOC started education and outreach workshops to enable people to get to know and gain experience of both ALI and Hyperion data in their applications. Australian researchers have contributed their knowledge to service the user community as part of extensive data buys from USGS.

This work done to develop an extended mission recognised that for these data to impact fully on applications and become accepted beyond their technical and scientific use in technology evaluation there is a need for visible results from applications and greatly increased data access for the wider community of researchers, information suppliers and end users. The SVT has shown that, with effective processing to overcome instrument

deficiencies and limitations, ALI and Hyperion can provide data sets of sufficiently high quality to be put to work in an operational setting. That work is ongoing and is currently filling a serious gap in space deployment of hyperspectral data.

6.3 Beyond Technology Evaluation

From the "proving of science" point of view, there is still a serious gap between the demonstrable quality of the data and its base processing by scientists and its further use in applications by applications oriented users. This issue needs some further research and much more development through applications involving both groups of people.

It seems to be possible and desirable to develop key activities on the base of the contributions of all of the scientists of the SVT to date and on the outcomes of the SVT meetings and publications. These include making accessible calibration and geometric findings, recommendations for pre-processing and atmospheric correction, the evaluation of time series products from the data and establishing clear environmental limits on applications products in others.

For example in Australia:

- Continuation of the temperate Coleambally agricultural test site as a time series study for crop health evaluation and support for precision agriculture;
- Development of complementary tropical sites for time series data with agricultural, coastal and forest applications;
- Evaluation of mineral mapping tools in more complex and diverse environments and enhanced processing speed and throughput;
- Proving and extending initial results on forest health, productivity monitoring and mapping;
- Evaluating coastal study sites in eutrophic waters;
- Assessing coral reef health and recovery from bleaching.

Due to the efforts of the SVT – in which the Australian scientists are proud to have participated – the users of EO-1 data can move beyond base data processing and engage in applications that will continue to build the demand for EO-1 and (equally significantly) for future hyperspectral and advanced multi-spectral sensor data. The requirements on those future sensors for operational sensitivity and resolution are now much sharper due to the EO-1 mission, and the need to maintain this activity is crucial to hyperspectral remote sensing as Hyperion is currently the only spaceborne hyperspectral instrument and will remain so for some time.

7 ACKNOWLEDGEMENTS

The Australian activity in the SVT has been successful in no small degree due to the interest, support and continued close collaboration and involvement of the NASA EO-1 Mission Chief Scientist, Steve Ungar and of members of the Hyperion instrument team from TRW and in particular the input and support of its leader Jay Pearlman. Their vision of extensive activity during the EO-1 mission in the southern hemisphere came to fruition with campaigns in Australia and Argentina and their role in the Australian activity is both gratefully appreciated and greatly valued. The Cover Picture and Figures 1.2.1 and 1.2.2 were kindly provided by and used with permission of NASA.

The activity recorded here has involved a wide range of Australian scientists and their Australian and international scientific collaborators. In addition to those mentioned in the site reports, scientists at the University of Queensland contributed extensively with the fieldwork done for the Moreton Bay study. In Coleambally, the help and support of the CRC for Sustainable Rice Production was highly valuable and appreciated as was the support of the Coleambally Irrigation Cooperative Limited and the Landholders. Every site involved more input than just that of the researchers and while it and they are too extensive to list here, the contribution to the outcomes is sincerely acknowledged.

At CSIRO, the work was supported in-kind and financially by the EOC and the Divisions for which the scientists involved work. Staff from the EOC office, while not listed among the investigators at the start of this report, have also undertaken many hours of work on behalf of the Australian members of the SVT and include particularly Jill Huntington and Ray Merton who put in great efforts in the early planning and logistics for the mission. In recent times, Beth Reid, Irenke Arthurson and others worked with EOC scientists to manage the communications, maintain records and manage data flow. It all mattered and it all contributed.

8 EO-1 RELATED PUBLICATIONS & PRESENTATIONS

This section provides a complete listing of papers and presentations by the Australian EO-1 Co-Investigators arising from their work. Some of these are also listed in the individual site reports in Section 3.0.

8.1 Journal Papers

8.1.1 Papers in 2002

Coops, N.C., Dury, S., Smith, M.L., Martin, M. and Ollinger, S. (2002). Comparison of Green Leaf Eucalypt Spectra using Spectral Decomposition. *Australian Journal of Botany.* **50**: 567 – 576.

Kutser T., A.G. Dekker and W. Skirving, (2002). Modelling spectral discrimination of Great Barrier Reef benthic communities by remote sensing instruments, *Limnology and Oceanography,* **48**: 497-510.

8.1.2 Papers in 2003-2004

V.E. Brando and A.G. Dekker (2003). Satellite hyperspectral remote sensing for estimating estuarine and coastal water quality. *IEEE - Transactions on Geoscience and Remote Sensing*, **41**(6), 1378-1387.

Coops, N.C., Smith, M.L., Martin, M.M, Ollinger, S. (2003). Prediction of Eucalypt Foliage Nitrogen Content from Satellite Derived Hyperspectral Data. *IEEE Transactions on Geoscience and Remote Sensing,* **41**(6), 1338-1346.

Coops, N.C., Smith, M.L., Jacobsen, K.L., Martin, M. and Ollinger, S. (2004). Estimation of plant and leaf area index using three techniques in a mature native eucalypt canopy. *Austral Ecology*, **29**(3), 332 – 341.

B. Datt, T.R. McVicar, T.G. Van Niel, D.L.B. Jupp, J.S. Pearlman (2003). Pre-processing EO-1 Hyperion Hyperspectral Data to Support the Application of Agricultural Indices. *IEEE - Transactions on Geoscience and Remote Sensing,* **41**(6), 1246-1259.

Liang, S. Fang H. L., Thorp L., Kaul, M., Van Niel, T.G., McVicar, T. R., Pearlman J. S., Walthall, C. L., Daughtry, C. S. T., and Huemmrich, F. (2003). Estimation of land surface broadband albedos and leaf area index from EO-1 ALI data and validation. *IEEE - Transactions on Geoscience and Remote Sensing*. **41**(6), 1260-1267.

8.2 Conference Proceedings

8.2.1 IGARSS

8.2.1.1 IGARSS 2001, Sydney, Australia

Barry, P.S., Jarecke, P., Pearlman, J.S., Jupp, D.L.B., Lovell, J.A. and Campbell, S.K. (2001). Use of Lake Frome Ground Truth Campaign as a Cross-Calibration of the Hyperion Instrument. *IGARSS'01 Special Session 40*, paper 1780.

S.K. Campbell, J.A. Lovell, D.L.B. Jupp, R.D. Graetz, P. Barry, P. Jarecke and J.S. Pearlman (2001). The Lake Frome Field Campaign in Support of Hyperion Instrument Calibration and Validation," *Proceedings of International Geoscience and Remote Sensing Symposium (IGARSS'01)*, Sydney, Australia, 2001.

N. Coops, M. Smith, M.M. Martin, S. Ollinger, A. Held and S. Dury (2001). Assessing the performance of Hyperion in Relation to Eucalypt Biochemistry: Preliminary Project Design and Specifications," *Proceedings of International Geoscience and Remote Sensing Symposium (IGARSS'01)*, Sydney, Australia, 2001.

T.J. Cudahy, R.D. Hewson, J.F. Huntington, M.A. Quigley, P. Barry (2001). The Performance of the Satellite-borne Hyperion Hyperspectral VNIR-SWIR Imaging System for Mineral Mapping at Mount Fitton, South Australia. *Proceedings of International Geoscience and Remote Sensing Symposium (IGARSS'01)*, Sydney, Australia, 2001.

A.G. Dekker, V.E. Brando, J. Anstee, N. Pinnel, A. Held (2001). Preliminary Assessment of the performance of Hyperion in Coastal waters. Cal/Val activities in Moreton Bay, Queensland, Australia. *Proceedings of International Geoscience and Remote Sensing Symposium (IGARSS'01)*, Sydney, Australia, 2001.

Liang, S., Fang, H., Kaul, M., Van Niel, T.G., McVicar, T.R., Campbell, S.K., Walthall, C., Daughtry, C. and Pearlman, J.S. (2001). Land Surface Bio/Geophysical Variable Estimation for EO-1 Data and Validation. *Proceedings of the International Geoscience and Remote Sensing Symposium*, Sydney, July 2001.

T.G. Van Niel, T.R. McVicar, S.K. Campbell, S. Liang, M. Kaul, J.S. Pearlman, P. Clancy, C. Segal (2001). The Coleambally Agricultural Component of Hyperion Instrument Validation. *Proceedings of International Geoscience and Remote Sensing Symposium (IGARSS'01)*, Sydney, Australia, 2001.

8.2.1.2 IGARSS 2002, Toronto, Canada

N. Coops, M. Smith, M. Martin, S. Ollinger, A. Held (2002). Predicting Eucalypt Biochemistry From Hyperion and HyMap Imagery. *Proceedings of International Geoscience and Remote Sensing Symposium (IGARSS'02)*, Toronto, Canada, 2002.

T.J. Cudahy, P.S. Barry, et al, (2002). Early Earth Magmatic-Seawater Hydrothermal Alteration Revealed through Processed Satellite-Borne Hyperion Imagery. *Proceedings of International Geoscience and Remote Sensing Symposium (IGARSS'02)*, Toronto, Canada, 2002.

J. Pearlman, T. McVicar, T. Van Niel, D. Jupp, B. Datt, *et al.* (2002). Using a Time Series of EO-1 Data for the Coleambally Irrigation Area, Australia, To Assess The Value of Co-registration, Atmospheric Correction and Multispectral Data for Agricultural Applications. *Proceedings of International Geoscience and Remote Sensing Symposium (IGARSS'02)*, Toronto, Canada, 2002.

8.2.1.3 IGARSS 2003, Toulouse, France

Datt, B., Jupp, D.L. B., McVicar, T. R., Van Niel, T. G., and Pearlman, J. S. (2003). Time Series Analysis of EO-1Hyperion Data for Yield Estimation at an Agricultural Site. *Proceedings of the International Geoscience and Remote Sensing Symposium*, Toulouse, France 21-25 July.

8.2.2 11th ARSPC, Brisbane, Australia, 2002

V.E. Brando, A.G. Dekker, and J.M. Anstee, "Estuarine Hyperspectral Remote Sensing from Space: Case Study Moreton Bay," *Proceedings of the 11th Australasian Remote Sensing and Photogrammetry Conference*, Brisbane, Australia, 2002.

B. Datt, D.L.B. Jupp, T.R. McVicar, T.G. Van Niel, J. Lovell, S.K. Campbell, "Spectral Feature Analysis of Crop, Soil and Stubble Using Hyperion and HyMap Data," *Proceedings of the 11th Australasian Remote Sensing and Photogrammetry Conference*, Brisbane, Australia, 2002.

V.H. Chewings, G.N. Bastin, M.M. Crawford and J.E. Kinloch, "Characterisation of Vegetation Components in the Australian Arid Zone Using EO-1 Hyperion Imagery," *Proceedings of the 11th Australasian Remote Sensing and Photogrammetry Conference*, Brisbane, Australia, 2002.

A. Held, K. Powell, A. Gonzalez, S.R. Phinn, C.H. Menges, "Application of Imaging Spectroscopy to Crop Monitoring and Precision Agriculture," *Proceedings of the 11th Australasian Remote Sensing and Photogrammetry Conference*, Brisbane, Australia, 2002.

8.2.3 Other Conferences

D.L.B. Jupp, B. Datt, T. R. McVicar, T. G. Van Niel, J. S. Pearlman, J. Lovell, and E. A. King (2002). Improving the Analysis of Hyperion Red Edge Index from an Agricultural area. *Proceedings of the SPIE*, Vol. **4898**, 78-92..

Kutser T, A. Dekker, W. Skirving (2002). Detecting coral reef substrate types by airborne and space borne hyperspectral sensors. *Proceedings of SPIE*, 4544: 93-102.

Kutser T., D.L.B Jupp (2002). Mapping coral reef benthic habitat with a hyperspectral space borne sensor. Proceedings of Ocean Optics XVI, Santa Fe, CD-ROM.

8.3 Technical Reports/Workshop Documents

T. R. McVicar, T. G. Van Niel, and D. L. B. Jupp, "Geometric Validation of Hyperion Data acquired by Earth Observing 1 Satellite at Coleambally Irrigation Area," CSIRO Land and Water Technical Report 46/01, 2001.

D.L.B. Jupp *et. al*., "Discussions around Hyperion Data: Background Notes for the Hyperion Data Users Workshop," CSIRO Earth Observation Centre, 2002.

B. Datt, and D.L.B Jupp, "Hyperion Data Processing Workshop: Hands-on Processing Instructions," CSIRO Earth Observation Centre, 2002.

8.4 Presentations at CSIRO EOC Annual Science Meetings

8.4.1 CSIRO EOC Annual Science Meeting, 2001

S. Campbell, G. Byrne, D.L.B. Jupp, E.A. King, J. Lovell, R.D. Graetz, P.S. Barry, P. Jarecke, J. Pearlman "The Lake Frome field campaign in support of Hyperion instrument calibration & Validation," C*SIRO EOC Annual Science Meeting*, Canberra, 2001.

T. McVicar, T. Van Niel, "The Coleambally Agricultural Component of Hyperion Instrument Validation," C*SIRO EOC Annual Science Meeting*, Canberra, 2001.

F. Prata, G. Rutter, D.L.B. Jupp, "Cal/Val Activities at the CIGSN Uardry Field Site, NSW, Australia in Support of the EO-1 Mission," C*SIRO EOC Annual Science Meeting*, Canberra, 2001.

T.J Cudahy, R. Hewson, J.F. Huntington, M.A. Quigley, P.S. Barry, "The Performance of the Satellite borne Hyperion Hyperspectral VNIR-SWIR Imaging System for Mineral Mapping at Mount Fitton, South Australia," C*SIRO EOC Annual Science Meeting*, Canberra, 2001.

A.G. Dekker, V.E. Brando, J. Anstee, N. Pinnel, A. Held, "Preliminary assessment of the performance of Hyperion in coastal waters. Cal/Val activities in Moreton Bay, Queensland, Australia," C*SIRO EOC Annual Science Meeting*, Canberra, 2001.

N. Coops, A. Held, "EO-1 SVT Site: Tumbarumba, Australia," C*SIRO EOC Annual Science Meeting*, Canberra, 2001.

M.A. Quigley, T.J. Cudahy, J.F. Huntington. "Hyperion Geoscience Group-Shoot". CSIRO EOC Annual Science Meeting, Canberra, 2001

8.4.2 CSIRO EOC Annual Science Meeting, 2002

B. Datt, D.L.B. Jupp, "The Hyperspectral task report," C*SIRO EOC Annual Science Meeting*, Canberra, 2002.

N. Coops, M. Smith, M. Martin, S. Ollinger, A. Held, "Predicting Eucalypt Biochemistry From Hyperion and HyMap Imagery," C*SIRO EOC Annual Science Meeting*, Canberra, 2002.

T. McVicar, T. Van Niel, D.L.B. Jupp, B. Datt, J. Pearlman, "Coleambally Irrigation Area (CIA) and EO-1: A Time Series Agricultural and Cal-Val Site," C*SIRO EOC Annual Science Meeting*, Canberra, 2002.

V.E. Brando, A. Dekker, *et al,* "Satellite hyperspectral remote sensing for estimating estuarine and coastal water quality," C*SIRO EOC Annual Science Meeting*, Canberra, 2002.

V.H. Chewings, G.N. Bastin, J.E. Kinloch, M.M. Crawford, "Characterisation of Vegetation Components in the Australian Arid Zone Using EO-1 Hyperion Imagery," C*SIRO EOC Annual Science Meeting*, Canberra, 2002.

T.J Cudahy, P. Barry, A.P. Rodger, P. Mason, M. Quigley, M. Folkman, J. Pearlman, "Assessment of the stability of the Hyperion SWIR module for hyperspectral mineral mapping using multi-date images from Mount Fitton, Australia," C*SIRO EOC Annual Science Meeting*, Canberra, 2002.

T.J. Cudahy, et al, "Hyperion Mineral Mapping Results: Panorama," C*SIRO EOC Annual Science Meeting*, Canberra, 2002.

8.5 NASA EO-1 Science Validation Team (SVT) Meetings

[Available as PDF files of original powerpoint presentations at the CSIRO EOC Web site (http://www.eoc.csiro.au) under Hyperspectral/Australian Science Validation Team/Presentations and Papers.]

8.5.1 First SVT Meeting, NASA Goddard, February 2001

D.L.B. Jupp *et al.*, "Evaluation & Hyperion Performance at Australian Calibration & Validation Sites", Goddard, February 2001.

8.5.2 SVT Meeting, Tuscon, May 2001

D.L.B. Jupp et al, "The Australian Summer EO-1 Southern Hemisphere (SH) Campaign," *EO-1 SVT Meeting*, Tuscon, May 2001.

D.L.B. Jupp, "Lake Frome Fieldwork and Analysis Of Hyperion Data," *EO-1 SVT Meeting*, Tuscon, May 2001.

T. Cudahy, J. Huntington, P. Barry, "Mount Fitton, South Australia Hyperion "SWIR - Spectral" Test Site," *EO-1 SVT Meeting*, Tuscon, May 2001.

J. Pearlman, T. G. Van Niel, T. McVicar, D.L.B. Jupp, S. Liang, M. Kaul, "Agriculture in Coleambally - Imaging the growing season," *EO-1 SVT Meeting*, Tuscon, May 2001.

F. Prata, D.L.B. Jupp, "Cal/ Val Activities at the CIGSN Uardry Field Site, NSW, Australia in Support of the EO- 1 Mission," *EO-1 SVT Meeting*, Tuscon, May 2001.

N. Coops, "EO-1 SVT Site: Tumbarumba," *EO-1 SVT Meeting*, Tuscon, May 2001.

A. G. Dekker, V. E. Brando, J. Anstee, N. Pinnel, A. Held, "Preliminary assessment of the performance of Hyperion in coastal waters. Cal/ Val activities in Moreton Bay, Queensland, Australia," *EO-1 SVT Meeting*, Tuscon, May 2001.

8.5.3 SVT Meeting, Buenos Aires, November 2001

D. L. B. Jupp, A. Held, "Summary of Australian EO- 1 activities," *EO-1 SVT Meeting*, Buenos Aires, 6-8 November 2001.

T. R. McVicar, T. G. Van Niel, D. L. B. Jupp, J. S. Pearlman , "Assessment of Precision Agriculture in Coleambally," *EO-1 SVT Meeting*, Buenos Aires, 6-8 November 2001.

A. Held, "Summary of Australian Land and Vegetation Based EO-1 Activities," *EO-1 SVT Meeting*, Buenos Aires, 6-8 November 2001.

V. E. Brando, A. G. Dekker, J. Anstee, N. Pinnel, A. Held. "Preliminary multitemporal assessment of the performance of Hyperion in coastal waters. Cal/ Val activities in Moreton, Bay, Queensland, Australia," *EO-1 SVT Meeting*, Buenos Aires, 6-8 November 2001.

T. Cudahy, "Mineral mapping at the Australian Mount Fitton and Panorama test sites," *EO-1 SVT Meeting*, Buenos Aires, 6-8 November 2001.

T. Cudahy, "An additive SWIR instrument/ processing artifact observed in recent Hyperion data," *EO-1 SVT Meeting*, Buenos Aires, 6-8 November 2001.

Jon Huntington, Melissa Quigley and Peter Mason "Geological Analysis of Hyperion Data of Virginia City, Nevada" *EO-1 SVT Meeting*, Buenos Aires, 6-8 November 2001.

Melissa Quigley, Peter Mason and Jon Huntington "Oatman Arizona Geological Validation Site, Hyperion Processing and Analysis" *EO-1 SVT Meeting*, Buenos Aires, 6-8 November 2001.

[The last two reports were presented as part of a combined report by Fred Kruze "Progress Report: Evaluation and Geologic Validation of EO-1 Hyperion" on behalf of the AIG/CSIRO Cooperative Project.]

8.5.4 SVT Meeting, Goddard, April 2002

Jupp, D.L.B. "Australian EO-1 Report: One year on – Applications and Experiences," *EO-1 SVT Meeting*, Goddard Visitors Center, April 2002.

Pearlman, J.S., D.L.B. Jupp, T.R. McVicar, T. Van Niel, B. Datt, J. Lovell," Hyperion Noise and Atmospheric Impacts on Vegetation Data,*" EO-1 SVT Meeting*, Goddard Visitors Center, April 2002.

Jupp, D.L.B. "Some Smiley Discussions," *EO-1 SVT Meeting*, Goddard Visitors Center, April 2002.

8.5.5 Final SVT Team Meeting, Hilo, Hawaii, November 2002.

Datt, B. *et al.* "The Australian EO-1 final Report: Activities and Outcomes from the CalVal sites", *Final EO-1 SVT Meeting*, Hawaii, November 2002.

Apan, A. and Held, A. "Mapping of sugarcane biophysical variables with Hyperion imaging spectrometer on the NASA EO-1 Mission." *Final EO-1 SVT Meeting*, Hawaii, November 2002.

8.6 Media Reports and Outreach

Coops, N. *Forests a blaze of colour from space* Date: 03/07/01, Ref 2001/54 **,** http://www.csiro.au/index.asp?type=mediaRelease&id=PrsatelliteA

Coops, N. CSIRO Media: May 2001. *A satellite eying our forests* (available on CD from CSIRO National Science radio).

Coops, N. ABC National Radio (South Australia) 10th March 2001.

A.G. Dekker, V.E. Brando, N. Pinnel, A. Held, "HYPERION: the first imaging spectrometer from space: also suitable for inland and coastal water observations," *Backscatter magazine (http://www.waterobserver.org/backscatter/issue-02-winter.html),* 2002.

EOC Press Release. (2000) "*See More, Colourfully, from Space*", [Scientists from NASA and TRW visit potential Hyperion calibration sites in Australia], February, 2000. Available on http://www.eoc.csiro.au under Media Releases.

EOC Press Release. (2001) "*Salt lake helps test 'sky eye'*", [A team of CSIRO scientists has just spent a week in a huge barren salt lake in Australia's interior helping to test a new NASA satellite], January, 2001. Available on http://www.eoc.csiro.au under Media Releases.

Kutser T, How looks health of coral reefs from space? *Horisont*, 5:10-15, 2002 (in Estonian).

McVicar, T.R. ABC Radio Wagga Wagga NSW "*NASA and Coleambally Irrigation Area*" September 5, 2001.

McVicar, T.R. The Weekend Australian "*NASA helps beat salinity*" September 1-2, 2001, pp 22.